

University of Nottingham
UK | CHINA | MALAYSIA

Targeting the Hypoxic Expression of Epidermal Growth Factor Receptor

Abdulmohsin J Alamoudi, Pharm.D., MSc.

Thesis submitted to the University of Nottingham for the degree of Doctor of Philosophy

November 2020

Abstract

Investigating translation regulation of epidermal growth factor receptor (EGFR) is a growing concern in the context of advanced breast cancer. The 5' untranslated region (UTR) of *EGFR* mRNA contains an internal ribosome entry site (IRES) that permits hypoxic expression. This allows targeting of the expression of EGFR in breast cancer cells under hypoxia and other stress conditions. Here we describe the role of the *EGFR* IRES in mediating protein expression under stress conditions commonly associated with malignant growth including DNA damage. The requirement for DDX3, a DEAD-box RNA helicase, was also investigated in terms of regulating the mRNA translation of *EGFR* via its 5' UTR. In addition, this study seeks to obtain data with regards to the feasibility of targeting the hypoxic expression of EGFR using the antisense technology and polymeric delivery systems.

The response of the *EGFR* IRES to different conditions of cell stress and DDX3 was examined utilising bicistronic plasmids in breast cancer cells. In addition, antisense oligonucleotides (ASOs) binding different regions of the *EGFR* 5' UTR have been used to target the expression of EGFR in breast cancer cell lines. To deliver these ASOs to hypoxic cancer cells, linear cationic polymers based on poly(β-amino ester) (PBAE) chemistry were synthesised incorporating the hypoxia-sensitive azobenzene bond.

Translation driven by the *EGFR* IRES responds to specific conditions of cell stress, notably those that induce genotoxic stress, suggesting an important role of the *EGFR* IRES in mediating translation initiation as a response to moderate

DNA damage. The second major finding was that DDX3 stimulates cap-independent translation initiation irrespective to the 5' UTR sequence. In addition, targeting the *EGFR* IRES using modified ASOs was found to be ineffective in preventing the internal landing of ribosomes, yet targeting the *EGFR* mRNA for degradation was found to significantly reduce the expression of EGFR and viability of breast cancer cells. Finally, azobenzene-containing PBAEs were synthesised and characterised showing promising results in terms of their ASO complexation stability and responsiveness to low oxygen tensions. Once established, these PBAEs can be used to deliver the anti-EGFR ASOs preferentially to hypoxic cells in breast-cancer tumours.

Acknowledgements

First, I would like to thank my principal supervisor Keith Spriggs for giving me the chance to work in his lab. Since I started around three years ago, he was always welcoming supportive and encouraging to the point where I feel privileged joining his group. Indeed, leaving his lab would never mean that I will stop seeking his guidance in my future endeavours.

In addition, many thanks to my secondary supervisor Hilary Collins for providing support and encouragement throughout my project and especially for being exceptionally patient with me as we spent hours looking at fluorescent cells in the confocal microscope room.

I would like also to thank Cameron Alexander for enabling me to work in his lab and especial thanks to Pratik Gurnani for being incredibly supportive which helped me a lot in advancing my project. Since I started working with polymers, Pratik generously provided knowledge and support especially during my transition stage from RNA biology to polymer chemistry.

Thanks also to my dear friend Abdul Hafeez for his unique sense of humour and all the side talks that we had in our way to and from Portland building where we did our prayers. I would also like to thank my lab buddy and my good friend Declan Grewcock for all the great discussions we had about science and about football, boxing, MMA, bodybuilding and sometimes cricket and rugby. Thanks also to my other group members Arnelle Edwards and Maksim Ivanov for being so nice and helpful.

Thanks to everyone in the gene regulation and RNA biology group and B15 lab who have helped me through my PhD project. Special thanks to Bismoy Mazumder and Jonathan Whitchurch for helping in the lab when I just started, Barbara Rampersad and Peter Wellham for the early morning chats, Christopher Roberts for pushing me towards a more plant-based diet, Ryan Morris for his help during his DTP rotation in our lab and Aalam Ameerul Moominin for being my out-of-hours buddy.

Thanks to King Abdelaziz University for providing this opportunity to complete my graduate studies in the UK. I have gained a lot from this journey and definitely increased my passion for science even more! Finally, I would like to thank my beloved family especially my parents who helped and encouraged me to become the best version of myself and my wife Shahad who has supported me all the way to the point where I cannot thank her enough!

Table of Contents

Abstract ..... **i**
Acknowledgements ..... **iii**
Table of Contents ..... **v**
List of Figures ..... **viii**
List of Tables ..... **xii**
List of Schemes ..... **xii**
List of Abbreviations ..... **xiii**
1 Introduction **1**
1.1 Background 2
1.2 Translation Initiation 4
1.2.1 Translation-Initiation Regulation 5
1.3 Internal Ribosome Entry Sites (IRESs) 9
1.3.1 IRES Function 12
1.3.2 IRES Structure 14
1.3.3 IRES Regulation 15
1.4 Cell Stress Responses 17
1.4.1 Cancer Cell Stress Responses 19
1.4.2 Translational Regulation of Cancer Stress Responses 21
1.5 DDX3 22
1.5.1 DDX3 in mRNA Translation 23
1.5.2 DDX3 in Cell Stress 26
1.5.3 DDX3 in Cancer 30
1.6 EGFR 31
1.6.1 EGFR in Cancer 33
1.6.2 EGFR Stress Responses 34
1.6.3 EGFR in Triple-Negative Breast Cancer 38
1.7 Antisense Technology 40
1.7.1 Pharmacodynamics of ASOs 41
1.7.2 Pharmacokinetics of ASOs 45
1.7.3 Chemical Modifications 47
1.8 Polymers 53
1.8.1 Cationic Polymers 53
1.8.2 Tumour-Targeting Strategies 56
1.8.3 PBAEs and PAAs 59
1.9 Hypothesis and Objectives 61
2 Materials and Methods **64**

2.1 Cell Culture Methods 65
2.1.1 Cell Lines and Maintenance 65
2.1.2 Transient Transfection and Treatment 65
2.1.3 Dual-Luciferase Assay 67
2.1.4 MTT Assay 68
2.2 Molecular Biology Methods 69
2.2.1 Total RNA Extraction 69
2.2.2 Determination of Purity of Extracted Total RNA 69
2.2.3 cDNA First-Strand Synthesis 69
2.2.4 Polymerase Chain Reaction 70
2.2.5 Agarose Gel Electrophoresis 70
2.2.6 Purification of DNA from Agarose Gel 71
2.2.7 Restriction Enzyme Digestion 71
2.2.8 Gibson Assembly 72
2.2.9 Site-Directed Mutagenesis 73
2.2.10 Total Protein Extraction 75
2.2.11 Total Protein Quantification 75
2.2.12 SDS Polyacrylamide Electrophoresis 76
2.2.13 Western Blotting 76
2.2.14 Immunocytochemistry 77
2.3 Bacterial Methods 78
2.3.1 Competent DH5α *Escherichia coli* Preparation 78
2.3.2 Transformation of Competent DH5α *E. coli* 78
2.3.3 Small-Scale Isolation of Plasmid DNA 79
2.3.4 Large-Scale Isolation of Plasmid DNA 80
2.4 Computational-Biology Methods 81
2.4.1 The Atlas of UTR Regulatory Activity 81
2.4.2 The Nucleotide Basic Local Alignment Search Tool 81
2.4.3 GGGenome 82
2.5 Physicochemical Methods 82
2.5.1 Syntheses of Base Monomers for Michael Addition 82
2.5.2 Purification of Base Monomers for Michael Reaction 83
2.5.3 Synthesis of Poly(β-Amino Ester) Polymers 84
2.5.4 Purification of PBAEs 84
2.5.5 Characterisation of PBAEs 85
2.5.6 Gel Retardation Assay 85
2.5.7 Nanoparticle Characterisation 86
2.6 Statistical Analysis 86
3 Cell Stress and the *EGFR* 5′ UTR 87
3.1 Introduction 88
3.2 Effect of Cell Stress 91

3.2.1 Effect of Genotoxic Stress 91
3.2.2 Effects of ER Stress, Iron Overload, Inflammation and Oxidative Stress 102
3.3 Discussion 106
3.3.1 Effect of Genotoxic Stress 107
3.3.2 Effect of ER Stress 110
4 DDX3 and the *EGFR* 5' UTR 113
4.1 Introduction 114
4.2 Bioinformatic Analysis 116
4.3 Cell-Based Analysis 120
4.4 Discussion 130
4.4.1 DDX3 and the *EGFR* 5' UTR 131
4.4.2 DDX3 and Bicistronic Plasmids 134
5 Targeting *EGFR* using the Antisense Technology 136
5.1 Introduction 137
5.2 Occupancy-Only ASOs 140
5.3 RNase H1-Dependent ASOs 145
5.4 Discussion 155
5.4.1 Occupancy-Only ASOs 157
5.4.2 RNase H1-dependent ASOs 158
6 Hypoxia Responsive Polymers 162
6.1 Introduction 163
6.2 Polymer synthesis 166
6.3 Polymer formulation 179
6.4 Polymer Cell-Based Activity 185
6.5 Discussion 191
6.5.1 Azobenzene Linkage 192
6.5.2 PAA-based Polymers 193
6.5.3 PBAE-based Polymers 194
7 Discussion and Future Work 198
7.1 Outlook 199
7.1.1 Effect of Cell Stress on the Activity of the *EGFR* IRES 199
7.1.2 Effect of DDX3 on the Activity of the *EGFR* 5' UTR 201
7.1.3 Targeting *EGFR* using the Antisense Technology 203
7.1.4 Targeting Hypoxia using Azobenzene-Containing Polymers 205
7.2 Conclusion 207
8 Appendix 209
9 References 219

List of Figures

Figure		Page
1.1	Cap-dependent translation initiation	**5**
1.2	Translational control by uORFs	**9**
1.3	IRES-mediated translation initiation	**10**
1.4	Bicistronic plasmids	**12**
1.5	Functions of DDX3 in translation initiation	**28**
1.6	RNase-H1 Dependent ASOs	**43**
1.7	ASO chemical modifications	**47**
3.1	Map of the pREF plasmid	**90**
3.2	Relative activity of the *EGFR* IRES following treatment with cryptolepine	**94**
3.3	Relative activity of the *EGFR* IRES following treatment with phleomycin	**95**
3.4	Relative activity of the *EGFR* IRES following treatment with etoposide	**97**
3.5	Relative activity of the *EGFR* IRES following exposure to UV-B radiation	**98**
3.6	The effect of genotoxic stress on the expression of γ-H2AX and the metabolic activity of MCF-7 cells	**100**
3.7	The effect of etoposide and UV-B radiation on the metabolic activity of MCF-7 cells	**101**
3.8	The relative activity of the *EGFR* IRES following treatment with thapsigargin and ammonium iron (III) citrate	**104**
3.9	The relative activity of the *EGFR* IRES following treatment with LPS and H_2O_2	**105**
4.1	The *EGFR* 5′ UTR was queried by sequence using AURA	**118**

4.2	The EGFR 5’ UTRs from 58 different species were aligned using Clustal Omega	**119**
4.3	Cloning of DDX3 into the mammalian expression vector pcDNA3.1	**121**
4.4	Characterisation of pDDX3	**122**
4.5	Firefly luciferase activity of plasmids containing the *EGFR* 5’ UTR upon DDX3 overexpression	**123**
4.6	Relative firefly activity of pREF in cells treated with ketorolac salt	**125**
4.7	Luciferase activity profile of the wild-type EGFR 5’ UTR and the mutant version lacking the identified stem-loop structure	**126**
4.8	The effect of DDX3 overexpression on pRF plasmids	**128**
4.9	The effect of overexpressing DDX3 on the protein expression of EGFR	**129**
5.1	Targeting the internal landing site of the 40S ribosomal subunit using 2’-O-methyl ASOs	**139**
5.2	Mutant versions of the *EGFR* 5’ UTR cloned into the bicistronic pRF plasmid	**141**
5.3	Relative firefly luciferase expression of pRF plasmids containing iAUGs within the *EGFR* 5’ UTR sequence	**142**
5.4	Relative firefly luciferase expression of pRF plasmids containing silent mutations within the *EGFR* 5’ UTR sequence	**143**
5.5	Relative firefly luciferase activity of pREF after transfection with modified RNA ASOs	**145**
5.6	Screening DNA ASOs for their anti-EGFR mRNA activity	**147**

5.7	Gapmer ASOs against the *EGFR* 5' UTR cloned into p15E	**149**
5.8	Effects of gapmers on the protein expression of EGFR	**152**
5.9	Effects of the anti-EGFR gapmers on the metabolic activity of breast cancer cells	**153**
5.10	The unassisted uptake of the gapmer ASOs by breast cancer cells	**154**
6.1	Synthesis of azobenzene diacrylamide	**168**
6.2	Characterisation of samples from the PAA-synthesis reaction	**170**
6.3	Effect of iodine catalysis on the PAA-synthesis reaction	**171**
6.4	Synthesis of azobenzene diacrylate	**173**
6.5	Characterisation of the azo-100% polymer	**174**
6.6	PBAE-based polymer synthesis	**176**
6.7	Characterisation of PBAE-based polymers	**178**
6.8	Formulation of polyplexes and mechanism for polymer function	**179**
6.9	ASO loading capacity of nanoparticles	**180**
6.10	Nanoparticles responsiveness to oxygen levels	**182**
6.11	Characterisation of ASO release from the PBAE-based polyplexes	**184**
6.12	Effects of PBAE-based polyplexes targeting *EGFR* on the metabolic activity of MCF-7 cells	**186**
6.13	Characterising the azo-25% polyplexes in cell culture media	**188**
6.14	Dose-response of the azo-25% polyplexes	**189**
6.15	Transfection efficiency of the azo-25% polyplexes	**190**

A.1	The relative activity of the *EGFR* IRES following treatment with lipopolysaccharide	**209**
A.2	The effect of overexpressing DDX3 on the protein expression of EGFR	**212**
A.3	FT-IR and mass spectra of azobenzene diacrylamide	**213**
A.4	Molecular weights of azo-0% polymers	**214**
A.5	Fourier Transform Infrared (FT-IR) spectra of the PABE polymers	**215**
A.6	Size distribution of PBAE polyplexes	**216**
A.7	Effects of PBAE-based polyplexes formulated with PEG-PEI on the metabolic activity of MCF-7 cells	**217**
A.8	Effects of PBAE-based polyplexes formulated with the HIV-1 Tat protein on the metabolic activity of MCF-7 cells	**218**

List of Tables

Table		Page
2.1	Breast cancer cell lines	**65**
2.2	Primers for *DDX3* amplification	**73**
2.3	Primers for Site-Directed Mutagenesis	**74**
5.1	Modified RNA ASOs	**144**
5.2	Unmodified DNA ASOs	**146**
5.3	2'-O-methyl gapmers	**148**
5.4	Analysis of the binding specificity of the gapmer ASOs performed using the GGGenome tool	**150**
6.1	Physicochemical characteristics of PBAE based polymers	**177**
6.2	Characterisation of PBAE-based polyplexes formulated at 30 w/w	**185**
A.1	Accession numbers of sequences included in the *EGFR* 5' UTR sequence-alignment analysis	**210**

List of Schemes

Scheme		Page
1.1	Hypoxia triggered cleavage of azobenzene bond	**58**
1.2	Synthesis of PBAEs and linear PAAs	**60**
6.1	Synthesis of the PAA-based polymer	**169**

List of Abbreviations

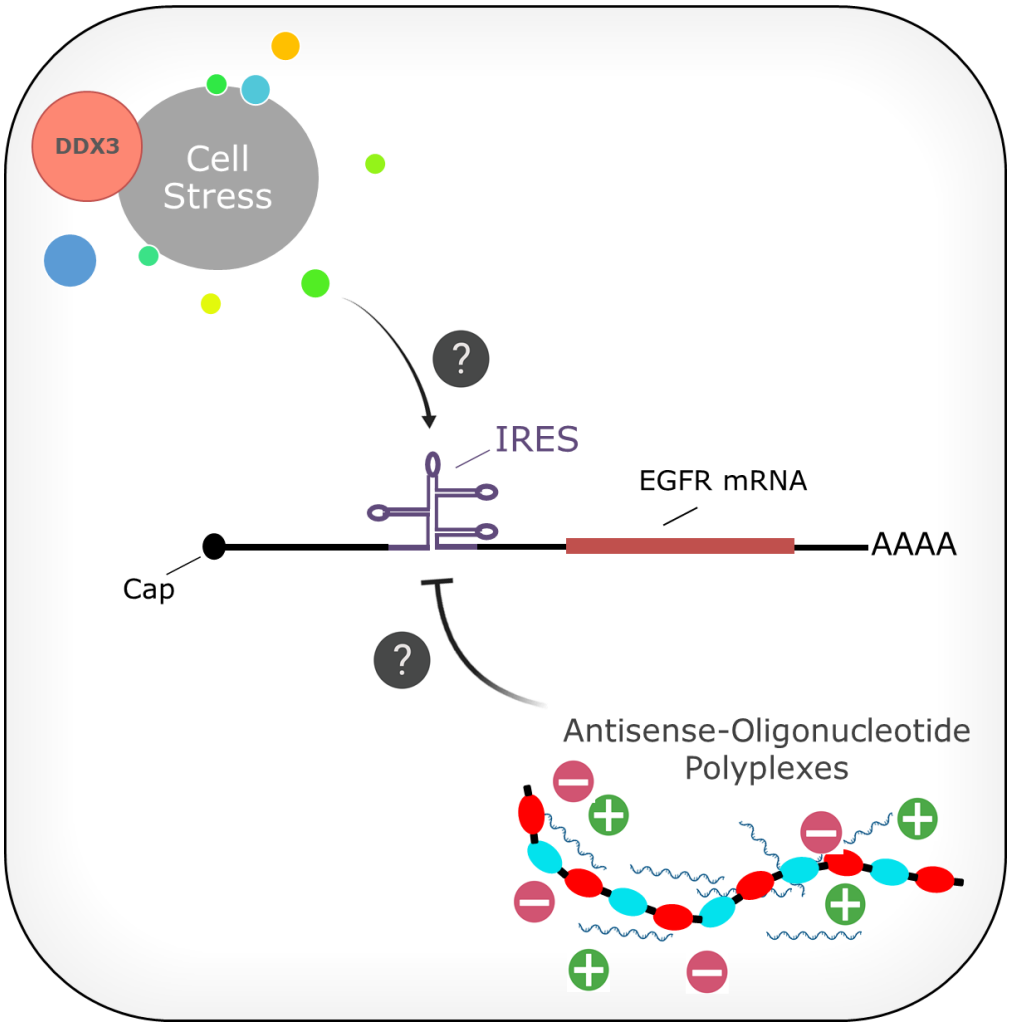
2'MOE	2'-O-methoxyethyl modification
4E-BP	eIF4E-binding protein
APP	Amyloid precursor protein
APS	Ammonium persulfate
ASO	Antisense oligonucleotide
AURA	The Atlas of UTR regulatory activity
BLAST	Basic local alignment search tool
BSA	Bovine serum albumin
CAT1	Cationic amino acid transporter-1
CMV	Cytomegalovirus
CPP	Cell-penetrating peptide
DCM	Dichloromethane
DDR	DNA damage response
DLS	Dynamic light scattering
DMF	Dimethylformamide
DMSO	Dimethyl sulfoxide
DOPE	1,2-dioleoyl-sn-glycero-3-phosphoethanolamine
eIF	Eukaryotic initiation factor
ER	Endoplasmic reticulum
EPR	Enhanced permeability and retention effect
FT-IR	Fourier transform infrared
GPC	Gel permeation chromatography
iAUG	Introduced out-of-frame start codons
IRES	Internal ribosome entry site
ITAF	IRES transacting factor
LB	Luria Bertani
LDL	Low-density lipoprotein cholesterol
m^6A	N^6-methyladenosine
m^7G	7-Methylguanylate group

MOF	Metal-organic framework
MTT	2-(3,5-diphenyltetrazol-2-ium-2-yl)-4,5,-dimethyl-1,3-thiazole bromide
NaAc	Sodium acetate
NHEJ	Non-homologous end-joining
NMR	Nuclear magnetic resonance
PAA	Polyamidoamine
PABP	Poly(A) binding protein
PBAE	Poly(β-amino ester)
PBS	Phosphate buffered saline
PCR	Polymerase chain reaction
PEG	Poly(ethylene glycol)
PEI	Polyethyleneimine
PLL	Poly(l-lysine)
PTBP	Polypyrimidine tract-binding protein
RG4	RNA G-quadruplex
RT	Reverse transcription
SDS	Sodium dodecyl sulphate
TBS-T	Tris-buffered saline with tween
TEA	Triethylamine
TEMED	Tetramethylethylenediamine
TNBC	Triple-negative breast cancer
uORF	Upstream open reading frame
UPR	Unfolded protein response
UTR	Untranslated region
UV	Ultraviolet radiation
w/w	Weight ratio
YB-1	Y-box-binding protein-1
γ-H2AX	Phosphorylated histone H2A variant

Chapter One

1 Introduction

Graphical abstract



1.1 Background

Breast cancer is one of the leading causes of death in women worldwide (Bray et al., 2018). It is a heterogeneous disease that could be classified into distinct entities that exhibit variable histopathological features and differential clinical outcomes (Viale, 2012). Among them is the triple-negative breast cancer (TNBC) which is immunohistochemically identified based on the absence of oestrogen receptors, progesterone receptors, and excess human epidermal growth factor receptor 2 (HER2) protein. It is an aggressive and common form of breast cancer that is associated with greater metastatic potential and poor clinical outcomes. Currently, this breast cancer subtype lacks effective targeted therapeutics, hence chemotherapy remains the standard of care (Garrido-Castro et al., 2019). In this regard, the epidermal growth factor receptor (EGFR) is known to be an important driver of cell proliferation in several cancers including TNBC (Rimawi et al., 2010).

EGFR, also known as ERBB1 and HER1, is a receptor tyrosine kinase with important physiological functions in promoting cellular growth and differentiation (Oda et al., 2005). It is found in nearly 80% of TNBC tumours and its expression is positively correlated with high clinical grade and lymphocytic infiltration (Changavi et al., 2015). The Spriggs lab has identified a posttranscriptional mechanism of regulation involving an internal ribosome entry site (IRES) in the 5’ untranslated region (UTR) of the *EGFR* mRNA which allows the expression of EGFR under hypoxic conditions (Webb et al., 2015). This IRES-mediated expression highlights the importance of EGFR as a survival factor in hypoxia and underscores the impact of EGFR

targeting to tackle hypoxic cancer cells (Hoogsteen et al., 2012, Swinson and O'Byrne, 2006).

Due to increased genetic diversity, cancer cells are known to adapt to cell stress including hypoxia, nutrient deprivation, exposure to immune responses and anticancer drugs (Xie and Zhou, 2017, Xie and Zhou, 2018, Liu et al., 2017). In addition, altered translational control is emerging as an important cellular response that contributes to cancer resilience against both intracellular and extracellular stress associated with tumour growth (El-Naggar and Sorensen, 2018). The expression of several proteins involved in translation initiation is adjusted in response to cellular stress. For instance, the DEAD-box helicase 3 (DDX3) is highly expressed in breast cancer cells in response to hypoxia and its expression was found to directly correlate with aggressiveness and virulence in a panel of breast cancer cell lines (Botlagunta et al., 2011, Botlagunta et al., 2008).

Accordingly, this research project was designed to gain further insight into the translational control of *EGFR* under stress and evaluate targeting the hypoxic expression of *EGFR* in the treatment of breast cancer. The IRES-mediated expression of *EGFR* was assessed in conditions of cell stress associated with malignant growth including DNA damage, endoplasmic reticulum stress, inflammation, iron overload and oxidative stress. The role of DDX3, a DEAD-box RNA helicase, was also investigated in this regard as a potential *trans*-acting factor for modulating the *EGFR* IRES activity. This project was also designed to evaluate targeting the hypoxic expression of the *EGFR* mRNA in breast cancer cells utilising the antisense technology while using linear cationic polymers including poly(beta-amino esters) as delivery systems.

1.2 Translation Initiation

Almost all cellular mRNAs have an N^7-methylguanosine cap added at their 5′ terminus during the maturation process inside the nucleus. This universal cap structure is utilised by the translation machinery to initiate the process of decoding almost all mRNAs into proteins (Walters and Thompson, 2016). In this canonical process, the trimeric eIF4F complex, composed of three eukaryotic initiation factors (eIF4E, eIF4A, and eIF4G) initiates cap-dependent translation by recruiting and loading the 40S ribosomal subunit to the 5′ cap structure (Figure 1.1).

The recognition of the cap structure is mediated specifically by the eIF4E subunit (Sonenberg et al., 1978). The DEAD-box RNA helicase subunit, eIF4A, facilitates the unwinding of RNA secondary structures, clearing the path for the scanning ribosomal subunit (Schmid and Linder, 1991). The scaffolding initiation factor, eIF4G, interacts with eIF3 to land the 40S ribosomal subunit on the mRNA. It also interacts with PABP (poly(A) binding protein) to mediate mRNA circularisation (Jackson et al., 2010, Gingras et al., 1999, Kozak, 2002, Wells et al., 1998).

After binding the cap structure, the 40S ribosomal subunit, recruited as a 43S preinitiation complex starts scanning the mRNA transcript in a 5′ to 3′ direction until the encounter of a start codon. This event results in the rearrangement of the scanning complex into a more closed configuration known as the 48S complex (Eliseev et al., 2018). The process of decoding the mRNA transcript into protein is then initiated by the formation of the elongation-competent 80S ribosome as a result of the recruitment of the 60S ribosomal subunit and the subsequent release of eIF1, eIF2–GDP, eIF3, eIF4A, eIF4B,

eIF4G and eIF5. This event, triggered by the release of eIF5B and eIF1A after GTP hydrolysis, marks the end of the initiation process of mRNA translation (Hinnebusch, 2014, Geissler et al., 2012).

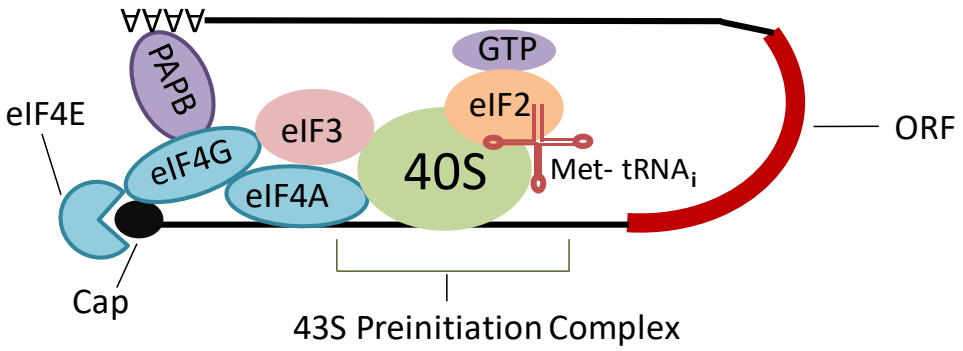


Figure 1.1 Cap-dependent translation initiation. Cellular mRNAs utilise the 5' cap structure to recruit ribosomes during the initiation phase of translation.

1.2.1 Translation-Initiation Regulation

The regulation of gene expression is an intricate biological process that occurs at all stages of gene expression including mRNA translation. The significance of regulating mRNA translation is highlighted by the high energy demands and by the large number of proteins and RNA components involved in protein synthesis. The importance of translation initiation is noticeable in the context of cellular adaptation to abrupt changes in the microenvironment (Sonenberg and Hinnebusch, 2009). Transcriptomic studies have also supported the importance of mRNA translation control by showing a low correlation between cellular mRNA and protein levels (Ghazalpour et al., 2011, Schwanhäusser et al., 2011). While

the regulation of mRNA translation occurs at the different stages of mRNA translation, translation initiation is generally regarded as the rate defining step (Aitken and Lorsch, 2012).

Cap-dependent translation initiation is subjected to tight regulatory mechanisms in response to several cellular conditions including mitosis, apoptosis, hypoxia, DNA damage, nutrient deprivation, heat shock, and viral infection (Walters and Thompson, 2016, Bonneau and Sonenberg, 1987, Holcik et al., 2000, Kaufman, 1999). In principle, the regulation of cap-dependent translation initiation mainly stems from the differential availability of initiation factors to facilitate ribosomal recruitment (Hellen and Sarnow, 2001). For instance, the phosphorylation of the α subunit of eIF2 by four distinct kinases, namely, HRI (also called EIF2AK1), PKR (EIF2AK2), PERK (EIF2AK3) and GCN2 (EIF2AK4) in response to different conditions of cell stress results in the competitive inhibition of eIF2B.

In this regard, GCN2 is activated by the binding of uncharged transfer RNAs under amino acid starvation while HRI and PKR are activated in response to heme deficiency and viral infection, respectively (Dong et al., 2000, Nanduri et al., 2000, Chen, 2007). Under endoplasmic reticulum stress, PERK dissociates from BIP to allow for dimerization and autophosphorylation leading to its activation and eIF2B inhibition (Bertolotti et al., 2000). As the function of eIF2B is to recycle eIF2-bound GDP to GTP, the inhibition of this initiation factor leads to a decline in the eIF2-GTP pool which in turn significantly decreases the translation rate due to decreased formation of the 43S preinitiation complex (Kimball, 1999).

In addition to eIF2α phosphorylation, global protein expression could be also inhibited by reducing the phosphorylation of eIF4E under conditions of cell stress such as mitosis, growth factor deprivation, and hypoxia (Bonneau and Sonenberg, 1987). This process is achieved through inhibiting the phosphorylation of eIF4E-binding protein (4E-BP). When hypo-phosphorylated, 4E-BP competitively inhibits the binding of eIF4G to eIF4E, leading to a reduction in eIF4E phosphorylation and activation by the eIF4G-associated MKNK1 (Gingras et al., 1998, Connolly et al., 2006).

Stable secondary structures located within the 5’ UTR could also influence cap-dependent translation initiation. For example, guanine-rich sequences can assemble into G-quadruplex secondary structures (RG4s), resulting in stable mRNA elements capable of regulating the translation of downstream open reading frames (Schofield et al., 2015). This mechanism of translation regulation is highly dependent on the expression levels of eIF4A (Wolfe et al., 2014, Rubio et al., 2014).

1.2.1.1 Upstream open reading frames

Cap-dependent translation initiation can be also regulated by sequence-specific mechanisms such as the presence of upstream open reading frames (uORFs). The translation of these ORFs located within the 5' UTR of mRNA affects translation from the main open reading frame primarily through controlling the accessibility to preinitiation complex (Figure 1.2). Once translating ribosomes recognise the stop codon of uORF, they terminate translation and undergo ribosomal recycling leading to their complete dissociation from the mRNA (Pöyry et al., 2007). Yet the 40S ribosomal subunits could

remain attached and continue scanning along the 5’ UTR to reinitiate translation at a proximal or distal AUG codon (Grant and Hinnebusch, 1994). However, the efficiency of reinitiation is critically dependent on the uORF length and the intercistronic distance. Long uORFs (~33 codons) promote the dissociation of critical regulatory factors from translating ribosomes that are necessary for reinitiation at the downstream AUG, hence negatively affect reinitiation (Somers et al., 2013, Hinnebusch et al., 2016, Kozak, 2001). On the other hand, short intercistronic regions were found to negatively affect reinitiation by decreasing the time window for scanning 40S ribosomal subunits to acquire factors necessary for start codon recognition and reinitiation (Luukkonen et al., 1995, Kozak, 1987). Therefore, the probability of the retained 40S subunit to reinitiate translation was found to be influenced by the availability of several factors including recycled ternary complex, eIF3 and eIF4F (Gunišová et al., 2017, Skabkin et al., 2013).

Additionally, the extent to which uORFs inhibit cap-initiated translation depends on its sequence. For instance, uORFs can have an occluding effect by stalling translating ribosomes via sequence-specific interactions between the encoded peptide and translating ribosomes (Ivanov et al., 2010). Furthermore, an upstream AUG that has a structured ORF and/or complies with Kozak’s consensus has a higher potential to inhibit cap-dependent translation (Calvo et al., 2009, Luukkonen et al., 1995). Leaky scanning of uORFs might occur when eIF2 is phosphorylated under stress conditions leading to improved translation from the main ORFs (Andreev et al., 2015). This is thought to be due to a reduction in ternary complex assembly which then allows the 40S ribosomal subunits to reach the

upstream AUG without yet acquiring a ternary complex necessary to initiate translation (Hinnebusch et al., 2016).

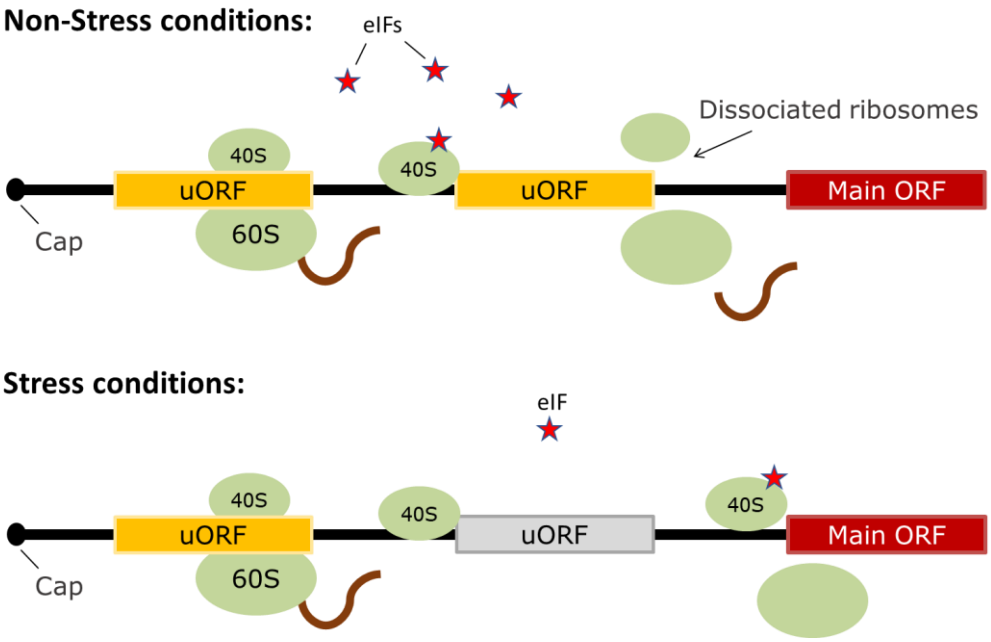


Figure 1.2 Translational control by uORFs. When scanning ribosomes translate the uORF, they could stall during the elongation/termination stage creating a roadblock; or they could dissociate from the mRNA after termination without translating the main ORF due to inefficient reinitiation. Under cell stress, however, there is an increased time required for scanning ribosomes to acquire initiation factors necessary for start codon recognition leading to poor reinitiation at the downstream uORF and hence increased reinitiation capacity at the main ORF.

1.3 Internal Ribosome Entry Sites (IRESs)

Despite the inhibition of cap-dependent translation under various stress conditions, a low proportion of mRNAs encoding proteins, mostly involved in cell survival and stress recovery, still manages to be translated. This subset of mRNAs appears to drive their protein expression via mechanisms that do not rely on the universal cap structure; bypassing the inhibitory

regulation situated on the primary mechanism of translation initiation (Holcik and Sonenberg, 2005).

The nucleotide sequence located before the start codon, namely the 5' UTR, is known to hold regulatory elements that could influence the efficiency and even the mechanism of translation initiation. While the average length in humans is 210.2 nucleotides, the 5' UTRs of mRNAs involved in growth and metabolic pathways are longer and loaded with secondary structures (Pesole et al., 2001, Davuluri et al., 2000). A growing body of literature has been published describing internal ribosome entry sites (IRESs) in highly structured 5' UTRs that have the ability for translation initiation (Figure 1.3). In this process, the 40S ribosomal subunit is recruited to the mRNA independent of either the 5' cap structure or the cap-binding protein, eIF4E (Walters and Thompson, 2016).

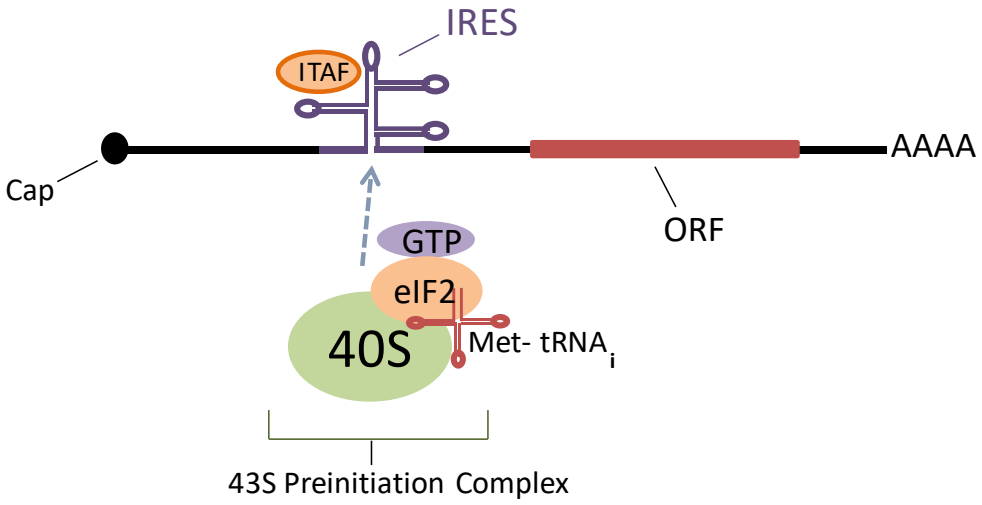


Figure 1.3 IRES-mediated translation initiation. Under conditions of limiting cap-dependent translation, a subset of mRNAs can recruit ribosomes through IRESs independent of the cap structure or the cap-binding protein, eIF4E.

Despite several reports arguing against the existence of cellular IRESs (Kozak, 2005), it is estimated that around 10% of all cellular mRNAs possess IRES activity necessary for their expression in conditions of cell stress where global protein expression is down-regulated (Truitt and Ruggero, 2017, Spriggs et al., 2008). An important reason for this contention is that the identification of these RNA elements depends exclusively on functional assays as IRESs do not share any obvious common secondary structures or consensus sequences (Thompson, 2012, Baird et al., 2006). Hence, these functional assays including bicistronic reporters must be combined with additional experimental measures to preclude the presence of splice variants or cryptic promoter activity (Figure 1.4).

Indeed, it has been shown previously that pGL3 and pGL4 vectors commonly used as backbones for the bicistronic plasmids contain a cryptic promoter within their origin of replication that can generate cryptic transcripts with artefactual reporter activities (Stoneley et al., 1998, Lemp et al., 2012). Thus, including promoter-less constructs is an essential control measure to confirm the absence of cryptic promoter activity in the examined sequences. Northern analysis is also an important measure to reveal cryptic promoter activity and aberrant splicing events that might result in false-positive signals (Terenin et al. 2017).

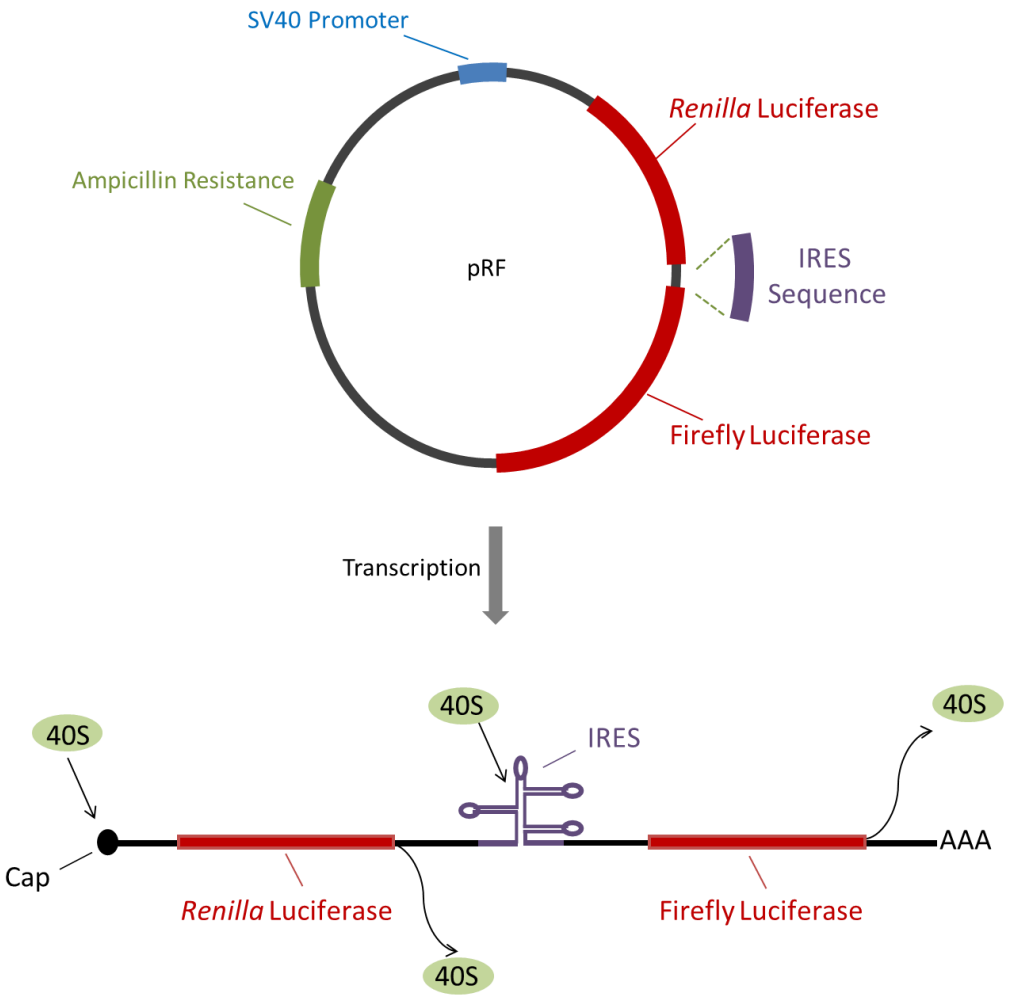


Figure 1.4 Bicistronic plasmids. The expression of *Renilla* and firefly cistrons from a single promoter results in the generation of a bicistronic mRNA in which the expression of the firefly luciferase is controlled by the IRES activity.

1.3.1 IRES Function

IRESs are recently recognised as important modulators in the context of homeostatic gene expression. The identification of structured IRESs in several mRNAs belonging to the homeobox gene family has shed new light on the function of IRESs during embryonic development. In this subset of mRNAs, it has been shown that cap-dependent translation initiation is constitutively depressed under physiological conditions by a newly described

inhibitory element located upstream of the IRES region (Xue et al., 2015). The joint function of this inhibitory element and the IRES is thought to mediate the differential expression of the homeobox mRNAs with regards to time and space during embryonic development.

IRES-mediated translation initiation is also important in several pathological conditions including cancer. Even though the impact of IRES-mediated expression in malignancy is currently understudied, aberrant IRES activity is linked to the pathogenesis of certain types of cancer (Piccirillo et al., 2014, Truitt and Ruggero, 2017). Mutations affecting the *MYC* IRES have been classified as pathogenic drivers in multiple myeloma. It has been demonstrated that several cell lines and bone marrow samples isolated from multiple myeloma patients exhibit high levels of the MYC protein without a concomitant increase in *MYC* mRNA levels. Analysis of the *MYC* mRNA has revealed a single nucleotide polymorphism that exchanges cytosine for uracil in the *MYC* IRES (Paulin et al., 1996). *In vitro* based assays demonstrated that this mutation resulted in a more active *MYC* IRES with increased binding affinity for regulatory proteins (Chappell et al., 2000, Paulin et al., 1998).

In ovarian cancer, a significant reduction in cellular viability was documented after the inhibition of cap-dependent protein expression via targeting PI3K/mTOR signalling. However, resistant cells were found to be overexpressing survival proteins that could be translated through IRES-dependent mechanisms (Muranen et al., 2012). It was also demonstrated that IRES dependent translation contributes to the formation of tumour emboli in advanced breast cancer (Silvera et al., 2009). This switch to cap-independent initiation of translation seems to be facilitated by the direct interaction between eIF4G and

regulatory elements in the 5' UTR (Braunstein et al., 2007, Hayashi et al., 2000). Overall, these studies suggest an important role of IRES mediated translation in the progression and development of highly resistant cancer cells.

1.3.2 IRES Structure

Cellular IRESs generally contain fewer structural elements in comparison to their viral counterparts (Komar and Hatzoglou, 2011). The activity of these eukaryotic IRESs can depend on short sequence motifs for internal initiation. Even though the entire sequence contributes to IRES activity, removal of sequences from either end of the *MYCL* 5' UTR substantially reduces IRES activity (Jopling et al., 2004). It was also demonstrated that the IRES activity of *XIAP* mRNA transcript is highly dependent on a 34-nucleotide polypyrimidine tract (Holcik et al., 1999). A motif in this tract which consists of the sequence $(CCU)_n$ was found even to permit internal initiation in artificial sequences (Mitchell et al., 2005). Furthermore, several studies have demonstrated the presence of complementary rRNA sequences in several viral and cellular 5' UTRs, suggesting direct interactions with ribosomes (Mauro and Edelman, 1997, Deforges et al., 2015, Panek et al., 2013).

In contrast to these studies, however, it has been shown that cellular IRESs including the *MYC* and *MYCN* IRESs are dependent on the entire sequence for full activity (Stoneley et al., 1998). In this regard, the activity of cellular IRESs appears to be derived from complex secondary structures composed of multiple non-contiguous nucleotide sequences which act in concert to obtain correct folding necessary for a functional IRES (Jopling and Willis, 2001). It has been reported that multiple

hairpin loop structures located in the 5' UTR of *BIP, FGF2, and MYC* mRNAs appear to collectively represent functional motifs that display internal initiation activity. Unlike viral IRESs, these functional motifs do not exhibit clear sequence or structural similarities (Le and Maizel Jr, 1997, Le Quesne et al., 2001, Yang and Sarnow, 1997). Thus, further studies are still necessary to characterise these complex structures present in the IRES region of cellular transcripts.

1.3.3 IRES Regulation

1.3.3.1 IRES *in cis* Regulation

Similar to cap-dependent translation, the IRES activity is also subjected to *cis*-regulatory mechanisms involving uORFs and RG4s. In the cationic amino acid transporter-1 (*CAT1*) mRNA, the translation of an uORF embedded in the IRES region transiently stimulates *in cis* the formation of an active IRES conformation. Interestingly, during amino acid deprivation, this activation mechanism is sustained potentially due to ribosomal stalling in the uORF as a result of a decrease in the charged tRNA pool (Fernandez et al., 2005, Tallóczy et al., 2002). Furthermore, the active IRES structure of *CAT1* is predicted to be stabilised by IRES transacting factors only expressed during amino acid deprivation and subsequent eIF2α phosphorylation (Fernandez et al., 2002).

By contrast, uORFs could also influence negative *in cis* type of regulation on IRES activity as in *VEGF* and *FGF9* mRNAs (Chen et al., 2013). It has been shown that translation of a small uORF located within the *VEGF* IRES structure down-regulates the IRES activity possibly through eliciting conformational changes leading to the unfolding of an active IRES structure (Bastide et

al., 2008). On the other hand, it was shown based on an *in vitro* study that the activity of the *VEGF* IRES depends on the presence of an RG4 domain situated within the 5' UTR. The deletion of this domain resulted in impaired internal initiation as it was found to disturb the binding of the 40S ribosomal subunit (Bhattacharyya et al., 2015). Consistent with cap-dependent translation, structural elements present in 5' UTR play an important function in regulating the IRES activity.

1.3.3.2 IRES *in trans* Regulation

The activity of cellular IRESs also depends on the availability of regulatory proteins including translation initiation factors such as eIF3, eIF4G, and eIF4A (Hellen and Sarnow, 2001). These proteins are thought to facilitate IRES-mediated translation initiation through either stabilizing functional IRES structures or inducing conformational changes necessary for ribosomal recruitment (Leppek et al., 2017, Spriggs et al., 2005). The multi-subunit translation initiating factor eIF3 seems to be greatly involved in regulating cap-independent mechanisms of translation initiation. Recent evidence suggests that eIF3 interacts with stem-loop structures in the 5' UTRs of a subset mRNAs to mediate their translation (Lee et al., 2015). Furthermore, the direct interaction between eIF3 and N^6-methyladenosine (m^6A), a frequent chemical modification of RNA, was reported to induce cap-independent translation by direct ribosomal recruitment (Meyer et al., 2015).

The eIF4G analogue, DAP5 (death-associated protein 5), is also considered an important modulator of cap-independent translation, especially in advanced breast cancer. Acting like a scaffold, DAP5 seems to stimulate IRES activity by recruiting

other translation initiation factors including eIF4A (Liberman et al., 2015). It seems that eIF4A recruitment is critical in the context of inducing conformational changes necessary for IRES-mediated translation initiation (Webb et al., 2015, Bordeleau et al., 2006).

In addition to translation initiation factors, IRES transacting factors (ITAFs) are also involved in regulating IRES activity. Stemming from a point mutation affecting the *MYC* IRES, the increased binding of the cellular ITAFs polypyrimidine tract-binding protein (PTBP) and Y-box-binding protein-1 (YBX1) has been found to upregulate *MYC* expression (Cobbold et al., 2010, Chappell et al., 2000). It was also shown that the IRES of *APAF1* interacts sequentially with Unr and PTBP to facilitate ribosomal recruitment by exposing an active ribosomal landing site (Mitchell et al., 2003). Similarly, the *BAG1* IRES interacts with PCBP1 (poly(rC) binding protein 1) and PTBP to induce structural changes and ribosomal recruitment, respectively (Pickering et al., 2004, Pickering et al., 2003). The regulation of IRES activity by the different ITAFs appears to enable the differential translation of certain IRES-containing mRNAs at defined cellular conditions or tissue-specific patterns.

1.4 Cell Stress Responses

Cells respond to stress by a wide range of molecular pathways that are involved in cellular survival and recovery in addition to apoptosis to eliminate damaged cells. Depending on the mode and intensity of stress, specific pro-survival pathways are activated to resolve the noxious stimulus; however, if these pathways are ineffective, then the programmed cell-death pathways are activated to eliminate cells with persistent and

irresolvable stress (Fulda et al., 2010). For instance, the heat shock response is one of the main pro-survival pathways that is activated in response to elevated temperature, oxidative stress and heavy metals (Shamovsky and Nudler, 2008). As these stress conditions result in protein damage and accumulation of unfolded proteins, the heat shock response is activated to alleviate the burden of unfolded proteins in the cell. While global protein synthesis is halted, the expression of the protective heat-shock factors and heat-shock proteins is increased to promote the refolding of misfolded proteins, thus reducing protein aggregation (Morimoto et al., 1996). These adaptive responses create a state known as thermotolerance in which cells are highly resistant to stressful stimuli (Samali et al., 1999).

Furthermore, the unfolded protein response (UPR) is activated in response to the accumulation of unfolded proteins in the endoplasmic reticulum (ER) causing ER stress. This condition is developed when cells are exposed to stressful stimulus affecting the ER environment such as glucose starvation and disturbance of calcium homeostasis (Ron and Walter, 2007). ER stress then results in the activation of ER-resident proteins including IRE1 (inositol-requiring enzyme 1) and PERK. Both are type-I-transmembrane protein kinases which are activated via dimerization and autophosphorylation in response to ER stress. While activated IRE1 is involved in upregulating the expression of UPR target genes, activated PERK results in global translation inhibition via eIF2α phosphorylation, hence improving the ER balance between the protein loading and folding capacities (Calfon et al., 2002, Harding et al., 1999).

In addition to protein damage, exposure to environmental or therapeutic genotoxic agents can cause DNA lesions that

activate specific DNA damage responses (Christmann et al., 2003). Single-strand lesions can be recognised and repaired by base excision repair, nucleotide excision repair, and DNA mismatch repair depending on the type of DNA lesion. Nucleotide excision repair is particularly important in resolving the bulky DNA adducts induced by UV radiation (Staresincic et al., 2009). Single strand breaks induced by chemical attacks or cellular nucleases activate a specialised repair pathway that is considered a sub-pathway of base excision repair in which PARP1 (poly(ADP-ribose) polymerase 1) and XRCC1 (X-ray repair cross complementing 1) are key regulators (Abbotts and Wilson III, 2017). On the other hand, the induction of double-strand breaks by many anticancer drugs including topoisomerase inhibitors primarily induces the activation of non-homologous end joining in mammalian cells (Valerie and Povirk, 2003). If the damage is unresolved, cell death is then triggered through various stress-inducible molecules, including p53, MAPK8 (mitogen-activated protein kinase 8) and NF-κB (nuclear factor kappa B) (Weston and Davis, 2007, Perkins and Gilmore, 2006).

1.4.1 Cancer Cell Stress Responses

Oncogenic mutations leading to reduced apoptotic or senescence potential result in the accumulation of genetic mutations, facilitating the emergence of virulent mutants resistant to immune destruction, cytotoxic and targeted therapies (Lowe et al., 2004). Mutations that either negatively affect pro-apoptotic regulators including caspase-8 and cell death receptors such as CD95 and TRAILR-1; or positively affect the expression of pro-survival factors including BCL2 (B-cell lymphoma 2), XIAP (X-linked inhibitor of apoptosis protein) and

survivin are frequently detected in cancer (Fulda et al., 1998, Shin et al., 2001, Hunter et al., 2007, Fulda, 2009, Adams and Cory, 2007). In addition, almost all solid tumours eventually will outgrow their local blood supply as the cancer progresses and develops creating stressful conditions in focal and then diffuse areas within the tumour microenvironment of low oxygen tensions, nutrient deprivation, and pH changes. In order to survive in this competitive microenvironment, stress-resilient clones must activate a range of cellular response pathways geared toward stress adaptation and recovery (Quaranta et al., 2008). Indeed, pathological stress response including resistance to therapy is a hallmark of cancer.

Under therapeutic pressure, tumour heterogeneity due to increased genomic instability allows the selection of cancer clones with resistance mutations to dominate the tumour population leading to disease relapse after temporary remission (Alexandrov et al., 2013). Resistance to therapy can also develop in cancer cells via non-genetic responses including feedback activation of upstream regulators (Sun and Bernards, 2014). For instance, the reactivation of the upstream EGFR was found to counteract the targeting of BRAF (B-Raf proto-oncogene, serine/threonine kinase) in colon cancer. In this adaptive response, inhibiting BRAF inactivates MAPK1 which then decreases activation of the phosphatase CDC25C that negatively regulates EGFR (Corcoran et al., 2012). On the other hand, melanomas are sensitive to BRAF targeting which could be attributed to their low levels of EGFR expression (Prahallad et al., 2012). Aberrant translation control also allows cancer cells to grow and survive under cell stress (Sriram et al., 2018).

1.4.2 Translational Regulation of Cancer Stress Responses

Translational upregulation of mRNAs involved in stress response is emerging as an important factor contributing to the increased capacity of cancer cells for stress adaptation (El-Naggar and Sorensen, 2018). Under conditions of amino acid deprivation and inflammation, translational reprogramming mediated by eIF2B inhibition via eIF2α phosphorylation was found to correlate with phenotypic plasticity and resistance to T-cell-mediated therapies in melanoma (Falletta et al., 2017). Inhibition of eIF2B in response to glutamine limitation and TNFα was found to decrease overall translation while selectively enhancing translation of ATF4 (activating transcription factor 4) which is involved in amino acid transport and coping with oxidative stress (Falletta et al., 2017, Piskounova et al., 2015). Furthermore, the cap-independent expression of the molecular chaperone HSPA4 (heat shock protein family A (Hsp70) member 4), mediated by a direct interaction between eIF3 and the m^6A mRNA modification, facilitates adaptation under stress conditions (Meyer et al., 2015). Interestingly, targeting METTL3 (methyltransferase like 3) which catalyses the formation of the m^6A modifications inhibited tumour growth and prolonged survival in mice bearing glioblastoma multiforme tumours, underscoring the promising utility of translation-initiation regulators as therapeutic targets (Visvanathan et al., 2018).

RNA-binding proteins including the Y-box binding protein 1 (YBX1) were also implicated in malignant transformation in a wide range of human cancers including breast cancer (Evdokimova et al., 2009). While repressing cap-dependent translation, it was found that YBX1 promotes metastatic spread in breast cancer by activating the IRES-mediated mRNA

translation of SNAI1 which is a transcription factor involved in epithelial-mesenchymal transition (Evdokimova et al., 2009, Evdokimova et al., 2006). Under hypoxia, YBX1 also promotes the translational upregulation of the hypoxia-inducible factor 1 subunit α (HIF1α), and depleting YBX1 *in vivo* was found to significantly reduce sarcoma metastasis, which was rescued by ectopic HIF1α expression (El-Naggar et al., 2015). In addition to YBX1, other regulators of translation initiation under cell stress have been described including DDX3.

1.5 DDX3

Also known as DDX3X, DBX, HLP2, DDX14, DEAD/H (Asp-Glu-Ala-Asp/His) box polypeptide 3, CAP-Rf, DEAD/H box-3 and helicase like protein 2; this protein and its yeast orthologue Ded1p are ATP-dependent helicases involved in regulating different stages of gene expression including mRNA translation (Sharma and Jankowsky, 2014). In contrast to the ubiquitous expression of DDX3, the expression of the highly-homologous DDX3Y located on the Y chromosome is restricted only to the male germ cells (Ditton et al., 2004).

As described earlier, once the cap structure is recognised and bound by the 43S preinitiation complex, the scanning along the 5’ UTR is facilitated by the helicase activity of the eIF4A subunit (Parsyan et al., 2011). The requirement for this canonical DEAD-box RNA helicase is directly correlated to the amount of complex secondary structures situated between the cap structure and the start codon (Svitkin et al., 2001, Pestova and Kolupaeva, 2002). It is known that mRNA transcripts having highly structured 5’ UTRs show considerable resistance for the helicase activity of eIF4A (Pickering and Willis, 2005, Kozak,

1991). For such mRNAs, various helicases including DDX3, DHX9 (DExH-box helicase 9) and DHX29 have been identified to assist in the ribosomal scanning process (Pisareva et al., 2008, Soto-Rifo et al., 2012, Parsyan et al., 2011, Hartman et al., 2006, Lai et al., 2008). While they appear mainly to assist in the unwinding of mRNA secondary structures within the 5' UTR, some of these helicases such as DHX29 have a characteristic ability in facilitating the scanning of the 40S ribosomal subunit over existing RNA secondary structures (Parsyan et al., 2009, Abaeva et al., 2011).

They also appear to have unique recruitment mechanisms to their target mRNAs. While the canonical RNA helicase eIF4A is recruited as part of the eIF4F complex, other helicases such as DHX9 appear to have a unique ability to recognise and bind post-transcriptional elements present in the 5' UTRs of specific mRNAs (Imataka and Sonenberg, 1997, Pisareva et al., 2008, Hartman et al., 2006, Hilliker et al., 2011). In this regard, DDX3 could be recruited universally as part of the 43S preinitiation complex to mRNAs via its interactions with the 40S subunit and eIF3 (Geissler et al., 2012). In addition, it seems that DDX3 could also bind stem-loop structures proximal to the universal cap end, facilitating its direct recruitment to a specific set of transcripts (Soto-Rifo et al., 2012).

1.5.1 DDX3 in mRNA Translation

DDX3 is known to both positively and negatively influence global mRNA translation (Shih et al., 2008, Geissler et al., 2012). Furthermore, it is notable that DDX3 supports the preferential translation of selected transcripts (Soto-Rifo et al., 2012). This reported multifaceted-function of DDX3 in mRNA

translation is thought to be mediated via its unique ability to interact directly with mRNAs and several translation initiation factors including eIF3, eIF4E, PABP, and eIF4G (Soto-Rifo et al., 2012, Lee et al., 2008, Geissler et al., 2012, Shih et al., 2008, Lai et al., 2008) The expression levels of DDX3 also appear to control its effects on mRNA metabolism (Hilliker et al., 2011). Steady-state levels of DDX3 expression seem to promote mRNA translation, while high levels of DDX3 expression appear to globally inhibit translation potentially as a stress response mechanism (Figure 1.5).

Mediated via its catalytic core domain, DDX3 partly affects RNA translation in an ATP-dependent manner through remodelling RNA structures and altering RNA-protein interactions (Linder and Jankowsky, 2011, Cordin et al., 2006). It was shown that inhibiting the function of its yeast orthologue Ded1p caused both ribosomal stalling and activation of near-cognate translation initiation codons proximal to secondary mRNA structures (Guenther et al., 2018). This observation might provide mechanistic insight into the main function of DDX3 in translation initiation which revolves around facilitating the ribosomal scanning of structured 5’ UTRs.

It has been shown that DDX3 could be also recruited directly to selected transcripts harbouring secondary structures proximal to their 5’ capped terminus (Soto-Rifo et al., 2012, Oh et al., 2016, Lai et al., 2008). By resolving these RNA structures, DDX3 seems to facilitate the anchoring of the trimeric complex to the cap structure to initiate translation of these selected transcripts. It is known that DDX3 could facilitate the mRNA binding of eIF4F through its double interaction with eIF4G and PABP (Soto-Rifo et al., 2012, Lai et al., 2008). Indeed, displacing eIF4G from the trimeric complex was found to disrupt

the preferential translation of these target transcripts, indicating a functional partnership between DDX3 and eIF4G (Adjibade et al., 2017). Overall, this direct recruitment of DDX3 appears to be important in resolving stable structures located near the 5’ end known to impair the landing of the trimeric complex eIF4F (Parkin et al., 1988, Kozak, 1989, Sagliocco et al., 1993, Pestova and Kolupaeva, 2002, Babendure et al., 2006).

Under conditions of cell stress, it is known that eIF4F concentrates in stress granules, reducing its concentration in the diffuse cytoplasm for initiating translation (Adjibade et al., 2015). Even though the mechanism is still unclear, it is possible that under cell stress, the initial binding of DDX3 to these selected transcripts facilitates the recruitment of the limiting eIF4F to initiate translation (Adjibade et al., 2017). DDX3 is also involved in other mechanisms for regulating translation initiation (Shih et al., 2008, Lai et al., 2008). DDX3 plays a defined role in facilitating the assembly of the elongation competent 80S ribosome (Soto-Rifo et al., 2012, Soto-Rifo and Ohlmann, 2013, Shih et al., 2012, Lee et al., 2008). Together with eIF3, DDX3 appears to assist in the remodelling process of the 48S preinitiation complex required for the efficient assembly of the 80S ribosome. This helicase-independent role of DDX3 was found to globally enhance translation in a sequence nonspecific manner (Geissler et al., 2012).

While the role of DDX3 in promoting translation is still not fully characterised, DDX3 has an established role in repressing translation. DDX3 is known to influence a negative type of regulation on cap-dependent translation under conditions of cell stress. It was found that overexpressing DDX3 results in the sequestration of the cap-binding protein eIF4E leading to global

inhibition of cap-dependent translation (Shih et al., 2008). This inhibitory interaction with eIF4E is mediated via a binding motif in the N-terminal tail of DDX3 (Shih et al., 2008). As a result, the availability of other translation initiation factors for eIF4E-independent translation mechanisms such as the internal recruitment of ribosomes is increased (Shih et al., 2008, Lai et al., 2008). Considering how the translation of stress-induced transcripts is largely dependent on the activity of different transacting factors, DDX3 may be also involved in the translation control of these highly structured transcripts especially during stress (Shih and Lee, 2014).

1.5.2 DDX3 in Cell Stress

Perhaps these different regulatory mechanisms of DDX3 in mRNA metabolism are optimised to regulate translation in both homeostatic and stress conditions (Shih and Lee, 2014). Indeed, it is known that DDX3 plays an important role in regulating the cellular response to various conditions of environmental stress. Under such conditions, DDX3 appears to inhibit cap-dependent translation via its direct interaction with the eIF4E subunit. As stated earlier, this effect is thought to stimulate cap-independent translation which could result in the preferential expression of stress-induced mRNAs containing IRES elements in their 5’ UTRs, yet this remains to be established by experimental evidence (Shih and Lee, 2014).

In addition, the induction of several stress conditions including UV irradiation, oxidative and endoplasmic stress was found to concentrate DDX3 inside the stress granules, indicating a possible regulatory role of DDX3 in their formation. Stress granules are known to sequester translation complexes and

coding RNAs, mainly halting translation in response to endogenous and exogenous stress (Anderson and Kedersha, 2009, Buchan and Parker, 2009).

Depleting DDX3 was found to result in defective stress granule formation and increased cell death while DDX3 supplementation restored these impairments (Hilliker et al., 2011). DDX3 appears also to be highly associated with eIF4E inside the stress granules, and a mutant DDX3 lacking the eIF4E-binding ability was found to be ineffective in facilitating their formation (Shih et al., 2012). In a coordinative role with eIF4E, DDX3 appears to facilitate the formation of the stress granules leading to global translation inhibition (Shih et al., 2012, Raman et al., 2016).

This multifunctional protein has been also heavily linked in mediating innate immune pathways against viral infection (Ariumi, 2014). In addition to the established antiviral role of DDX3 at the gene transcription level, it was also found that DDX3 could stimulate the mRNA translation of antiviral proteins including PRKRA (protein activator of interferon induced protein kinase EIF2AK2) (Lai et al., 2016, Schroder et al., 2008). Upregulating the expression of PRKRA activates the pattern recognition receptor RIG-I (retinoic acid-inducible gene I) to mediated viral detection and globally inhibits translation in infected cells (Schroder et al., 2008, Patel et al., 2000). Indeed, several viruses including the hepatitis B virus (HBV) are known to target DDX3 for immune evasion, highlighting the importance of this protein in this context (Oshiumi et al., 2010, Wang and Ryu, 2010).

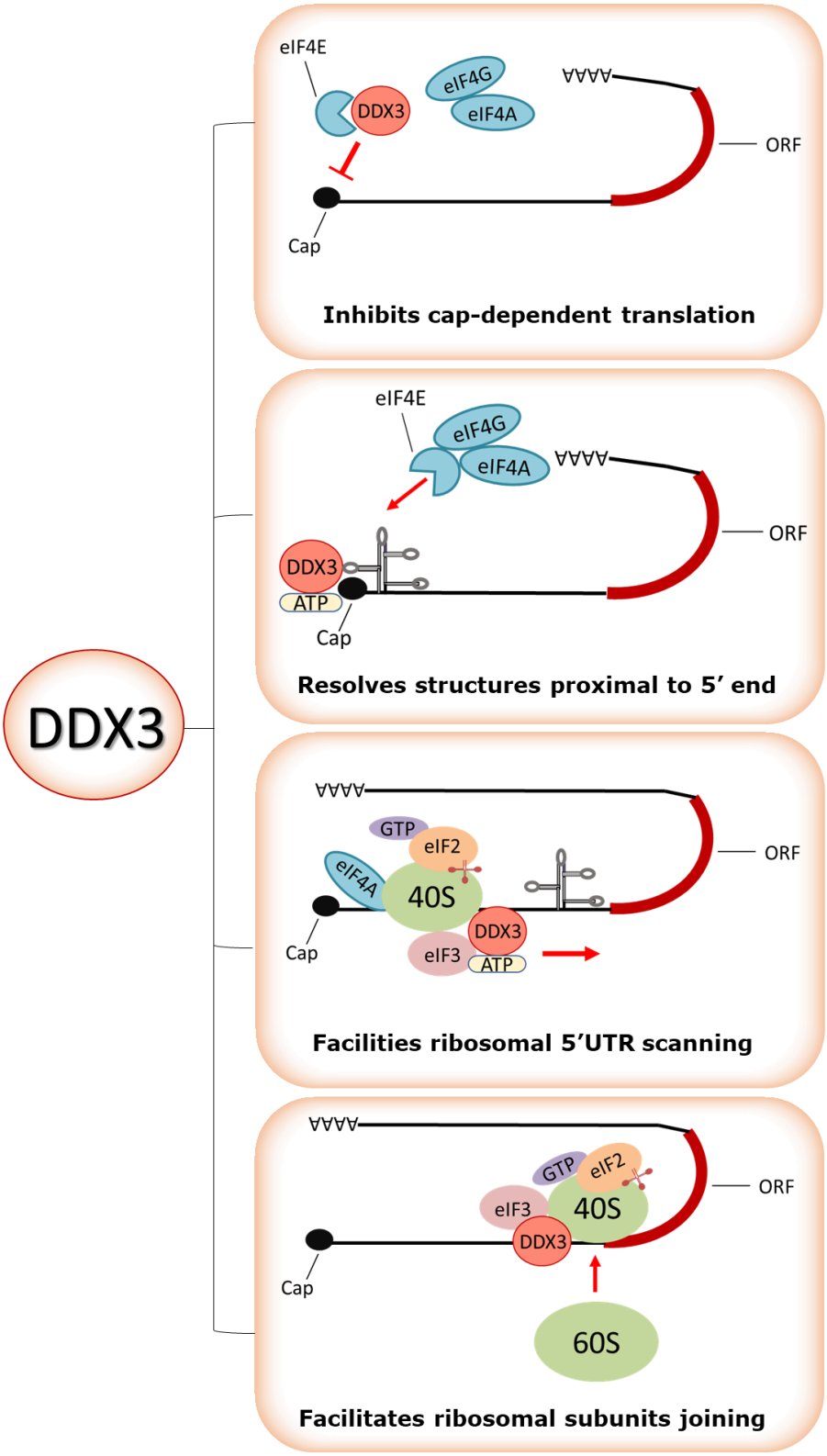


Figure 1.5 Functions of DDX3 in translation initiation. Schematic illustration demonstrating the described functions of DDX3 in mRNA translation initiation.

It was shown that HBV polymerase blocks interferon signalling by disturbing the interaction between DDX3 and IKKε (Schroder et al., 2008). Some viruses such as HCV and HIV-1 have even managed to utilise DDX3 to support their replication (Yedavalli et al., 2004, Ariumi et al., 2007). In addition to its established antiviral functions, DDX3 also appears to mediate immune responses against bacterial infection. It was reported that DDX3 is involved in regulating phagocytosis and proinflammatory cytokine production in macrophages (Ku et al., 2019). This response is thought to be partly mediated by the ability of DDX3 to control the mRNA translation of STAT1 (signal transducer and activator of transcription 1), GNB2 (G protein subunit beta 2), and RAC1 (Rac family small GTPase 1) (Ku et al., 2019).

DDX3 is also involved in cell cycle regulation (Li et al., 2014, Lai et al., 2010). Either inhibiting or depleting DDX3 was found to hinder cellular proliferation; specifically affecting the transition from G1 to S phase (Fukumura et al., 2003, Bol et al., 2015, Lee et al., 2008). DDX3 appears to be involved in cell cycle control via regulating the translation of cyclin E1, which has an established role in the context of the G_1/S phase transition (Lai et al., 2010). Furthermore, DDX3 was found to regulate the activity of p53 at three different levels. In addition to controlling its transcription and localisation, knocking down DDX3 was found also to inhibit p53 translation (Chen et al., 2017). Thus, these studies indicate a critical role of DDX3 in regulating mRNA translation during cell division.

DDX3 is also involved in regulating cellular adhesion and mobility. It has been shown that DDX3 modulates the expression of *RAC1* mRNA, which is a pleiotropic regulator known to be involved in cellular motility and cell-to-cell adhesion via the actin network (Gungabissoon and Bamburg,

2003, Chen et al., 2015, Lai et al., 2010). It was also shown that the translation of PKACA (protein kinase cAMP-activated catalytic subunit alpha) is controlled by DDX3, and as a part of a larger protein complex, PKACA activates the RAC1 protein (Goto et al., 2011). The importance of DDX3 in controlling the PKACA-RAC1 signalling is highlighted by the impaired dendritic outgrowth of hippocampal neurons upon depleting DDX3 or inhibiting its activity in neonatal mice (Chen et al., 2016).

1.5.3 DDX3 in Cancer

Even though it has been assigned as a tumour suppressor and an oncogene, a growing body of evidence has demonstrated a significant association between DDX3 overexpression and poor prognosis in cancer patients (Botlagunta et al., 2008, Wu et al., 2011, Chao et al., 2006). DDX3 has been linked with the development of malignant tumours potentially as an implication of its function in regulating cell cycle, adhesion and mobility (Miao et al., 2013, Heerma van Voss et al., 2015).

Apparent expression of DDX3 has been found in several types of cancer including breast cancer (Botlagunta et al., 2008, Epling et al., 2015, Chang et al., 2006, Huang et al., 2004, Kandoth et al., 2013). In a HIF-1α dependent fashion, DDX3 has been implicated in the development of the hypoxic response in breast cancer cells (Bol et al., 2013). In addition, certain cancer-associated mutations of DDX3 were shown to drive the hyper assembly of stress granules which subsequently affects mRNA translation (Valentin-Vega et al., 2016). Considering the high recurrence of these mutations, this abnormal translation control could be an important survival measure for cancer cells against the stressful tumour microenvironment (Ruggero,

2013, Oh et al., 2016) Indeed, targeting DDX3 by different small molecules was found to reduce the viability and invasiveness of breast cancer cells (Kondaskar et al., 2013, Xie et al., 2015).

As stated earlier, it was found that DDX3 is a translational regulator of several cancer-related genes including *RAC1* (Ku et al., 2019). By activating *RAC1* translation, DDX3 plays an important role in promoting cancer cell metastasis (Chen et al., 2015). DDX3 is also known to influence the transcription of oncogenes such as *SNAI1* and *KRAS*, leading to increased cell motility and invasiveness (Sun et al., 2011, Botlagunta et al., 2008, Wu et al., 2016). In cells expressing non-functional or mutant p53, DDX3 expression was found to associate with reduced caspase activation and subsequently reduced apoptotic potential (Sun et al., 2013). DDX3 could also form an antiapoptotic signalling complex with GSK3 (glycogen synthase kinase 3) and BIRC2 (baculoviral IAP repeat-containing 2) that has a characterised function in maintaining cell death receptors in quiescence (Sun et al., 2008). These findings suggest that DDX3 is heavily involved in regulating cancer progression and metastasis.

1.6 EGFR

The epidermal growth factor receptor (EGFR/ERBB1/HER1) is a 170-kDa plasma-membrane glycoprotein characterised by tyrosine kinase activity. It is composed of four extracellular domains, a transmembrane domain, and three cytoplasmic domains, namely the juxtamembrane domain, the tyrosine kinase domain and the carboxyl-terminal domain. The phosphorylation of specific tyrosine residues in the carboxyl-

terminal domain correlates with functional activation of EGFR (Schlessinger, 2002).

EGFR is activated by the binding of several ligands including epithelial growth factor, transforming growth factor-α, epigen, epiregulin, betacellulin, amphiregulin, and heparin-binding EGF-like growth factor (Harris et al., 2003). These described EGFR ligands appear to induce distinct downstream signalling pathways which could be due to the differential ability of each ligand to stabilise an active conformation of EGFR (Wilson et al., 2012, Freed et al., 2017). Binding of these ligands to the extracellular domains induces a series of conformational changes leading to asymmetric receptor homodimerization and allosteric activation of the tyrosine kinase domain. The activated tyrosine kinase then stimulates *in trans* the autophosphorylation of specific tyrosine residues located in the carboxyl-terminal tail. Ligand activation could also result in the formation of heterodimers with other members of the ERBB family especially ERBB2, resulting mainly in stronger and more diverse signals (Lemmon et al., 2014).

After that, several regulatory molecules interact with the phosphorylated tyrosine residues, resulting in the activation of downstream signalling pathways including AKT and MAPK pathways that in turn activate transcription factors important in the context of cellular proliferation, differentiation, migration and survival (Zhu et al., 2015). In addition to ligand activation, a growing body of evidence indicates that the activity of EGFR can be upregulated by non-canonical stimuli including receptor transactivation and ultraviolet radiation (Castagliuolo et al., 2000, Daub et al., 1996). Once activated, EGFR is subjected to ubiquitination by the ubiquitin E3 ligase-Grb2 adaptor complex (Waterman et al., 2002). Ligand-bound EGFR is then

internalised into early endosomes which then can be recycled back to the cell surface or processed further into late endosomes and lysosomes resulting in the termination of the EGFR activity (Tomas et al., 2014). Nuclear translocation of EGFR could also occur following endocytosis (Brand et al., 2013). This nuclear fraction of EGFR was shown to influence gene transcription, DNA repair and drug resistance (Han and Lo, 2012). In the nucleus, EGFR acts mainly as a transcription factor, regulating the expression of several genes including the gene for the breast cancer resistance protein (Huang et al., 2011, Lo et al., 2005). Furthermore, it was demonstrated that EGFR nuclear translocation stimulates the DNA damage response following radiotherapy (Dittmann et al., 2005). The impact of nuclear translocation in cancer is reflected by the inverse correlation between the nuclear fraction of EGFR and the overall survival of breast cancer patients (Lo et al., 2005).

1.6.1 EGFR in Cancer

EGFR is well characterised for playing a key role in the development of several types of cancer including breast cancer. There is also a growing body of literature that recognises the importance of EGFR in facilitating cancer cell adaptation to the tumour microenvironment (Nijkamp et al., 2013). Indeed, EGFR is an established target for several cancer therapeutic agents. These agents can be grouped into two classes depending on their mechanism of action. Monoclonal antibodies such as cetuximab and trastuzumab have been developed to target the extracellular domains of EGFR, while small molecule inhibitors including gefitinib, erlotinib, and lapatinib have been developed to target the tyrosine kinase domain (Baselga and Arteaga, 2005).

The overexpression of EGFR in cancer can stem from genetic abnormalities including *EGFR* amplification and mutated EGFR with constant basal activity (Normanno et al., 2006, Bache et al., 2004). Yet these genetic abnormalities mostly occur in certain types of cancer such as non-small-cell lung cancer or glioblastoma multiforme (Halatsch et al., 2006, Sharma et al., 2007). Furthermore, cancer tumours overexpressing the wild-type EGFR appear to be even more resistant to small molecule inhibitors (Mok et al., 2009). It has been also shown that EGFR overexpression is correlated with poor response to hormonal therapy (Massarweh et al., 2006). Indeed, the overexpression of EGFR in breast cancer is often regarded as a prognostic sign for virulence, drug resistance, and advanced tumour stages (Arteaga, 2002, Rimawi et al., 2010).

1.6.2 EGFR Stress Responses

Hypoxia

Growing cancer lesions tend to have hypoxic regions located in the inner part of the tumour where there is a shortage of blood supply. In breast cancer carcinogenesis, the development of these hypoxic regions is a critical outcome that signals the development of a more aggressive phenotype characterised by increased proliferation, invasiveness, resistance to therapy and poorer survival (Bos et al., 2005, Greijer et al., 2005, Brown and Wilson, 2004). To facilitate tumour cells adaptation to low oxygen levels, the activity of several regulatory proteins is induced including the hypoxia-inducible factors (HIFs) and EGFR. In this regard, it was shown that EGFR activation leads to the induction of HIF1α levels (Lee et al., 2009). On the other hand, EGFR protein levels could be induced following the

activation of HIF2 in the absence of genetic mutations or even increased *EGFR* mRNA levels (Franovic et al., 2007).

As addressed earlier, the activity of the cap-binding protein eIF4E is reduced under hypoxic conditions. Thus, to initiate EGFR protein expression under hypoxia, it seems that HIF2 forms a trimeric complex with the RNA binding proteins RBM4 (RNA binding motif protein 4) and eIF4E2 (an analogue of eIF4E) that can initiate translation of the *EGFR* mRNA independently of the canonical initiation factor eIF4E (Uniacke et al., 2012). In addition, the 5' UTR of *EGFR* contains an IRES element that is capable of maintaining the expression of EGFR under hypoxic conditions (Webb et al., 2015). Therefore, the hypoxic expression of EGFR, mediated mainly by translational control, appears to be an important cellular mechanism for adaptation to low oxygen levels in the tumour microenvironment.

Oxidative Stress and Inflammation

Oxidative stress and inflammation are cancer-associated conditions that have been linked to cancer pathogenesis via inducing DNA mutations and genomic instability (Bartsch and Nair, 2006). Inflammation is a complex biological process that involves several immune cells and inflammatory mediators including EGFR. It was shown that the Fas ligand (FASLG), a member of the tumour necrosis factor family, stimulates the release of the EGFR ligand amphiregulin. Consequently, ligand-activated EGFR appears to facilitate the expression of a subset of cytokines involved in epidermal inflammation (Farley et al., 2008, Koff et al., 2008). EGFR is also involved in the amplification of the inflammatory response mediated via COX2

in inflammatory breast cancer (Wang et al., 2017). In addition to inflammation, EGFR is involved in mediating the cellular response to oxidative stress. Oxidative stress is a state of imbalance between the generation of reactive oxygen species and their elimination mechanisms in the cell. Evidence suggests that oxidative stress could affect the activity and cellular trafficking of EGFR, as it was demonstrated that hydrogen peroxide induces the activity of EGFR independent of ligand binding and results in abnormal dimerization and phosphorylation of EGFR which in turn impairs trafficking and subsequent degradation (Filosto et al., 2011, Ravid et al., 2002).

Endoplasmic Reticulum Stress and Iron Overload

Oxidative stress can lead to endoplasmic reticulum (ER) stress which is another stress condition associated with malignancy (Plaisance et al., 2016). The endoplasmic reticulum is a vital cellular organelle responsible mainly for protein folding and trafficking. It has been reported that inducing ER stress by tunicamycin resulted in aberrant EGFR expression and activity mainly through inhibiting EGFR N-glycosylation (Ling et al., 2009). However, during vascular remodelling, EGFR activation seems to be dependent on ER stress (Takayanagi et al., 2015). These conflicting findings highlight the complex dynamics between the endoplasmic reticulum and EGFR.

Cancer patients often receive frequent blood transfusions over their treatment course, resulting in systemic iron overload (de Ville de Goyet et al., 2013). In addition, breast cancer cells appear to have high intracellular levels of iron which is thought to be mediated through decreasing the expression of the iron

transporter ferroportin (Pinnix et al., 2010). In this regard, EGFR is known to be involved in the regulation of iron metabolism to support cancer development and progression, yet it is still unclear whether the translation control of EGFR could be affected by intracellular iron levels (Wang et al., 2016).

Genotoxic Stress

Perhaps DNA damage is one of the most well-known stress conditions associated with cancer growth. The integrity of DNA could be affected by various agents or conditions including ultraviolet and ionising radiation, cigarette smoking, industrial chemicals, and various chemotherapeutic agents. The induction of this DNA damage subsequently results in the activation of the DNA damage response (DDR) (Lord and Ashworth, 2012). This response encompasses a network of molecular pathways involved in minimising the impact of DNA damage on the integrity of DNA molecules. The importance of these pathways in human physiology in highlighted by a broad spectrum of disorders including breast cancer which are characterised by mutations in genes involved in the DDR such as *BRCA1* and *BRCA2* (Farmer et al., 2005). Indeed, these DDR defects are widely exploited in conventional and targeted cancer treatments (Lord and Ashworth, 2012). For instance, radiation therapy is an important therapeutic option in breast cancer, inducing DNA double-strand breaks that are particularly lethal to cancer cells (Group, 2006). However, following radiotherapy many patients eventually develop adaptive resistance, resulting in tumour recurrence and metastasis (Li et al., 2011). Interestingly, the upregulation of EGFR activity has been linked to the development of resistance to radiotherapy and chemotherapy in breast cancer (Golding et al., 2009, Liccardi et

al., 2011, Hsu et al., 2009, Dent et al., 1999, Reardon et al., 1999). EGFR appears to be involved in the development of resistance to radiotherapy by enhancing DDR directed against the DNA lesions induced by radiation. It has been demonstrated that EGFR nuclear translocation mediates non-homologous end joining (NHEJ) via the interaction with the catalytic subunit of DNA-protein kinase (Liccardi et al., 2011). It has been also shown that blocking EGFR with cetuximab decreases NHEJ activity while improving overall survival after radiation exposure (Kriegs et al., 2010, Bossi and Platini, 2017). Thus, the activation of EGFR seems to play an important role in the context of DNA damage response following exposure to genotoxic stress in breast cancer patients.

1.6.3 EGFR in Triple-Negative Breast Cancer

EGFR is expressed in around 30% of malignant tumours affecting breast tissues. Yet EGFR is more frequently expressed in triple-negative breast cancer (TNBC), a highly aggressive subtype of breast cancer (Changavi et al., 2015). TNBC, defined by the lack of progesterone, oestrogen and HER2 receptors, approximately accounts for 20% of breast cancer incidence. Due to the lack of HER2 and hormonal receptors, TNBC is regarded as the only major subtype of breast cancer that lacks effective targeted therapies to improve patient outcomes (Costa et al., 2017). Combined with surgery and radiotherapy, the standard cytotoxic chemotherapy for metastatic TNBC consists of taxanes, anthracyclines, capecitabine, and ixabepilone. Yet poor therapeutic outcomes in terms of progression-free survival and overall survival are generally observed in these patients (Kassam et al., 2009). Accordingly, there is an urgent need to address this lack of effective treatment options for TNBC

patients. In TNBC, genetic abnormalities affecting the *EGFR* gene only account for a minute percentage of patients, suggesting that other abnormalities including aberrant posttranscriptional regulation could be implicated in the overexpression of EGFR in these patients (Kersting et al., 2004, Grob et al., 2012, Pintens et al., 2009). Profiling the *EGFR* mRNA and protein expression in TNBC tumours has revealed interesting findings. In analysed tumour samples, the protein expression levels of EGFR were shown to be significantly higher than their respective mRNA levels, indicating an abnormal translation rate of EGFR in TNBC tumours (Gumuskaya et al., 2010, Meseure et al., 2012).

Despite the established role of EGFR in driving the growth of malignant tumours, it is still unclear whether targeting EGFR overexpression in TNBC can produce positive outcomes. In many phase II clinical trials where targeted therapies were used against EGFR, the response rate was not encouraging, indicating that TNBC tumours do not rely solely on EGFR for survival (Costa et al., 2017). Yet the poor response rate in these clinical trials could be attributed to several confounding factors including the genetic heterogeneity of the TNBC subtypes (Pintens et al., 2009). Non-small-cell lung cancer (NSCLC) patients tend to have a significantly higher response rate to tyrosine kinase inhibitors than TNBC patients. Unlike TNBC tumours, it has been shown that NSCLC tumours are characterised by the presence of common activating mutations affecting the tyrosine kinase domain of EGFR that could be targeted by small-molecule inhibitors (Lynch et al., 2004).

In addition, due to the critical physiological function of EGFR in the context of cellular growth and differentiation, targeting EGFR expression in normal tissues could lead to severe side

effects affecting the skin and gastrointestinal tract that result in the discontinuation of treatment (Morse and Calarese, 2006). Developing selective therapies against malignant EGFR expression confers the advantage of using relatively large but safe doses, resulting potentially in improved therapeutic outcomes. Furthermore, combining anti-EGFR antibodies directed against distinct epitopes was found to be synergistic in the downregulation of EGFR in TNBC models (Ferraro et al., 2013). Combining anti-EGFR treatments with other therapeutic options including PARP and immune checkpoint inhibitors is also a new promising concept in tackling TNBC (Sonnenblick et al., 2015, Postow et al., 2015).

1.7 Antisense Technology

Antisense technology and RNA interference have emerged as powerful platforms for drug discovery. In principle, these antisense modalities exert their therapeutic effects by altering the complex metabolism of target mRNA. While similar to traditional approaches in its reversible nature, targeting mRNA metabolism significantly expands the library of potential therapeutic targets to proteins or RNAs not amenable to small-molecule or protein-based therapeutics (Bennett et al., 2017, Janssen et al., 2013). Furthermore, the antisense technology also complements current treatment options such as small molecules inhibitors and antibodies by targeting mRNAs upstream of their protein targets, underscoring potential synergistic effects (Stephenson and Zamecnik, 1978).

Combination therapy is currently of great interest in cancer treatment as tumour heterogenicity is known to occur not only among patients but also within a single tumour population

(Nickel et al., 2012). Thus, single-drug treatment plans are often incapable of exterminating all malignant cells in a given tumour. Treatment with a single drug often results in the selective survival of inherently resistant cells or mutated cells with acquired resistance. In this regard, the antisense technology provides a practical platform to generate multiple therapeutic antisense oligonucleotides (ASOs) targeting different survival pathways within a single dosage form, thus greatly minimising the development of resistance (Bennett et al., 2017).

1.7.1 Pharmacodynamics of ASOs

The therapeutic effects of ASOs start from the interaction with a disease-related mRNA through Watson–Crick base complementarity. This direct binding then modulates the RNA metabolism via occupancy-only mechanisms or cleavage and degradation mechanisms (Bennett et al., 2017). Even though screening is required for optimal activity, it is possible to rationally design ASOs to alter the processing of a given RNA just based on the ASO chemistry and the targeted RNA sequence (Bennett, 2019).

Occupancy-only ASOs induce their pharmacological effects via hybridising to specific sequence elements in their target RNAs necessary for splicing or translational events. In this category, the modulation of RNA splicing is the most widely adopted strategy, in which exon skipping could be induced as with eteplirsen or exon inclusion as with nusinersen (Kinali et al., 2009, Passini et al., 2011). In addition to splice-site modulation, these occupancy-only ASOs could also alter specific translational events. It has been shown that ASOs hybridising

to domain IIId of the hepatitis C virus IRES prevent the landing of the 40S ribosomal subunit via steric hindrance (Martinand-Mari et al., 2003, Tallet-Lopez et al., 2003). However, once the ribosomal binding is established, scanning ribosomes are thought to become capable of displacing bound ASOs via their helicase activity. Indeed, targeting the coding region with these ASOs was found to be ineffective due to the robust helicase activity of translating ribosomes (Dias and Stein, 2002, Summerton, 1999).

ASOs could be also designed to induce the degradation of target RNAs. Through chemical and structural features, cleavage-inducing ASOs mediate their pharmacological effects via the recruitment of endogenous enzymes mainly ribonuclease H1, also known as RNase H1 (Bennett and Swayze, 2010). RNase H1 is a ubiquitously-expressed ribonuclease that catalyses the degradation of RNA heteroduplexed with DNA in a sequence non-specific manner (Wu et al., 1999, Cerritelli and Crouch, 2009). To recruit RNase H1, the ASO has to contain 7 to 10 consecutive DNA nucleotides with 5 nucleotides being the minimum (Bennett, 2019). While targeted RNA is degraded in this process, the duplexed ASO is released intact (Figure 1.6).

Mipomersen is an FDA-approved ASO that was used for the management of homozygous familial hypercholesterolemia (Hair et al., 2013). It is a chemically-modified single-stranded ASO designed to complementary bind and degrade the apolipoprotein B mRNA via an RNase-H1 dependent mechanism. As apolipoprotein B is an essential component of the low-density lipoprotein cholesterol (LDL), treatment with mipomersen results in the reduction of LDL levels in the blood (Wong and Goldberg, 2014). In addition to mipomersen, inotersen is another RNase-H1 inducing ASO that has been

approved by the FDA for the treatment of transthyretin amyloidosis. By decreasing circulating transthyretin levels, it was recently shown in a phase III study that inotersen was associated with limited disease progression and improved quality of life (Benson et al., 2018).

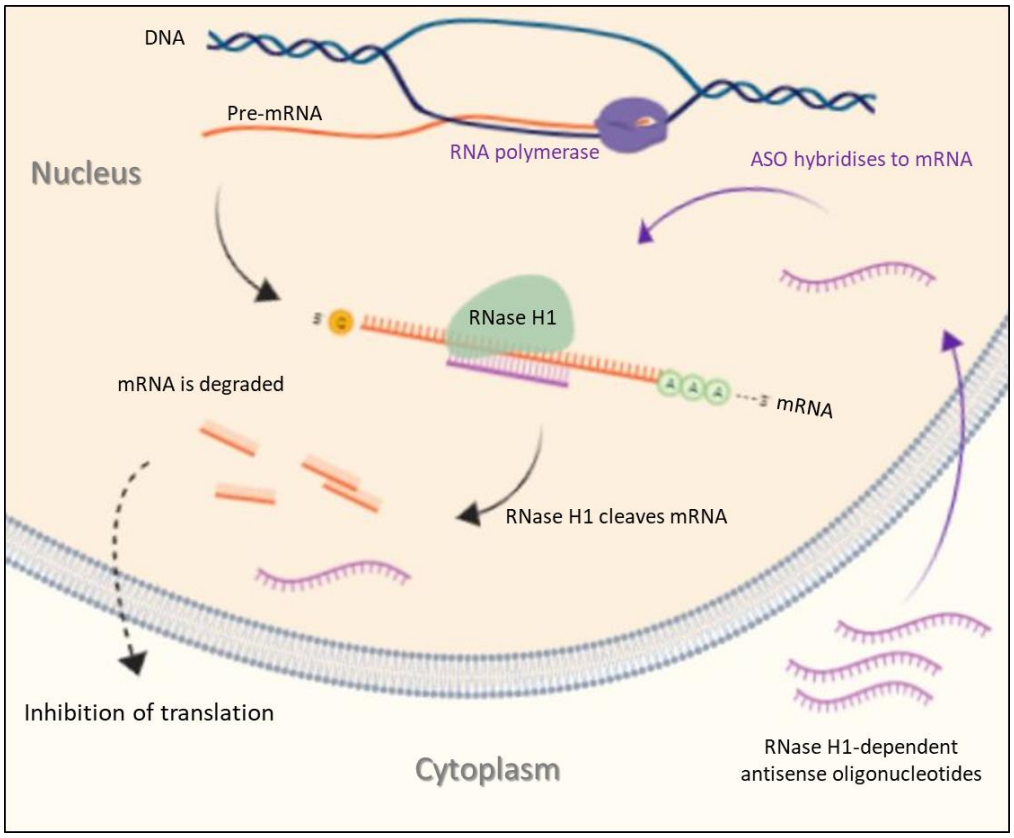


Figure 1.6 RNase-H1 Dependent ASOs. Schematic illustration, based on (Levin, 2019, Bennett, 2019), showing the mechanism of action of cleavage-inducing ASOs exerting their effects via RNase-H1.

Potential toxicity of ASOs

As short ASOs are inclined to have more off-target effects, ASOs of around 16-20 nucleotides bases in length are considered to have a unique binding ability to their targeted transcripts (Bennett, 2019). In addition, conducting a bioinformatics

analysis to screen for predicted targets with perfect or partial matches is an important characterisation measure to minimise off-target hybridisations (Burel et al., 2015). On the other hand, ASOs longer than 20 nucleotides are inclined to form self-structures that could impair hybridisation or have poor access to their targeted sequence (Hagedorn et al., 2018).

Potential toxicities derived from the administration of ASOs could be categorised into hybridisation-dependent or hybridisation-independent toxicities. Hybridisation-independent toxicities, derived from non-nucleic acid interactions, can be also sub-classified into sequence-dependent or sequence-independent interactions with cellular proteins. For instance, sequence-independent interactions have been documented with proteins belonging to the coagulation and complement systems (Sheehan and Phan, 2001, Henry et al., 2016), while sequence-dependent interactions include the activation of Toll-like receptors (Krieg et al., 1995). It was shown that unmethylated CpG motifs such as GTCGTT, GACGTT or AACGTT especially at a particular nucleotide context are associated with increased activation of human leukocytes (Hartmann et al., 2000, Krieg et al., 1998).

The second source of potential toxicities can be mediated through hybridisation dependent mechanisms. This category of potential toxicities can be driven by either off-target hybridisation or excessive on-target hybridisation. This source of potential toxicities could be greatly minimised through careful selection of target RNA sequences and sufficient preclinical characterisation of potential ASO candidates. Nevertheless, several clinical trials have demonstrated the relative safety of ASOs as a therapeutic intervention in humans (Bennett et al., 2017). Indeed, the safety of antisense technology has been

validated by the FDA approval of several nucleotide-based drugs including inotersen for the treatment of transthyretin amyloidosis (Benson et al., 2018, Rader and Kastelein, 2014).

1.7.2 Pharmacokinetics of ASOs

In contrast to small-molecule drugs, unmodified oligonucleotides are unstable in biological matrices and have limited access to the intracellular compartment due to their nuclease sensitivity and hydrophilic nature (Bennett, 2019). To address these pharmacokinetic restrictions, chemical modifications and formulations are employed to improve the drug-like properties of these oligonucleotides. As a result, the pharmacokinetics of ASOs is driven substantially by their modified chemistries and formulations. Hence, modifications within the same chemical class usually confer similar pharmacokinetic properties and exhibit comparable pharmacokinetic profiles across different species including humans (Geary et al., 2015, Rosie et al., 2009). A major advantage of this consistency is the potential of reducing the high attrition rate of the drug-development pipeline (Yu et al., 2013).

Naked ASOs can be spontaneously internalised into cells via a passive yet inefficient process known as gymnosis, by which ASOs pass through the cell membrane into the cytoplasm. Once in the diffuse cytoplasm, these oligonucleotides must access their complementary nucleotide sequences within their RNA targets to exert their pharmacological effects. As RNAs are often bound to regulatory proteins and have secondary and tertiary structures, the accessibility of ASOs to their targets is a major concern. This is often addressed in practice by screening a

library of ASOs that target different regions in a given mRNA (Vickers et al., 2000, Gredell et al., 2008). In comparison to small-molecule drugs, screening a library of ASOs for an active pharmacophore is more practical and efficient considering the ease of designing and synthesising novel ASOs. Furthermore, the homogenous nature of ASOs regarding their physicochemical properties provides added efficiencies to the drug development pipeline (Levin, 2019).

Due to their low molecular weight, naked ASOs are readily excreted by the kidneys, therefore, plasma protein binding is a major pharmacokinetic parameter that controls their bioavailability (Bennett, 2019). Weak plasma protein binding usually results in rapid filtration of ASOs out of the blood and into the urine, causing minimal tissue distribution (McMahon et al., 2002). Consequently, a balanced affinity to plasma proteins is critical for target-tissue bioavailability following systemic administration (Bennett et al., 2017). Conjugation strategies to improve the selective distribution of ASOs were also implemented especially for oligonucleotides targeting the liver. Through efficient delivery, these conjugation strategies aim to improve the therapeutic index of ASOs targeting specific tissues in the body. It was shown that conjugation with N-acetylgalactosamine, cholesterol, tocopherol and several fatty acids increased exposure to hepatocytes while it minimised renal elimination (Crooke et al., 1996, Herbert et al., 2005, Nishina et al., 2015, Prakash et al., 2014). When distributed into tissues, clearance of ASOs is then catalysed mainly by cellular exonucleases (Eder et al., 1991, Wójcik et al., 2007), resulting in small fragments that are readily excreted in urine due to their low plasma protein binding (Geary et al., 2015).

1.7.3 Chemical Modifications

Due to the inherent instability of unmodified nucleic acids in both the intracellular and extracellular compartments, a continuing effort has been invested to improve the stability and efficacy of ASOs. An important outcome of this effort is the development of chemically modified ASOs that show enhanced resistance to degradation, binding affinity and tissue distribution (Crooke et al., 2018, Bennett, 2019). These chemical modifications are broadly classified into three dominating classes, namely, backbone modifications, nucleobase modifications and sugar modifications (Figure 1.7).

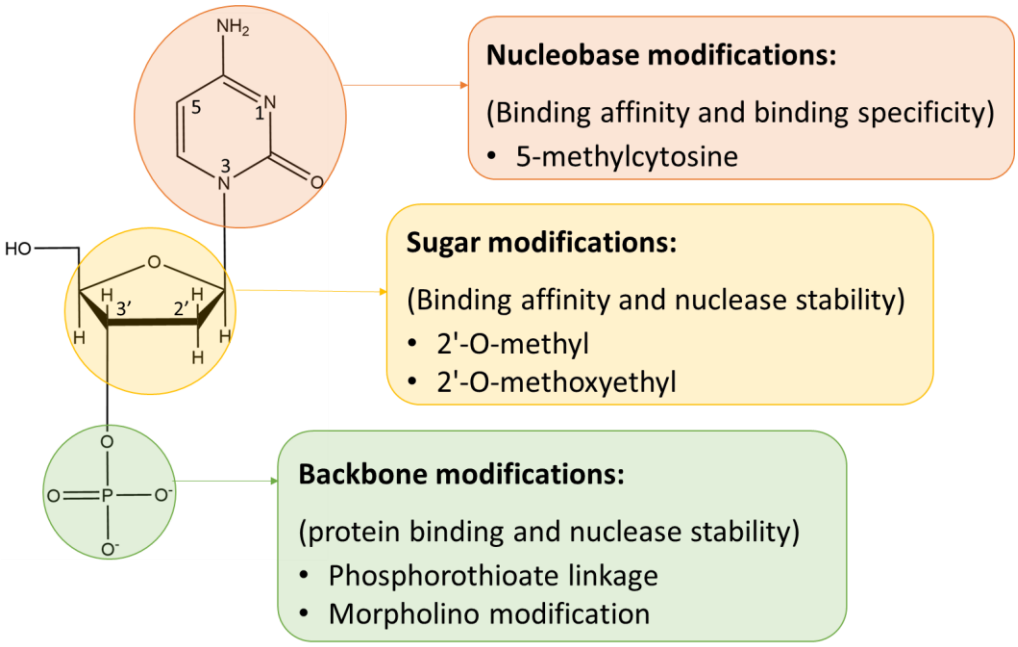


Figure 1.7 ASO chemical modifications. Schematic illustration showing the main classes of chemical modifications used to improve the stability and efficacy of ASOs.

Backbone Modifications

The phosphodiester backbone linking different nucleotide bases is inherently susceptible to the action of exo- and endonucleases. Thus, several backbone modifications have been developed to address this issue which could be classified into two subcategories: phosphate modifications such as the phosphorothioate linkage and phosphate-sugar modifications including the morpholino modification (Smith and Zain, 2019).

Often considered as a first-generation modification, the replacement of a non-bridging phosphate oxygen atom with a sulphur atom is a common backbone modification to confer a high degree of nucleolytic resistance (Stein et al., 1988). Despite the increased resistance to nuclease degradation, ASOs bearing this phosphorothioate linkage are still capable of eliciting RNase-H1-induced cleavage of target RNA (Stein et al., 2009). It was also shown that oligonucleotides containing this modification achieve detectable intracellular distribution without any requirement for targeting ligands or transfecting reagents (Stein et al., 2009, Sands et al., 1994, Agrawal et al., 1991). Even though it is still rudimentary, it seems that these phosphorothioate ASOs bind initially to proteins on the cell surface including EGFR before being endocytosed (Juliano and Carver, 2015, Wang et al., 2018). After escaping the intracellular vesicles, these ASOs bind mainly to the paraspeckle proteins such as P54NRB (non-POU domain-containing octamer binding) and SFPQ (splicing factor proline and glutamine-rich) to form electron-dense structures of 150-300 nm in diameter known as the phosphorothioate bodies. The formation of these nuclear foci is thought to facilitate RNA hybridisation by retaining ASOs in the intracellular

compartment (Bailey et al., 2017, Shen et al., 2014, Lorenz et al., 1998).

In addition, phosphorothioate-modified ASOs are characterised by increased bioavailability after systemic administration especially to organs with high blood supply such as the liver and kidneys. This effect stems from the increased binding affinity for proteins present in the circulation such as serum albumin (Geary et al., 2007, Koller et al., 2011). To prevent renal clearance, it seems that a minimum of ten phosphorothioate linkages is required to ensure robust oligonucleotide-protein interaction (Liang et al., 2014). After subcutaneous or intravenous administration, ASOs containing this modification have a distribution phase ranging from minutes to hours followed by an elimination phase that proceeds for weeks with a half-life of 2 to 3 days (Geary et al., 2015).

However, phosphorothioate ASOs cannot cross the blood-brain barrier mainly due to their high polarity (Rigo et al., 2014). Furthermore, the proinflammatory nature of this chemical modification could result in side effects mainly related to the activation of innate immune responses. Local skin reactions were frequently observed in patients after mipomersen administration as a subcutaneous injection (van Meer et al., 2016). In rarer instances, marked thrombocytopenia has been also reported after inotersen treatment in patients with hereditary transthyretin amyloidosis (Benson et al., 2018). As these side effects were found to be dose-dependent reactions, efficient delivery of these modified ASOs is recommended to reduce the amount of dose required (Levin, 2019).

The isosteric replacement of the sugar-phosphate backbone with methylene-morpholine rings attached by phosphorodiamidate groups is another widely utilised backbone

modification. This modification confers resistance against nuclease degradation in conditions where the induction of RNase-H1 activity is not desirable. In addition, these neutral ASOs exhibit increased RNA binding affinity compared to the unmodified oligonucleotides. However, due to their low plasma protein binding, these ASOs have limited tissue distribution as they are rapidly excreted by kidneys (Blum et al., 2015).

Nucleobase Modifications

In addition to backbone modifications, modifications targeting the heterocyclic bases have also been developed. The main aim of these modifications is to increase the binding affinity to the target sequence while retaining unaltered binding conformation (Bennett et al., 2017, Smith and Zain, 2019). It was found that the addition of substituent groups mainly to the fifth position of the pyrimidine bases resulted in increased binding affinity by improving duplex thermal stability.

Several modifications of this chemical category were developed including the commonly used methyl to cytosine modification (Smith and Zain, 2019). The introduced methyl group appears to fit in a major groove between the stacked nucleobases, inducing a thermal shift into more stabilising binding conditions (Herdewijn, 2000). Comparable to the phosphorothioate modification, ASOs bearing this type of modification could activate the RNase-H1 degradation pathway (Shen et al., 2003, Freier and Altmann, 1997).

Sugar Modifications

Often considered as a second-generation modification, modifying the sugar moiety at the second carbon atom appears to be an effective strategy to increase both nuclease resistance and binding affinity for target mRNAs (Bennett et al., 2017). In principle, RNA homoduplexes are more stable than their DNA counterparts due to the presence of the hydroxyl group, an electron-withdrawing group, at 2’ position of the RNA ribose ring. Accordingly, several electron-withdrawing groups including the 2'-O-methyl modification have been incorporated into the ASO structure at the same position to obtain an A-form or an RNA-like conformation upon hybridisation with their targets (Monia et al., 1993, Smith and Zain, 2019). The improved binding affinity associated with this type of modification appears to be directly correlated with the electronegativity of the substituent at the 2’ position. ASOs containing a 2’-fluoro modification exhibit a superior binding affinity than their analogues containing 2’-O-alkyl groups. Yet ASOs containing 2’-O-alkyl groups are more widely adopted due to their substantial resistance to nuclease degradation (Freier and Altmann, 1997). Derived from their high resistance to degradation, the 2'-O-alkyl modification has been found to extend the half-life of phosphorothioate ASOs from 48 hours to up to 4 weeks (Geary et al., 2015). Consequently, these ASOs have the potential to be administered weekly (Rigo et al., 2014).

In addition, it has been shown that the 2'-O-methyl modification abrogates the immunostimulatory activity of ASOs containing the immunostimulatory motif 5’-UGUGU-3’ (Judge et al., 2006). Currently, the 2’-O-methoxyethyl (2’MOE) modification is

considered the most effective 2’-substituent; substantially increasing binding affinity for target RNA while reducing non-specific protein interactions (Henry et al., 2000). Indeed, 2’MOE-modified ASOs including inotersen appear to be well tolerated even in comparison to chemical modifications from other classes including the phosphorothioate modification. Nevertheless, sporadic cases of severe thrombocytopenia in patients administered 2’MOE-modified ASOs have been documented (Henry et al., 2000, Crooke et al., 2016, Crooke et al., 2017).

In contrast to the unmodified oligonucleotides, ASOs containing the 2’-O-alkyl modification cannot activate the RNAase-H1 degradation pathway. This potential limitation could be overcome by having a core nucleotide sequence capable of instigating the RNAase-H1 activity flanked by 2’-O-alkyl modified nucleotides. This chimeric design, designated the ‘gapmer’ design, has the advantage of activating RNAase-H1 while retaining the improved stacking and high resistance to exonuclease degradation derived from the terminal 2’-O-alkyl-modified nucleotides (Lima et al., 2007).

As far as the binding affinity is concerned, constraining the ASO structure with a 2’-O-4’ methylene bridge has increased the binding affinity to target RNA to unprecedented levels (Henry et al., 2000, Wengel, 1999). However, this type of modification seems to be associated with increased hepatic toxicity (Burdick et al., 2014, Swayze et al., 2006). Yet several analogues including the stereoisomers and bridge heteroatom analogues have been developed to resolve these toxicity issues, underscoring the potential of this modification in facilitating the production of highly active ASOs (Prakash et al., 2010, Seth et al., 2012).

1.8 Polymers

The delivery of ASOs to the intracellular compartment of target tissues is probably the main challenge for the widespread adoption of the antisense technology (Levin, 2019). This challenging component is due to the nuclease instability of ASOs and their limited ability to penetrate the cell membrane because of their relatively high molecular weight and hydrophilic nature (Juliano et al., 1999). Hence, protection and transportation are important characteristics of any potential gene-transfer strategy, which could be broadly classified into a viral and non-viral delivery system.

Viral gene delivery strategies, based mainly on adenoviruses and retroviruses, are known to produce efficient expression in cells of interest but also known to have major disadvantages including the high immunogenicity, random genomic integration, and limited cargo capacity (Smith, 1995). Conversely, non-viral vectors are less immunogenic and more practical in terms of their gene loading capacity and large-scale manufacture. Yet, these non-viral carriers have also challenges to overcome including their low transfection efficiency and toxicity (Gonzalez et al., 1999).

1.8.1 Cationic Polymers

Non-viral gene transfer strategies are mainly based on the use of cationic lipids and cationic polymers. Due to their amphiphilic nature, cationic lipids can cluster into vesicles known as liposomes which have been extensively developed for gene delivery applications (Koynova and Tenchov, 2009, Howard, 2009). On the other hand, cationic polymers such as

polyethyleneimine (PEI), poly(l-lysine) (PLL), linear polyamidoamine (PAA), and poly(β-amino ester)s (PBAEs) are polycations that can bind and condense nucleic acid via electrostatic interactions into compact nanoparticles known as polyplexes. The formation of these polyplexes facilitates the intracellular delivery of nucleic acid cargo via the endocytic pathway while protecting it against enzymatic degradation. In comparison to liposomes, these polycations have high stability and improved design flexibility achieved by modulating their molecular weight, chemical composition, and architecture (Kabanov, 1999).

Cationic polymers also interact electrostatically with the negatively charged cell membrane, thus facilitating the cellular uptake of nucleic acid cargo (Verma and Stellacci, 2010, Hafez et al., 2001). In addition, incorporating hydrophobic moieties such as bisphenol A can also enhance the interaction of polymers with both nucleic-acid and plasma membrane which in turn facilitate cargo encapsulation and endocytosis (Jeong et al., 2007, Liu et al., 2010, Rui et al., 2019). Yet excessive hydrophobicity in polymers could disrupt the integrity of the cell membrane leading to cell toxicity (Neamnark et al., 2009). Surface modifications such as the conjugation with cell-penetrating peptides (CPPs) could further enhance the cellular uptake of polyplexes (Heitz et al., 2009).

Once internalised into the endosomal–lysosomal compartment, polymers must escape into the diffuse cytoplasm for successful gene delivery. It has been shown that PAAs undergo pH-induced conformational changes that enable physical interactions with the vesicular membranes of endosomes, facilitating their release to the cytoplasm (Richardson et al., 2010). Hydrophobic moieties including phenyl groups and lipids were found to

facilitate this process via improved hydrophobic interactions (Urade et al., 1988, Chang et al., 2017, Habrant et al., 2016). Similarly, CPPs can also fuse with the endosomal membrane facilitating cargo release into the diffuse cytoplasm (Plank et al., 1994). On the other hand, certain cationic nanoparticles such as PBAEs and PEI get reversibly protonated inside the endosomes, acting as a "proton sponge" preventing excessive acidification (Boussif et al., 1995, Akinc and Langer, 2002). This reversible protonation event leads to the build-up of an electrical gradient resulting in an influx of chloride ion which is followed by water due to osmotic pressure. Eventually, this causes the rapture of endosomes and the release of polyplexes into the diffuse cytoplasm (Nel et al., 2009).

In the diffuse cytoplasm, polyplexes then release their oligonucleotide load which is an event that can be triggered by polymer degradation (Luo and Saltzman, 2000). PBAEs get degraded by hydrolysis in the cytoplasm within hours while they are relatively stable in the endosomal acidic environment. At endosomal pH, protonated PBAEs are less likely to generate the ^{-}OH nucleophile by deprotonating the surrounding water molecules, hence the increased stability (Lynn and Langer, 2000). As other polymers like PLA and PLGA have different degradation kinetics, selecting a suitable release rate depends on the location of the targeted transcript. For instance, RNA-interference requires a release mechanism that is fast and selective to the cytosolic environment. This could be achieved by the incorporation of bioreducible moieties in the polymer chemical composition, thus triggering polymer degradation in the reducing environment of cytosol (Son et al., 2012).

In the systemic circulation, polyplexes are often cleared by the reticuloendothelial system (Wightman et al., 2001). To extend

their half-life, several physicochemical strategies were developed to reduce this interaction including grafting of poly(ethylene glycol) (PEG) chains (Ogris et al., 1999). However, extensive PEGylation could reduce the transfection efficiency, therefore, a balanced approach to polymer design should consider a combination of physicochemical parameters optimised to achieve the desired outcomes (Williford et al., 2016).

1.8.2 Tumour-Targeting Strategies

A serious problem related to conventional cancer therapeutics is off-target toxicity. To address this issue, differential features of cancer cells such as overexpressed surface molecules or tumour-microenvironment properties are often exploited to actively target cancer cells. Passive targeting for nanoscale delivery vehicles with a size range of 10–200 nm can be also achieved utilising the enhanced permeability and retention (EPR) effect observed around rapidly growing tumours (Matsumura and Maeda, 1986, O'Brien et al., 2004). In this regard, reducing clearance by the reticuloendothelial system via incorporating PEG chains and adopting non-spherical geometries was found to enhance the circulation time, which in turn improves tumour targeting by EPR (Perrault et al., 2009, Champion and Mitragotri, 2006). Passive tumour targeting, however, is a highly variable process that is controlled by the degree of vascularization in addition to the type and size of the targeted tumour (Maeda, 2015).

In addition to passive targeting, polymers could be designed to include functional moieties that enable specific interactions with cancer-related targets including surface receptors and

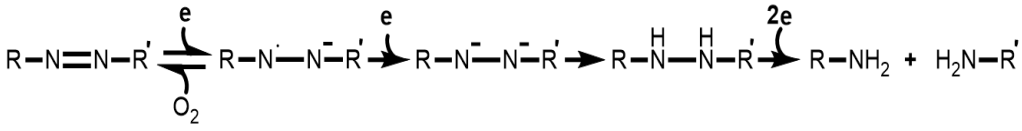
integrins. Particles functionalised with antibodies were found to be highly precise in targeting tumours expressing the relevant antigen (Stuchinskaya et al., 2011). Due to their smaller size, next-generation antibodies such as nanobodies and single-chain antibodies were found to be even safer and more effective in facilitating tumour-cell uptake of conjugated nanoparticles (Hansel et al., 2010, Yang et al., 2009). Functional moieties could also include ligands for surface receptor-like EGFR and transferrin that are frequently overexpressed in cancer (Vaughan et al., 2019). Nevertheless, tumour heterogenicity, tumour penetration and increased immunogenicity remain challenging issues regarding active tumour targeting using these modalities (Juweid et al., 1992, Cheng et al., 2012).

Polymers could include responsive chemistries to certain triggers present in the cancer microenvironment including the abnormally low pH and oxygen levels (Whiteside, 2008). Furthermore, external triggers such as a magnetic field, light, and temperature could be applied to provide temporal and spatial control over the release mechanism (Zintchenko et al., 2006, Oliveira et al., 2007, Plank et al., 2011, Sirsi et al., 2012). Once triggered, polymers could expose a binding domain, release a therapeutic load or transform into a biologically active form (Vaughan et al., 2019). For instance, zwitterionic polymers have a neutral charge at physiological pH which helps in reducing non-specific interactions with macromolecules and increasing their stability against clearance. Yet these polymers become rather protonated and cationic in the acidic extracellular microenvironment of tumours. Acquiring a positive charge then facilitates their interactions with the negatively charged cell membrane of cancer cells (Yuan et al., 2012). As described earlier, polymers could be also designed to include

responsive moieties to the reducing environment of the cytosol. Polymers functionalised with bioreducible disulphide bonds are characterised by efficient targeted delivery to the cytosol with reduced toxicity (Zhao et al., 2020).

Azobenzene Linkage

It was also shown that polymers containing the azobenzene bond are characterised by hypoxia sensitivity and specificity (Perche et al., 2014, Kulkarni et al., 2016). In addition, azobenzene-based fluorescent probes and nanogels were also effective in targeting hypoxic cancer cells in breast cancer (Kiyose et al., 2010, Si et al., 2020). Under low oxygen levels, the azobenzene derivatives, in general, are reduced by several reductases including the rat liver microsomal cytochrome P-450 in two one-electron steps, in which the first step is an oxygen-dependent process (Zbaida and Levine, 1991). As shown in Scheme 1.1, the dianion intermediate then becomes spontaneously protonated by water to the corresponding arylhydrazine which gets fully reduced to the aniline derivative (Sadler and Bard, 1968, Kiyose et al., 2010).



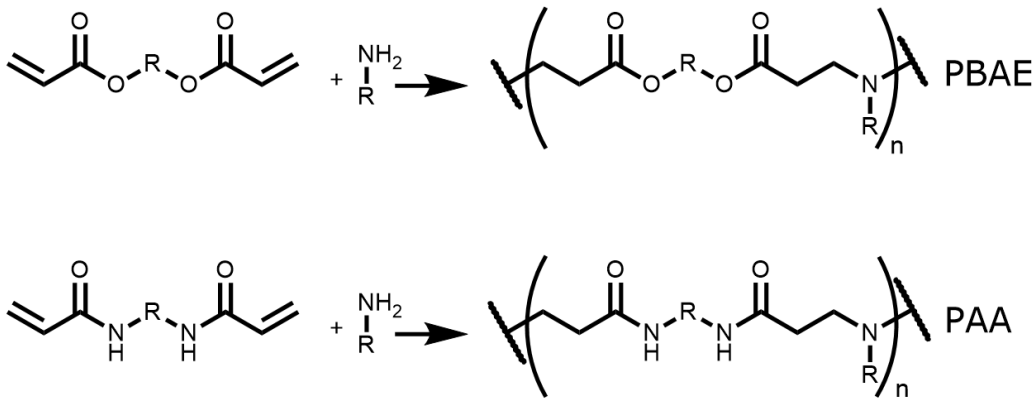
Scheme 1.1 Hypoxia triggered cleavage of azobenzene bond. This figure shows the reductive cleavage of the azo bond (N=N) in azobenzene under low oxygen levels (Kiyose et al., 2010).

1.8.3 PBAEs and PAAs

Poly(β-amino ester)s (PBAEs) are a class of cationic polymers studied widely for the delivery of nucleic acids. This class is characterised by the presence of hydrolytically degradable ester linkages which makes them less toxic in comparison to non-biodegradable polymers like PEI (Akinc et al., 2003). Comparable to PBAEs are linear polyamidoamines (PAAs), a different class of cationic polymers in which the degradable ester linkages are replaced with more stable amide bonds (Christensen et al., 2006). In addition to their biodegradable nature, PBAEs and PAAs also contain important characteristics that make them an attractive foundation for the development of novel gene delivery systems. First, PBAEs and PAAs contain intrinsically the required positive charge necessary to complex the nucleic acid. Furthermore, their ease of manufacture has resulted in the generation of PBAEs and PAAs with various chemical and physical properties (Green et al., 2008, Ferruti et al., 2002). Due to their versatile chemistry, these polymers can be equipped with functional groups conferring chemical as well as biological abilities. For instance, PBAEs and PAAs have been synthesised containing PEG chains and disulphide bonds to improve their biodistribution and cytoplasmic delivery, respectively (Tzeng et al., 2012, Christensen et al., 2006, Vader et al., 2012, Kim et al., 2016).

PBAEs and PAAs are mainly synthesised by the step-wise, conjugate polyaddition of amine and diacrylate or diacrylamide molecules (Scheme 1.2). In this reaction, a primary or secondary amine launches a nucleophilic attack on the electrophilic alkene of an α, β-unsaturated carbonyl compound after initial hydrogen bond interactions. The resulting enolized

intermediate then undergoes quick tautomerization to generate the aza-Michael adduct (Lynn and Langer, 2000, Yang et al., 2014). This is a one-step, one-pot reaction that generally does not require catalysts, protective strategies for functional groups, or additional purification steps to remove products of side reactions (Lynn et al., 2001, Ranucci and Manfredi, 2019). To minimise hydrolytic degradation, PBAE synthesis is typically carried out in anhydrous organic solvents or solvent-free conditions (Anderson et al., 2005). On the other hand, the synthesis reaction of PAAs is best preformed in protic solvents like water and methanol as the reaction in aprotic organic solvents is generally not suitable (Manfredi et al., 2007). As the rate-limiting step in Michael addition reaction is the proton-transfer step, only protic solvents are recommended with the less reactive amide group in comparison to the ester group in PBAE (Ranucci and Manfredi, 2019).



Scheme 1.2 Synthesis of PBAEs and linear PAAs. This scheme shows the synthesis of PBAEs and linear PAAs via bis-Michael addition reaction.

Driven mainly by electrostatic interactions, PBAEs and PAAs can condense nucleic acid into nanoparticles simply by mixing them in slightly acidic conditions. Cationic polymers are known to

bind oligonucleotides less efficiently than large plasmids, yet higher concentrations or improved variants of these relatively less toxic polymers are often used to compensate for the reduced avidity (Dosta et al., 2018). While considering the toxicity limits, an excess of cationic polymers can also facilitate the association between the polyplexes and the negatively charged cell membrane (Lopez-Bertoni et al., 2018). Interestingly, the flexibility in formulating these polymers allows loading multiple nucleic acids in a single formulation for combinatorial delivery (Kozielski et al., 2019). It has been shown that PBAEs containing disulphide bridges can co-deliver two cancer stem-cell inhibiting microRNAs, namely, miR-296-5p and miR-148a to *in vitro* and *in vivo* models of human glioblastoma. Both miRNAs in combination were more effective than using a single sequence alone according to tumour-size over time and long-term survival rate, highlighting the potential of combinatorial nucleic acid therapy (Lopez-Bertoni et al., 2018).

1.9 Hypothesis and Objectives

The overexpression of EGFR in breast cancer correlates with poor prognosis and advanced tumour stages. Even though targeted therapies proved to be effective in other types of cancer, limited success has been achieved in targeting EGFR in breast cancer. An important limitation of these targeted therapies is the lack of specificity in targeting the malignant expression of EGFR while keeping homeostatic expression unaffected. Following the identification of the *EGFR* IRES and characterising its function in maintaining the hypoxic expression of EGFR, the first aim of this work was to further characterise the IRES-mediated expression of *EGFR* in the

context of cell stress associated with advanced breast cancer. The second aim of this project was to investigate the trans-regulation of the *EGFR* IRES. As the 5′ UTR of the *EGFR* mRNA is relatively long, GC rich and perhaps highly structured, it is possible, therefore, that an RNA helicase other than the canonical eIF4A is involved in its regulation.

- To these effects, bicistronic reporter systems were used to investigate whether treatment with agents that induce DNA damage, ER stress, iron overload, inflammation and oxidative stress could have any effect on the relative expression of the downstream firefly luciferase, controlled by the *EGFR* 5′ UTR, in MCF-7 cells. The results of this work are presented in chapter three.
- DDX3, a hypoxia-responsive member of the DEAD-box RNA helicase family, has been identified as a potential regulator of the *EGFR* 5′ UTR in breast cancer cells. The requirement of the *EGFR* 5′ UTR for DDX3 was examined by overexpressing DDX3 or inhibiting its function using ketorolac salt in breast cancer cells transfected with a reporter plasmid containing the *EGFR* 5′ UTR. The results of this investigation are found in chapter four.

The third aim of this thesis was to target the expression of EGFR under conditions of cell stress including hypoxia utilising the antisense technology. To deliver the anti-EGFR ASOs preferentially into hypoxic cancer cells, the fourth aim of my project was to generate novel polymeric gene vectors that are responsive to low oxygen levels.

- The antisense technology was utilised in two distinct approaches. The first approach aimed to inhibit the *EGFR* IRES activity under cell stress using occupancy-only ASOs

targeting the internal landing site of ribosomes. This targeting strategy is thought to selectively inhibit the hypoxia-induced expression of EGFR while homeostatic expression remains unaffected as scanning ribosomes recruited via the universal cap structure could displace these ASOs via their helicase activity. The second approach utilised to target the hypoxic expression of EGFR was based on cleavage-inducing ASOs. An efficient screening strategy was designed, based on the IRES activity of the *EGFR* 5' UTR, to examine a library of ASOs targeting the *EGFR* mRNA for degradation. The results of this investigation are detailed in chapter five.

- To deliver these ASOs into hypoxic cancer cells, hypoxia-responsive polymers have been designed and synthesised based on the chemistries of PBAEs and PAAs. These polymers were then characterised for their ability to complex with the anti-EGFR ASOs via electrostatic interactions and then preferentially release them under low oxygen levels in an event that is triggered by the cleavage of the hypoxia-responsive azobenzene bond. The results of this work are described in chapter six.

Chapter Two

2 Materials and Methods

2.1 Cell Culture Methods

2.1.1 Cell Lines and Maintenance

Breast cancer cell lines used throughout this project are listed in Table 2.1. MCF-7 cells, which express oestrogen receptors, were cultured in DMEM (Sigma Aldrich, Cat# D5671), and MDA-MB-231 cells were cultured in RPMI (Sigma Aldrich, Cat# R8758) using tissue culture treated, gamma sterilised plasticware (TPP). Both media were supplemented with 10% foetal bovine serum (Gibco, Cat# 10500064) and 2 mM L-glutamine, and both cell lines were maintained at 37°C under a humidified atmosphere containing 5% CO_2. When cells reached 70-80% confluence, they were either sub-cultured or seeded after enzymatic dissociation using 1x trypsin-0.5 mM EDTA.

Table 2.1 Breast cancer cell lines

Cell line	ATCC reference	Origin	Description
MCF-7	HTB-22	Human breast adenocarcinoma	Adherent cell line with oestrogen receptor expressed
MDA-MB-231	CRM-HTB-26	Human breast adenocarcinoma	Adherent triple-negative breast cancer cell line

2.1.2 Transient Transfection and Treatment

Commercially available lipid-based systems were used to transfect plasmid DNA and antisense oligonucleotides (ASOs)

into breast cancer cells. FuGENE HD (Promega, Cat# E2311) was used for plasmid DNA transfection according to the manufacturer's instructions. Using 24-well plates, MCF-7 cells were seeded at a density of $2x10^4$ per well 24 hours before transfecting with plasmid DNA at a 3:1 FuGENE HD transfection reagent to DNA ratio. After 24 hours, cells were incubated with cryptolepine (provided by Patrick Ayande, University of Nottingham), phleomycin (Source Bioscience, Cat# ABE8567), thapsigargin (Sigma Aldrich, Cat# 586006), lipopolysaccharide from *E. coli* serotype O111:B4 (Cell Signalling, Cat# 14011S), hydrogen peroxide (VWR Chemicals, Cat# 7722-84-1), ammonium iron (III) citrate (Sigma Aldrich, Cat# W527106) or ketorolac tris salt (Sigma Aldrich, Cat# K1136) for 24 hours or 48 hours. Regarding ultraviolet radiation (UV), the exhausted medium was first removed before exposing the cells to UV-B radiation (1-10 seconds) using a UVBM-57 lamp (UVBP Products UVP). Then, cells were supplemented with fresh media and allowed to recover for 24 hours before assessing the luciferase activity.

Transfection of ASOs

For transfection of ASOs (Sigma Aldrich), Oligofectamine transfection reagent (Invitrogen, Cat# 12252011) was used according to manufacturer's recommendations. Briefly, cells were seeded into 24 well plates at a density of $1x10^4$ per well or 96 well plates at a density of $2x10^3$ per well. After 24 hours, cells were transfected with ASOs at 200 nM after replacing exhausted media with Opti-MEM (Gibco, Cat# 31985062). Transfection was carried out using a mixture of diluted Oligofectamine and diluted ASOs incubated for 20 minutes to allow for complexation and then added to cells. After 4 hours,

cells were supplemented with FBS and incubated for an additional 48 to 72 hours.

Polymer-Based Transfection of ASOs

In addition to Oligofectamine, ASOs were delivered to cells using the synthesised poly(β-amino ester) (PBAE) polymers. For 96-well plate transfections, polymers were solubilised in DMSO (dimethyl sulfoxide) at 100 mg/ml and then differentially diluted in 25 mM sodium acetate (NaAc, pH=5) to produce polyplexes with a varied polymer to DNA weight ratios when combined with a fixed ASO dosage. ASOs were also diluted in 25 mM NaAc (pH=5) to 2 μM before being combined and thoroughly mixed via pipetting or a syringe pump (WPI, Cat# 941-371-1003) with the diluted polymer solutions in a 1:1 volume ratio. In addition, branched PEI-g-PEG (Sigma Aldrich, Cat# 900926) and HIV-1 Tat protein (Sigma Aldrich, Cat# H0292) were also incorporated into some of the formulations to a final well concentration of 8.3 μg/ml and 1 μ/ml, respectively. After incubating for 10 minutes at room temperature to allow for complexation, 20 μl of each formulation was then diluted in 100 μl Opti-MEM and added to each well of cells after aspirating exhausted media. Cells were then incubated for two hours, at which point the media was replaced (Wilson et al., 2019). 72 hours post-transfection, MTT analysis was carried out to assess the metabolic activity of cells as described below.

2.1.3 Dual-Luciferase Assay

The dual-luciferase reporter assay system (Promega, Cat# E1980) was used according to manufacturer's protocol to assess the expression of firefly and *Renilla* luciferases in the

bicistronic constructs used in this study. Briefly, transfected cells were washed with ice-cold phosphate-buffered saline (PBS) and then lysed on ice using 50 µl of Passive Lysis Buffer. After scraping the bottom of wells to facilitate cell dissociation and lysis, 5 µl of each lysate was transferred into an individual well of a black 96-well plate. Using Promega's GloMax-96 microplate luminometer, the luminescence of each sample was measured twice over a 10 second integration time. The first measurement was after the addition of 25 µl of Lar II reagent to activate the firefly luciferase and the second measurement was after the addition of 25 µl of Stop & Glo reagent to quench the firefly luciferase activity and stimulate the activity of the *Renilla* luciferase.

2.1.4 MTT Assay

The viability of cultured cells was assessed using the MTT assay. This colourimetric assay is a sensitive indicator of the cellular metabolic activity as reflected by the activity of NAD(p)H-dependent oxidoreductase enzymes in reducing the water-soluble 2-(3,5-diphenyltetrazol-2-ium-2-yl)-4,5,-dimethyl-1,3-thiazole bromide (MTT) to its insoluble purple-coloured formazan product. The formation of formazan then can be easily quantified by measuring the spectral absorbance after solubilisation. Briefly, cells were seeded at a density of $2x10^3$ per well in 96-well plates and incubated for 24 hours before any treatment or transfection. To assess for viable cells, a solution of 2 µg/ml MTT (Sigma Aldrich, Cat# 298-93-1) dissolved in PBS was added to each well to achieve a final concentration of 0.8 µg/ml before incubating for 2 hours at 37°C. Next, 150 µl of DMSO was then added to each well to resuspend the formazan product after discarding the exhausted medium. The

spectral absorbance was then measured at 560 nm following shaking for 5 minutes using a Synergy HT spectrophotometer.

2.2 Molecular Biology Methods

2.2.1 Total RNA Extraction

Total RNA was isolated and purified from MCF-7 cells using the RNeasy Plus mini kit (Qiagen, Cat# 74134) according to the manufacturer's instructions. Briefly, pelleted cells were lysed using Buffer RLT Plus, a high-salt buffer containing guanidine isothiocyanate to ensure inactivation of RNases. The lysate was then passed through a gDNA Eliminator spin column to selectively remove genomic DNA. The flow-through was then applied to a silica-containing RNeasy spin column after mixing with 70% ethanol to provide favourable binding conditions. After washing contaminants with Buffers RW1 and RPE, total RNA was eluted using 30 µl of nuclease-free water.

2.2.2 Determination of Purity of Extracted Total RNA

The concentration of total RNA was determined using a Nanodrop spectrophotometer 1000 (Thermo Scientific) at a wavelength of 260 nm.

2.2.3 cDNA First-Strand Synthesis

Total RNA isolated was used as a template for reverse transcription (RT) reactions to synthesise cDNA using the SuperScript III first-strand synthesis system (Invitrogen, Cat# 18080051). Briefly, 100 ng of total RNA was primed with 1 µl of 10 mM dNTPs and 1 µl of 50 ng/µl random hexamers in a

total 14.25 µl reaction mixture at 65°C for 5 minutes and then on ice for 5 minutes. In the second step, the reaction mixture was mixed with 4 µl of 5X RT Buffer containing 25 mM $MgCl_2$, 1 µl of 0.1 M dithiothreitol (DTT), 0.25 µl of RNase inhibitor, and 0.5 µl of SuperScript III. Finally, the resulting mixture was incubated sequentially at 25°C for 2 minutes, 50°C for 1 hour (cDNA synthesis step) and 70°C for 15 minutes. cDNA template was then stored at -20°C after Nanodrop analysis.

2.2.4 Polymerase Chain Reaction

DNA of interest was amplified from vectors or cDNA templates using the polymerase chain reaction (PCR) mediated by Phusion high-fidelity DNA polymerase (NEB, Cat# M0530S) according to the manufacturer's recommendations. Briefly, 200 ng of template DNA was added to the DNA synthesis mix containing 10 µl of 5X Phusion GC buffer, 2 µl of 5 mM dNTPs, 2.5 µl of 10 µM forward primer, 2.5 µl of 10 µM reveres primer, 1.5 µl of DMSO and 0.5 µl of Phusion polymerase in a total 50 µl reaction. In a Techne TC-512 gradient PCR machine, the reaction was performed in typical thermocycling conditions consisting of initial denaturation at 98°C for 30 seconds before entering a cycle of denaturation at 98°C for 10 seconds, annealing at 60.8°C for 20 seconds and extension at 72°C for 60 seconds. After 35 cycles, the thermocycling reaction was terminated by a final extension phase at 72°C for 10 minutes.

2.2.5 Agarose Gel Electrophoresis

To separate a mixed population of nuclear acids, agarose gel electrophoresis was utilised in which resolution of DNA is based on the molecular weight. To prepare 1% (w/v) agarose gels,

0.5 g of agarose was melted in 50 ml of 1x TEA (40 mM Tris, 40 mM acetic acid, 1 mM EDTA, pH 8.0) and cast in a gel tray after supplementing with ethidium bromide (Sigma Aldrich, Cat# E1510) to a final concentration of 0.5-1 µg/ml. DNA samples were then mixed with 6X gel loading dye (NEB, Cat# B7024S) and loaded into the agarose gel. After submerging in an electrophoresis tank filled with 1X TEA, DNA samples typically run for 30-45 minutes at 100 V and then visualised using a Gel Doc XR+ System (Bio-Rad).

2.2.6 Purification of DNA from Agarose Gel

After excising the DNA fragments using a scalpel, the collected gel slices were purified using the Monarch DNA gel extraction kit (NEB, Cat# T1020S) according to the manufacturer's instructions. Briefly, DNA-containing gel slices were completely dissolved in Gel Dissolving buffer at 50°C with periodic vertexing before loading onto columns and spinning for 1 minute. Columns were then washed twice with DNA Wash buffer and then DNA was eluted by adding 13 µl of DNA Elution buffer and spinning for 1 minute.

2.2.7 Restriction Enzyme Digestion

DNA was digested using restriction enzymes as recommended by the manufacturer (NEB). In general, DNA was digested in a 50 µl reaction including the restriction enzyme and the recommended buffer for 1 hour at 37°C.

2.2.8 Gibson Assembly

This is an efficient cloning method that allows the joining of adjacent DNA fragments with overlapping ends in a single isothermal reaction that is catalysed by three different enzymes. First, the activity of a 5' to 3' exonuclease on the DNA fragments results in the formation single-stranded 3' overhangs which then anneal due to their matching complementarity. After that, a fully sealed double-stranded DNA of interest is produced due to the actions of a DNA polymerase and a DNA ligase. This DNA template can be used for further applications including direct transformation (Gibson et al., 2009). In this regard, a Gibson assembly master mix (NEB, Cat# E2611) was used to clone *DDX3* into the mammalian expression vector pcDNA3.1 (Invitrogen, Cat# V385-20). Briefly, *DDX3* cDNA sequence was amplified by PCR from MCF-7 cDNA using the forward and reverse primers designed by NEBuilder v2.0.5 assembly tool (Table 2.2). The resulting PCR products were separated according to their size via agarose gel electrophoresis and the *DDX3* cDNA fragment was then isolated from the agarose gel using Monarch DNA gel extraction kit (NEB, Cat# T1020S). On the other hand, pcDNA3.1 was digested and linearized with HindIII (NEB, Cat# R0104S) and EcoRI (NEB, Cat# R0101S) in 1X NEBuffer 2.1 (NEB, Cat# B7202S) for 1 hour at 37°C. Finally, *DDX3* cDNA and pcDNA3.1 were combined at 2:1 molar insert: vector ratio and incubated in an equal volume of Gibson assembly master mix at 50°C for 15 minutes before the transformation.

Table 2.2 Primers for *DDX3* amplification

Primer Name	Sequence (5'-3')
DDX3 HindIII F	ACTGTGCTGGATATCTGCAGTTAGTTACCCCACCAGTC
DDX3 EcoRI R	CTGGCTAGCGTTTAAACTTAATGAGTCATGTGGCAGTG

2.2.9 Site-Directed Mutagenesis

This method was used to create specific, targeted changes to the *EGFR* 5' UTR in pREF. Briefly, overlapping primers were designed to contain the desired mutations in the middle of the sequence flanked by 15 perfectly matched nucleotides (Table 2.3). The incorporation of these primers to target DNA using a PCR machine creates mutated plasmids with staggered nicks. Due to the presence of these staggered nicks, mutated plasmids cannot serve as templates for further amplification, hence a large amount of parent vector DNA (200 ng) is critically required. This thermocycling reaction was performed using Phusion DNA polymerase as described earlier, yet with thermocycling conditions consisting of initial denaturation at 98°C for 3 minutes before entering a cycle of denaturation at 98°C for 10 seconds, annealing at 55°C for 30 seconds and extension at 72°C for 20 minutes. After 25 cycles, the thermocycling reaction was terminated by a final extension phase at 72°C for 10 minutes. After this step, the parental methylated DNA template was digested with DpnI (NEB, Cat# R0176S), selecting the synthesized DNA containing the required mutations. Finally, these nicked mutated plasmids were transformed into competent cells.

Table 2.3 Primers for Site-Directed Mutagenesis. Forward primers for site-directed mutagenesis in which the introduced mutations are highlighted

Primer Name	Sequence (5'-3')
iAUG 1 EGFR F	GTCCCCGGCGCAGCGATGCCGCAGCAGCCTC
iAUG 2 EGFR F	GCCCGACGCGGCCGATGCGGCCGGAGTCCCGA
Con 2 EGFR F	GCCCGACGCGGCCGAAGCGGCCGGAGTCCCGA
iAUG 3 EGFR F	CGGAGTCCCGAGCTATGCCCGGCGGCCGCCGC
Con 3 EGFR F	CGGAGTCCCGAGCTATTCCCGGCGGCCGCCGC
iAUG 4 EGFR F	CGAGCTAGCCCCGGCGGCAATATGAGCCCAGACCGGA-CGACAG
Con 4 EGFR F	CGAGCTAGCCCCGGCGGCAATATTAGCCCAGACCGGA-CGACAG
iAUG 5 EGFR F	CCAGACCGGACGACATGCCACCTCGTCGGCG
Con 5 EGFR F	CCAGACCGGACGACAAGCCACCTCGTCGGCG
iAUG 6 EGFR F	CCGCCTCGCCGCCAATGCCACAACCACCGCG
Con 6 EGFR F	CCGCCTCGCCGCCAAAGCCACAACCACCGCG
iAUG 7 EGFR F	CACAACCACCGCGCATGGCCCCCTGACTCCG
Con 7 EGFR F	CACAACCACCGCGCAAGGCCCCCTGACTCCG
iAUG 8 EGFR F	CCACCGCGCACGGCCCCATGACTCCGTCCAGTATTG
Con 8 EGFR F	CCACCGCGCACGGCCCCTTGACTCCGTCCAGTATTG
iAUG 9 EGFR F	GACTCCGTCCAGTATGGATCGGGAGAGCCGG
Con 9 EGFR F	GACTCCGTCCAGTATCGATCGGGAGAGCCGG

2.2.10 Total Protein Extraction

Total protein extraction from MCF-7 and MDA-MB-231 cells was performed using RIPA buffer (150 mM sodium chloride, 1.0% NP-40, 0.5% sodium deoxycholate, 0.1% SDS (sodium dodecyl sulphate) 50 mM Tris, pH 8.0) supplemented with 1 tablet of protease inhibitors per 10 ml of extraction solution (Roche, Cat# 11836153001). Briefly, cells grown in 24-well plates were washed with ice-cold PBS before being lysed with 500 µl of RIPA buffer per well. The resulting cell suspension was then transferred into a pre-cooled microcentrifuge tube and incubated for 20 minutes on ice. After centrifugation at 14,000 rpm for 20 minutes at 4°C, the supernatant was collected and kept on ice for further applications or stored at -80°C.

2.2.11 Total Protein Quantification

Bradford protein assay was used to measure the concentration of proteins in samples. In principle, this assay is based on the interaction between the amino-acid residues of proteins and the Coomassie dye under acidic conditions resulting in a colour change detected at 595 nm (Bradford, 1976). Briefly, 2 µl of each sample was mixed with 200 µl of 1X Bradford reagent (Bio-Rad, Cat# 5000006) before measuring the optical absorbance at 595 nm. To determine the protein concentration, the optical absorbance of each sample was compared to a standard curve of bovine serum albumin (BSA) standards. Six standards including a blank, and 2 µg/ml, 4 µg/ml, 6 µg/ml, 8 µg/ml and 10 µg/ml standards were used to perform a linear regression with an R value between 0.99 and 0.95 to calculate the protein concentration of unknown samples.

2.2.12 SDS Polyacrylamide Electrophoresis

SDS polyacrylamide gel electrophoresis was utilised to separate a mixed population of proteins based on their molecular weight using a Bio-Rad vertical mini-gel electrophoresis system. Briefly, 10% gels were prepared by combining 3.3 ml of 30% w/v acrylamide (Protogel, Cat# A2-0072) with 2.5 ml of 1.5 M Tris pH 8.8, 0.1 ml of 10% SDS and 4 ml of water. Just before casting the gel, 0.1 ml of 10% ammonium persulfate (APS) and 0.006 ml of TEMED were added to the mixture to initiate the polymerisation reaction. After that, the resulting mixture was poured between the two glass plates to set and covered with 100% propan-2-ol. After 20 minutes, the propan-2-ol layer was poured off and replaced with a stacking-gel mixture composed of 0.33 ml of 30% w/v acrylamide, 0.25 ml of 1.0 M Tris pH 6.8, 0.02 ml of 10% SDS, 1.4 ml of water, 0.02 ml of 10% APS and 0.002 ml of TEMED before adding a comb to make the wells. Once completely set, gels were immersed in 1X SDS-PAGE running buffer (25 mM Tris-HCl; 192 mM glycine; 0.1% SDS) after removing combs. A protein ladder and samples were then loaded after denaturing in 1X SDS loading dye (50 mM Tris-HCl pH 6.8, 2% SDS, 10% glycerol, 5% β-mercaptoethanol, 0.002% bromophenol Blue) at 95°C for 10 minutes. The gel was run at 100 V until the separation required was achieved.

2.2.13 Western Blotting

After protein separation, the gel was placed on a methanol-activated PVDF (polyvinylidene fluoride) transfer membrane, 45 µm (Thermo Scientific, Cat# 88518) layered in between blot absorbent filter papers (Bio-Rad, Cat# 1703965) soaked in blotting buffer (25 mM Tris, 192 mM glycine, 20% methanol).

After assembling the transfer block, proteins were blotted for 16.65 hours at 30 V using Mini Trans-Blot Cell (Bio-Rad). After that, the membrane was blocked for 1 hour with 5% skimmed milk (Marvel) in tris-buffered saline with tween (TBS-T, 150 mM NaCl, 50 mM Tris, 0.1% tween-20) before incubating with a primary antibody in fresh blocking solution overnight at 4°C with agitation. The membrane was then washed three times in TBS-T for 15 minutes before incubating with a species-specific horseradish peroxidase-conjugated secondary antibody in blocking solution for 1 hour at room temperature with agitation. Antibodies used were the rabbit anti-EGFR antibody 1:5000 (Sigma Aldrich, PLA0101), mouse anti-DDX3 antibody 1:1000 (Abcam, Cat# ab196032), mouse anti-β-actin antibody 1:5000 (Sigma-Aldrich, Cat# A5441), anti-rabbit IgG, HRP-linked antibody 1:2000 (Cell Signalling Technology, Cat# 7074) and anti-mouse IgG, HRP-linked antibody 1:2000 (Cell Signalling Technology, Cat# 7076). After a second washing step, blots were visualised by chemiluminescence using Pierce ECL western blotting substrate (Thermo Scientific, Cat# 32209), scanned using Fujifilm LAS- 4000 luminescent image analyser and quantified using ImageJ (US National Institutes of Health, Bethesda, Maryland, USA).

2.2.14 Immunocytochemistry

Indirect immunofluorescence was carried out to assess the expression of γ-H2AX following the induction of genotoxic stress. After seeding MCF-7 cells at a density of 1 x 10^4 cells/well in 8 well chamber slides (Ibidi, Cat# 80826) and exposing them to genotoxic agents, the cells were fixed with 4% paraformaldehyde solution for 10 minutes before being permeabilised with 0.2% Triton-X100 solution for 2 minutes.

After blocking with 3% BSA, the cells were incubated sequentially with the rabbit anti-phospho-histone H2A.X antibody 1:800 (Cell Signalling Technology, Cat# 2577), anti-rabbit IgG, Alexa Fluor 488 secondary antibody at 2 µg/ml (Invitrogen, Cat# A-21206) and DRAQ 5 fluorescent probe solution at 1:5000 (Invitrogen, Cat# 62251). Fluorescent microscopy images were taken using a confocal microscope (Zeiss LSM 510).

2.3 Bacterial Methods

2.3.1 Competent DH5α *Escherichia coli* Preparation

The first step in this process was to grow a 5 ml Luria Bertani (LB) starter culture from a single *Escherichia coli* (*E. coli*) colony (Invitrogen, Cat# 18288019) overnight at 37°C with agitation. The starter culture was then inoculated into 250 ml of LB medium supplemented with 20 mM $MgSO_4$ and incubated until the optical density was between 0.4 and 0.6 at 600 nm. After centrifugation at 4000 rpm for 10 minutes at 4°C, the cells were gently resuspended in 100 ml of ice-cold TBF1 (30 mM KOAc, 10 mM $CaCl_2$, 50 mM MnCl2, 100 mM RbCl, 15% glycerol) and incubated on ice for 5 minutes. The cells were then resuspended in 10 ml of ice-cold TBF2 (10 mM MOPS (pH 6.5), 75 mM $CaCl_2$, 10 mM RbCl, 15% glycerol) and incubated for 60 minutes on ice before aliquoting and snap freezing in liquid nitrogen. Aliquots were stored at -80°C for future use.

2.3.2 Transformation of Competent DH5α *E. coli*

In this process, plasmids were gently mixed with 50 µl of competent DH5α *E. coli* and then incubated on ice for 20

minutes. After that, cells were exposed to a heat shock at 42°C for 1 minute followed by incubation on wet ice for 2 minutes. After that, the cells were grown in 1 ml of LB media for 1 hour in a shaking incubator at 37°C before spreading onto an LB plate containing ampicillin at 100 µg/ml and incubated overnight at 37°C. After purification, the resulting plasmids were confirmed by diagnostic digest and sequencing.

2.3.3 Small-Scale Isolation of Plasmid DNA

Wizard Plus SV Miniprep DNA purification kit (Promega, Cat# A1460) was used to isolate plasmids from 5-10 ml of LB cultures according to the manufacturer's recommendations. Briefly, a single colony was inoculated in 5-10 ml of liquid LB supplemented with ampicillin at 100 µg/ml and incubated overnight at 37°C with agitation. After that, bacterial cells were resuspended in a solution composed of 50 mM Tris-HCl, pH 7.5, 10 mM EDTA and 100 µg/ml RNase and then lysed using Lysis solution (0.2 M NaOH and 1% SDS) supplemented with alkaline protease to induce degradation of cellular proteins. After incubation for 5 minutes at room temperature, Neutralisation solution (4.09 M guanidine hydrochloride, 0.759 M potassium acetate and 2.12 M glacial acetic acid, pH 4.2) was added to stop the reaction before centrifuging at 13,000 rpm for 10 minutes at room temperature. The supernatant was then applied to one of the provided DNA binding columns and centrifuged at 13,000 rpm for 1 minute. After washing the column twice with Column Wash solution (60% ethanol, 60 mM potassium acetate, 8.3 mM Tris-HCl, 0.04 mM EDTA), 50 µl of nuclease-free water was added to elute the DNA by centrifugation at 13,000 rpm for 2 minutes. Plasmid DNA was stored at -20°C for future use.

2.3.4 Large-Scale Isolation of Plasmid DNA

To prepare a large plasmid stock, Plasmid Maxi kit (Qiagen, Cat# 12163) was used following the manufacturer's instructions. Briefly, a starter culture was prepared by inoculating a single *E. coli* colony into 5 ml of LB containing 100 µg/ml ampicillin at 37°C for 8 hours. After that, the starter culture was inoculated into 300 ml of LB media supplemented with ampicillin and incubated overnight with agitation at 37°C. Next, the bacterial pellet was resuspended in Buffer P1 (50 mM Tris·HCl, pH 8.0, 10 mM EDTA, and 100 µg/ml RNase A) after centrifugation at 4000 rpm for 30 minutes at 4°C. The bacterial cells were lysed by mixing with Buffer P2 (200 mM NaOH, 1% SDS) before incubating for 5 minutes at room temperature. To stop the reaction, the lysate was mixed with P3 buffer (3.0 M potassium acetate, pH 5.5) and incubated on ice for 20 minutes.

The resulting mixture was then centrifuged at 4000 rpm for 45 minutes at 4° C before allowing the supernatant to pass through one of the provided DNA binding columns by gravity. Following two washing steps with Buffer QC (1.0 M NaCl; 50 mM MOPS, pH 7.0; 15% propan-2-ol), the DNA was eluted using Buffer QF (1.25 M NaCl; 50 mM Tris·HCl, pH 8.5; 15% propan-2-ol). Next, the DNA was precipitated by the addition of chilled 0.7X-volume 100% propan-2-ol and subsequently centrifuged at 6500 rpm for 30 minutes at 4° C. The DNA pellet was then collected by 500 µl of nuclease-free water and then mixed with 1 ml of chilled absolute ethanol to precipitate DNA. Following centrifugation at 13000 rpm for 2 minutes, the DNA pellet was washed with 70% ethanol, vacuum dried, and then re-suspended in nuclease-free water. DNA aliquots were stored at -20°C for future use. To examine the purity and concentration

of the DNA yield, the spectral absorbance was assessed using a Nanodrop 100 spectrophotometer.

2.4 Computational-Biology Methods

2.4.1 The Atlas of UTR Regulatory Activity

To investigate a potential RNA-protein interaction between the *EGFR* 5' UTR and the RNA-helicase DDX3, the Atlas of UTR Regulatory Activity (AURA) version 2.5.0 was used to investigate the presence of a binding site of DDX3 on the *EGFR* 5' UTR. Accordingly, the EGFR 5' UTR was queried by the gene name through the web interface of this manually curated catalogue of human UTRs. All relevant 5' UTRs were then selected, and their regulatory annotations were viewed using the explore option.

2.4.2 The Nucleotide Basic Local Alignment Search Tool

To investigate the consensus of the identified stem-loop structure located on the *EGFR* 5' UTR proximal to the predicted binding site of DDX3, the Nucleotide Basic Local Alignment Search Tool (BLAST) engine was used to find regions of similarities between the reported sequences of the *EGFR* 5' UTR across available species. The resulting database was then processed and visualised for multiple sequence alignment using Clustal Omega and Jalview Desktop with default parameters.

2.4.3 GGGenome

To evaluate the specificity of nucleic acid hybridisation of the developed gapmer ASOs, GGGenome was utilised to find complementary target sequences while allowing for varying degrees of mismatching. The transcript database RefSeq Human RNA Release 90 was used by this ultrafast sequence search engine to generate the results summarised in Table 5.3.

2.5 Physicochemical Methods

2.5.1 Syntheses of Base Monomers for Michael Addition

Azobenzene diacrylamide and azobenzene diacrylate were synthesised by reacting azobenzene-4,4'-dicarbonyl dichloride (Tokyo Chemical Industry, Cat# A1575) with N-hydroxyethyl acrylamide (Sigma Aldrich, Cat# 697931) and 2-hydroxyethyl acrylate (Sigma Aldrich, Cat# 292818), respectively. Briefly, these base monomers were synthesised by reacting a solution of azobenzene-4,4'-dicarbonyl dichloride (1.04916 g, 1 equivalence), triethylamine (TEA, 1900 µl, 4 equivalence) and dichloromethane (DCM, 100 ml) with either N-hydroxyethyl acrylamide (1.57312 g, 4 equivalence) or 2-hydroxyethyl acrylate (0.872685 g, 2.2 equivalence) to get azobenzene diacrylamide and azobenzene diacrylate, respectively. The reaction was carried out overnight at room temperature after starting the reaction on ice for 20 minutes under argon atmosphere. Azobenzene diacrylamide: ^{1}H NMR (400 MHz, C_2D_6OS) δ_H 8.42 (t, 2H, H_2C=CHCON**H**), 8.23 (d, 4H, C_{12}**H**$_8N_2$), 8.06 (d, 4H, C_{12}**H**$_8N_2$), 6.24 (dd, 2H, **H**$_2$C=CHCONH), 6.14 (dd, 2H, H_2C=C**H**CONH), 5.63 (dd, 2H, **H**$_2$C=CHCONH), 4.38 (t, 4H,

$CH_2C\mathbf{H}_2CO_2$), 3.55 (q, 4H, $C\mathbf{H}_2CH_2CO_2$). ^{13}C NMR (100 MHz, C_2D_6OS) δ_c 165 ($CH_2CH_2\mathbf{C}O_2$), 154 ($H_2C{=}CH\mathbf{C}ONH$), 132 ($\mathbf{C}_{12}H_8N_2$), 131 ($\mathbf{C}_{12}H_8N_2$), 131 ($H_2C{=}\mathbf{C}HCONH$), 126 ($H_2\mathbf{C}{=}CHCONH$), 123 ($\mathbf{C}_{12}H_8N_2$), 64 ($CH_2\mathbf{C}H_2CO_2$), 38 ($\mathbf{C}H_2CH_2CO_2$). FTIR v cm-1: 3296 (s, N-H), 1785 (s, C=O ester), 1718 (s, C=O amide), 1644 (s, aromatic C=H), 1264 (s, C-O ester), 1405 (m, N=N), 951 (s, C=C alkene). ESI-MS: *m/z* = 487.16 $[M+Na]^+$. Azobenzene diacrylate: ^1H NMR (400 MHz, $CDCl_3$) δ_H 8.25 (d, 4H, $C_{12}\mathbf{H}_8N_2$), 8.00 (d, 4H, $C_{12}\mathbf{H}_8N_2$)**,** 6.50 (dd, 2H, $\mathbf{H}_2C{=}CHCO_2$), 6.20 (dd, 2H, $H_2C{=}C\mathbf{H}CO_2$), 5.90 (dd, 2H, $\mathbf{H}_2C{=}CHCO_2$)**,** 4.62 (t, 4H, $CH_2C\mathbf{H}_2CO_2$-Ar), 4.57 (t, 4H,$C\mathbf{H}_2CH_2CO_2$-Ar). FTIR ν cm^{-1}: 1722 (s, C=O ester), 1633 (m, aromatic C=H), 1495 (m, C-H alkane), 1409 (m, N=N), 1264 (m, C-O, aromatic ester), 996 (s, C=C alkene).

2.5.2 Purification of Base Monomers for Michael Reaction

Based on their solubility, the synthesised base monomers were purified using two different approaches. As it was insoluble in DCM, azobenzene diacrylamide was filtered out of the reaction using a Büchner filter system. On the other hand, azobenzene diacrylate was isolated using column chromatography. In brief, the reaction mixture was vacuumed dried until the total volume was reduced to approximately 20 ml then placed on the top of a column packed with silica gel 60-angstrom pore size, 35-70 micron (Fisher Scientific, Cat# 10773124). DCM was then applied as the mobile phase to differentially elute azobenzene diacrylate. Compounds travel at different rates due to their differential adsorption to the silica gel, allowing them to be separated according to their polarity into small fractions as they elute off the column. DCM was then removed from the fractions

containing azobenzene diacrylate as indicated by TLC (thin layer chromatography) via a rotary evaporator after washing with water to remove hydrophilic contaminants and then drying with sodium sulphate (Fisher Scientific, Cat# 7757-82-6).

2.5.3 Synthesis of Poly(β-Amino Ester) Polymers

Poly(β-amino ester)s (PBAEs) were synthesised using Michael addition in a single-pot reaction. Azobenzene diacrylate (200 mg, 1 molar equivalence) and 1,4-butanediol diacrylate (Sigma Aldrich, Cat# 411744) were reacted at varied ratios with 4-amino-1-butanol (Sigma Aldrich, Cat# 178330) dissolved in 1 ml dimethylformamide (DMF). In this reaction, the required amounts of azobenzene diacrylate and 1,4-butanediol diacrylate were first dissolved in DMF before adding 4-amino-1-butanol to initiate the polymerisation reaction. After 72 hours at 90°C with stirring, PBAEs were end-capped by reacting with an additional 0.2 M 4-amino-1-butanol in the dark at room temperature for 1 hour.

2.5.4 Purification of PBAEs

Polymers were then purified by double precipitation in diethyl ether. First, polymers dissolved in DMF were added dropwise to 10X-volume diethyl ether to precipitate before centrifugation at 4750 rpm for 5 minutes. After that, the supernatant was carefully aspirated and 5X-volume diethyl ether was added and thoroughly mixed. After the second round of centrifugation, the supernatant was removed and polymers were placed in a desiccator under vacuum for three days to remove residual solvent. Polymers were then stored at 4°C protected from light for future applications.

2.5.5 Characterisation of PBAEs

Polymers and synthesised base monomers were characterised via nuclear magnetic resonance (NMR) spectroscopy, Fourier transform infrared (FT-IR) spectroscopy and gel permeation chromatography (GPC). The chemical structure was characterised via ^{1}H NMR and ^{13}C NMR in a deuterated solvent (Bruker NMR400) and analysed using MestreNova 14.0.1 software. For additional structural investigations, the FT-IR spectrum was determined using Agilent FT-IR spectrometer. Polymers dissolved in DMF with 0.05 M LiBr were also characterised using PL-GPC 50 Plus Integrated GPC system to determine polymer molecular weight and polydispersity against linear polystyrene standards.

2.5.6 Gel Retardation Assay

The complexation stability of polyplexes and the hypoxic release of ASOs was investigated using the gel retardation assay. First, polymers dissolved in DMSO at 100 mg/ml and ASOs were diluted to achieve the same volume in 25 mM NaAc buffer (pH 5.0) before mixing them at a fixed ASO dose to achieve the required weight ratios. Polyplexes were then incubated for 10 minutes to self-assemble into nanoparticles. To investigate the hypoxic release of ASOs, formulated polyplexes were incubated in PBS with rat liver microsomes at 0.5 mg/ml (Sigma Aldrich, Cat# M9066) and 50 µM NADPH (Sigma Aldrich, Cat# 10107824001) for 2 hours while purging with argon for 20-120 minutes. After that, samples were mixed with 6X gel loading dye, no SDS (NEB, Cat# B7025S) and loaded onto a 1% agarose gel containing ethidium bromide at 1 µg/ml. Gel

electrophoresis was carried out in TEA at 100 V for 20 minutes prior to visualisation under UV.

2.5.7 Nanoparticle Characterisation

Nanoparticle size and zeta potential were characterised using Malvern's Zetasizer ZS particle and zeta potential analyser. For particle size measurements, polyplexes were formulated in 25 mM NaAc (pH 5.0) at a varied ASO dosage and a fixed polymer concentration of 0.1 mg/ml and then the hydrodynamic diameter was assessed by dynamic light scattering (DLS) in disposable micro cuvettes. Samples were then mixed with 10 mM NaCl at a dilution factor of 2 to assess the zeta potential by electrophoretic light scattering in zeta cuvettes (Malvern Panalytical, Cat# DTS1070) at 25°C.

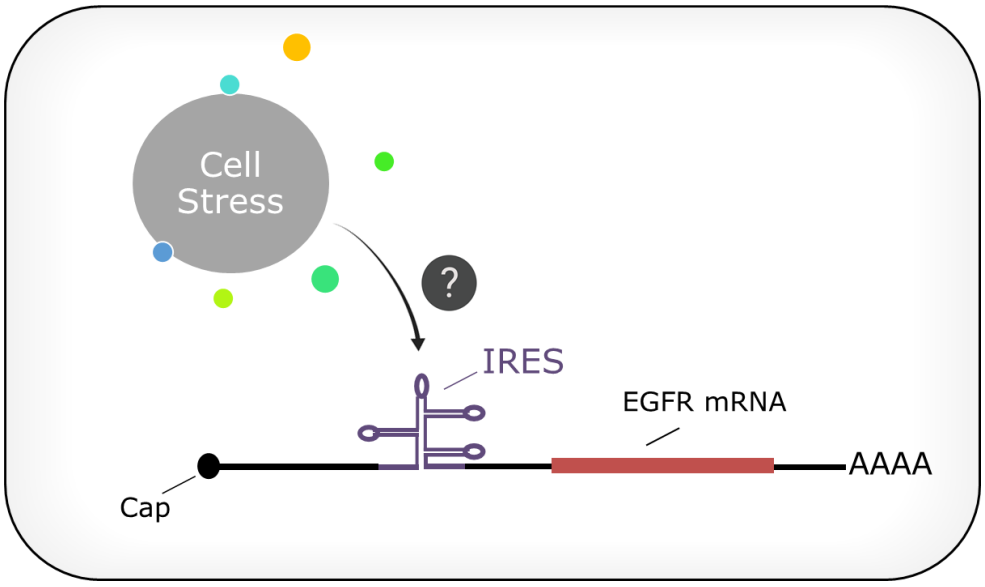
2.6 Statistical Analysis

Unpaired student t-test or ordinary one-way ANOVA followed by Dunnett's multiple comparison test were performed using GraphPad Prism version 7.02 (GraphPad Software Inc, La Jolla, CA, USA). A difference in mean of two data sets with a p-value less than 0.05 was considered statistically significant. Data are expressed as mean ± standard deviation.

Chapter Three

3 Cell Stress and the *EGFR* 5’ UTR

Graphical summary



3.1 Introduction

During RNA synthesis in eukaryotic cells, most precursor messenger RNAs are capped with a 7-methylguanylate group (m^7G) on their 5′ ends (Moteki and Price, 2002). This universal cap structure is utilised by the translation machinery to initiate translation for protein synthesis. This cap-dependent process requires the interaction of eukaryotic initiation factor 4E (eIF4E) as part of the trimeric complex eIF4F with the mRNA 5′ end and the subsequent recruitment of the 43S preinitiation complex containing the 40S ribosomal subunit and the ternary initiator tRNA–eIF2–GTP complex. The 40S ribosomal subunit then scans the 5′ untranslated region (5′ UTR) in a 5′-to-3′ direction until the encounter of an appropriate initiation codon where it joins the 60S large ribosomal subunit, forming the 80S ribosomes to initiate peptide synthesis. This highly regulated process is the primary mode of translation initiation in eukaryotes (Sonenberg and Hinnebusch, 2009).

Translation control with a focus on the initiation phase is a key regulator of gene expression under conditions of cell stress, and it is primarily based on the availability of translation initiation factors. Cells often respond to cell stress by inhibiting cap-dependent translation mainly via limiting the availability of the ternary complex and the cap-binding protein eIF4E (Gebauer and Hentze, 2004). In order for the cells to survive under such conditions, alternative mechanisms of translation initiation including initiating translation through internal ribosome entry sites (IRESs) act to allow the expression of proteins important for cellular survival and recovery (Spriggs et al., 2008). As not all cellular IRESs respond to all types of cell stress, the activation of cellular IRESs is also dependent on the expression

and subcellular localisation of specific IRES trans-acting factors (ITAFs). For instance, the IRES-mediated expression of *BAG1* mRNA following genotoxic stress was found to be dependent on the re-localisation of the *BAG1* IRES ITAFs, PCBP1 and PTBP from the nucleus to the cytoplasm (Dobbyn et al., 2008). Therefore, the IRES activity does not only depend on its structural elements but also on *in trans* assistance from translation initiation factors and ITAFs (Yang and Wang, 2019).

In this regard, it was reported previously that the *EGFR* 5' UTR contains an IRES that allows hypoxic expression and has a high requirement for eIF4A in SH-SY5Y cells (Webb et al., 2015). Dependence on the IRES-mediated expression of EGFR was also found to be increased under serum starvation and rather decreased in endoplasmic stress in the U87-MG cell line (Daniel Smalley, 2016). To gain further insight about the activity of the *EGFR* IRES in other conditions of cells stress in the context of breast cancer, this chapter aims to investigate whether the induction of genotoxic stress, endoplasmic reticulum (ER) stress, iron overload, inflammation and oxidative stress could lead to increased IRES-mediated expression of EGFR in MCF-7 cells.

A widely-adopted method for assessing IRES activity is to clone the DNA sequence encoding a potential IRES into the intercistronic region of a bicistronic reporter. The co-expression of both reporter genes from a single promoter results in the generation of a bicistronic mRNA transcript in which the first cistron is expressed through cap-dependent translation while the translation of the second cistron is mediated by IRES activity. Firefly (*Photinus pyralis*) and *Renilla* (*Renilla reniformis*) luciferases are frequently used as reporter genes in these bicistronic plasmids. These proteins generate their

bioluminescent signals immediately after translation as they do not require post-translation modifications. These enzymes have also distinct substrate requirements, allowing discrete detection of their luminescence signals in the same experiment (Thompson, 2012).

In this regard, the bicistronic vector pREF, which encodes both the *Renilla* and firefly luciferases, was used to assess the activity of the *EGFR* IRES. In this vector, the 5' UTR of the *EGFR* mRNA (NM_201283.1), was previously inserted into the intercistronic region of pRF, controlling the expression of the downstream open reading frame of the firefly luciferase (Webb et al., 2015). To account for variations in cell viability and transfection efficiency among replicates, the firefly luciferase readings were normalised to the respective readings of *Renilla* luciferase (Figure 3.1).

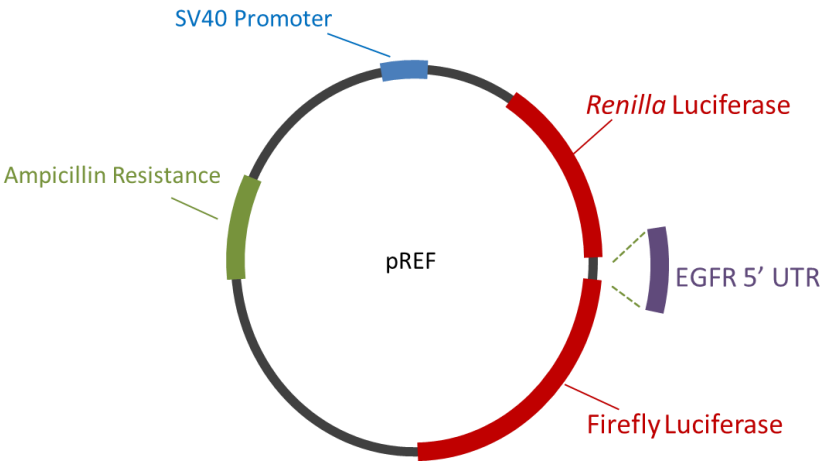


Figure 3.1 Map of the pREF plasmid. Transcription of pREF from a single promoter generates a bicistronic mRNA in which the expression of the firefly luciferase is controlled by the *EGFR* 5' UTR.

3.2 Effect of Cell Stress

3.2.1 Effect of Genotoxic Stress

Genotoxic stress results from exposure to a wide variety of exogenous and endogenous factors including reactive oxygen species, inflammation, ionizing and non-ionizing radiation, genotoxic chemicals and even through DNA replication. Exposure to genotoxic stress elicits highly sophisticated biochemical responses that detect and repair DNA lesions preventing the acquisition and transmission of potentially deleterious mutations (Coates et al., 2005).

In this regard, the upregulation of EGFR activity has been linked to mediating resistance to radiotherapy and chemotherapy in cancer via enhancing the DNA damage response (Reardon et al., 1999, Mendelsohn and Baselga, 2003, Yu et al., 2012, Liccardi et al., 2011). After exposure to ionising radiation and induction of DNA damage, EGFR translocates into the nucleus to activate DNA-protein kinase (DNA-PKcs) which is involved in the formation of the DNA end-binding complex necessary for the non-homologous end-joining (NHEJ) response to double-strand breaks (Dittmann et al., 2005, Dittmann et al., 2008).

EGFR can also modulate DNA synthesis and repair via tyrosine phosphorylation of histone H4; thereby facilitating the recruitment of histone methyltransferases and subsequent methylation of the lysine residue K20 that is involved in DNA replication and repair. Indeed, disrupting this interaction demonstrated tumour-suppressive activity in breast cancer cells, underscoring the importance of EGFR in the context of the DNA damage response (Chou et al., 2014).

Translational reprogramming also protects against genotoxic stress by initiating general repression of mRNA translation while promoting the translation of selected mRNAs encoding DNA repair enzymes. For instance, UV-B radiation was found to reduce the rate of protein synthesis by increasing the phosphorylation of eIF2α. Yet mRNAs encoding proteins involved in DNA repair were found to be efficiently translated under such conditions due to increased polysomal association (Powley et al. 2009). Conversely, ionising radiation, bleomycin and etoposide were found to reduce global protein expression via inhibiting the activity of eIF4E (Jeffrey et al., 2002, Le Bouffant et al., 2006, von Stechow et al. 2015).

Therefore, to investigate whether genotoxic stress could increase EGFR production through translational control, the IRES-activity of the *EGFR* 5' UTR was examined using pREF following treatment with different genotoxic chemicals (cryptolepine, phleomycin, and etoposide) or exposure to UV-B radiation. The induction of DNA damage using these genotoxic measures can induce distinct types of DNA lesions. Cryptolepine, a plant alkaloid, is considered a topoisomerase II inhibitor similar to etoposide, resulting mainly in double strands breaks (Pal and Katiyar, 2016). On the other hand, phleomycin, a natural glycopeptide, is a DNA intercalator that is highly efficient in inducing DNA single-strand breaks (Sleigh, 1976). In contrast to the induction of DNA strand breaks associated with cryptolepine, phleomycin and etoposide treatment; UV-B radiation mainly leads to the development of DNA adducts, leading to the distortion of DNA structure (de Lima-Bessa et al., 2008).

As shown in Figure 3.2, treatment with cryptolepine resulted in differential changes in the normalised expression of the firefly luciferase in pREF ($p < 0.01$). Treatment with cryptolepine at 5 µg/ml for 24 hours significantly decreased the activity of the *EGFR* IRES in mediating the expression of firefly luciferase ($p = 0.0073$). Conversely, cryptolepine at a lower concentration, 2.5 µg/ml, has significantly increased the relative activity of firefly luciferase by 54.39% (±0.1120; $p = 0.0067$).

It should be noted that the half-life of the firefly luciferase is 3.5 hours which is slightly shorter than the half-life of the *Renilla* luciferase (4.5 hours). Hence, this could negatively affect the observed increase in the relative activity of the firefly luciferase, while positively affect the relative decrease in firefly to *Renilla* luminescence (Leclerc et al., 2000, Thorne et al., 2010). Nevertheless, the effects associated with cryptolepine treatment suggest that inducing moderate DNA damage by cryptolepine has resulted in more significant inhibition of the cap-dependent translation of the *Renilla* luciferase in comparison to the IRES-mediated translation of the firefly luciferase.

To confirm whether these changes in the *EGFR* IRES activity were caused by the genotoxic effects of cryptolepine, the normalised expression of pREF was assessed after treating MCF-7 cells with the radiomimetic drug phleomycin (Figure 3.3). As can be seen from Figure 3.3A, there was also a significant increase in the relative activity of firefly luciferase following 24-hour treatment with phleomycin in a concentration-dependent manner ($p = 0.0044$). In particular, 1 µg/ml phleomycin treatment significantly increased the relative firefly activity by 25.08% (±0.1769; $p = 0.0016$).

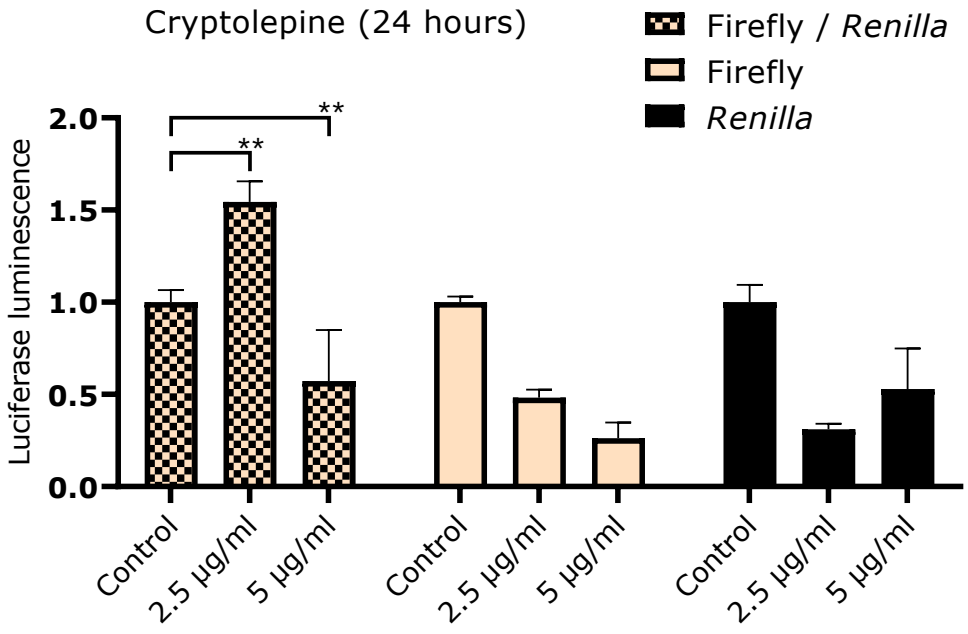


Figure 3.2 Relative activity of the *EGFR* IRES following treatment with cryptolepine. After 24 hours of plasmid transfection, MCF-7 cells were treated with cryptolepine at 2.5 µg/ml or 5 µg/ml for 24 hours before assessing the relative activity of firefly luciferase (the activity ratio of firefly to *Renilla* luciferase). N = 3 – 6. Data derived from two independent experiments. Control treated with an equivalent solvent amount. Error bars represent standard deviation. Ordinary one-way ANOVA followed by Dunnett's post hoc test. ** indicates $P < 0.01$.

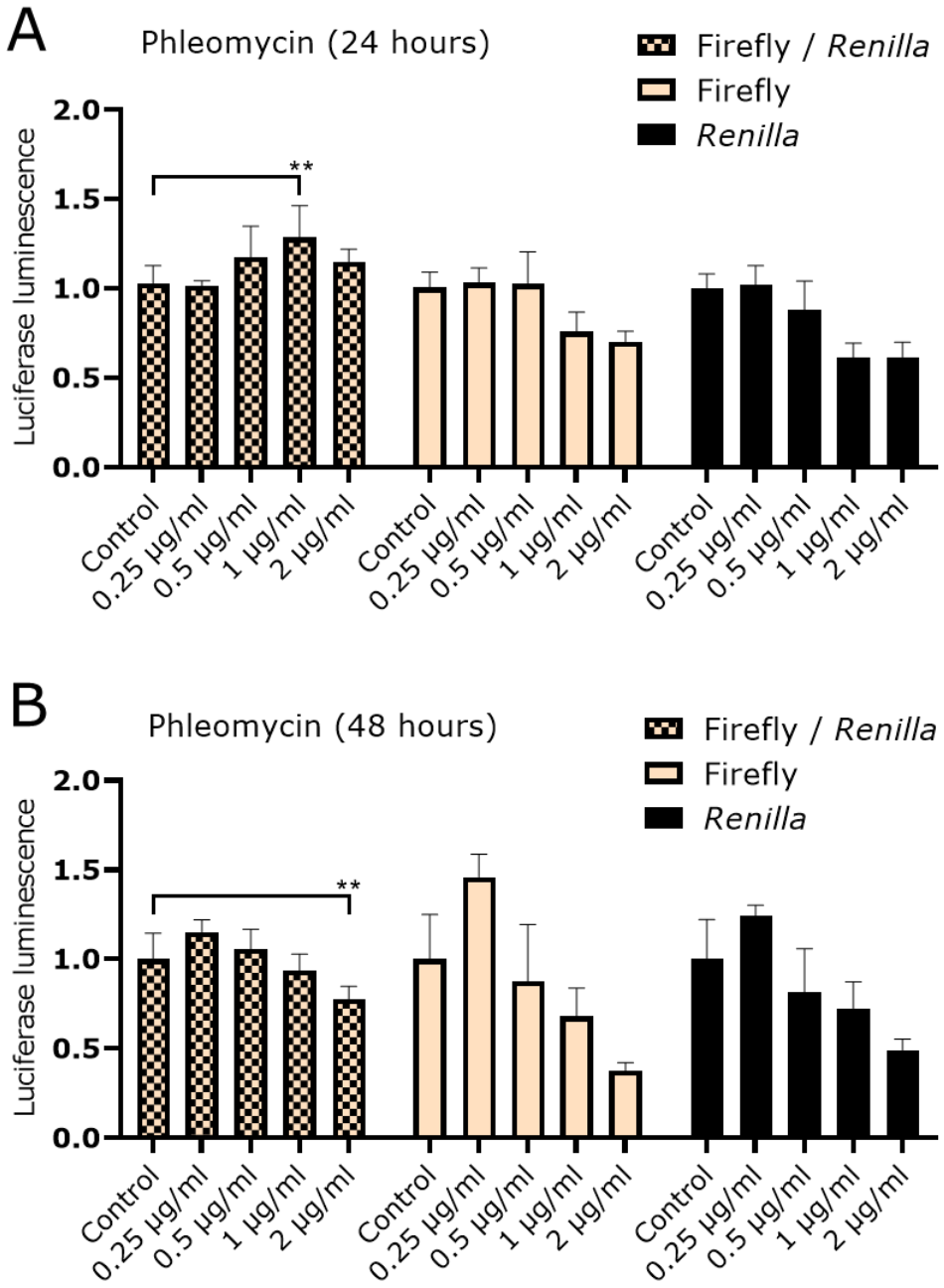


Figure 3.3 Relative activity of the *EGFR* IRES following treatment with phleomycin. After 24 hours of plasmid transfection, MCF-7 cells were treated with phleomycin at 0.25 µg/ml, 0.5 µg/ml, 1 µg/ml, or 2 µg/ml for 24 hours **(A)** and 48 hours **(B)** before assessing the relative activity of firefly luciferase. N = 3 – 9. Data derived from three independent experiments. Control treated with an equivalent solvent amount. Error bars represent standard deviation. Ordinary one-way ANOVA followed by Dunnett's post hoc test. ** indicates $P < 0.01$.

After that, we assessed whether increasing the incubation time of phleomycin could induce any further changes, hence the same concentrations of phleomycin were used for 48 hours before assessing for luciferase activity. From the data in Figure 3.3B, it is apparent that increasing the incubation time of phleomycin has differentially affected the response of the *EGFR* IRES to phleomycin treatment ($p < 0.01$). Treatment with phleomycin for 48 hours resulted in a trend of increase in the relative activity of firefly luciferase at concentrations different than incubating for just 24 hours. As shown in Figure 3.3B, the most notable increase in the relative expression of firefly luciferase occurred at 0.25 µg/ml, highlighting the positive effect of increasing the incubation time on increasing the potency of phleomycin treatment. In concordance with cryptolepine findings, higher concentrations of phleomycin for 48 hours induced a decrease in the *EGFR* IRES activity (Figure 3.3B). Treatment with phleomycin at 2 µg/ml has induced a significant decrease in the relative activity of firefly luciferase ($p = 0.0090$).

Similarly, treatment with the topoisomerase II inhibitor etoposide resulted in comparable changes in the relative expression of firefly luciferase. While there was a trend of increase in the relative activity of firefly luciferase following treatment with etoposide for 24 hours (Figure 3.4A), there was a significant decrease in the activity following treatment for 48 hours in a concentration-dependent manner (Figure 3.4B, $p < 0.001$).

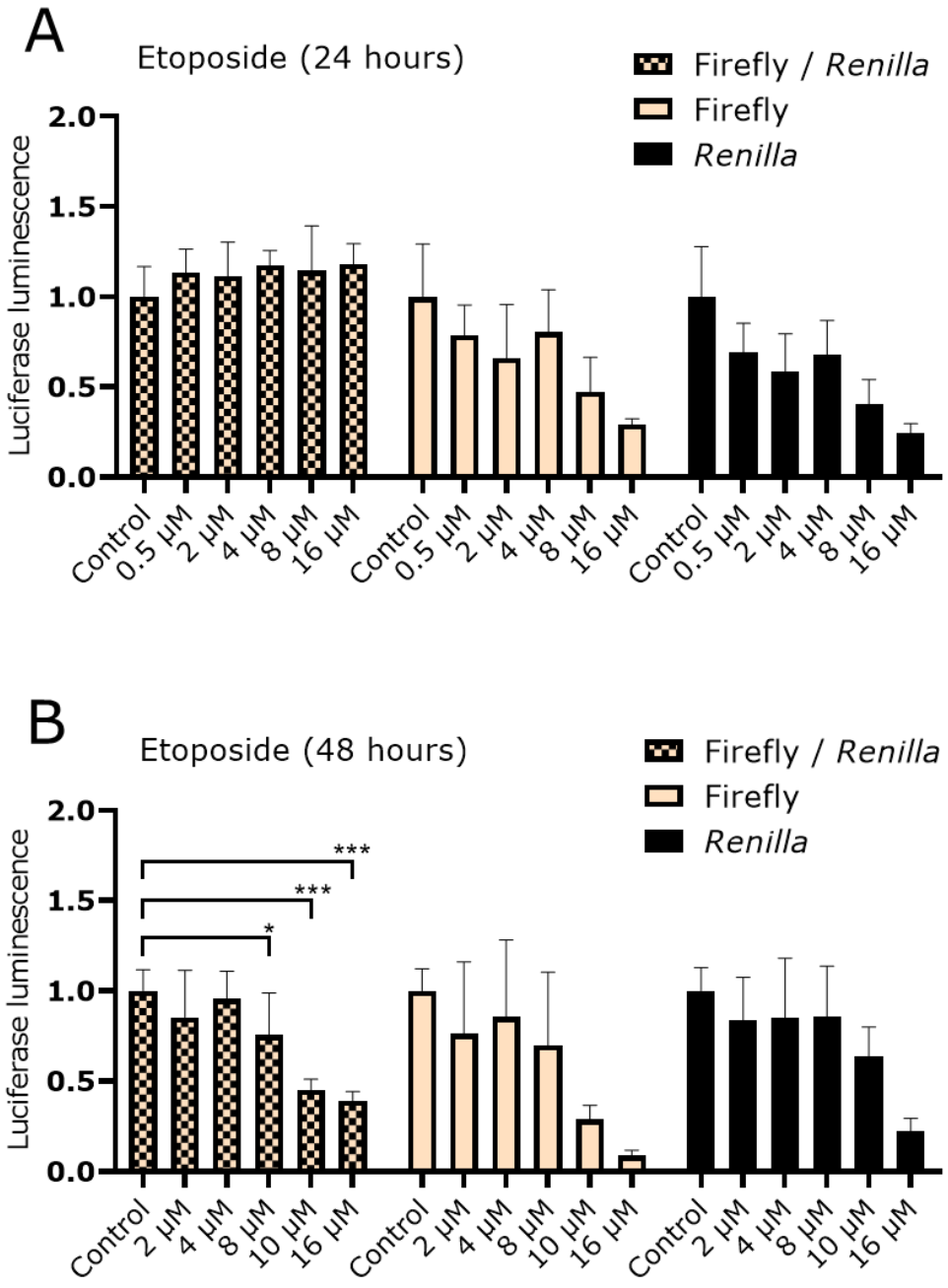


Figure 3.4 Relative activity of the *EGFR* IRES following treatment with etoposide. After 24 hours of plasmid transfection, MCF-7 cells were treated with etoposide at 0.5 µM, 2 µM, 4 µM, 8 µM, 10 µM, or 16 µM for 24 hours **(A)** and 48 hours **(B)** before assessing the relative activity of firefly luciferase. N = 3 – 9. Data derived from three independent experiments. Control treated with an equivalent solvent amount. Error bars represent standard deviation. Ordinary one-way ANOVA followed by Dunnett's post hoc test. * indicates $P<0.05$, *** indicates $p < 0.001$.

The normalised expression of the firefly luciferase was also assessed after exposing MCF-7 cells to sub-lethal doses of UV-B radiation. As can be seen from Figure 3.5, UV-B radiation at all tested doses resulted in no significant changes, as the activity of both luciferases was increased to the same extent, leading to a lack of any significant changes in the relative activity of the firefly luciferase.

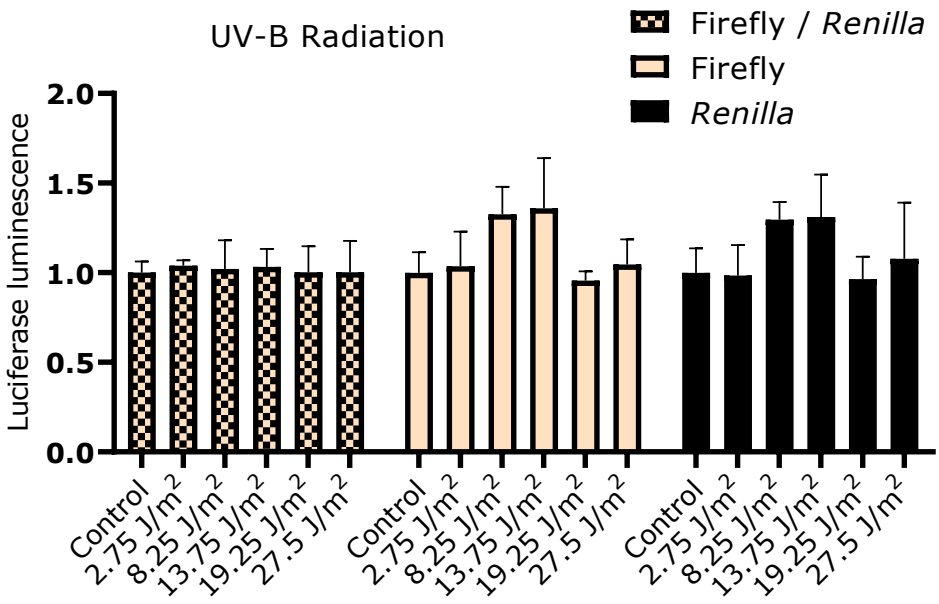


Figure 3.5 Relative activity of the *EGFR* IRES following exposure to UV-B radiation. After 24 hours of plasmid transfection, MCF-7 cells were exposed to 2.75 J/m^2, 8.25 J/m^2, 13.75 J/m^2, 19.25 J/m^2, or 27.5 J/m^2 of UV-B radiation after discarding exhausted medium. Then, the relative activity of firefly luciferase was assessed after 24 hours of incubation. N = 3 – 6. Data derived from two independent experiments. Values are normalised to control which represents untreated cells. Error bars represent standard deviation.

What stands out in these genotoxic findings is the differential expression of the firefly luciferase in response to the concentration and incubation time of cryptolepine and

phleomycin. Using low doses of either agent has increased the relative expression of the firefly luciferase that is mediated by the *EGFR* 5′ UTR. Yet increasing their potency by increasing the concentration or incubation time has negatively affected the expression of the firefly luciferase. This non-linear hormetic relationship between the EGFR IRES activity and the extent of DNA damage is consistent with other stress conditions and their response mechanisms including the impact of oxidative stress on cancer cell proliferation (Zelenka et al., 2018). Taken together, these results might indicate that inducing moderate DNA damage in breast cancer cells could prefer IRES-mediated translation of EGFR by influencing a more significant inhibition on cap-dependent translation. Conversely, high levels of DNA damage have led to a greater reduction in IRES-mediated translation.

Effects of Genotoxic Stress on the Development of DNA Double-Strand Breaks and Cellular Viability

The phosphorylation of the histone H2A variant is considered an early step in the DNA damage response against double-strand breaks (Kuo and Yang, 2008). To distinguish between the applied genotoxic measures with regards to their ability to induce double-strand breaks, the expression level of the phosphorylated histone H2A variant (γ-H2AX) was determined after exposing MCF-7 cells to phleomycin, etoposide or UV-B radiation. In accordance with previous studies, the expression of γ-H2AX was only increased following treatment with etoposide (Figure 3.6A).

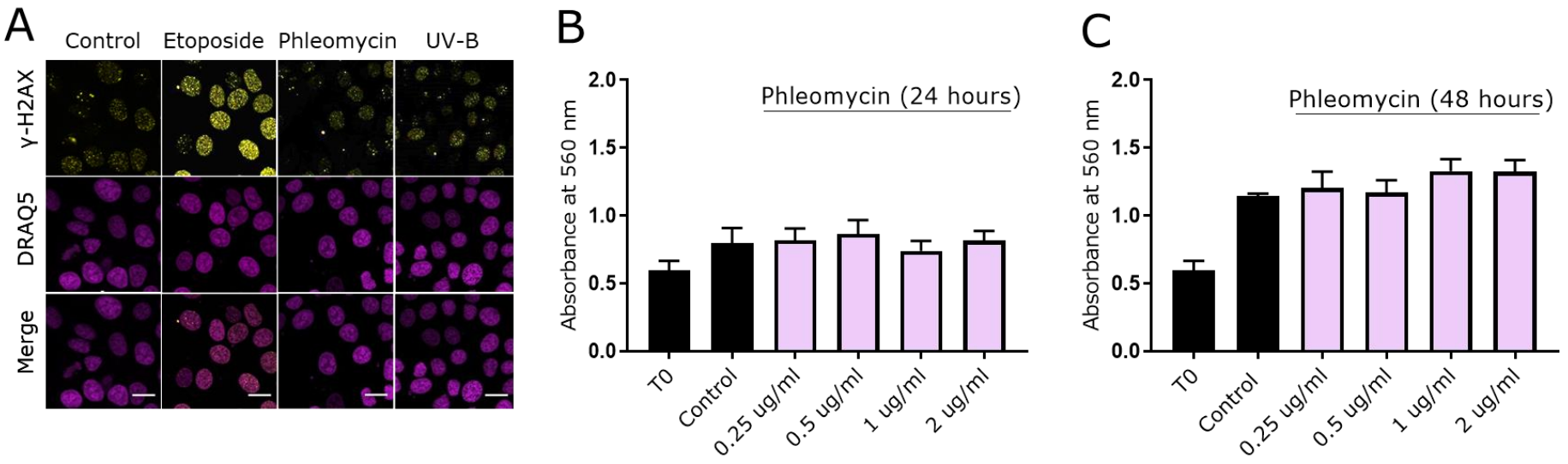


Figure 3.6 The effect of genotoxic stress on the expression of γ-H2AX and the metabolic activity of MCF-7 cells. (A) Fluorescent images of MCF-7 cells stained for γ-H2AX following treatment with etoposide at 2 μM, phleomycin at 1 μg/ml for 24 hours, or UV-B at 19.25 J/m². Scale bar length is 10 μm. MTT assay results after treatment with phleomycin at 2 μg/ml, 1 μg/ml, 0.5 μg/ml, or 0.25 μg/ml for **(B)** 24 hours and **(C)** 48 hours. Control cells were treated with an equivalent solvent amount. T0 indicates the metabolic activity of cells immediately before starting treatment. Error bars represent standard deviation. N = 6. Data derived from a single experiment.

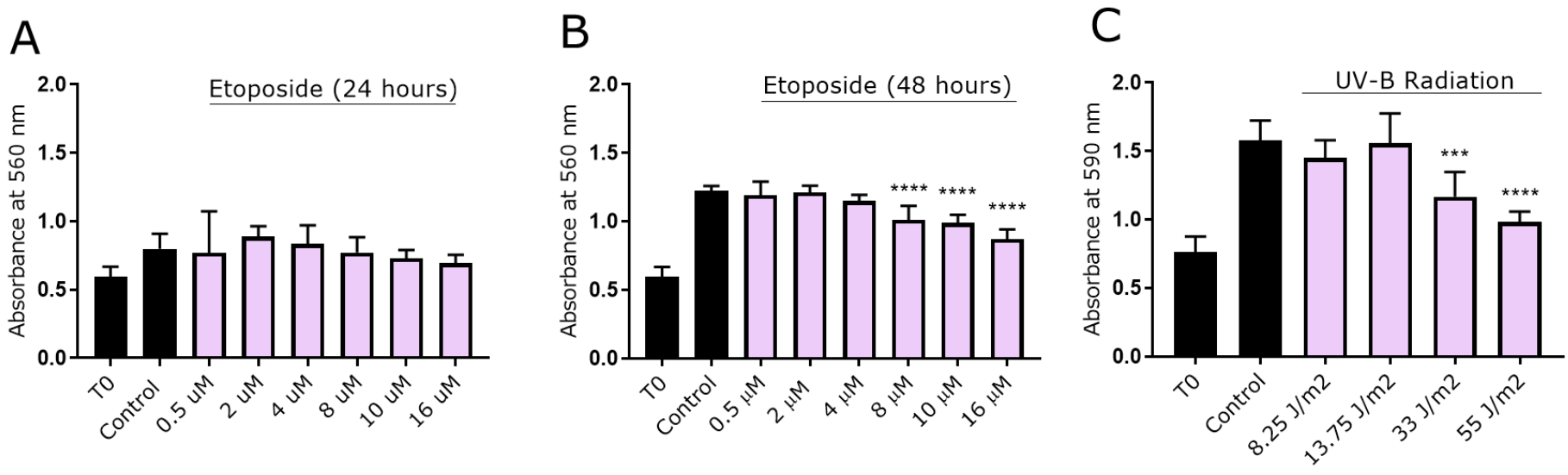


Figure 3.7 The effect of etoposide and UV-B radiation on the metabolic activity of MCF-7 cells. Treatment with etoposide at 0.5 µM, 2 µM, 4 µM, 8 µM, 10 µM, or 16 µM for **(A)** 24 hours and **(B)** 48 hours. The cellular metabolic activity was similarly assessed after 24 hours of exposing MCF-7 cells to **(C)** UV-B radiation at 8.25 J/m2, 13.75 J/m2, 33 J/m2, or 55 J/m2. Control cells were treated with an equivalent solvent amount. T0 indicates the metabolic activity of cells immediately before starting treatment. Error bars represent standard deviation. N = 6. Data derived from a single experiment. Ordinary one-way ANOVA followed by Dunnett's post hoc test. *** indicates $p < 0.001$, **** indicates $p < 0.0001$.

To investigate whether phleomycin, etoposide or UV-B radiation could have affected the viability of cultured cells, the MTT assay for assessing the mitochondrial redox potential was carried out on treated MCF-7 cells. Metabolically active cells contain NAD(P)H-dependent oxidoreductases which reduce the tetrazolium-based MTT to formazan. Hence, the quantification of this product is indicative of cell viability. As shown in Figures 3.6B and 3.6C, show, the viability of MCF-7 cells was not affected by phleomycin treatment at different concentrations and incubation times. Similarly, the viability of MCF-7 cells was not altered after 24 hours of etoposide treatment or exposure to UV-B radiation (Figure 3.7). Yet, etoposide treatment at high doses for 48 hours or exposure to UV-B levels beyond those tested in the luciferase experiments induced a reduction in the viability of MCF-7 cells. Overall, these results indicate that the observed effects of phleomycin and UV-B radiation on the expression of pREF are not derived from any changes in the viability of MCF-7 cells.

3.2.2 Effects of ER Stress, Iron Overload, Inflammation and Oxidative Stress

To confirm the inhibitory effect of ER stress on the activity of the *EGFR* IRES in U87-MG and MCF-7 cells (Daniel Smalley, 2016), the relative activity of firefly luciferase was assessed following treatment with 1 μM thapsigargin for 24 hours. Acting as an inhibitor of the endoplasmic/sarcoplasmic reticulum calcium pump, thapsigargin induces the development of ER stress via depleting calcium stores (Lytton et al., 1991).

It can be seen from Figure 3.8A that treatment with 1 μM thapsigargin has inhibited the activity of the *EGFR* IRES in MCF-7 cells ($p = 0.0002$), confirming previous findings. In addition

to the positive regulation of the *EGFR* IRES induced by genotoxic stress, these results suggest that the *EGFR* IRES is also subjected to a negative type of regulation under certain cellular conditions such as ER stress.

Based on evidence indicating an important role of EGFR in regulating iron metabolism in cancer cells, the activity of the *EGFR* IRES has been assessed following the induction of iron overload using ammonium iron (III) citrate (Wang et al., 2016, Li et al., 2016). The relative activity of firefly luciferase appeared to be unaffected by treatment with 250 μM ammonium iron (III) citrate in MCF-7 cells (Figure 3.8B). Despite the involvement of EGFR in iron metabolism, there was no evidence that iron overload influences the *EGFR* IRES activity in breast cancer cells.

Evidence also suggests that inflammation and oxidative stress can upregulate the activity of EGFR (Farley et al., 2008, Ravid et al., 2002). To investigate whether IRES meditated translation of EGFR could be influenced by inflammation or oxidative stress, the effects of stimulating MCF-7 cells with lipopolysaccharide (LPS) or hydrogen peroxide (H_2O_2) were assessed against the relative activity of firefly luciferase. As shown in Figure 3.9, no significant differences in the relative activity of firefly luciferase were found following treatment with LPS or H_2O_2. Similar results were observed in LPS-treated MDA-MB-231 cells, which can be found in the appendix (Figure A.1). These results might indicate that inflammation and oxidative stress are not important regulators of the IRES-mediated translation control of *EGFR* in breast cancer.

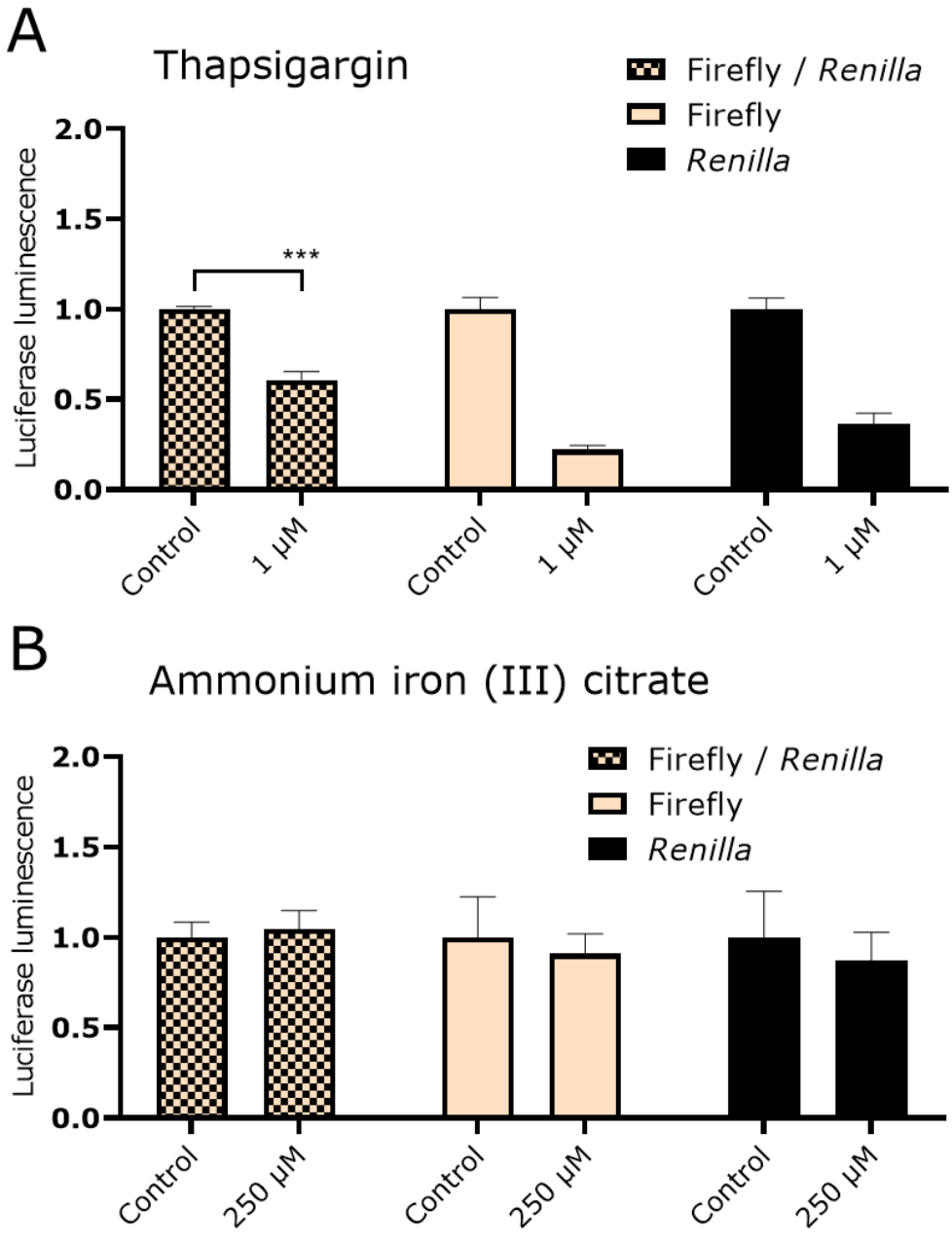


Figure 3.8 The relative activity of the *EGFR* IRES following treatment with thapsigargin and ammonium iron (III) citrate. Quantification of the relative activity of firefly luciferase in MCF-7 cells following 24-hour treatment with **(A)** 1 μM thapsigargin and **(B)** 250 μM ammonium iron (III) citrate. Control cells received an equivalent solvent amount. Error bars represent standard deviation. N = 3. Data generated from a single experiment. Unpaired t-test. *** indicates $p < 0.001$.

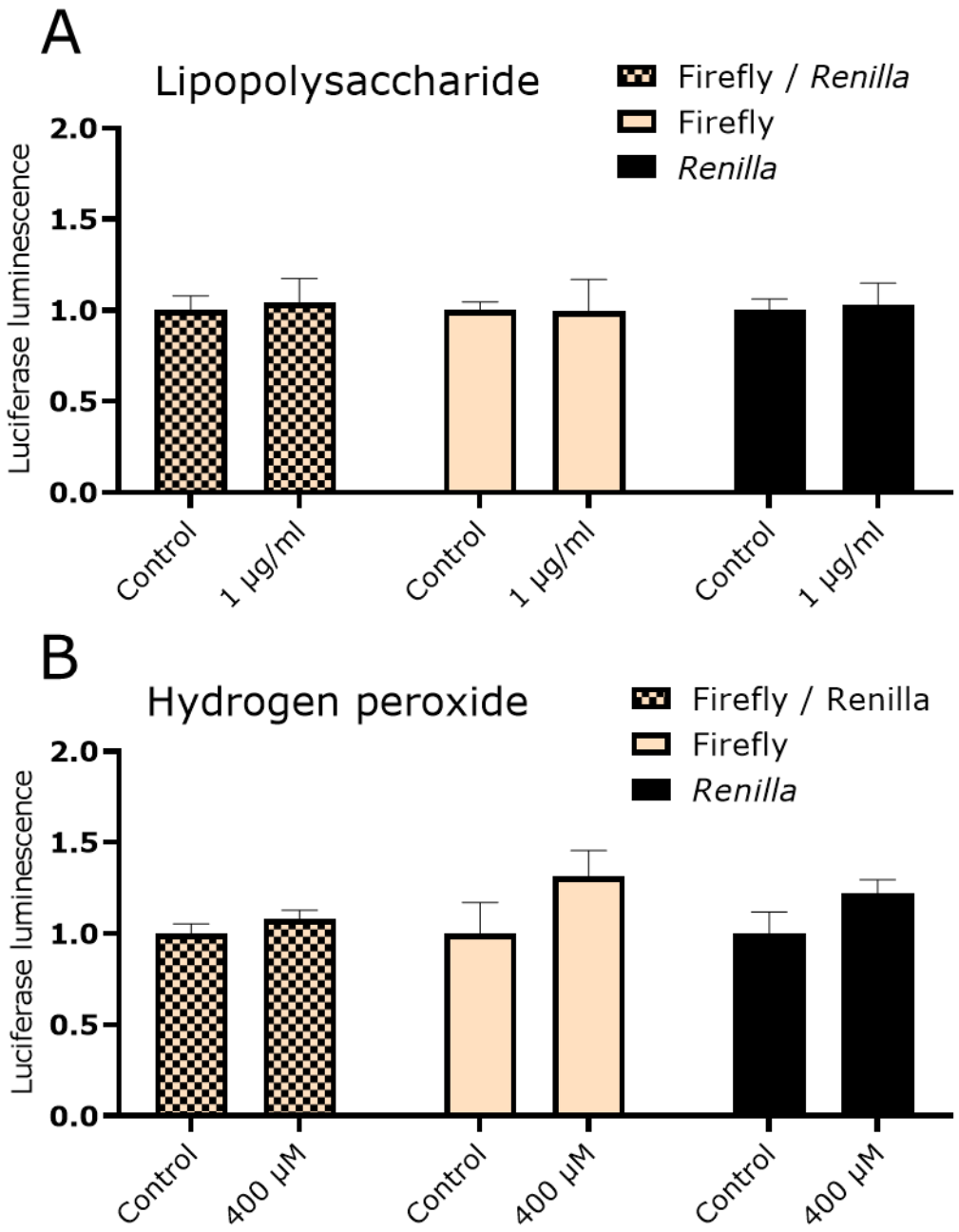


Figure 3.9 The relative activity of the *EGFR* IRES following treatment with LPS and H_2O_2. Quantification of the relative activity of firefly luciferase in MCF-7 cells following 24-hour treatment with **(A)** 1 µg/ml LPS or **(B)** H_2O_2 at 400 µM. Control cells received an equivalent solvent amount. Error bars represent standard deviation. N = 3-6. Data derived from two independent experiments.

Overall, the present study was designed to determine the effect of cell stress on the IRES-mediated expression of EGFR via exposing breast cancer cells to several cell stress inducers. It was found that treatment with the genotoxic chemicals cryptolepine and phleomycin can result in a condition of translation control that prefers the IRES-mediated translation of EGFR. In this condition, IRES-mediated translation appears to be inhibited significantly less than cap-dependent translation, leading to increased dependency on the *EGFR* IRES activity. On the other hand, UV-B radiation resulted in no significant changes in the translation profile of pREF. Collectively, these results indicate that the translation control induced by genotoxic stress can influence EGFR expression in breast cancer.

3.3 Discussion

One of the important signs of drug resistance and advanced tumour stages in breast cancer is the overexpression of EGFR (Arteaga, 2002). As investigating translation control is a growing concern in advanced breast cancer, the present chapter was designed to investigate the effect of cell stress on the translation control of EGFR (Kersting et al., 2004, Grob et al., 2012). It has been previously shown by our group that an IRES in the 5' UTR of the *EGFR* mRNA is capable of maintaining EGFR expression under hypoxia, where global protein expression is reduced (Webb et al., 2015). Thus, this study set out with the aim of assessing the importance of the *EGFR* IRES in mediating translation in other stress conditions associated with malignant growth, including genotoxic stress, ER stress, iron overload, inflammation and oxidative stress. Using bicistronic reporter plasmids, the activity of the *EGFR* IRES in driving the expression

of firefly luciferase was assessed to the cap-dependent expression of *Renilla* luciferase following treatment of MCF-7 cells with different cell stress inducers.

3.3.1 Effect of Genotoxic Stress

Several reports have shown that EGFR is involved in the development of resistance to radiotherapy in breast cancer by enhancing the cellular response to the induced DNA damage (Liccardi et al., 2011, Kriegs et al., 2010). Therefore, we aimed to investigate the effect of inducing different types of DNA lesions on the activity of the *EGFR* IRES in initiating cap-independent translation. The most interesting finding was that treatment with the genotoxic chemicals cryptolepine and phleomycin has resulted in a cellular condition in which cap-dependent translation is inhibited significantly more than IRES-mediated translation. Yet UV-B radiation resulted in no significant downregulation of both translation mechanisms. There would therefore seem to be a requirement for EGFR under the stress of damaged DNA.

Partially maintaining the expression of EGFR in a genotoxic condition where global protein expression is downregulated highlights the importance of EGFR in promoting cancer resistance and survival. Previous studies have demonstrated that EGFR nuclear translocation is involved in the DNA damage response by enhancing NHEJ directed against DNA strand breaks induced by ionising radiation (Kriegs et al., 2010). It seems possible that the nuclear response of EGFR can partly stem from the relative stimulation of the IRES-mediated expression of EGFR under the stress of damaged DNA. In response to genotoxic stress, it is known that cancer cells

induce translational reprogramming tailored toward translating mRNAs that are involved in the DNA damage response (Badura et al., 2012). Consistent with the literature, this study demonstrates the potential of translational control in directing the preferential expression of EGFR under genotoxic stress.

These findings must be interpreted with caution because there was no evidence that the induction of DNA damage by UV-B radiation has affected the *EGFR* IRES activity. In contrast to cryptolepine, phleomycin and etoposide findings, the relative activity of the *EGFR* IRES did not change after 24 hours of exposing MCF-7 cells to sublethal doses of UV-B radiation. However, this discrepancy could be attributed to several factors that could modulate the response of the *EGFR* IRES to different types of genotoxic stress. In accordance with these findings, it was shown previously that EGFR responds differentially to different types of DNA lesions. Lesions induced by ionising radiation were shown to induce the association between the catalytic subunit of DNA-protein kinase and EGFR within 20 minutes, while this association peaked at 18 hours following cisplatin treatment (Liccardi et al., 2011). Indeed, it is known that the type of DNA lesions greatly influences the mechanism of the DNA damage response. Ionising radiation and topoisomerase II inhibitors impair the integrity of DNA through the induction of DNA strand breaks. The induction of these breaks by ionising radiation causes a reduction in mTOR activity, leading to decreased phosphorylation of eIF4E-binding protein (4E-BP). As addressed earlier, hypophosphorylated 4E-BP binds and inactivates the cap-binding protein eIF4E leading to a preferential suppression of cap-dependent translation (Braunstein et al., 2009).

Conversely, the activity of the mTOR pathway is increased following UV-B exposure (Brenneisen et al., 2000). UV-B radiation induces primarily two types of DNA lesions: cyclobutane pyrimidine dimers (CPDs) and pyrimidine (6-4) pyrimidone photoproducts (6-4PPs) (de Lima-Bessa et al., 2008). The induction of these DNA lesions leads to the distortion of the DNA double helix, affecting DNA replication and transcription. In contrast to ionising radiation and topoisomerase II inhibitors, UV-B exposure results in global downregulation of protein synthesis via eIF2α inhibition. Reducing the activity of eIF2α by phosphorylation negatively affects the formation of the ternary complex necessary for both cap-dependent and IRES-mediated translation (Deng et al., 2002). It has been shown that the phosphorylation of eIF2α is responsible for developing resistance to viral infection by suppressing viral IRES-mediated translation (Sanz et al., 2013, White et al., 2011). In concordance with these previous studies, the activity of the *EGFR* IRES appears to be dependent on eIF2α following DNA damage.

Yet this activity concept could be challenged by reports in the literature demonstrating an increased IRES activity in stress conditions characterised by eIF2α inactivation (Chan et al., 2013, Fernandez et al., 2002). There is still uncertainty, however, eIF2α-independent mechanisms of translation initiation mediated by viral and cellular IRESs have been described. It has been demonstrated that IRESs of swine fever virus and *XIAP* mRNA require the initiating factor eIF5B instead of eIF2α for ribosomal initiation (Pestova et al., 2008, Thakor and Holcik, 2011). Considering the dissimilarities in structure and sequence among cellular IRESs, it seems that the EGFR

IRES might lack the necessary *in trans* regulation for initiating eIF2α-independent translation (Spriggs et al., 2009).

In addition, gene expression differences between cell lines may help explain the difference in response of cellular IRESs to certain conditions of cell stress. For instance, the expression of the cellular ITAF IGF2BP1 (insulin like growth factor 2 mRNA binding protein 1) was found to be increased in certain cancer tumours when compared to normal tissues (Faye et al., 2015). By regulating the IRES-mediated translation of the oncogene cIAP1, IGF2BP1 is involved in the development of resistance to apoptosis in rhabdomyosarcoma. Thus, mRNA translation under cellular stress could be differentially regulated based on the cellular genetic profile (Faye and Holcik, 2015, Hać et al., 2020).

3.3.2 Effect of ER Stress

It has been shown that disturbing the function of the ER leads to aberrant EGFR expression and activity, as proper ER function is necessary for the maturation of the EGFR protein (Ling et al., 2009). In this study, it was found that treatment with thapsigargin, an inducer of ER stress, reduced the *EGFR* IRES activity in breast cancer cells. It seems possible that this inhibitory effect is partly due to the downregulation of factors including eIF2α necessary for the *EGFR* IRES function. When the endoplasmic reticulum is under stress, it responds by inducing global protein down-regulation to decrease the accumulation of unfolded proteins in its lumen. This global protein downregulation is achieved through eIF2α phosphorylation (Saito et al., 2011). In concordance with the

DNA damage findings, functional eIF2α seems to be required for the *EGFR* IRES to initiate translation.

Furthermore, this inhibitory effect could stem from the inability of the *EGFR* IRES to interact with translation initiation factors or ITAFs necessary for proper function under ER stress. The induction of endoplasmic stress was reported, conversely, to stimulate the IRES-mediated translation of *SREBP1* mRNA, a transcription factor involved in lipid metabolism (Damiano et al., 2013). It has been found that IRES-mediated translation of SREBP1 is dependent on the cytosolic translocation of HNRNPA1, a cellular ITAF (Damiano et al., 2013). Once more, *in trans* regulation mediated by initiation factors and ITAFs appears to be important in regulating IRES activity under cell stress, potentially accounting for the differential activity of the *EGFR* IRES under different stress conditions.

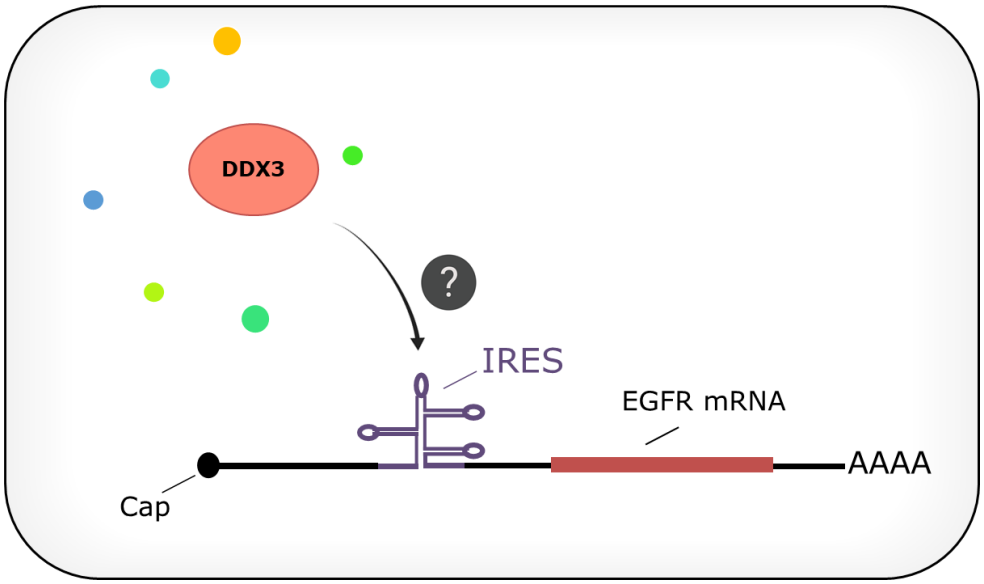
Overall, the present results appear to support the hypothesis that the stress of damaged DNA could relatively lead to the upregulation of EGFR via increased dependency on IRES-mediated translation. These results are significant in at least two major respects. In addition to the established role of EGFR in promoting proliferation and differentiation of malignant cells, the preferential expression of EGFR under the stress of damaged DNA highlights the importance of EGFR in facilitating cancer cell recovery and resistance. Consequently, combining conventional cytotoxic therapy with targeted therapy for EGFR might have the potential to hinder the development of resistance to cytotoxic drugs, rendering EGFR targeting as a potential chemosensitisation measure (Jian et al., 2010). As cancer cells are inclined to accumulate genetic mutations during cell division, characterising the *EGFR* IRES activity under genotoxic stress is also important for our understanding of how

cancer tumours adapt and develop inside the body (Yao and Dai, 2014). Understanding the link between the translation control of EGFR and DNA damage helps to provide some insights into how cancer cells adapt to genetic mutations affecting their survival.

Chapter Four

4 DDX3 and the *EGFR* 5’ UTR

Graphical summary



4.1 Introduction

DDX3, also known as DDX3X because of its location on the X chromosome, is a DEAD-box RNA helicase that has a multifaceted function in gene expression including mRNA translation (Rocak and Linder, 2004). While the helicase activity of this protein allows the unwinding of complex RNA structures, DDX3 is also known to be involved in translation initiation via helicase independent mechanisms such as supporting the assembly of functional 80S ribosomes and limiting the availability of the cap-binding protein eIF4E (Geissler et al., 2012, Shih et al., 2008, Lai et al., 2008). The sequestration of eIF4E by DDX3 was found to stimulate IRES-mediated translation via increasing the availability of other translation initiation factors for cap-independent translation mechanisms (Shih et al., 2008). Furthermore, it was shown that DDX3 is required for the translation of selected transcripts harbouring complex secondary structures proximal to their 5’ ends (Soto-Rifo et al., 2012, Lai et al., 2010). The direct binding of DDX3 to those transcripts and the subsequent partial unwinding of the 5' proximal RNA structures is thought to allow the entry of the translation machinery to initiate protein synthesis (Soto-Rifo et al., 2012).

Despite conflicting evidence indicating both tumour-enhancing and repressing properties, DDX3 has an established role in promoting cellular transformation and proliferation especially in breast cancer (Botlagunta et al., 2008). Indeed, targeting this helicase was even found to reduce the evasiveness of breast cancer cells in preclinical models (Xie et al., 2015, Kondaskar et al., 2013). Similar to EGFR, DDX3 has been also linked to the development of the hypoxic response and resistance to

radiotherapy in breast cancer cells (Van Voss et al., 2018, Bol et al., 2013). With regards to the hypoxic response, DDX3 was found to be a direct downstream target of the hypoxia-inducible factor 1α (HIF-1α), the principal transcriptional regulator in the mammalian hypoxic response (Botlagunta et al., 2011). In addition to HIF-1α, this overexpression of DDX3 was found to be directly correlated with other hypoxia-related proteins including EGFR in patient samples of breast cancer (Bol et al., 2013). EGFR appears to be involved in regulating the expression levels of DDX3 under hypoxic conditions via the HER2/EGFR-Akt1-HIF-1α-DDX3 signal-transduction cascade (Gort et al., 2006, Mattoon et al., 2004).

Considering the structured nature of the *EGFR* 5' UTR and the presence of a stem-loop structure proximal to its 5' end (Daniel Smalley, 2016), it might be possible that the increased expression of DDX3 in hypoxia could further stimulate the hypoxic expression of EGFR via translation control in a positive feedback loop. Therefore, this chapter aimed to investigate whether DDX3 could facilitate translation initiation of the *EGFR* mRNA via its 5' UTR. To investigate this possible RNA-protein interaction, the relationship between DDX3 and the *EGFR* 5' UTR was bioinformatically assessed for the presence of predicted binding sites prior to cell-based analysis. The cDNA sequence of *DDX3* was then cloned into the mammalian expression vector pcDNA3.1 to induce the expression of DDX3 in breast cancer cells to further understand the link between DDX3 and the *EGFR* mRNA. In addition, the DDX3 inhibitor ketorolac salt was used to investigate the helicase activity of DDX3 in the context of the *EGFR* 5' UTR.

4.2 Bioinformatic Analysis

In consequence to the rising interest in the post-transcriptional regulation of gene expression, large volumes of data continue to be generated primarily through high throughput techniques including protein-RNA interaction mapping methods such as ultraviolet cross-linking and immunoprecipitation (CLIP) and its variants (Ule et al., 2003, Schwanhäusser et al., 2011). In this regard, meta-databases complemented by data-mining tools were created to enable comprehensive investigations of this wealth of data scattered throughout published papers and discrete databases (Richardson et al., 2009).

To gain insight into the relevance of DDX3 on the translation regulation of the *EGFR* mRNA, the first set of analyses examined the bioinformatic association between the *EGFR* mRNA and DDX3. The results were generated by The Atlas of UTR Regulatory Activity (AURA), a bioinformatic catalogue of human mRNA UTRs and their experimentally-determined regulatory annotations (Dassi et al., 2014). This comprehensive database allows access to a manually curated dataset of human UTRs bound by regulators since 1994 derived from mechanistic or single-gene experiments (Dassi et al., 2014). The purpose of using AURA was to investigate the presence of predicted DDX3 binding motifs on the *EGFR* 5’ UTR. In this regard, DDX3 was identified by AURA as a potential trans-acting factor that directly binds the *EGFR* 5’ UTR proximal to the universal cap structure. This is consistent with findings by Daniel Smalley (2016) via deletion analysis indicating both the first 57 nucleotides and the last 36 nucleotides of the *EGFR* 5’ UTR sequence to have a greater influence over IRES activity in comparison to the other 5’ UTR segments, signalling the

presence of important translational elements including binding sites of regulatory proteins. As shown in Figure 4.1, the proposed binding site of DDX3 is located between the 5’ cap end and a stem-loop structure with high consensus. This stem-loop structure, as predicted by mfold and LocARNA, was previously identified by Daniel Smalley (2016) via selective 2’ hydroxyl acylation analysed by primer extension (SHAPE) analysis (Zuker, 2003, Raden et al., 2018).

As it is located proximal to the predicted binding site of DDX3, the consensus of the identified stem-loop structure was further examined using the Nucleotide Basic Local Alignment Search Tool (BLAST) engine across the different species available. After that, the resulting database was processed for multiple sequence alignment using Clustal Omega with default parameters and then visualised using Jalview Desktop, an open-source bioinformatics software (Sievers and Higgins, 2018). As shown in Figure 4.2, this stem-loop structure was found to be almost present in all examined 58 different species listed in the appendix (Table A.1). These findings highlight the importance of this RNA structure in the topography of the *EGFR* mRNA. Interestingly, this highly conserved RNA structure is located in close proximity to the predicted binding site of DDX3 on the *EGFR* mRNA, signalling a potential interaction between them especially after considering the role of DEAD-box RNA helicases in resolving secondary structures during translation (Soto-Rifo et al., 2012, Cordin et al., 2006).

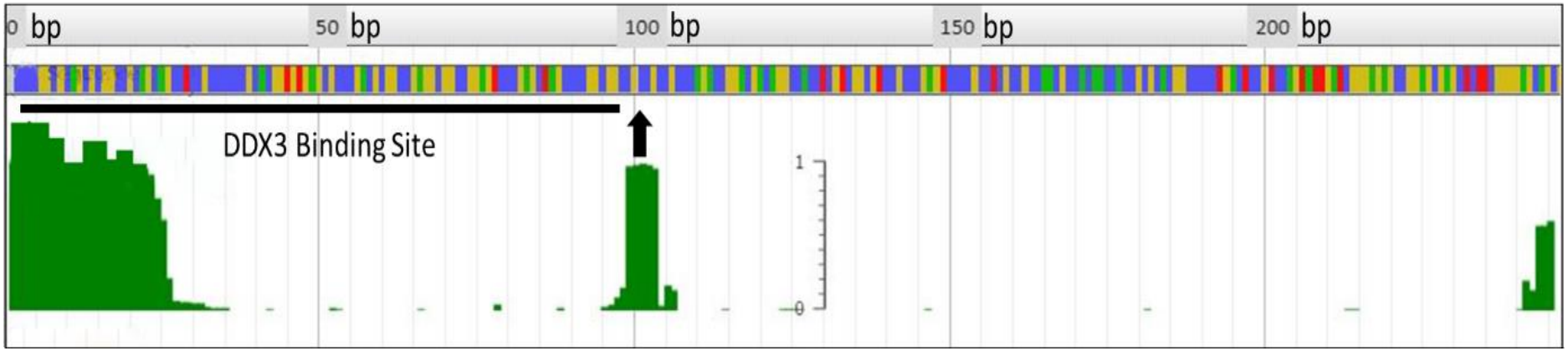


Figure 4.1 The *EGFR* 5' UTR was queried by sequence using AURA. Diagram was generated via AURA 2 website (http://aura.science.unitn.it) and then annotated accordingly. The stem-loop structure is indicated by an arrow while the predicted binding site belonging to DDX3 is underlined. The degree of conservation is reflected by the intensity of the green columns.

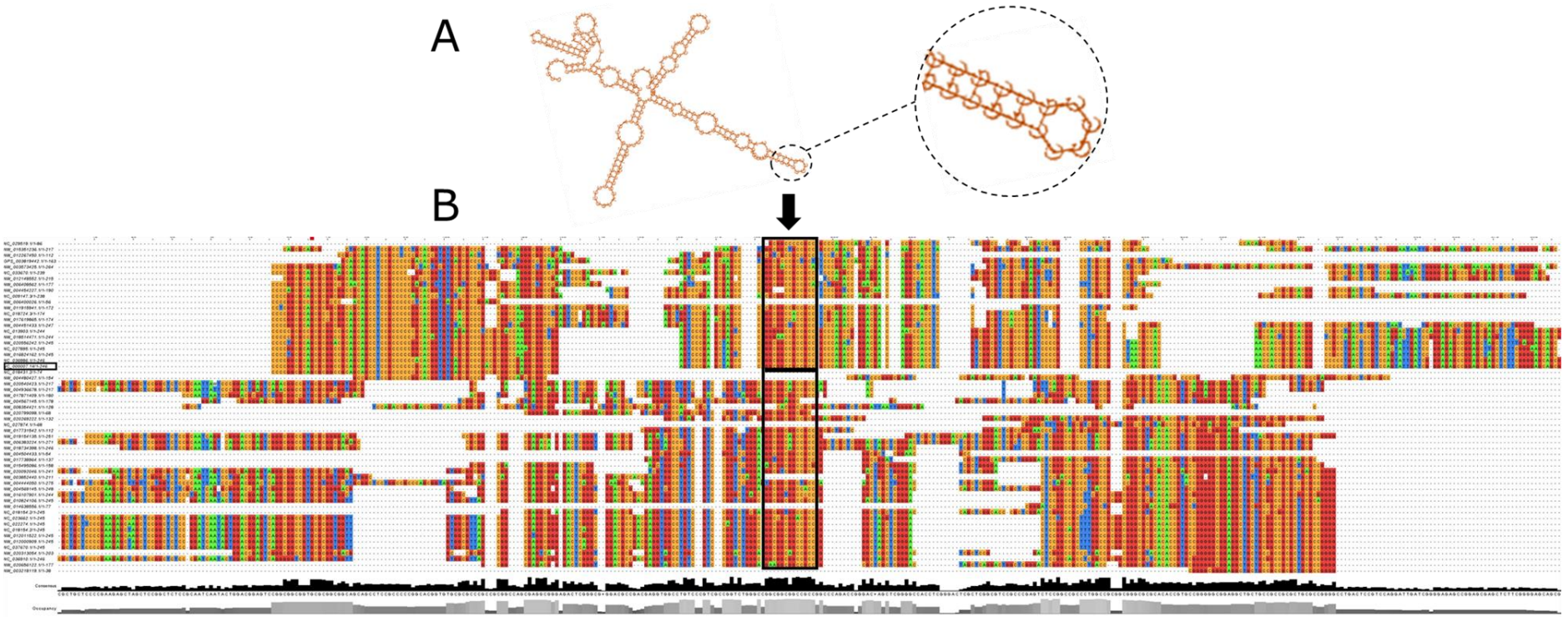


Figure 4.2 The *EGFR* 5′ UTRs from 58 different species were aligned using Clustal Omega. (A) A schematic diagram representing the *EGFR* 5′ UTR as predicted by mfold (Zuker, 2003) highlighting the highly conserved stem-loop structure. **(B)** A multiple sequence alignment diagram of the *EGFR* 5′ UTRs from 58 different species in which the stem-loop structure is enclosed in a box and the sequence belonging to the human genome is underlined. Accession numbers of the sequences included in the analysis are listed in the appendix (Table A.1).

4.3 Cell-Based Analysis

To experimentally assess the interaction between the *EGFR* mRNA and DDX3, the coding sequence of *DDX3* was cloned into the mammalian expression vector pcDNA3.1, containing the cytomegalovirus (CMV) promoter (Invitrogen, Cat #V385-20). The *DDX3* sequence was amplified from cDNA extracted from MCF-7 cells using primers that add HindIII and EcoRI restriction sites to the 5' and 3' ends, respectively (Figure 4.3). Successful cloning was confirmed by sequencing the generated plasmid, referred to in this thesis as pDDX3. The plasmid was then tested for activity by transfection into MCF-7 cells in which the DDX3 antigen was assessed via western blotting after 72 hours (Figure 4.4).

To investigate potential interactions between the *EGFR* 5' UTR and DDX3, pREF was co-expressed with pDDX3 in MCF-7 cells for 48 hours before assessing for luciferase activity. As shown in Figure 4.5A, overexpressing DDX3 in MCF-7 cells has increased the expression of the firefly luciferase in a dose-dependent manner. As shown in figure 4.5B, a similar increase pattern was also observed when DDX3 was overexpressed in the presence of the monocistronic plasmid p15E, containing the *EGFR* 5' UTR upstream to the main open reading frame of the firefly luciferase. Interestingly, the increase in luciferase activity was significantly higher in the bicistronic plasmid in comparison to the monocistronic counterpart.

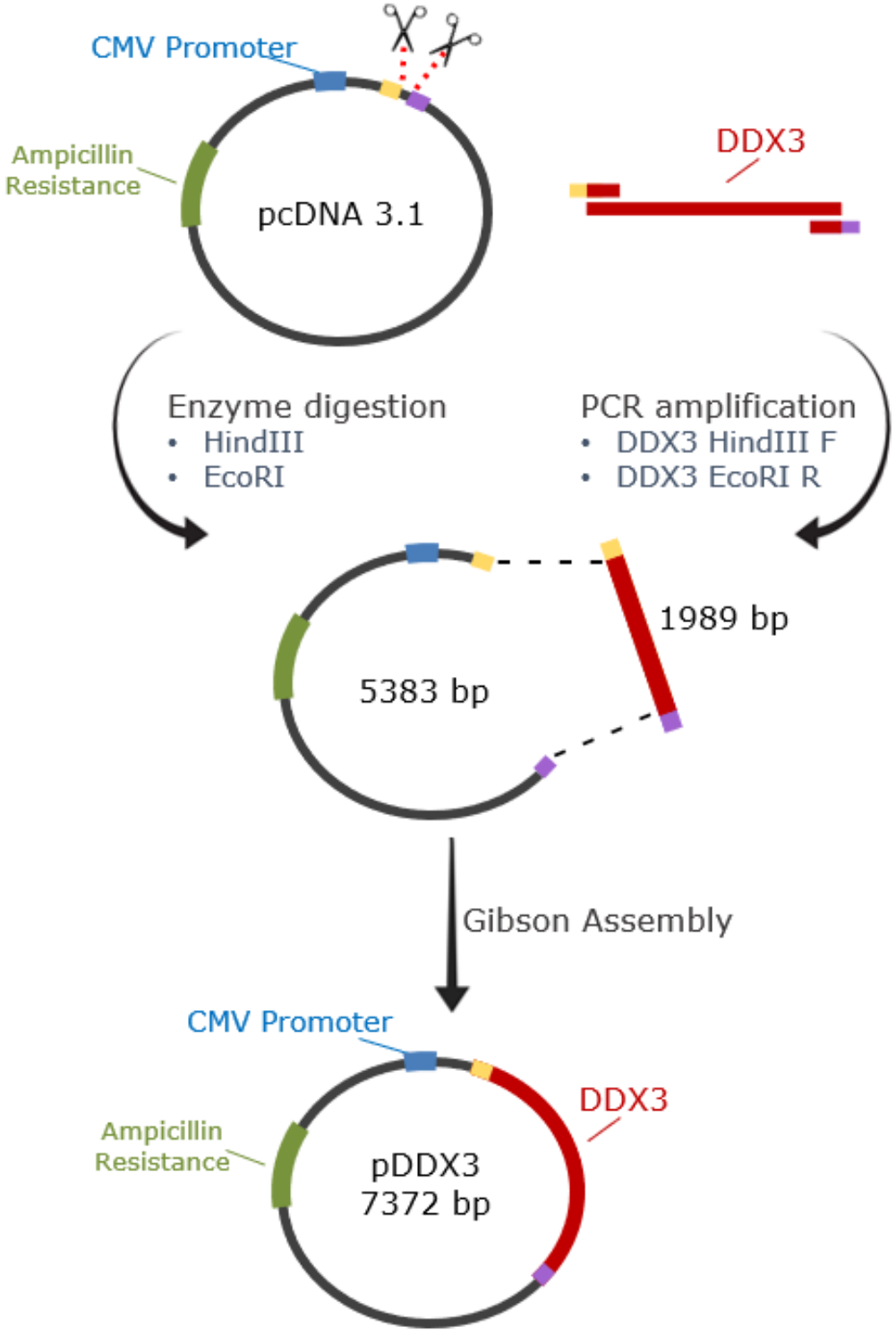


Figure 4.3 Cloning of *DDX3* into the mammalian expression vector pcDNA3.1. Human *DDX3* was PCR amplified from MCF-7 cDNA and Gibson cloned into the mammalian expression vector pcDNA3.1 using HindIII and EcoRI restriction sites.

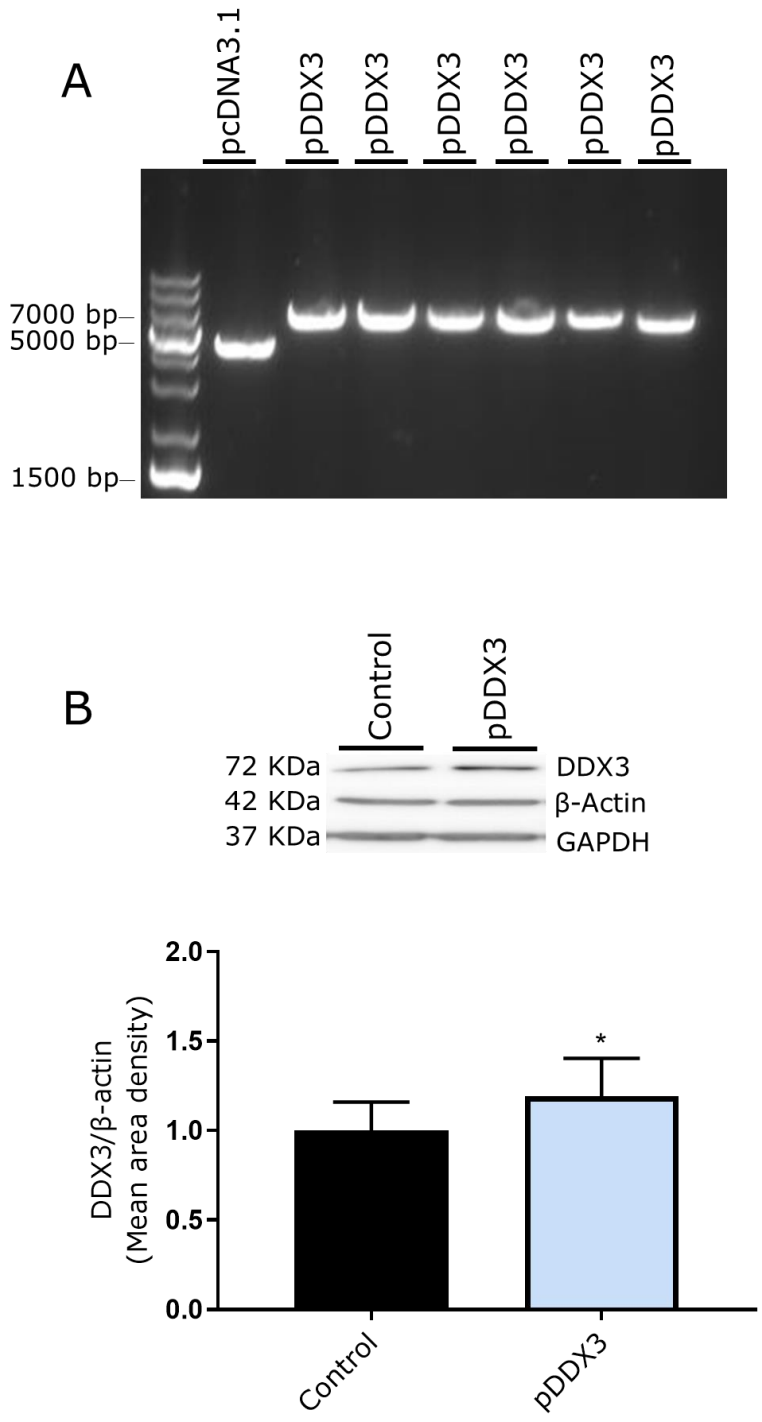


Figure 4.4 Characterisation of pDDX3. (A) Diagnostic enzyme digestion by BspHI. **(B)** A representative western blot and densitometric analysis of DDX3 normalised to β-actin in MCF-7 cells transfected with pDDX3 for 72 hours. Control cells were transfected with pcDNA3.1. Error bars represent standard deviation. N = 9. Three independent experiments. Unpaired t-test. * indicates $p < 0.05$.

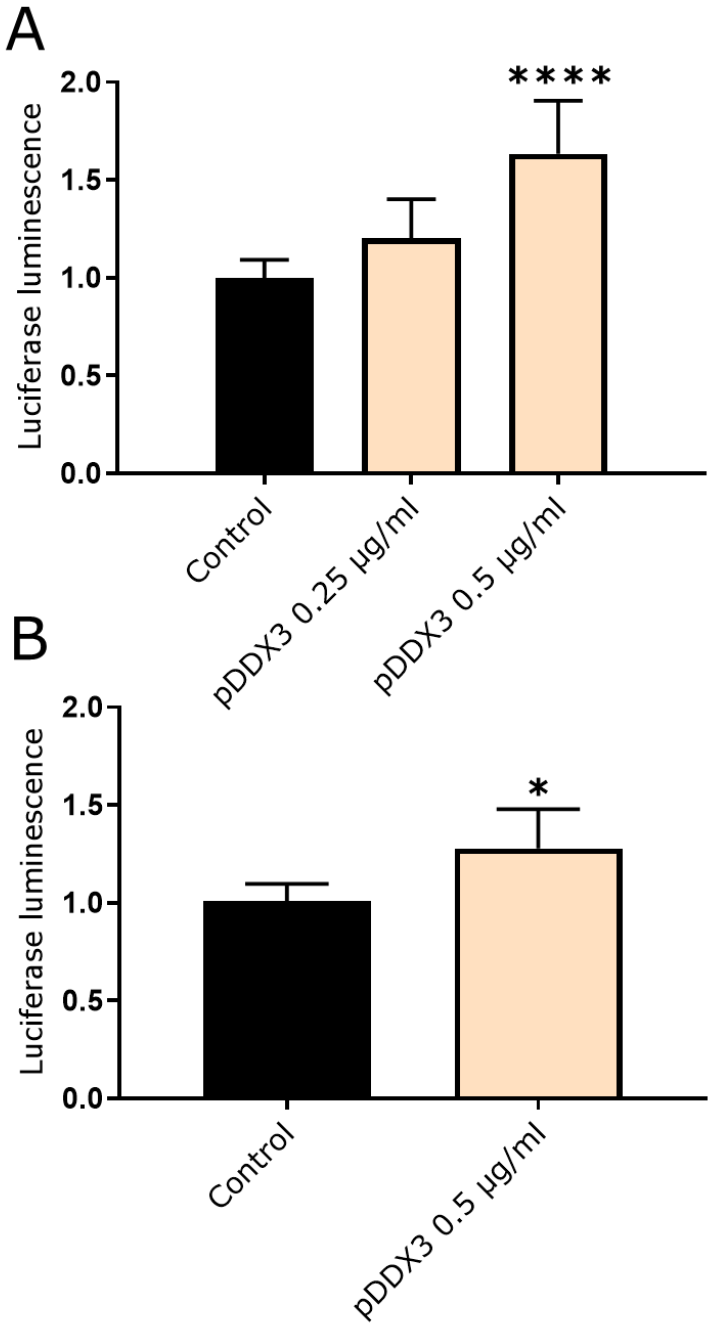


Figure 4.5 Firefly luciferase activity of plasmids containing the *EGFR* 5' UTR upon DDX3 overexpression. A luciferase assay showing the relative firefly activity of **(A)** the bicistronic pREF and **(B)** the monocistronic p15E upon pDDX3 transfection in MCF-7 cells. Control cells were transfected with pcDNA3.1. Data is relative to total protein. Error bars represent standard deviation. Three independent experiments. N=9 except for pDDX3 0.25 µg N=3. Ordinary one-way ANOVA followed by Dunnett's post hoc test for (A), unpaired Student t-test for (B). * indicates $P < 0.05$, *** indicates $p < 0.001$.

Thus, these results indicate that DDX3 can increase the expression of an open reading frame connected to a structured 5’ UTR in a mechanism that is independent of the universal 5’ cap structure. It should be noted that the expression of the *Renilla* luciferase in pREF was also increased upon DDX3 overexpression, hence total protein was used to normalise the expression data for the firefly luciferase. This increase in *Renilla* expression could be similar in mechanism to the observed increase in expression of the firefly luciferase of p15E as both cistrons are linked to a cap structure via a 5’ UTR.

Considering the function of DDX3 in homeostasis and disease, the constitutive helicase activity of DDX3 was examined using the ketorolac salt ((±)-5-benzoyl-2,3-dihydro-1H-pyrrolizine-1-carboxylic acid, tris (hydroxymethyl) aminomethane salt). Ketorolac salt is a DDX3 inhibitor that showed promising results against oral cancer with high DDX3 expression (Samal et al., 2015). After transfection with pREF, MCF-7 cells were treated with ketorolac salt at 5 μM to examine the effect of inhibiting the helicase activity of DDX3 on the translation control of the *EGFR* 5’ UTR (Samal et al., 2015). As shown in Figure 4.6, treatment with ketorolac for 24 hours did not change the translational profile of pREF, suggesting that the helicase activity of DDX3 is not important for regulating translation initiation in the context of the *EGFR* 5’ UTR under homoeostasis.

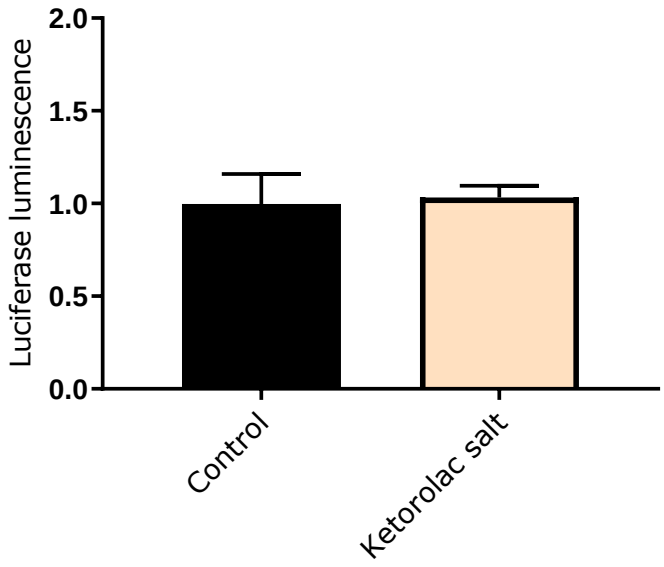


Figure 4.6 Relative firefly activity of pREF in cells treated with ketorolac salt. A luciferase assay showing the relative firefly activity to the respective *Renilla* activity of pREF transfected into MCF-7 cells 24 hours before treatment with 5 μM ketorolac salt for 48 hours. Control indicate cells treated only with solvent. N=6. Two independent experiments. Error bars represent standard deviation.

To establish the importance of the highly conserved stem-loop structure in the translation control of the *EGFR* 5' UTR, the nucleotide sequence of this stem-loop structure was disrupted via site-directed mutagenesis using the iAUG 4 EGFR primers listed in Table 2.3 to generate a pREF mutant lacking this conserved RNA structure but retaining the exact length of the original plasmid (Figure 4.7A). As shown in Figure 4.7B, disrupting this RNA structure resulted in no significant changes in the expression profile of the mutant plasmid in comparison to pREF. This indicates that this stem-loop structure might not have a direct impact on the translation control of the *EGFR* 5' UTR.

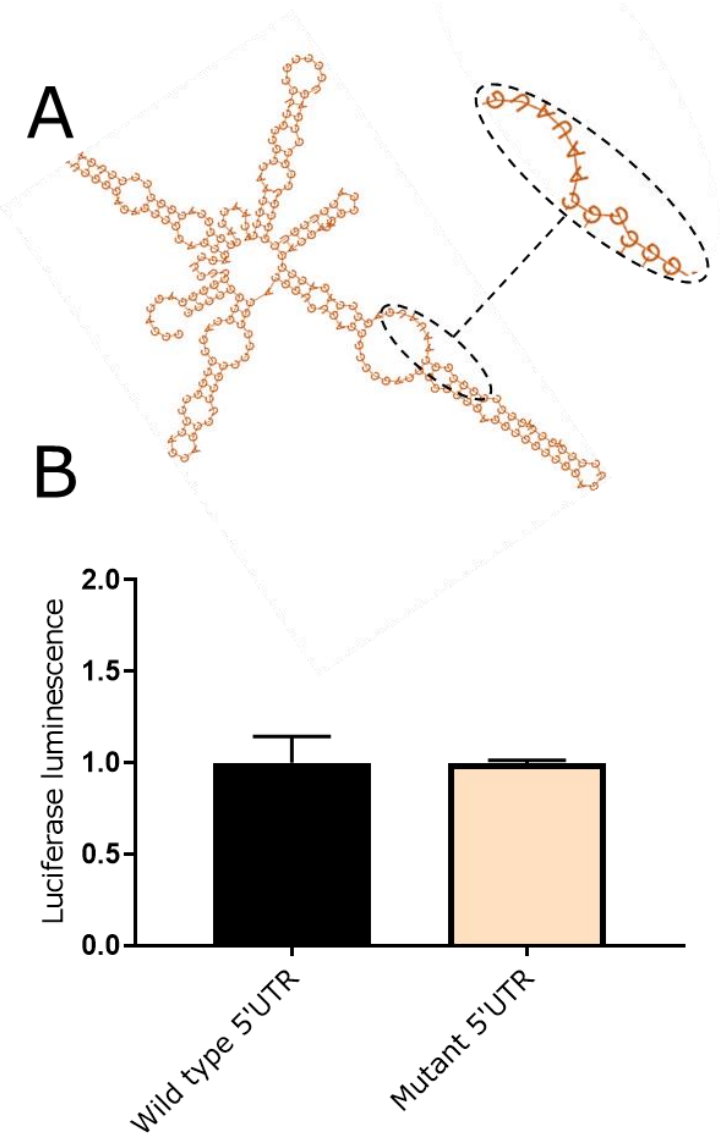


Figure 4.7 Luciferase activity profile of the wild-type EGFR 5' UTR and the mutant version lacking the identified stem-loop structure. (A) A schematic diagram of the mutant *EGFR* 5' UTR, highlighting the mutated sequence that disturbed the formation of the highly conserved stem-loop structure present in the wild type 5' UTR as predicted by mfold (Zuker, 2003). **(B)** Luciferase assay results comparing the ratio of firefly activity to Renilla activity for pRF plasmids containing the wild type and the mutant version of the EGFR 5' UTR transfected into MCF-7 cells for 48 hours. N=3. Data derived from a single experiment. Error bars represent standard deviation.

To address the global nature of the DDX3 function in mRNA metabolism, the effect of overexpressing DDX3 was examined on the translational control of different 5′ UTRs cloned into the intercistronic region of pRF. As demonstrated in Figure 4.8, the overexpression of DDX3 significantly increased the firefly luciferase expression by at least 50% of all screened 5′ UTRs, namely, the tubulin, amyloid precursor protein (*APP*), and tau protein 5′ UTRs. These results indicate that the observed increase in translation of the firefly luciferase is a global effect of DDX3 on translation initiation and it is not specific to the *EGFR* 5′ UTR.

There was also no evidence that the change in intercistronic length has an influence on the expression of the firefly cistron. The examined 5′ UTRs were all associated with increased firefly expression despite their variation in length which ranges from 127 nucleotides (β tubulin 5′ UTR) to 321 nucleotides (Tau 5′ UTR). Interestingly, the obtained results also show that the increase in firefly translation with DDX3 overexpression is irrespective to the IRES activity of the upstream 5′ UTR. In contrast to all 5′ UTRs tested in this study, the tubulin 5′ UTR lacks an IRES activity, yet DDX3 overexpression has permitted the expression of its downstream cistron (Beaudoin et al., 2008, Veo and Krushel, 2012). Overall, these results indicate that observed changes in translation are not related to increased IRES activity but rather to a novel mechanism that DDX3 is involved in its regulation.

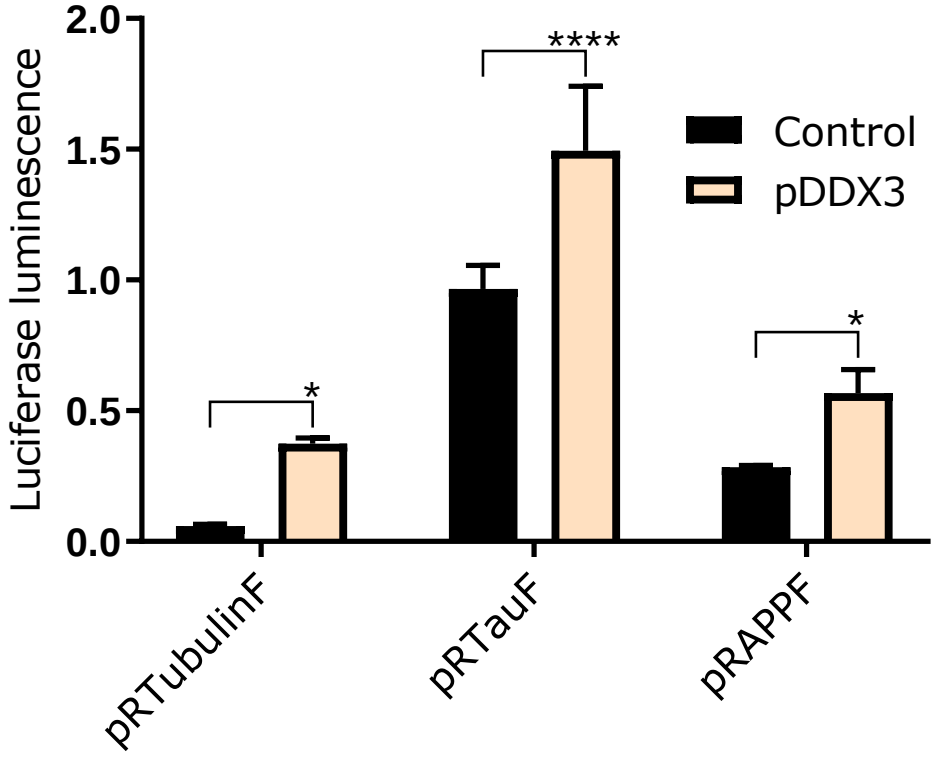


Figure 4.8 The effect of DDX3 overexpression on pRF plasmids. Luciferase assay results demonstrating the firefly activity of pRF plasmids containing the 5' UTRs of the tubulin, tau and *APP* mRNAs transfected with pDDX3 into MCF-7 cells for 48 hours. Data is relative to total protein. Error bars represent standard deviation. N=3. Data generated from a single experiment. Control cells were transfected with pcDNA3.1. Ordinary one-way ANOVA followed by Turkey's post hoc test. * indicates $P < 0.05$, **** indicates $P<0.0001$.

To assess the impact of overexpressing DDX3 on EGFR at the protein level, a western blotting analysis was carried out for EGFR expression after transfecting pDDX3 into MCF-7 cells for 72 hours. In addition to β-actin, EGFR protein levels were also normalised to GAPDH levels to confirm the findings as it has been reported that DDX3 could influence the actin network in the cell (Lai et al., 2008).

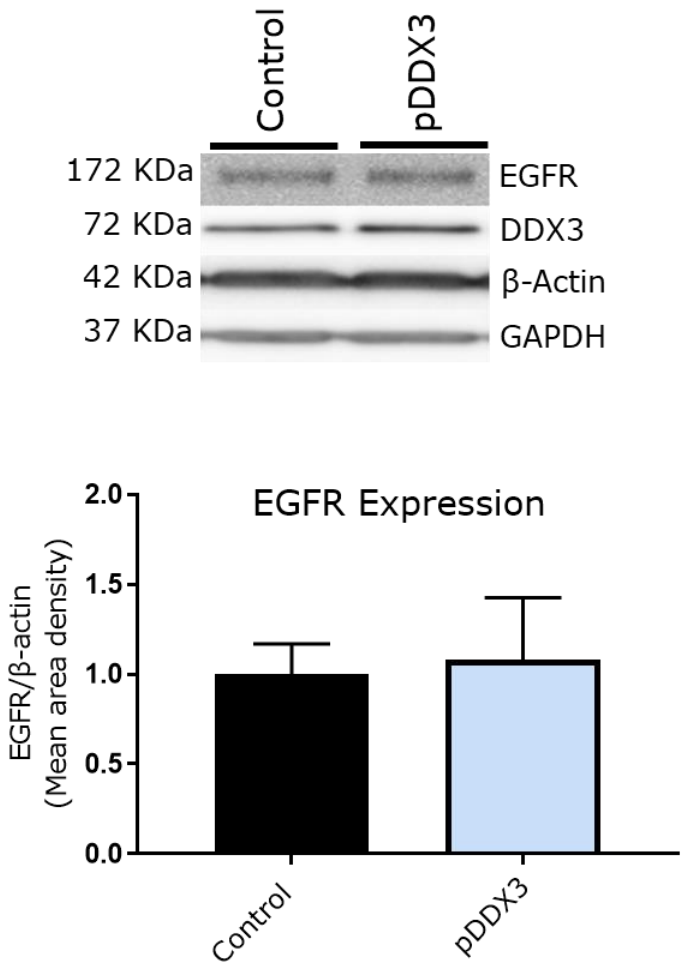


Figure 4.9 The effect of overexpressing DDX3 on the protein expression of EGFR. A representative western blot and densitometric analysis of the EGFR protein normalised to β-actin in MCF-7 cells transfected with pDDX3 for 72 hours. N = 9. Three independent experiments. Control cells were transfected with pcDNA3.1. Error bars represent standard deviation.

As can be seen from Figure 4.9, overexpressing DDX3 resulted in no significant changes in the cellular expression of the EGFR protein. Similar results were also obtained with MDA-MB-231 cells transfected with pDDX3 (Figure A.2). The obtained results indicate that the expression levels of DDX3 might not be closely correlated with the expression levels of EGFR.

In conclusion, a series of analyses were conducted to examine the impact of DDX3 on the translational control of the *EGFR* 5' UTR. This investigation started with a bioinformatic analysis that demonstrated a predicted binding site for DDX3 on the *EGFR* 5' UTR situated between the universal 5' cap end and a highly conserved stem-loop structure. After cloning the cDNA sequence of *DDX3* into the mammalian expression vector pcDNA3.1, the effect of overexpressing DDX3 on the *EGFR* 5' UTR was examined using bicistronic luciferase vectors including pREF. Upon DDX3 overexpression, it was found that the activity of the downstream cistron was significantly increased irrespective to the connected 5' UTR sequence. As this downstream cistron is not closely linked to a 5' cap structure via untranslated region nor in the case of the tubulin 5' UTR an upstream IRES element, DDX3 appears to facilitate translation reinitiation of ribosomes that has just terminated translation at the upstream cistron. Therefore, these results further support the reported functions of DDX3 in regulating translation initiation in eukaryotic cells and highlight a potentially novel role of DDX3 in translation reinitiation.

4.4 Discussion

DDX3 is a DEAD-box helicase that has a characterised multifaceted function in cellular gene expression including translation initiation (Chuang et al., 1997). As prior studies have noted the importance of trans-acting factors including ITAFs in the translation control of cellular IRESs and considering the importance of DDX3 and EGFR in the development of the hypoxic response in breast cancer cells, this current chapter was designed to determine the effect of DDX3 as a potential

trans-acting factor on the activity of the *EGFR* IRES (Webb et al., 2015, Bol et al., 2013)

The first part of this chapter was aimed to investigate the presence of potential binding sites of DDX3 via bioinformatic-resource portals including AURA and BLAST. The results of this bioinformatic analysis indicated a possible interaction between the *EGFR* 5' UTR and DDX3 via a binding motif present between the 5' cap end and a highly conserved stem-loop structure. After that, this investigation was oriented towards characterising this predicted interaction in cell-based systems utilising bicistronic plasmids. Even though the experiments implemented did not detect conclusive evidence about a specific type of regulation between DDX3 and the *EGFR* 5' UTR, the most interesting finding was that DDX3 can significantly influence the expression profile of bicistronic plasmids irrespective of the sequence inserted into the intercistronic region.

4.4.1 DDX3 and the *EGFR* 5' UTR

Based on the bioinformatics results, DDX3 appears to have a potential binding site situated between the 5' cap end and a highly conserved stem-loop structure. This is consistent with a study showing that this RNA helicase is recruited preferentially to mRNAs containing proximal stem-loop structures to their 5' ends (Soto-Rifo et al., 2012). It is therefore likely that such interaction exists between DDX3 and the *EGFR* 5' UTR, considering the functions of EGFR and DDX3 in driving the hypoxic-response and invasiveness of breast cancer cells. As these findings supported the conceptual premise that DDX3 could be a trans-acting regulator of the *EGFR* IRES, further cell-

based experiments investigating this potential interaction have been implemented.

Subsequently, the cDNA of *DDX3* was cloned into the mammalian expression vector pcDNA3.1 to be co-expressed with different bicistronic plasmids including pREF that contains the *EGFR* 5' UTR cloned upstream of the downstream firefly-luciferase cistron. It has been found that overexpressing DDX3 in MCF-7 cells has significantly increased the activity of firefly luciferase in a concentration-dependent manner. Conversely, neither inhibiting the helicase function of DDX3 nor disrupting the identified stem-loop structure resulted in any significant changes in the activity of the firefly luciferase. Furthermore, overexpressing DDX3 resulted in no significant changes in the protein expression of EGFR.

This absence of significant changes in the protein expression of EGFR could be attributed to the low expression levels of DDX3 induced in transfected cells. Despite using a mammalian expression construct with a strong promoter, the expression levels of DDX3 detected in transfected cells were only slightly elevated in comparison to the control cells transfected with the 'empty' vector. As shown in the literature, only high levels of DDX3 appear to be associated with the stress response mechanisms that involve limiting cap-dependent translation and the preferential translational of selected transcripts (Shih et al., 2008, Hilliker et al., 2011). This is thought to be mediated through two main molecular pathways. The first pathway involves the direct sequestration of the cap-binding protein, eIF4E by DDX3 via a consensus eIF4E-binding sequence (Shih et al., 2008). The second pathway is related to the formation of translationally inactive complexes with mRNAs and eIF4F in stress granules in an ATP-dependent manner (Hilliker et al.,

2011). Under such conditions, the selective recruitment of DDX3 to a specific set of mRNA transcripts seems to facilitate their translation as a result of the subsequent recruitment of the limiting trimeric complex eIF4F via the interaction between DDX3 and eIF4G (Hilliker et al., 2011, Geissler et al., 2012). As the induced DDX3 levels were probably not elevated enough to elicit a cell-stress response, the effect of selective DDX3 recruitment to the *EGFR* mRNA might have been masked by the high abundance of the trimeric complex under the homoeostatic conditions used in this study. Experiments with more focus on evaluating the role of DDX3 in the translational control of the *EGFR* mRNA under cell stress is therefore more suitable, hence the role of DDX3 in this regard could be more significant (Adjibade et al., 2017).

In addition to the selective recruitment to stress-induced mRNAs, DDX3 was previously found to be universally recruited to both cellular and viral mRNAs attached to the 40S ribosomal subunit and eIF3 (Geissler et al., 2012). This universal recruitment of DDX3 is important in the context of mRNA translation in homeostasis, as DDX3 seems to facilitate the formation of the elongation competent 80S ribosomes (Geissler et al., 2012). Associated with these observations, the overexpression of DDX3 was found to induce the expression of the downstream cistron to the different 5’ UTRs cloned into monocistronic and bicistronic plasmids. Furthermore, treatment with ketorolac salt (predicated to inhibit the helicase activity of DDX3) resulted in no significant changes in the expression profile of these plasmids. This lack of response suggests that the increased expression of the downstream open reading frames observed with DDX3 overexpression is independent of the helicase activity of DDX3. Indeed, it has been shown that

the role of DDX3 in facilitating the assembly of the 80S ribosomes is a helicase independent process (Geissler et al., 2012).

4.4.2 DDX3 and Bicistronic Plasmids

An interesting finding was that upon DDX3 overexpression, all tested pRF plasmids showed an increase in the expression of the downstream firefly cistron irrespective of the sequence inserted in the intercistronic region. The four different 5' UTR sequences inserted into pRF belong to the *EGFR, tau, APP, and* tubulin mRNAs. Apart from the tubulin 5' UTR, these tested sequences were reported previously to have intrinsic IRES activity (Veo and Krushel, 2012, Beaudoin et al., 2008, Webb et al., 2015). Yet one unanticipated finding was that overexpressing DDX3 has increased the expression of the firefly cistron tethered to the 5' UTR of the tubulin mRNA that has no reported IRES activity. Thus, these results indicate that the increased expression of firefly luciferase associated with DDX3 overexpression is not driven by increased IRES activity, especially for the tubulin 5' UTR.

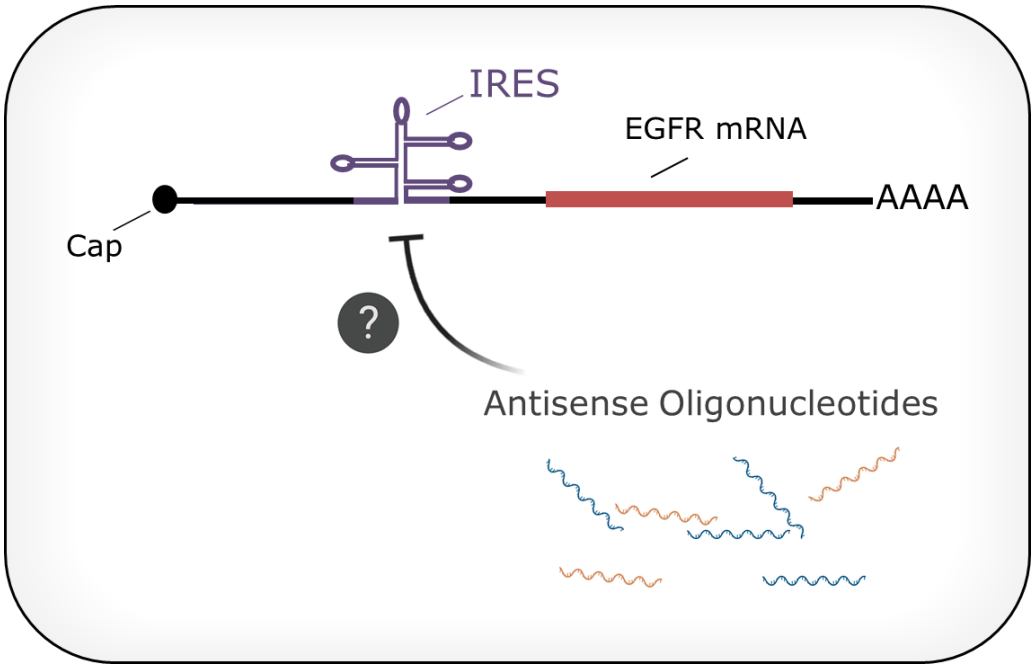
A possible explanation for these findings is that DDX3 might increase the rate of translation reinitiation following termination of translation of the first cistron in pRF. Several reports have shown that the 40S ribosomal subunits occasionally remain connected to mRNA during ribosome recycling after the encounter of a stop codon to reinitiate translation (Gould et al., 2014). In this regard, the availability of translation initiation factors including eIF4F and ternary complex was found to be required for these ribosomal subunits to reinitiate translation at a nearby AUG (Skabkin et al., 2013, Kozak, 1987). The data

generated in this study supports the notion that DDX3 could be one of these factors that positively influence the process of translation reinitiation in eukaryotic cells. An implication of this is the possibility of utilising DDX3 overexpression to increase the translation initiation rate of transfected transcripts especially circular mRNAs. Considering the novelty of these findings, the results, therefore, need to be interpreted with caution and further studies will need to be undertaken.

Chapter Five

5 Targeting *EGFR* using the Antisense Technology

Graphical summary



5.1 Introduction

Triple-negative breast cancer (TNBC) is an aggressive type of breast cancer that lacks target-specific therapies (Costa et al., 2017). EGFR is frequently expressed in TNBC tumours, highlighting its potential as a therapeutic target (Changavi et al., 2015). In this regard, the antisense technology has emerged as a powerful platform to generate therapeutic agents to inhibit the expression of EGFR at the mRNA level (Kang et al., 2006, Witters et al., 1999, Ciardiello et al., 2001). Antisense oligonucleotides (ASOs) are short lengths of single-stranded DNA/RNA molecules with complementary base sequence to specific mRNA targets. Upon target hybridisation by Watson–Crick base pairing, ASOs can modulate RNA processing through an array of distinct mechanisms leading to altered protein expression. These mechanisms of action are dependent on the design and chemistry of the ASO in addition to the hybridisation position on target RNA (Bennett, 2019). They can be broadly classified as those that bind and modulate RNA processing without inducing its degradation such as inhibiting translation, and those that induce sequence-specific degradation of target mRNA mediated by the activity of the endonuclease RNase H1 (Wu et al., 1999).

Firstly, ASOs can be designed to induce RNA degradation by RNase H1 which cleaves RNA in an RNA-DNA heteroduplex (Wu et al., 1999). RNase H1 is a ubiquitously expressed endonuclease that is involved in the resolution of R loops and removing RNA from Okazaki fragments (Ruhanen et al., 2011, Lima et al., 2016). To elicit RNase H1 activity, the ASO must contain a minimum of 5 consecutive DNA nucleotides with 10 nucleotides for optimal activity. Interestingly, RNase-H1

inducing ASOs are widely adopted to target the expression of the *EGFR* mRNA in different diseases including cancer (Najar et al., 2013, Nourazarian et al., 2012, Jian et al., 2010, Kagiyama et al., 2003, Qiu, 2003).

In addition, ASOs can modify RNA metabolism via several occupancy-only, steric blocking mechanisms (Bennett, 2019). This concept was first introduced by Zamecnik and Stephenson in their seminal work about blocking viral protein translation using synthetic oligonucleotides binding the 5’ and 3’ ends of Rous sarcoma virus 35S RNA (Zamecnik and Stephenson, 1978). Most steric blocking ASOs that inhibit translation are directed against sequences in the 5’ leader of target mRNA including the translational start site; as targeting the coding sequence was found to be ineffective due to the robust unwinding activity of translating ribosomes (Shakin and Liebhaber, 1986, Stein et al., 1997, Summerton, 1999). About blocking the IRES activity, it was shown that 2’-O-methyl ASOs targeting the domain IIId of the hepatitis C virus IRES can prevent *in vitro* viral-protein translation by competing with the 40S ribosomal subunit for binding to the IRES sequence (Tallet-Lopez et al., 2003). Interestingly, it was also shown that 2’-O-methyl ASOs targeting an inhibitory upstream open reading frame can increase protein translation from a downstream primary open reading frame (Liang et al., 2016). It seems that these ASOs can hinder the recognition of the upstream start codon, but not completely block the scanning process leading to enhanced initiation at the downstream primary AUG (Liang et al., 2016). Taken together, it appears feasible to selectively target the internal landing site of ribosomes using 2’-O-methyl ASOs without affecting translation mediated by ribosomes recruited through the universal cap structure (Figure 5.1).

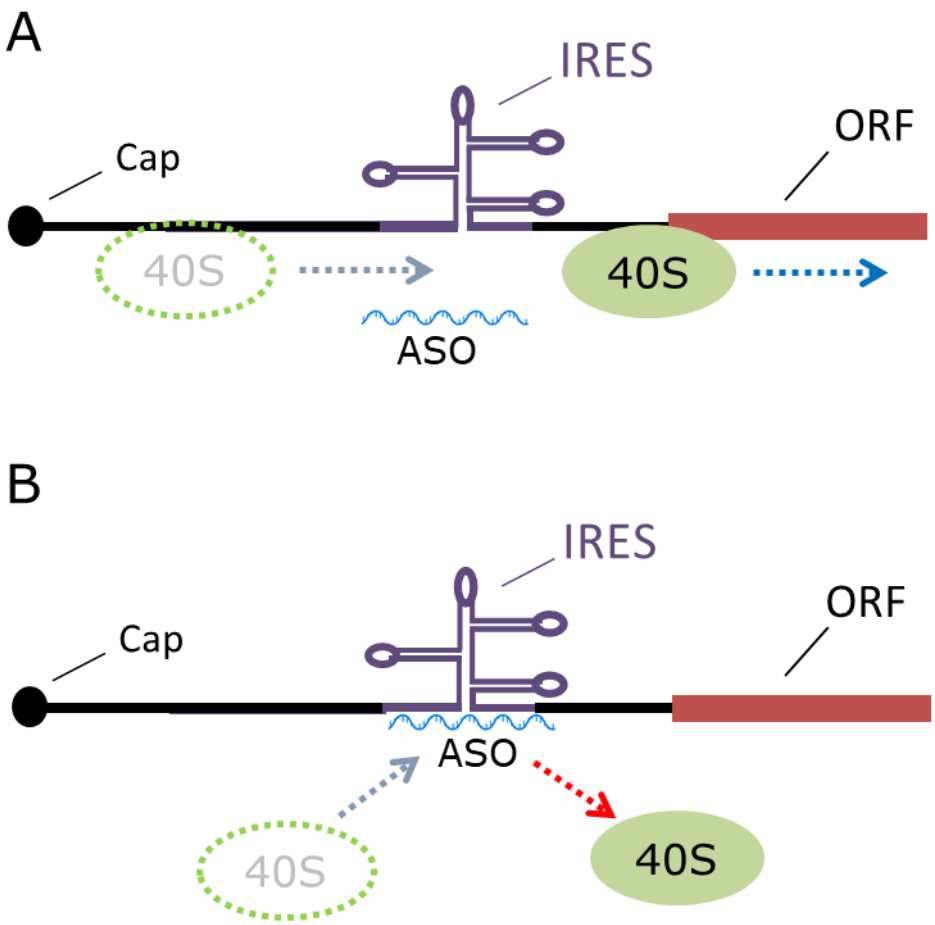


Figure 5.1 Targeting the internal landing site of the 40S ribosomal subunit using 2'-O-methyl ASOs. Under homeostatic conditions **(A)**, the 40S ribosomal subunit is recruited via a cap-dependent mechanism resulting in the displacement of inhibitory ASOs. However, the recruitment of the 40S subunit to an IRES is inhibited under cell stress **(B)**.

Therefore, the first section of this chapter will examine the use of 2'-O-methyl ASOs to selectively inhibit the *EGFR* IRES activity whilst cap-dependent translation remains unaffected (Webb et al., 2015). By inhibiting the internal landing of ribosomes, the IRES-mediated expression of EGFR under hypoxic conditions would be selectively inhibited without affecting the cap-dependent expression under homeostasis; limiting the toxic effects of systemic EGFR targeting. In the second antisense approach, modified ASOs were employed to

target different regions of the *EGFR* 5' UTR for degradation via the RNase-H1 pathway. By combining these ASOs with a drug delivery system responsive to low oxygen levels, this approach would allow the selective targeting of hypoxic cancer cells of solid tumours.

5.2 Occupancy-Only ASOs

To extend the analysis of Webb et al. (2015) with regard to specifically locating the 40S landing site within the IRES region, nine mutant versions of pREF were created in which the *EGFR* 5' UTR was mutated to induce out-of-frame start codons (iAUG) at 9 different positions along the *EGFR* 5' UTR starting from mutation 1 until mutation 9, which are located 13 and 206 nucleotides from the start of the sequence, respectively (Figure 5.2A). Each iAUG was introduced independently into a separate construct to distinguish their influence on translation initiation as these iAUGs were designed to induce the formation of non-functional peptides once recognised by the scanning ribosomes (Figure 5.2B). These mutant non-functional peptides would only be expressed if the ribosomal landing site is upstream of the mutant iAUG, and therefore quantified luciferase levels would be negatively affected. However, if the landing site is located downstream of the mutant iAUG, the wild-type firefly luciferase would be generated and quantified luciferase levels would be unaffected (Jopling et al., 2004).

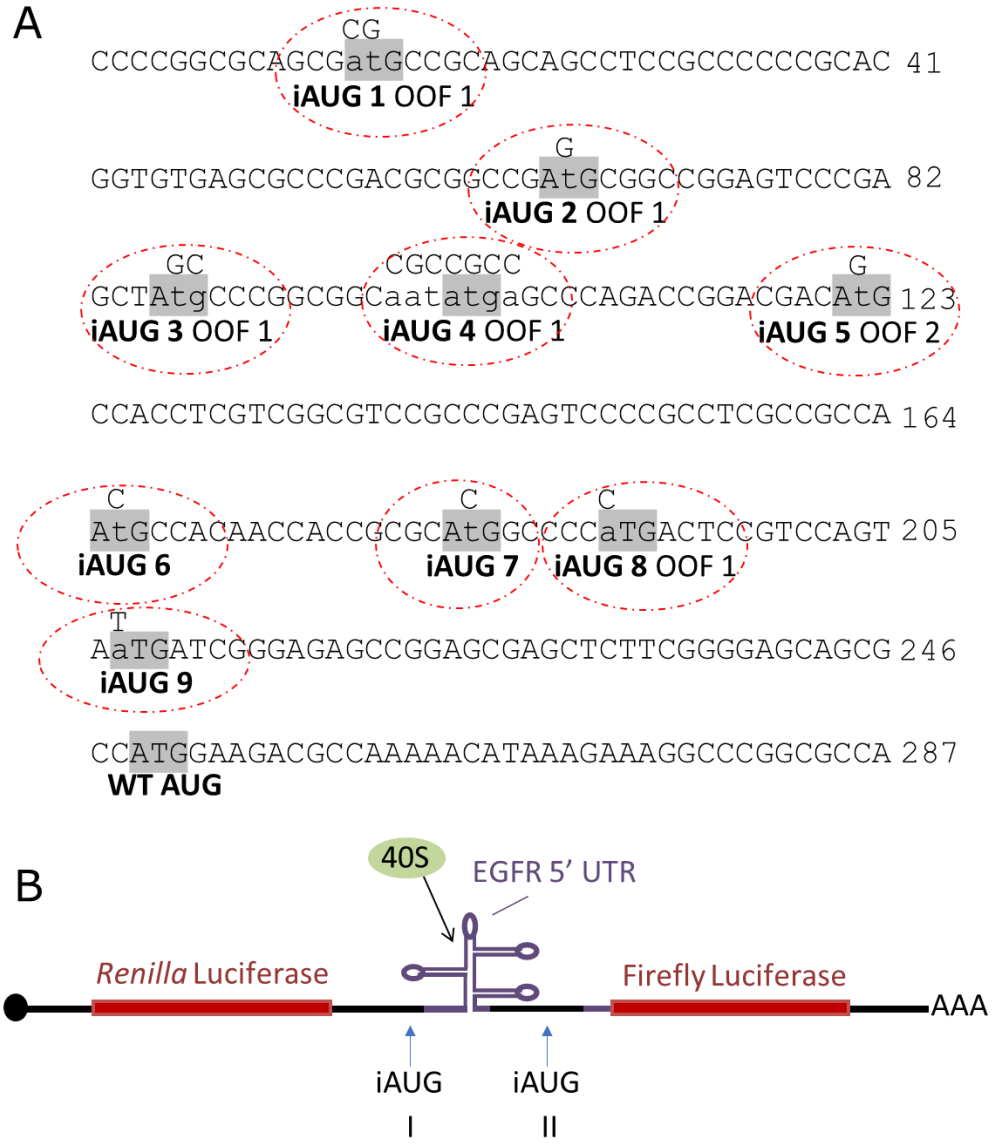


Figure 5.2 Mutant versions of the *EGFR* 5' UTR cloned into the bicistronic pRF plasmid. (A) The introduced start codons are highlighted in grey, where mutated bases are presented in lower case within the *EGFR* 5' UTR sequence. The wild-type sequence is presented on top of the mutated nucleotides. OOF: Out of Frame, WT: Wild Type. **(B)** A schematic illustration showing introduced AUGs (iAUGs) flanking the internal landing site of ribosomes. Opposite to (I), the downstream iAUG (II) would result in the formation of a non-functional protein.

The luciferase expression of these mutant pREF plasmids was assessed in MCF-7 cells at 48 hours after transfection. As it can be seen from Figure 5.3, these mutated plasmids have

differentially expressed the wild-type firefly luciferase in comparison to pREF, containing the wild-type *EGFR* 5' UTR. It seems that the introduction of these mutant iAUGs has affected the expression of the wild type luciferase in a manner dependent on their location. Consistent with previous findings, AUGs introduced downstream on the *EGFR* 5' UTR sequence appear to strongly affect the luciferase expression, whereas upstream AUGs affects the expression in a less significant manner with mutation 1 being the least effective (Webb et al., 2015).

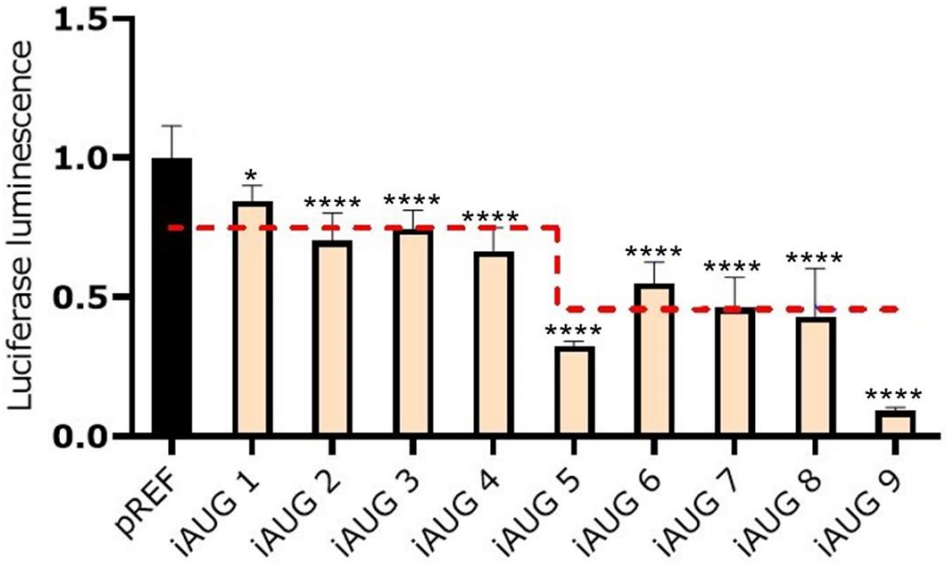


Figure 5.3 Relative firefly luciferase expression of pRF plasmids containing iAUGs within the *EGFR* 5' UTR sequence. Quantification of the firefly luciferase activity to *Renilla* luciferase activity of the different mutant versions of pREF following transfection in MCF-7 cells for 48 hours. The number assigned to each mutation represents the location within the *EGFR* 5' UTR as illustrated in Figure 5.2A. The dashed red line represents an interpretation of the trend of decline in expression of the wild-type firefly luciferase. N = 6. Two independent experiments. Error bars represent standard deviation. One-way ANOVA with Dunnett's correction. * indicates $p < 0.05$, **** indicates $p < 0.0001$.

In addition to the mutants containing introduced start codons, the same locations on the *EGFR* 5' UTR sequence were once more independently mutated but without introducing an upstream start codon. The purpose of this experiment was to assess whether the introduction of start codons could have affected possible binding sites of regulatory proteins or secondary structures important for optimal IRES activity. As shown in Figure 5.4, the introduction of these silent mutations has only affected the translation control of the *EGFR* 5' UTR at two distinct locations.

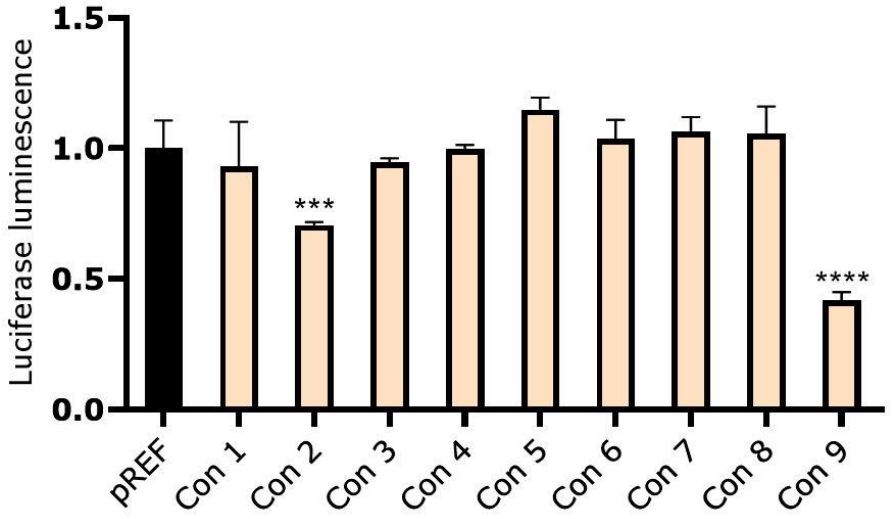


Figure 5.4 Relative firefly luciferase expression of pRF plasmids containing silent mutations within the *EGFR* 5' UTR sequence. The quantification of firefly luciferase activity to *Renilla* activity of the different mutant versions of pREF following transfection in MCF-7 cells for 48 hours. N = 3. Data generated from a single experiment. The number assigned to each mutation represents the location within the *EGFR* 5' UTR as illustrated in Figure 5.2A. Error bars represent standard deviation. One-way ANOVA with Dunnett's correction. *** indicates $P < 0.001$, **** indicates $p < 0.0001$.

Both mutation 2 and 9 have resulted in a significant reduction in the relative expression of the firefly luciferase, indicating the presence of potential regulatory-protein binding sites or

important structural features at these defined locations (Kieft et al., 1999). Thus, the observed decrease in translation with the introduced AUGs in the other locations appears to be related to altered 40S ribosomal activity. In addition, the descending pattern of the wild-type luciferase expression represented by the red dashed line in Figure 5.3 could suggest that the 40S landing site is located before iAUG 5. Yet further experiments are still required to confirm these results. As the internal landing site of ribosomes was not clearly identified, the *EGFR* 5' UTR was targeted at three different locations including the start of the 5' UTR sequence using occupancy-only RNA ASOs fully modified with 2'-O-methyl groups (Table 5.1). As can be seen from Figure 5.5, utilising these ASOs in MCF-7 cells transfected with pREF resulted in no significant changes in the expression of the firefly luciferase. Collectively, these results indicate that the concept of targeting the *EGFR* IRES with occupancy-only ASOs to prevent the internal landing of ribosomes remains to be established.

Table 5.1 Modified RNA ASOs. Nucleotide sequences of the fully modified RNA ASOs with the 2'O-methyl modification and their hybridisation targets in pREF.

Name	Sequence 5'-3'	Description
1st RNA ASO	CUGCUGCGGCC-GCGCUG	Hybridises to *EGFR* 5' UTR between nucleotides 8-25
2nd RNA ASO	AUACUGGACGG-AGUCAG	Hybridises to *EGFR* 5' UTR between 191-207
3rd RNA ASO	GCGUCUUCCAU-GGCGCUGCU	Hybridises to the start codon of firefly luciferase
Scrambled RNA ASO	UCAGAGAGUUA-CGGCGA	Scrambled nucleotide sequence

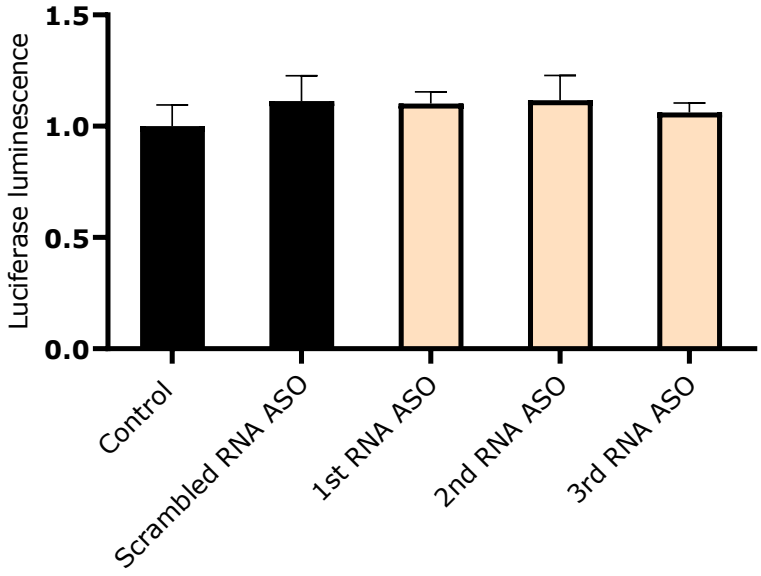


Figure 5.5 Relative firefly luciferase activity of pREF after transfection with modified RNA ASOs. A luciferase assay of MCF-7 cells transfected with pREF 24 hours before transfecting with modified RNA ASOs for 48 hours. N = 5. Data generated from a single experiment. Error bars represent standard deviation. Control represents cells with no ASO transfection.

5.3 RNase H1-Dependent ASOs

With regards to the second antisense approach utilised in this study, a small library of DNA ASOs was designed to target the different regions of the *EGFR* 5' UTR (Table 5.2). These DNA ASOs were assigned numbers from 1 to 10, in which 1 corresponds to the first segment while 10 corresponds to the last segment of the *EGFR* 5' UTR. This initial screening was conducted to assess the accessibility of the unmodified DNA ASOs to their respective targeted regions. For screening these RNase-H1-dependent ASOs, the p15E vector that contains a single firefly luciferase open reading frame downstream to the *EGFR* 5' UTR was co-transfected with the p80 plasmid, encoding the *Renilla* luciferase, as a control.

Table 5.2 Unmodified DNA ASOs. Nucleotide sequences of the unmodified DNA ASOs and their hybridisation targets in pREF.

Name	Sequence 5'-3'	Description
1st DNA ASO	CTGCGGCCGCGCT-GCGCCGG	Hybridises to *EGFR* 5' UTR between nucleotides 2-22
2nd DNA ASO	GGCGGAGGCTGCT-GCGGCCG	Hybridises to *EGFR* 5' UTR between nucleotides 13-33
3rd DNA ASO	GGCGCTCACACCG-TGCGG	Hybridises to *EGFR* 5' UTR between nucleotides 35-55
4th DNA ASO	GACTCCGGCCGCC-TCGGCCG	Hybridises to *EGFR* 5' UTR between nucleotides 58-78
5th DNA ASO	TGGCCTGTCGTCC-GGTCTGG	Hybridises to *EGFR* 5' UTR between 106-126
6th DNA ASO	GGCGGACGCCGA-CGAGGTGG	Hybridises to *EGFR* 5' UTR between 123-143
7th DNA ASO	TGGCGTTGGCGGC-GAGGCGG	Hybridises to *EGFR* 5' UTR between 150-170
8th DNA ASO	GGCCGTGCGCGGT-GGTTGTG	Hybridises to *EGFR* 5' UTR between 168-188
9th DNA ASO	CAATACTGGACGG-AGTCAGG	Hybridises to *EGFR* 5' UTR between 189-209
10 DNA ASO	GAAGAGCTCGCTC-CGGCTCTCC	Hybridises to *EGFR* 5' UTR between 213-233

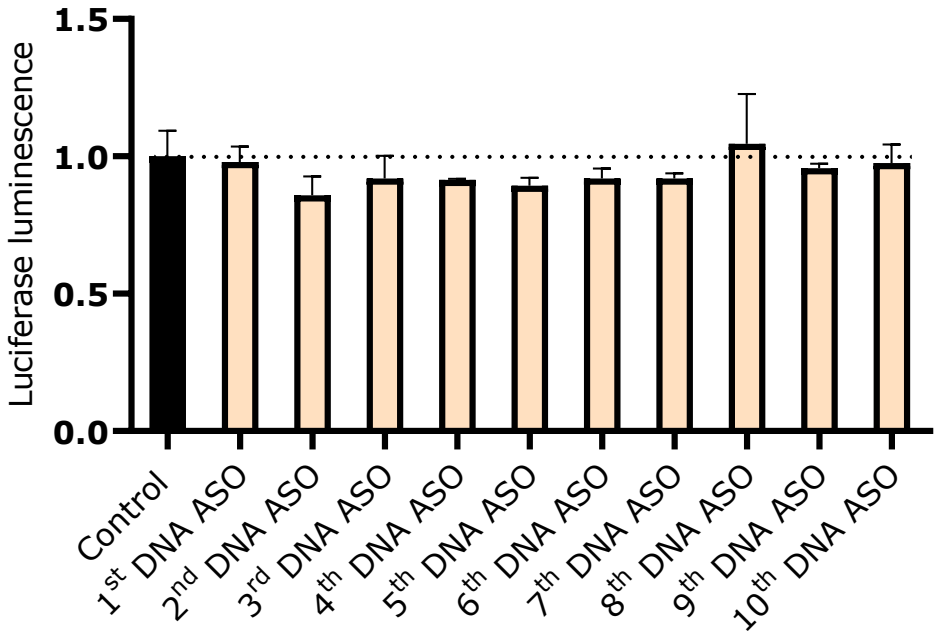


Figure 5.6 Screening DNA ASOs for their anti-EGFR mRNA activity. Luciferase assay results after transfection of unmodified DNA ASOs for 48 hours in MCF-7 cells transfected with p15E. Values are normalised to p80, a reporter plasmid expressing the *Renilla* luciferase. N = 3. Data generated from a single experiment. Error bars represent standard deviation. Control represents cells with no ASO transfection.

As shown in Figure 5.6, transfecting the different DNA ASOs has resulted in differential changes in the relative activity of the firefly luciferase. It should be noted that it was expected to have changes of moderate-intensity as these unmodified ASOs are known to be inherently unstable against the activity of nucleases (Crooke et al., 2018, Wickstrom, 1986). After that, three new ASOs were designed targeting the central region of the *EGFR* 5' UTR, while considering the feasibility of producing them as having exceptionally high GC content could impair the synthesis reaction.

Based on the widely-adopted gapmer design, these ASOs were designed to have a phosphorothioate backbone and a stretch of ten DNA monomers flanked by five 2'-O methyl modified nucleotides (Table 5.3). These modifications were adopted to increase the affinity for target mRNA and increase resistance to nuclease degradation while retaining efficacy for RNase-H1-mediated degradation (Stein et al., 1988, Freier and Altmann, 1997).

Table 5.3 2'-O-methyl gapmers. Nucleotide sequences of 2'O-methyl gapmers having a phosphorothioate backbone and a core DNA sequence of 8-10 nucleotides flanked by 5 RNA nucleotides modified by 2'O-methyl groups. The modified nucleotides are indicated in bold font.

Name	Sequence 5'-3'	Description
1st gapmer	**GGCGC**TCACACCG-**UGCGG**	Hybridises to 5' UTR between 35-54 nucleotides
2nd gapmer	**UGGCC**TGTCGTCC-GG**UCUGG**	Hybridises to 5' UTR between 105-126 nucleotides
3rd gapmer	**UGGCG**TTGGCGG-CGA**GGCGG**	Hybridises to 5' UTR between 150-171 nucleotides
Scrambled gapmer	**UUGUC**GGTGAAG-GTT**CCUCC**	Scrambled nucleotide sequence

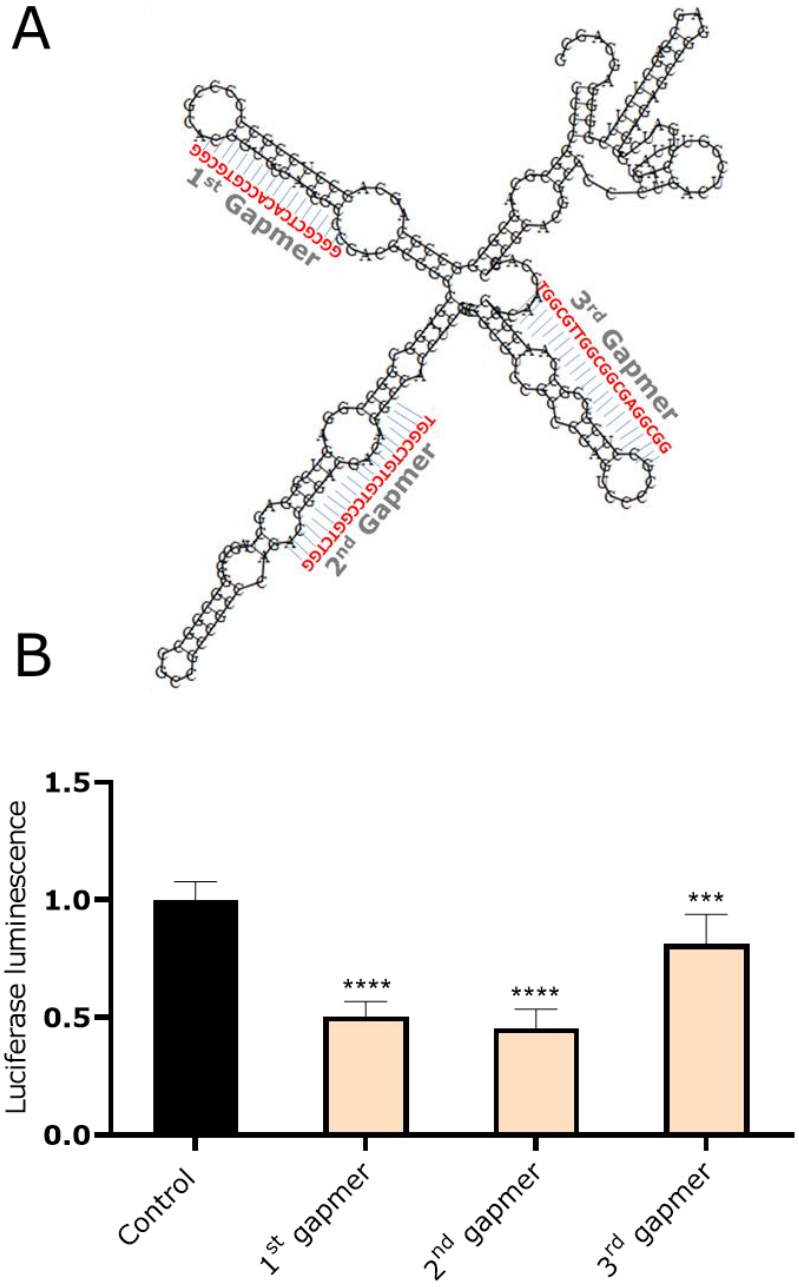


Figure 5.7 Gapmer ASOs against the *EGFR* 5' UTR cloned into p15E. (A) A schematic diagram representing the *EGFR* 5' UTR as predicted by mfold (Zuker, 2003) showing the binding sites of the gapmers used in this experiment. **(B)** A bar graph showing the quantification of luciferase activity after 48 hours of transfecting the gapmers targeting the *EGFR* 5' UTR in MCF-7 cells (N=9). Control group includes cells without ASO transfection. Three independent experiments. Values normalised to p80. Ordinary one-way ANOVA with Dunnett's post hoc test. *** indicates P < 0.001, **** indicates p < 0.0001**.**

As demonstrated in Figure 5.7, these gapmer ASOs especially the first and second gapmers have resulted in a significant decrease in the activity of firefly luciferase ($p = <0.0001$). In contrast, the relative activity of the firefly luciferase was unaffected by the transfection of the modified RNA ASOs lacking the DNA core sequence necessary for the RNAase-H1 activity (Figure 5.5).

In addition, the binding specificity of the designed gapmers was examined via *in silico* analysis using GGGenome (http://GGGenome.dbcls.jp/). GGGenome is a genomic and transcript bioinformatic tool for querying oligonucleotides, allowing gaps and mismatches (Yoshida et al., 2018). As it can be seen from Table 5.4, the designed gapmers only target the *EGFR* transcript, even after increasing the complementarity mismatches to 10% as in the case of the second gapmer ASO.

Table 5.4 Analysis of the binding specificity of the gapmer ASOs performed using the GGGenome tool. Except for the scrambled control, the *EGFR* mRNA is targeted by all gapmers at all given percentages of complementarity mismatches.

		Complementarity mismatches				
	Targeted transcripts	**0%**	**5%**	**10%**	**15%**	**20%**
ASO	**1st Gapmer**	1	1	5	11	879
	2nd Gapmer	1	1	1	4	93
	3rd Gapmer	1	1	2	19	302
	Scrambled gapmer	0	0	0	4	136

To confirm these findings, western blotting analysis was conducted to investigate the protein levels of EGFR following the transfection of these gapmers in two breast cancer cell lines, MCF-7 and MDA-MB-231. As it can be seen from Figure 5.8, there is a significant reduction in the expression of the EGFR protein in both MCF-7 ($p = <0.0001$) and MDA-MB-231 cells ($p = <0.0001$) with the anti-EGFR gapmers. Yet transfecting the scrambled gapmer resulted in no significant changes in the expression of EGFR, underscoring the specificity of the anti-EGFR gapmers.

In addition to the expression levels of the EGFR protein, the metabolic activity and hence the viability of breast cancer cells was assessed using the MTT assay following transfection with the anti-EGFR gapmers. From Figure 5.9, it can be seen that the viability of the cells was significantly reduced with all three gapmers in both the MCF-7 ($p = <0.0001$) and MDA-MB-231 cell lines ($p = <0.0001$). In this regard, the scrambled control also did not induce any significant changes in the viability of transfected cells. These described results collectively indicate that inhibiting the expression of the EGFR protein via gapmer ASOs is an effective strategy to inhibit the growth of breast cancer cells.

Finally, the unassisted uptake of these gapmers has been investigated in both cell lines by assessing the expression of EGFR in cells incubated for several days in culture media containing the anti-EGFR gapmers. As shown in Figure 5.10, the incubation of these gapmers without any transfection reagent has resulted in a significant decrease in the expression of the EGFR protein in both the MCF-7 ($p = 0.0157$) and MDA-MB-231 cell lines ($p = 0.0107$).

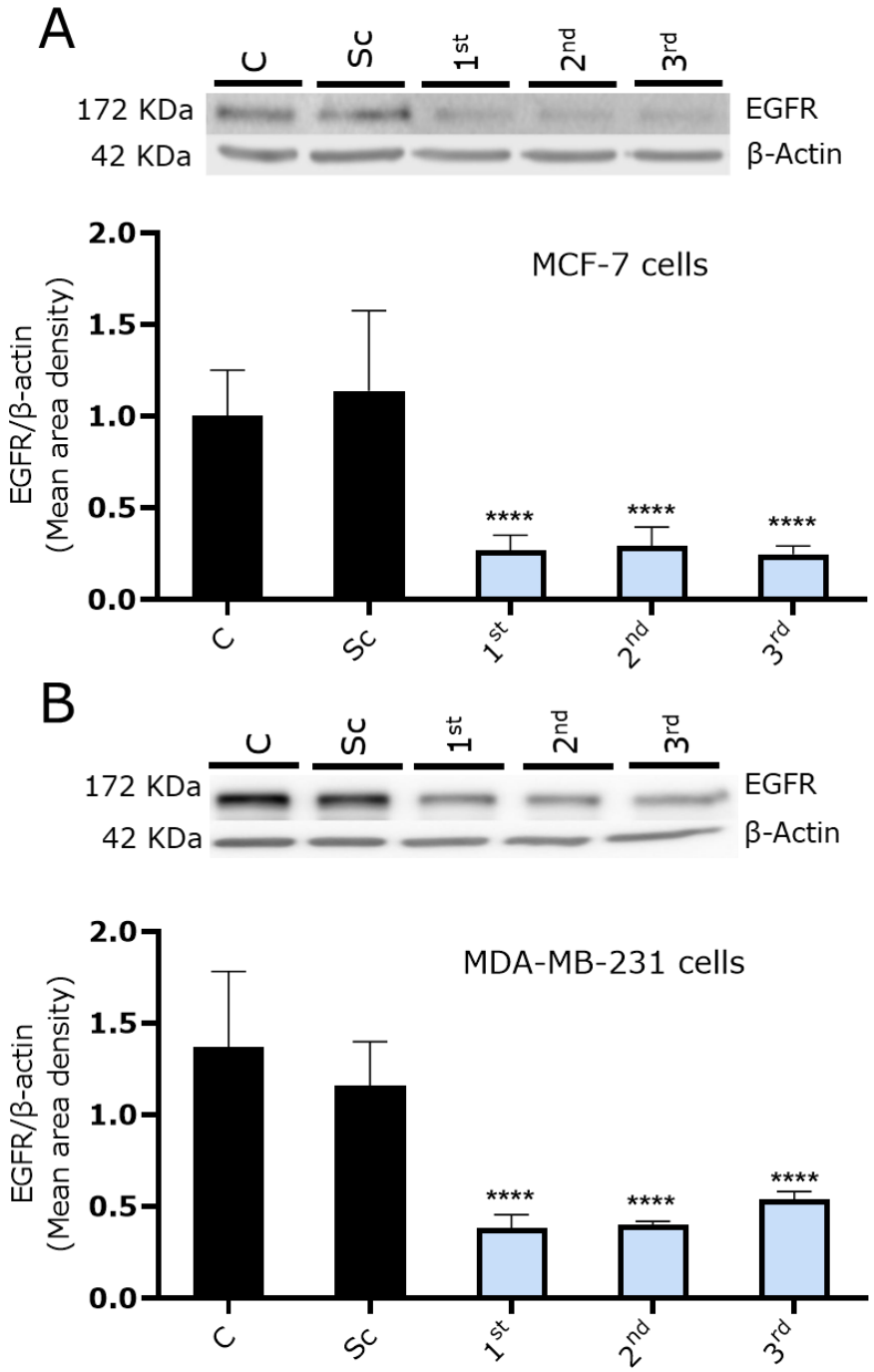


Figure 5.8 Effects of gapmers on the protein expression of EGFR. Representative western blots and densitometric analysis of EGFR normalised to β-actin in **(A)** MCF-7 and **(B)** MDA-MB-231 cells following transfection with gapmers for 48 hours. N = 3-6 for MCF-7 cells and N = 6 for MDA-MB-231 cells. Two independent experiments. One-way ANOVA with Dunnett's correction. **** indicates $p < 0.0001$. C – Control; Sc – Scrambled gapmer; 1st – 1st Gapmer; 2nd – 2nd Gapmer; 3rd – 3rd Gapmer.

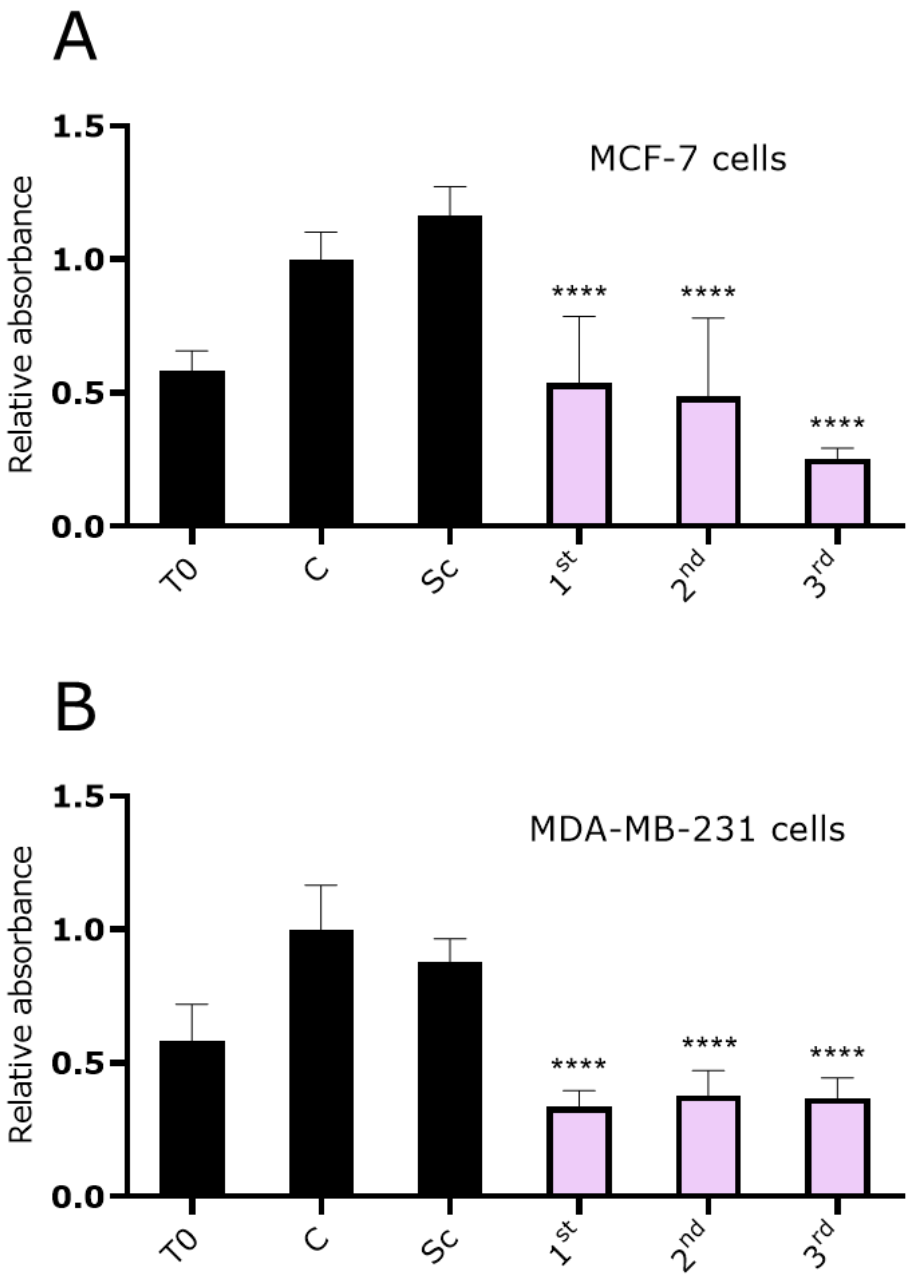


Figure 5.9 Effects of the anti-EGFR gapmers on the metabolic activity of breast cancer cells. MTT assay results after the transfection of the gapmer ASOs into **(A)** MCF-7 cells (N = 8-12) and **(B)** MDA-MB-231 cells (N = 8) for 48 hours. Two independent experiments. Error bars represent standard deviation. One-way ANOVA with Dunnett's correction. **** indicates $p < 0.0001$. T0 indicates the metabolic activity of cells immediately before ASO transfection. C – Control (without ASO transfection); Sc – Scrambled gapmer; 1st – 1st Gapmer; 2nd – 2nd Gapmer; 3rd – 3rd Gapmer.

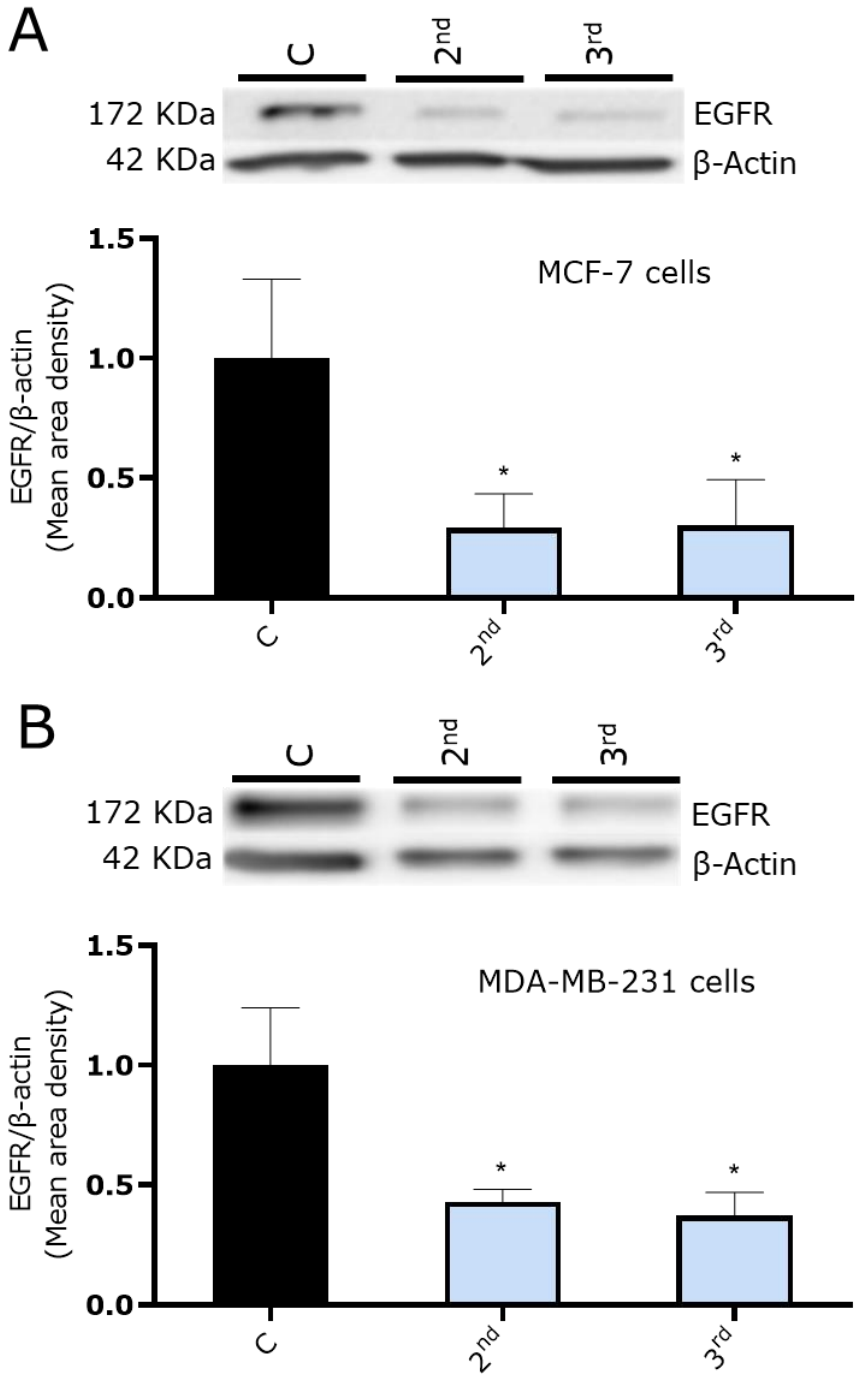


Figure 5.10 The unassisted uptake of the gapmer ASOs by breast cancer cells. Representative western blots and results of densitometric analysis of the EGFR expression normalised to β-actin in **(A)** MCF-7 cells (N = 3) and **(B)** MDA-MB-231 cells (N = 3) following incubation with the gapmers at 5 μM for 4 and 3 days, respectively. Data generated from a single experiment. One-way ANOVA with Dunnett's correction. * indicates $p < 0.05$. C – Control (without ASO treatment); 2nd – 2nd Gapmer; 3rd – 3rd Gapmer.

In summary, the present research aimed to examine the potential of the antisense technology in targeting EGFR in breast cancer cells. The first approach utilised was to inhibit the internal landing of ribosomes via modified RNA ASOs targeting the *EGFR* IRES. However, this approach was ineffective probably due to the lack of a defined landing site of ribosomes. The second approach was to target the *EGFR* 5' UTR for degradation using modified ASOs that induce the RNase H1 pathway. Utilising this approach, the expression of the EGFR protein has been effectively inhibited in breast cancer cells. Furthermore, the viability of these cells was significantly compromised, highlighting the therapeutic potential of these gapmers.

5.4 Discussion

A strong relationship between EGFR and hypoxia has been reported in the literature including reports demonstrating that the colocalization of EGFR and hypoxia is associated with poor clinical prognosis, signalling an important role of EGFR in promoting the survival of hypoxic cancer cells (Hoogsteen et al., 2012, Swinson and O'Byrne, 2006). To inhibit the expression of EGFR under low oxygen levels, the antisense technology was utilised through the use of ASOs targeting the *EGFR* 5' UTR harnessing different mechanisms of action. First, ASOs were designed to preferentially inhibit the *EGFR* IRES activity by blocking the internal landing site of ribosomes. Yet using these ASOs resulted in no significant changes in the *EGFR* IRES activity. The second group of ASOs were developed to induce degradation of the *EGFR* mRNA via the RNase H1 pathway. These gapmers targeting different regions of the *EGFR* 5' UTR were found to be effective in reducing the

expression of EGFR and cellular viability in two breast cancer cell lines. These results further support the concept of employing the antisense technology in targeting EGFR in cancer (He et al., 2010).

An important advantage of utilising the antisense technology is that the main requirement to identify a drug candidate is to locate targetable regions in a pathogenic RNA. To fulfil this requirement, a luciferase-based screening strategy was utilised harnessing the *EGFR* IRES activity to locate an active pharmacophore within the *EGFR* 5' UTR (Webb et al., 2015). In this target-based assay, the bicistronic reporter construct pREF containing the *EGFR* 5' UTR was used to assess both the specificity and efficacy of the hybridisation interactions between the occupancy-only ASOs used and the *EGFR* 5' UTR. On the other hand, the monocistronic p15E vector that contains the *EGFR* 5' UTR upstream of the firefly luciferase cistron was used to screen the activity of the RNase-H1-dependent ASOs. Considering the high throughput capabilities of these screening tools, cell lines stably expressing pREF and p15E could be used to screen large libraries of ASOs targeting the *EGFR* 5' UTR. This would facilitate not only the identification of an active pharmacophore but also assessing the effect of chemical modifications and formulation strategies on the ASO activity. This characteristic is of special importance with the advent of automation in drug discovery. Hit generation and target identification including the unravelling of the underlying pharmacological networks are resource-intensive processes in modern drug discovery that are often depicted as "finding a needle in a haystack" (Laraia et al., 2018, Rodrigues and Bernardes, 2020). In contrast, the design parameters of ASOs with regards to their nucleotide sequence and chemical

properties for target specificity and mechanism of action are more defined and validated (Hessler and Baringhaus, 2018, Putz et al., 2016). Hence in this study, three ASOs targeting different pharmacophores within the *EGFR* 5' UTR were developed in a relatively effective manner.

5.4.1 Occupancy-Only ASOs

Firstly, the antisense technology was utilised to prevent the internal landing of ribosomes on the *EGFR* 5' UTR; as this process was associated with maintaining EGFR expression under stress conditions associated with malignant growth such hypoxia (Webb et al., 2015). Thus, this antisense approach would be intrinsically selective in targeting EGFR in the stressed cancer cells while maintaining homeostatic, cap-dependent EGFR expression unaffected. To locate the internal landing site of ribosomes, 18 mutant versions of the *EGFR* 5' UTR were generated including mutants containing out-of-frame start codons introduced at different locations. These introduced start codons were designed to generate mutant nonfunctional peptides once inserted after the landing site of ribosomes.

Considering the dramatic decrease in reporter expression associated with iAUG 5, the results of this mutagenesis study signalled the possible recruitment of the 40S ribosomal subunits to the IRES region at a point between positions 104 and 120 from the start of the *EGFR* 5' UTR sequence. However, further experiments including computational resources of ribosomal profiling under stress are required to confirm the findings of this mutagenesis study and provide more details about the process of internal entry of ribosomes within the *EGFR* IRES region (Ingolia et al., 2011). In addition, the dramatic decrease in

luciferase expression induced by iAUG 5 can be further explored by additional iAUGs and occupancy-only ASOs specifically targeting that region in the *EGFR* 5’ UTR sequence.

As the location of the internal landing site of ribosomes is still unclear, the lack of efficacy of the modified RNA ASOs designed to prevent the ribosomal landing could be explained by the displacement of almost any bound ASO via the ATP-driven helicase activity of scanning ribosomes landed upstream to the hybridised ASO. Only landing ribosomes are thought to lack the helicase activity of eIF4A and DHX29 necessary to displace the hybridised ASOs from their landing site, thus physically blocking their mRNA binding and translation (Tallet-Lopez et al., 2003, Liang et al., 2016, Özeş et al., 2011).

5.4.2 RNase H1-dependent ASOs

In this study, it was also found that using gapmer ASOs targeting the *EGFR* 5’ UTR at three different locations has significantly reduced the expression of EGFR in two breast cancer cell lines, MCF-7 and MDA-MB-231. These gapmers at 5 μM were even found to be effective in targeting EGFR without any requirement for a transfecting agent. Despite differences in their nucleotide sequences and hence their targeted regions, these EGFR gapmers have produced a comparable phenotypic feature of reduced cellular viability, indicating a common mechanism of action. Furthermore, the negative control used with a mismatched nucleotide sequence has produced no significant changes in either cellular viability or EGFR expression. Yet additional experimental measures are still required including RNA interference and fluorescence-activated cell sorting to confirm the importance of RNase H1 in this regard

and to provide insight into the observed effects on cellular metabolism associated with ASO transfection (Liang et al., 2017). Overall, the obtained results indicate that the gapmer ASOs developed in this project are effective in targeting the expression of the *EGFR* mRNA.

With the advent of high throughput sequencing technologies, the cost of sequencing the human genome is increasingly on the decline, making personalised medicine more affordable and advisable. This is of special importance when EGFR is looked at in context as acquired resistance to anti-EGFR therapies ultimately develops in almost all colorectal and lung cancer patients (Lim et al., 2018, Parseghian et al., 2019). The development of this secondary resistance stems from the *de novo* acquisition of genetic mutations or the selective pressure exerted by the anti-EGFR therapies resulting in the outgrowth of resistant subclonal populations (Misale et al., 2014). By sequencing the *EGFR* gene in circulating tumour DNA, it is possible and practical to tackle this issue by tailoring the design of anti-EGFR ASO to address the presence of sequence mutations that could interfere with the efficacy of therapy.

Furthermore, combination therapy has been also suggested to overcome this problem by simultaneously surmounting different resistance mechanisms present in a single patient (Yang and Tam, 2018). A multimodal therapeutic approach could be utilised in which more than one pathogenic signalling cascade is targeted by ASOs in a single formulation. The activation of ERBB3/HER3 receptor has been implicated in the development of acquired resistance to EGFR therapy (Engelman et al., 2007). By the concomitant targeting of this receptor, EGFR ASOs would likely be more effective and less prone to the development of resistance. It was reported that combining antisense based

therapeutics against multiple targets including *EGFR* has enhanced their therapeutic efficacy which allowed the reduction of their effective concentrations by more than 80% (Kozielski et al., 2019). Reducing the effective concentration could even help in diluting dangerous off-target effects as observed with small-molecule oncology drugs (Chen et al., 2013).

In comparison to the double-stranded RNA-mediated interference, the nucleotide bases of ASOs could be modified extensively by chemical modifications as integration into the RNA-interference machinery is not required for their pharmacological actions. The possession of these chemical modifications has been shown to result in ASOs with higher affinity and improved stability in both biological and pharmaceutical settings (Chery, 2016). In this regard, two widely adopted ASO modifications were utilised to produce the anti-EGFR gapmers, namely, the phosphorothioate and 2-O-methyl modifications. As demonstrated earlier, the modified ASOs were dramatically more effective than naked ASOs in inhibiting reporter activity. In addition, double-stranded RNAs are more hydrophilic than ASOs due to the internalisation of the aromatic residues in the overall double-stranded structure and surfacing of the heavily hydrated phosphate groups. This improved hydrophilicity can negatively affect the interaction with the hydrophobic cell membrane surface, causing the delivery of duplex RNA to be more challenging than ASOs (Watts and Corey, 2012). Indeed, ASOs developed in this study have achieved effective intracellular concentrations in target cells without using any transfection aid. On the other hand, RNA interference is more robust and reproducible considering the widespread adoption of this technology in molecular biology laboratories. Nevertheless, both platforms can produce

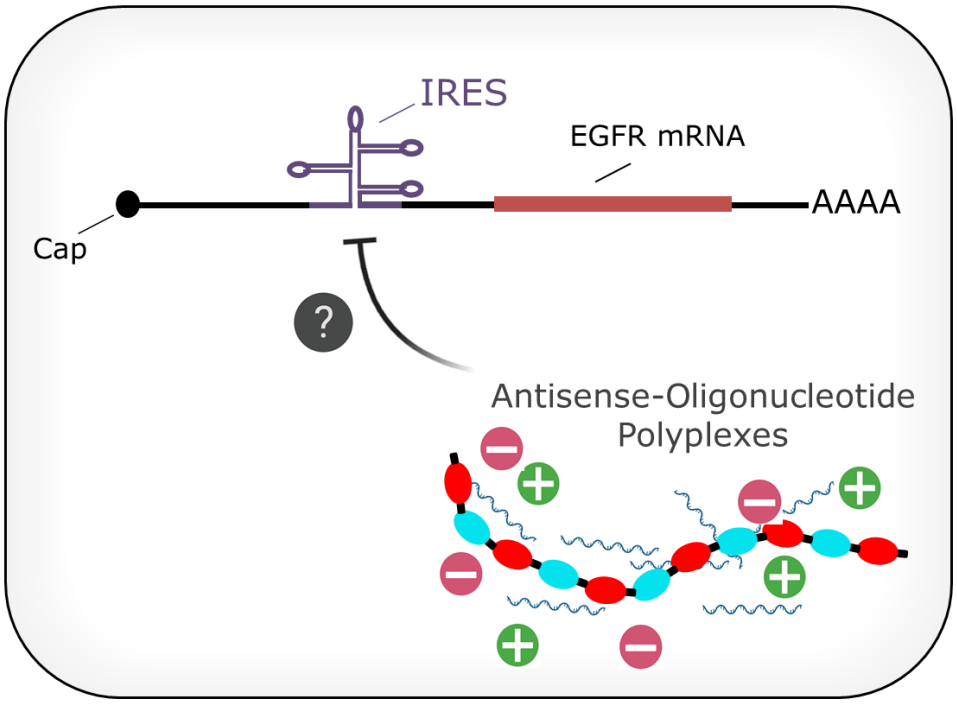
effective therapeutics as long as they are properly optimised. Therapeutic nucleotides including ASOs and siRNAs form a new class of drugs that requires novel pharmaceutical development to allow for the mainstream adoption of this technology. In comparison, antibody-based therapeutics required many years of development to be widely used in medical practice (Watts and Corey, 2012).

Overall, chemically modified ASOs were developed to target the expression of the *EGFR* mRNA. It was demonstrated that the gapmer ASOs developed in this study were capable of both inhibiting the expression of EGFR and reducing the viability of breast cancer cells. The development of these effective RNase-H1-dependent gapmers highlights the potential of targeting EGFR using the antisense technology in breast cancer. Yet combining these ASOs with a selective delivery system is required to ensure the preferential and effective targeting of breast cancer cells.

Chapter Six

6 Hypoxia Responsive Polymers

Graphical summary



6.1 Introduction

The delivery of nucleic acid into host cells is a critical step in gene therapy applications as genetic material has to overcome several barriers for successful transfection including avoiding nuclease degradation and crossing cell membrane. To address these issues, gene delivery is mainly achieved through vectors such as cationic polymers that can facilitate cellular internalisation while shielding against catalytic degradation (Geary et al., 2015). Among cationic polymers, linear poly(amidoamines) (PAAs) and poly(β-amino esters) (PBAEs) are promising candidates. PBAE and PAA refer to polymers synthesised by the conjugate addition of acrylates or acrylamides and amines and thus have inherent properties to esters and amides such as biodegradability (Ranucci and Manfredi, 2019, Cordeiro et al., 2019).

Perhaps the most important advantage of using these polymers is the versatility of their building blocks which can provide diverse physicochemical properties to the resulting polymers (Lynn and Langer, 2000). As a result, combinatorial libraries were used to study the structure-property relationship of these polymers. The results of the first initial screening of 140 different PBAEs indicated that polymers with molecular weights between 3,180 and 9,170 $g \cdot mol^{-1}$ can transfect DNA efficiently (Lynn et al., 2001). Yet short polymers are known to be less efficient in condensing nucleic acid while very long polymers are prone to restrain the "unpacking" of nucleic acid required for successful transfection (Schaffer et al., 2000). In a following paper from the Langer lab in which they examined the biophysical characteristics of polymers with regards to overcoming cellular barriers to gene delivery, it was found that

polymers which impart polyplexes with small mean diameters (<240 nm) and positive surface charge were associated with higher levels of transfection activity (Akinc et al., 2003).

In a different study in which 2,350 structurally unique PBAEs were examined for transfection efficiency, the best performing polymers were characterised by common structural features including a hydrophobic acrylate monomer (Bisphenol A glycerolate (1 glycerol/phenol) diacrylate) and a linear amine molecule with hydroxyl side groups (Anderson et al., 2003). The hydrophobic bisphenol A group was also found to improve DNA complexation via improved hydrophobic interactions (Zhang et al., 2010). The polymer end group was also found to significantly affect transfection efficiency. By varying the amine/diacrylate stoichiometric ratio in the synthesis reaction, high molecular weight polymers with amine end groups were found to transfect cells more effectively than acrylate-terminated polymers (Akinc et al., 2003). Based on these seminal studies by Langer's research group, a second-generation library of 70 structurally-different PBAEs was prepared in which 20 PBAEs were found to produce polyplexes with particle sizes of less than 150 nm and transfection efficiencies at least comparable to Lipofectamine 2000 (Anderson et al., 2005). Further combinatorial modifications have even resulted in polymers with transfection efficiencies similar to those registered with adenovirus, indicating that small structural changes can significantly influence the biophysical characteristics of the resulting polymers (Green et al., 2007). Even if these polymeric systems do not perform as well as adenoviruses with regards to transfection efficiency, there are manufacturing, safety and immunogenicity benefits to these systems in comparison to viral vectors (Gonzalez et al., 1999,

Smith, 1995). Due to the presence of amino groups in the polymer backbone, PAA and PBAE intrinsically carry a net positive charge that enables complexation with the negatively charged nucleic acid to form stable polyplexes via electrostatic interactions. These polyplexes not only allow the delivery of nucleic acid cargo into target cells but also protect against degradation by nucleases (Ranucci and Manfredi, 2019). The release of nucleic acid from these polyplexes is triggered by the hydrolysis of the ester/amide bonds embedded along the polymer backbone. As this hydrolytic degradation is on the time scale of several hours to a few days, it is difficult to control where the nucleic acid release will occur (Sunshine et al., 2012). To enhance intracellular targeting, disulphide bonds were incorporated along the polymer backbone of several PBAEs and PAAs (Kozielski et al., 2014). These disulphide bonds are degraded via glutathione which is predominantly present in the cytosol, triggering polymer degradation and hence intracellular nucleic acid release. However, this process is fairly non-selective as glutathione is found in every cell at relatively high concentrations in the range of 1–10 mM (Meister, 1988). Therefore, we have designed novel linear PBAE polymers incorporating the azobenzene bonds along the polymer backbone to specifically target the release of nucleic acid into hypoxic cancer cells. These azobenzene bonds are preferentially degraded reductively in cells under low oxygen tensions (1% oxygen or less) which are present predominantly in cancers (Brown and Wilson, 2004, Zbaida and Levine, 1991, Kiyose et al., 2010, McKeown, 2014). This property can be harnessed to target the release of the anti-EGFR ASOs to hypoxic cancer cells by employing these azobenzene-containing polymers as vectors. Indeed, the azobenzene bond is widely used to impart hypoxia sensitivity and specificity to imaging agents, prodrugs

and polymers (Zhang et al., 2016, Kulkarni et al., 2016, Si et al., 2020, Piao et al., 2013, Liu et al., 2019). For nucleic acid delivery, the first example was documented by Perche et al in which azobenzene was used to link a protective layer of polyethylene glycol (PEG) molecules with polyethyleneimine (PEI) and 1,2-dioleoyl-sn-glycero-3-phosphoethanolamine (DOPE) units. The degradation of azobenzene under low oxygen levels allowed the removal of the protective PEG molecules, releasing the DOPE/PEI complexes to mediate siRNA delivery (Perche et al., 2014). Another published strategy is based on metal−organic frameworks containing azobenzene units (Huang et al., 2019). In contrast to these existing systems, incorporating the azobenzene bond into PAAs and PBAEs would allow the generation of novel hypoxia-selective gene delivery systems that can be easily synthesised and their physicochemical properties can be finely modified (Cordeiro et al., 2019, Ranucci and Manfredi, 2019).

6.2 Polymer synthesis

The first set of experiments in this chapter was designed to synthesize biodegradable PAA and PBAE based polymers containing the azobenzene bond. The synthesis strategy utilised to make these hypoxia-responsive polymers is based on the step-growth Michael polyaddition. This polymerisation reaction involves the addition of nucleophiles to α, β-unsaturated carbonyl compounds to form first dimers and then trimers before the generation of longer oligomers and eventually the required polymer species. This reaction allows access to polymers containing azobenzene bonds distributed evenly across the polymer backbone. Therefore, the preferential cleavage of this bond under low oxygen levels triggers a uniform

polymer degradation, allowing the release of complexed ASOs for target hybridisation. To utilise this strategy to synthesise the hypoxia-responsive PAAs, azobenzene-4,4'-dicarbonyl dichloride was transformed into a Michael acceptor group by the reaction with N-hydroxyethyl acrylamide in dichloromethane (DCM) containing triethylamine (TEA). In this reaction, the oxygen atom in the hydroxyl group, especially once deprotonated by TEA, launches a nucleophilic attack on the δ-positive carbon atoms of the acyl groups of azobenzene giving a tetrahedral intermediate. The resulting intermediate then loses chloride and proton to form the amide, referred to as azobenzene diacrylamide in this thesis. After 24 hours, the reaction product was collected via Büchner filtration and analysed via nuclear magnetic resonance (NMR) spectroscopy, Fourier transform infrared (FT-IR) spectroscopy, and mass spectrometry (Figure 6.1 and A.3). The Michael acceptor azobenzene diacrylamide was then reacted at equimolar ratio with 4-aminobutanol, acting as a Michael donor in the presence of TEA as a base catalyst. Selecting a suitable solvent for this reaction was limited by the poor solubility of azobenzene diacrylamide in all protic solvents tested including methanol, ethanol, isopropanol and water. Acting as a source of mobile hydrogen, protic solvents have been shown to increase the rate of internal proton transfer which is the rate-determining step in Michael addition (Manfredi et al., 2007). The aprotic solvent dimethyl sulfoxide (DMSO) was then used to run this reaction at 90°C for up to 7 days (Scheme 6.1). The high temperature used in this reaction was required to increase the solubility of azobenzene diacrylamide in DMSO and it was also shown to increase the reaction rate in aprotic solvents (Ranucci and Manfredi, 2019).

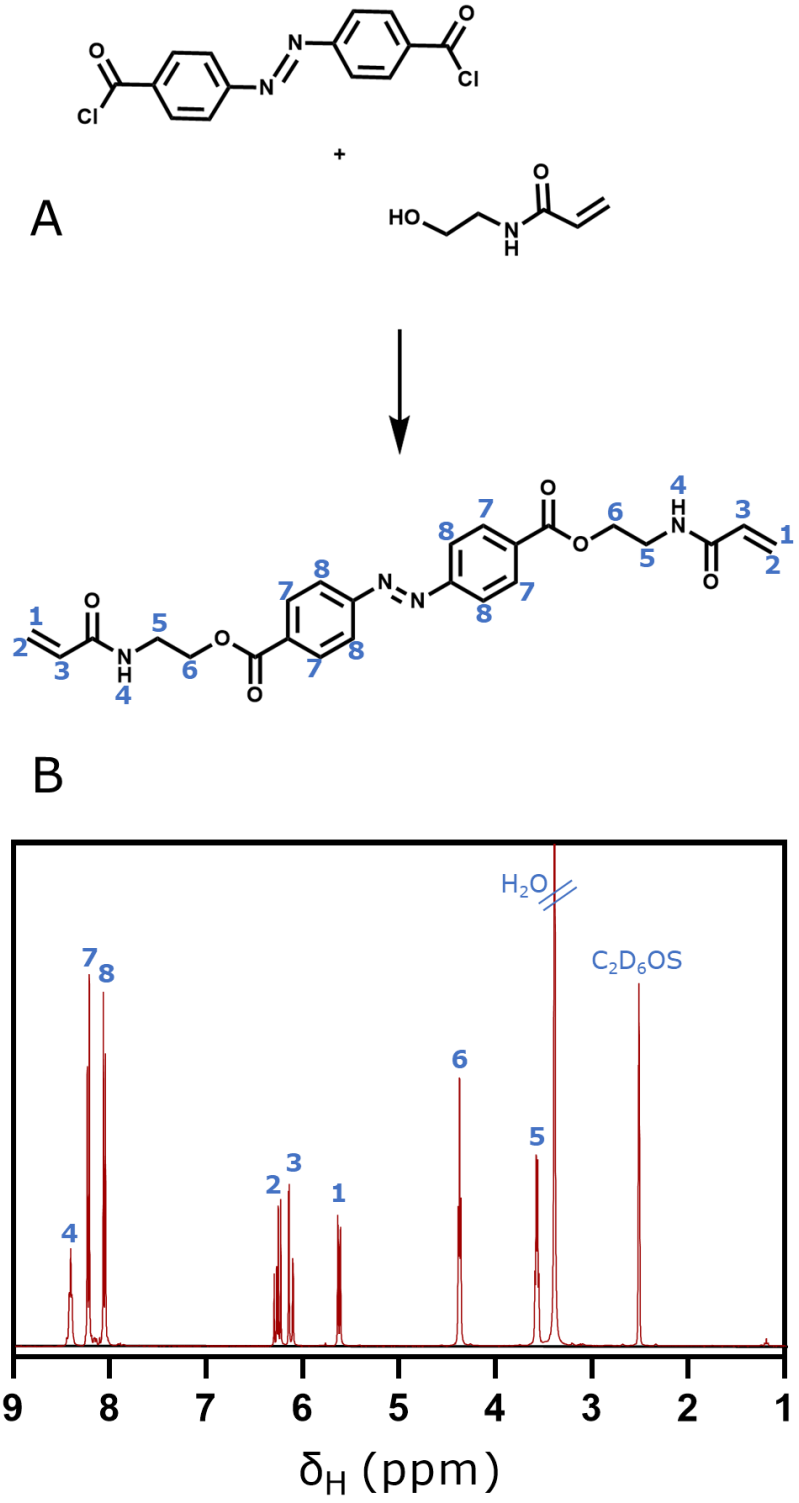
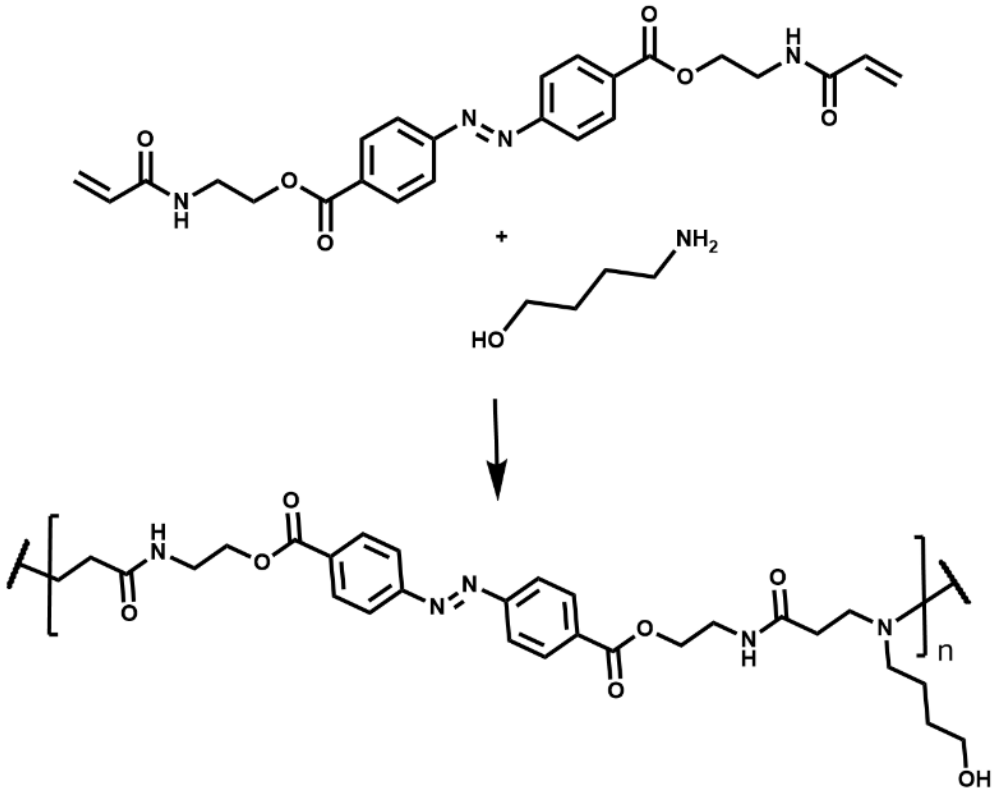


Figure 6.1 Synthesis of azobenzene diacrylamide. This figure shows **(A)** the reaction scheme and **(B)** the ^{1}H NMR spectrum of azobenzene diacrylamide resulting from the reaction of azobenzene-4,4'-dicarbonyl dichloride and N-hydroxyethyl acrylamide.



Scheme 6.1 Synthesis of the PAA-based polymer. In this aza-Michael reaction, azobenzene diacrylamide is reacted with 4-amino-1-butanol at equimolar ratios in DMSO at 90°C.

As shown in Figure 6.2A, the polymerisation reaction started to generate higher molecular weight species over the course of the reaction. Furthermore, the characteristic acrylamide peaks located around 6 ppm were gradually consumed over time consistent with the mechanism of polymerisation (Figure 6.2B). However, the gel permeation chromatography (GPC) results also show a considerable amount of azobenzene diacrylamide unable to be incorporated into long polymer chains (Figure 6.2A). Considering these results, it seems that the reactivity of the resulting 2° amine mono-addition adduct is drastically reduced, thus affecting the synthesis of the step-growth PAA polymer via bis-Michael reaction (Love et al., 2019).

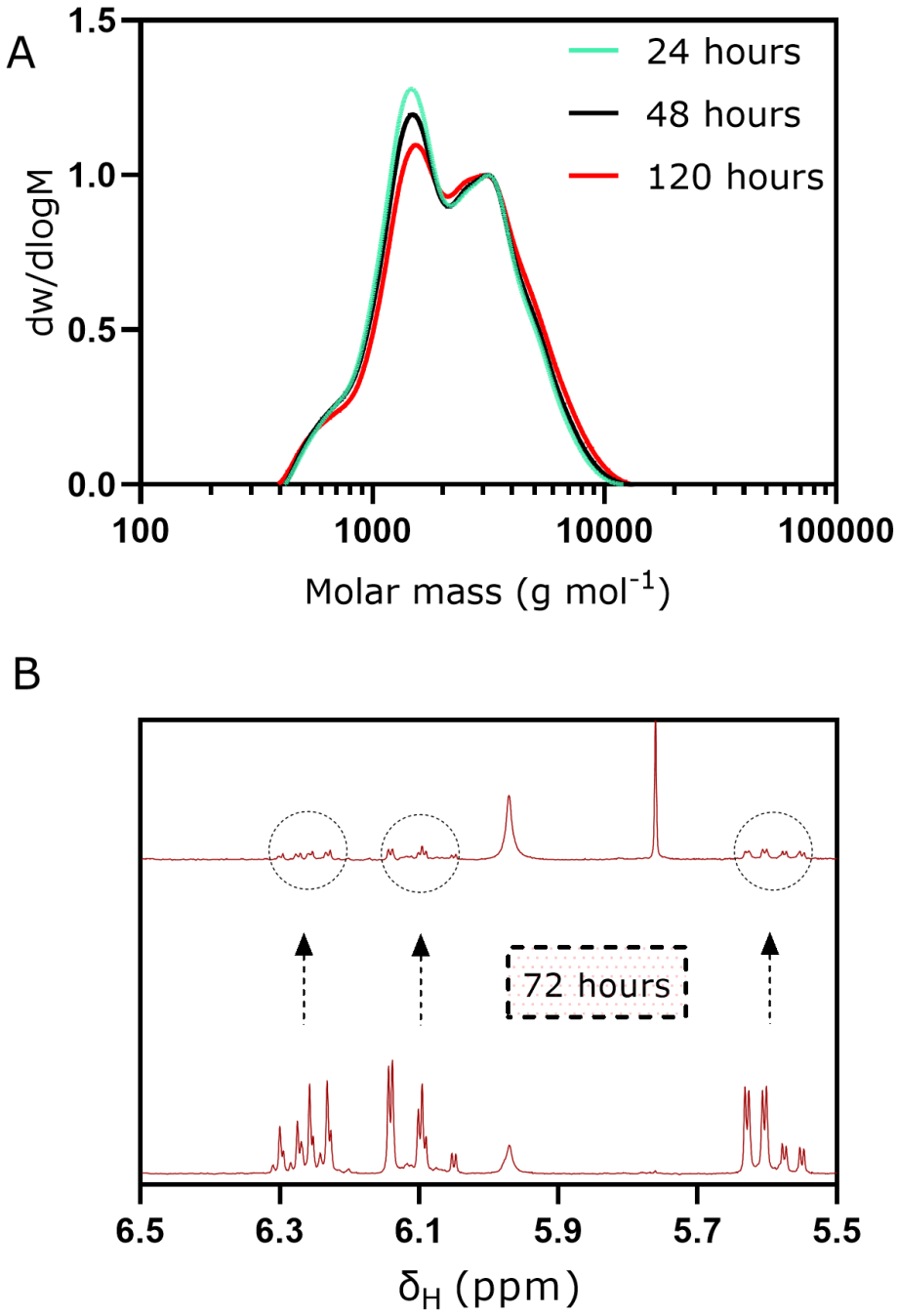


Figure 6.2 Characterisation of samples from the PAA-synthesis reaction. (A) Normalised GPC results that show the molecular weights and weight distributions of samples collected at different time points. A value of dw/dlogM on the Y-axis represent the relative amount of weight fraction with respect to a logarithmic molecular weight value on the X-axis. **(B)** Horizontally stacked ^{1}H NMR spectra showing the characteristic acrylamide peaks at 5.59, 6.09 and 6.25 ppm of samples collected at 24 hours and 96 hours.

To address this poor reactivity issue, molecular iodine was added to the reaction as a catalyst to activate the α,β-unsaturated carbonyl for the nucleophilic attack by the amine group (Breugst and von der Heiden, 2018, Borah et al., 2010). As can be seen from Figure 6.3, molecular iodine has resulted in a notable improvement in the generation of polymer species of higher molecular weights, however, there is still a significant fraction of unreacted secondary amine adducts present in the reaction.

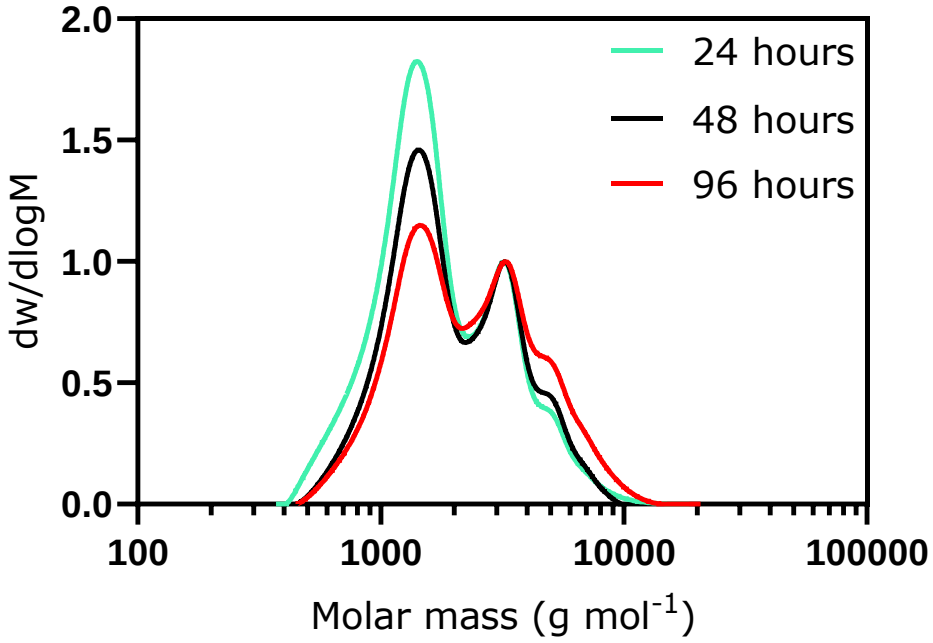


Figure 6.3 Effect of iodine catalysis on the PAA-synthesis reaction. Normalised GPC results that show the effect of iodine as a catalyst on the molecular weights and weight distributions of samples collected at different time points from the PAA-synthesis reaction.

To improve the yield of the Michael addition reaction, a different Michael acceptor was synthesised in which the azobenzene-4,4'-dicarbonyl moiety is flanked by the 2-hydroxyethyl acrylate groups. This ester-based monomer is more reactive than in its

amide counterpart due to the high electronegativity of the ester oxygen in comparison to the amide nitrogen which leads to less stable resident structures. To synthesise this hypoxia-responsive base monomer, azobenzene-4,4'-dicarbonyl dichloride was reacted with 2-hydroxyethyl acrylate for 24 hours in DCM containing TEA under argon atmosphere. The reaction product, designated azobenzene diacrylate, was then isolated via silica-gel column chromatography and purified via aqueous extraction (Figure 6.4).

Through Michael addition reaction, the acrylate-based monomer synthesised was then reacted with 4-aminobutanol at equimolar ratios in dimethylformamide (DMF) at 90°C for three days. Opposite to the diacrylamide monomer, the step-growth polymerisation reaction using this diacrylate counterpart proceeded rapidly within the first 24 hours, generating polymer species of high molecular weights (Figure 6.5). The resulting polymer was then end-capped with 4-aminobutanol to increase the overall cationic charge of the resulting polymer, hence enhancing its transfection efficiency (Sunshine et al., 2012). End capping also protects polymers from autopolymerisation and cross-linking via radical polymerisation which could negatively affect polymer solubility and function (Barner-Kowollik, 2009). End capping was confirmed by the absence of the characteristic acrylate peaks in the ^{1}H NMR spectrum. Before vacuum drying, the end-capped polymer, referred to as azo-100% polymer, was precipitated twice in diethyl ether to remove unreacted starting materials that might be present.

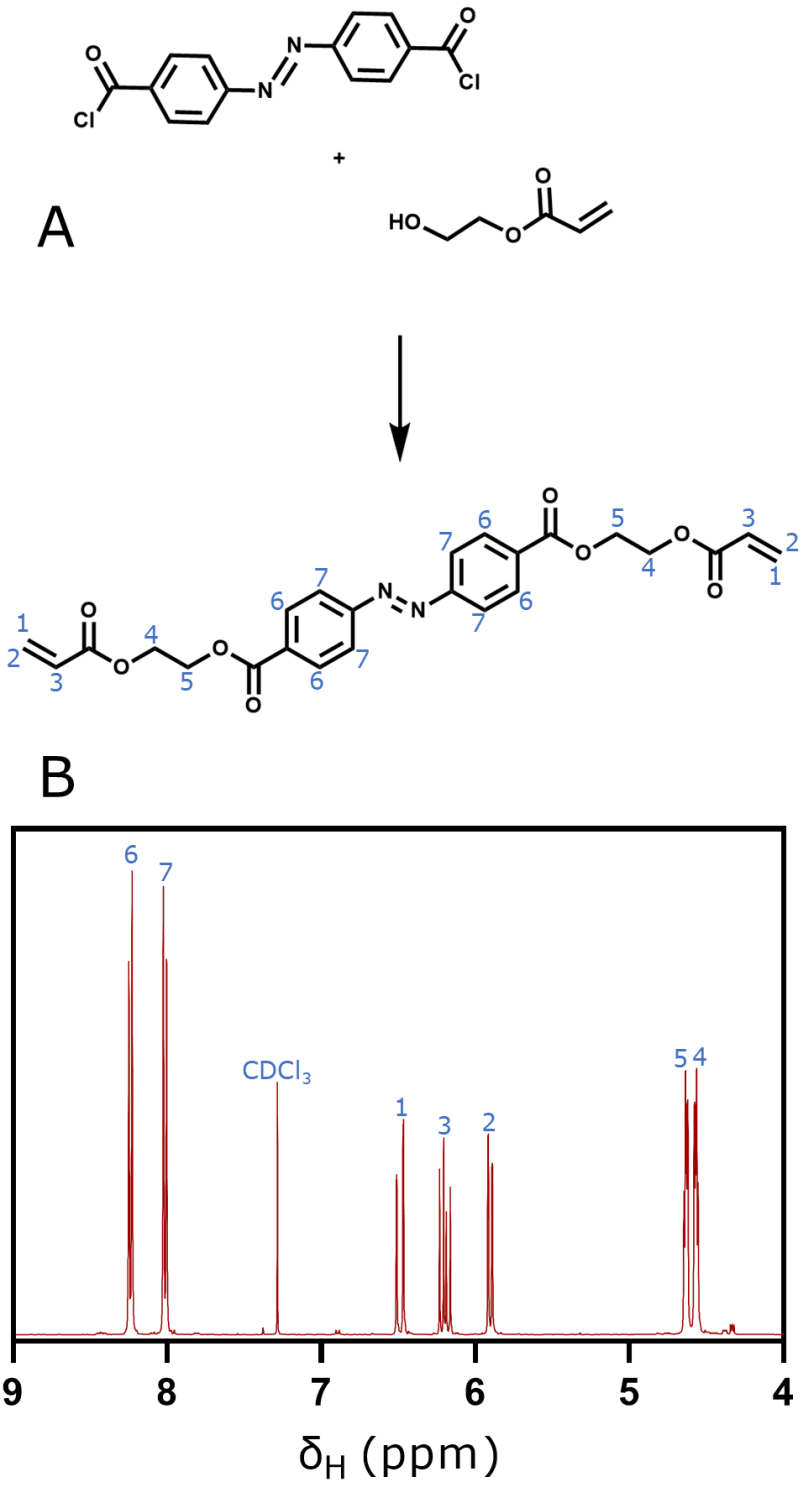


Figure 6.4 Synthesis of azobenzene diacrylate. This figure shows **(A)** the reaction scheme and **(B)** the ^{1}H NMR spectrum of azobenzene diacrylate resulting from the reaction of azobenzene-4,4'-dicarbonyl dichloride and N-hydroxyethyl acrylate.

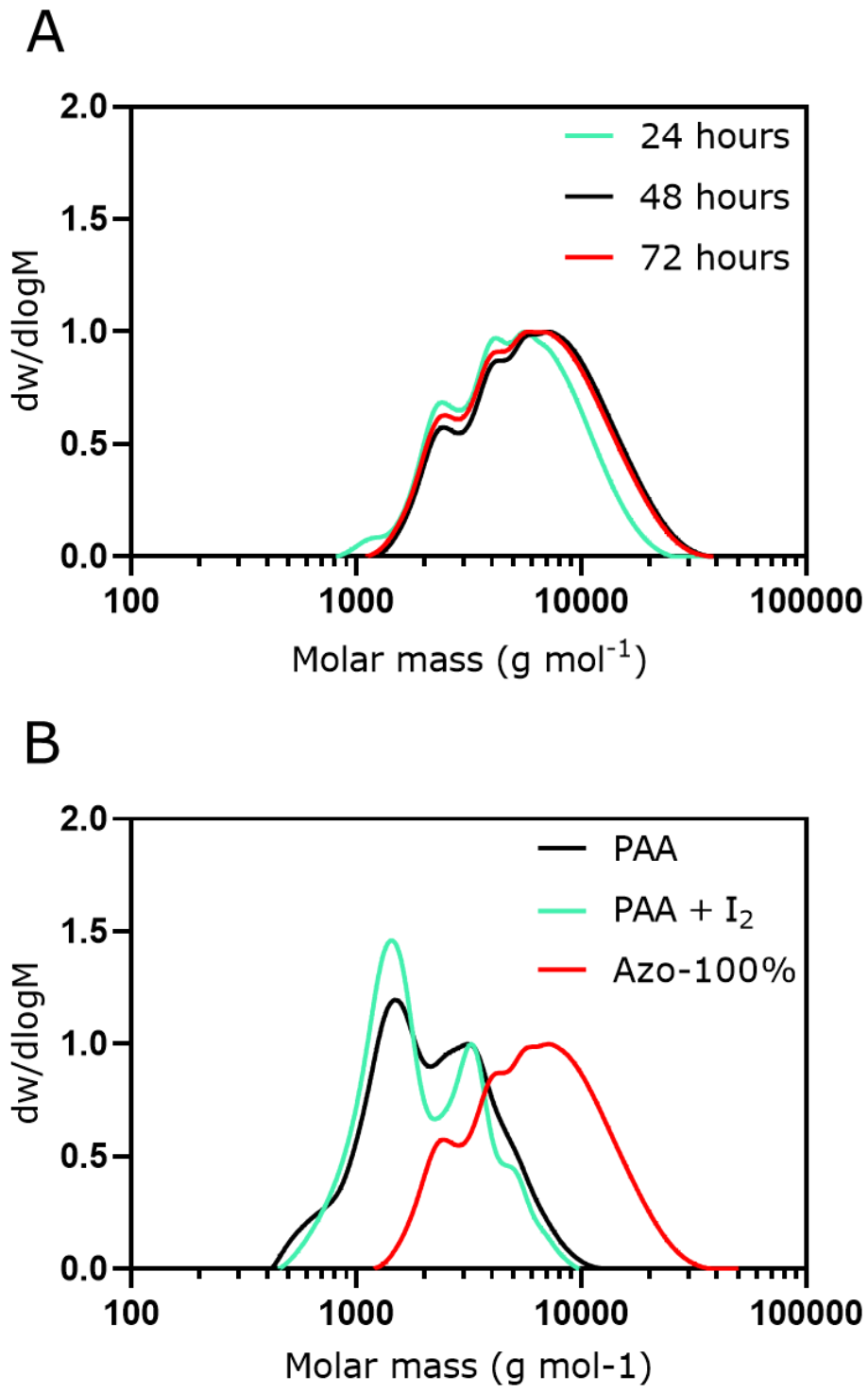


Figure 6.5 Characterisation of the azo-100% polymer. GPC analysis of the complete molecular weight distribution of the azo-100% polymer **(A)** at different time points, and **(B)** in comparison with the reaction products from the PAA-synthesis reactions.

In addition to the azo-100% polymer, four more PBAE polymers were synthesised in which the azobenzene diacrylate content was diluted to different levels by the incorporation of 1,4-butanediol diacrylate as an additional base monomer in the synthesis reaction according to the ratios in Figure 6.6 and Table 6.1.

1,4-butanediol diacrylate was incorporated into these polymers at different ratios to assess the interplay between the interchain spacing of azobenzene units and the hypoxic response of the resulting polymers. Furthermore, 1,4-butanediol diacrylate was previously found to produce polymers with high transfection activity (Anderson et al., 2004). It should be noted that 1,4-butanediol diacrylate was assumed to be 85% pure as calculating the required amount based on this purity percentage was found to result in the synthesis of polymer species of higher molecular weights opposite to the 90% purity indicated on the product label (Figure A.4). The resulting polymers were analysed using GPC, NMR spectroscopy, and FT-IR spectroscopy (Figure 6.7, A.5, A.6). In Figure 6.7A, the stacked ^{1}H NMR spectra show the varied content of azobenzene across the five different polymers reflected by the intensity of the azobenzene peaks around 8 ppm. Furthermore, all polymers were comparable in weight distribution and the FT-IR spectra show the characteristic peak of the azobenzene bond at 1400 cm^{-1} for all polymers except the azo-0% polymer (Figure 6.7B, A.5). Overall, these results indicate that the designed polymers were successfully synthesised via step-growth polymerisation incorporating various doses of the hypoxia-responsive moiety, the azobenzene linkage.

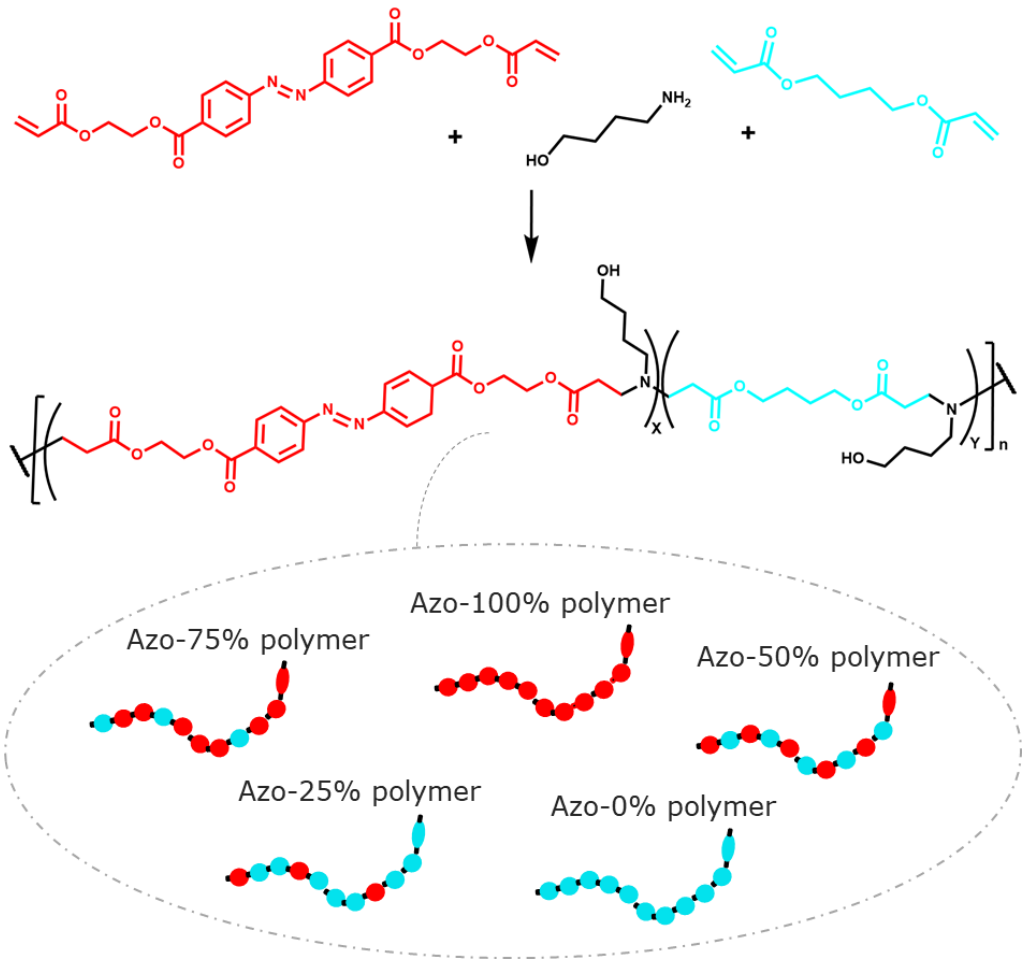


Figure 6.6 PBAE-based polymer synthesis. Backbone monomers azobenzene diacrylate and 1,4-butanediol diacrylate were randomly copolymerised at five different ratios with the side chain 4-aminobutanol to generate five different PBAE polymers.

Table 6.1 Physicochemical characteristics of PBAE based polymers. This table shows the mole fractions of azobenzene diacrylate (AZB), 1,4-butanediol diacrylate (BDDA), and 4-aminobutanol (ABOL) in addition to Malls GPC molecular weights ($M_{n,SEC}$, $M_{w,SEC}$) and the dispersity ($Đ$) of the PBAE based polymers.

Polymer	AZB mol%	BDDA mol%	ABOL mol%	$M_{n,SEC}$ (g mol^{-1})	$M_{w,SEC}$ (g mol^{-1})	$Đ$
Azo-0%	0	1	1	4000	5000	1.26
Azo-25%	0.25	0.75	1	5200	6400	1.23
Azo-50%	0.5	0.5	1	4900	6000	1.23
Azo-75%	0.75	0.25	1	4300	6100	1.43
Azo-100%	1	0	1	4900	7400	1.51

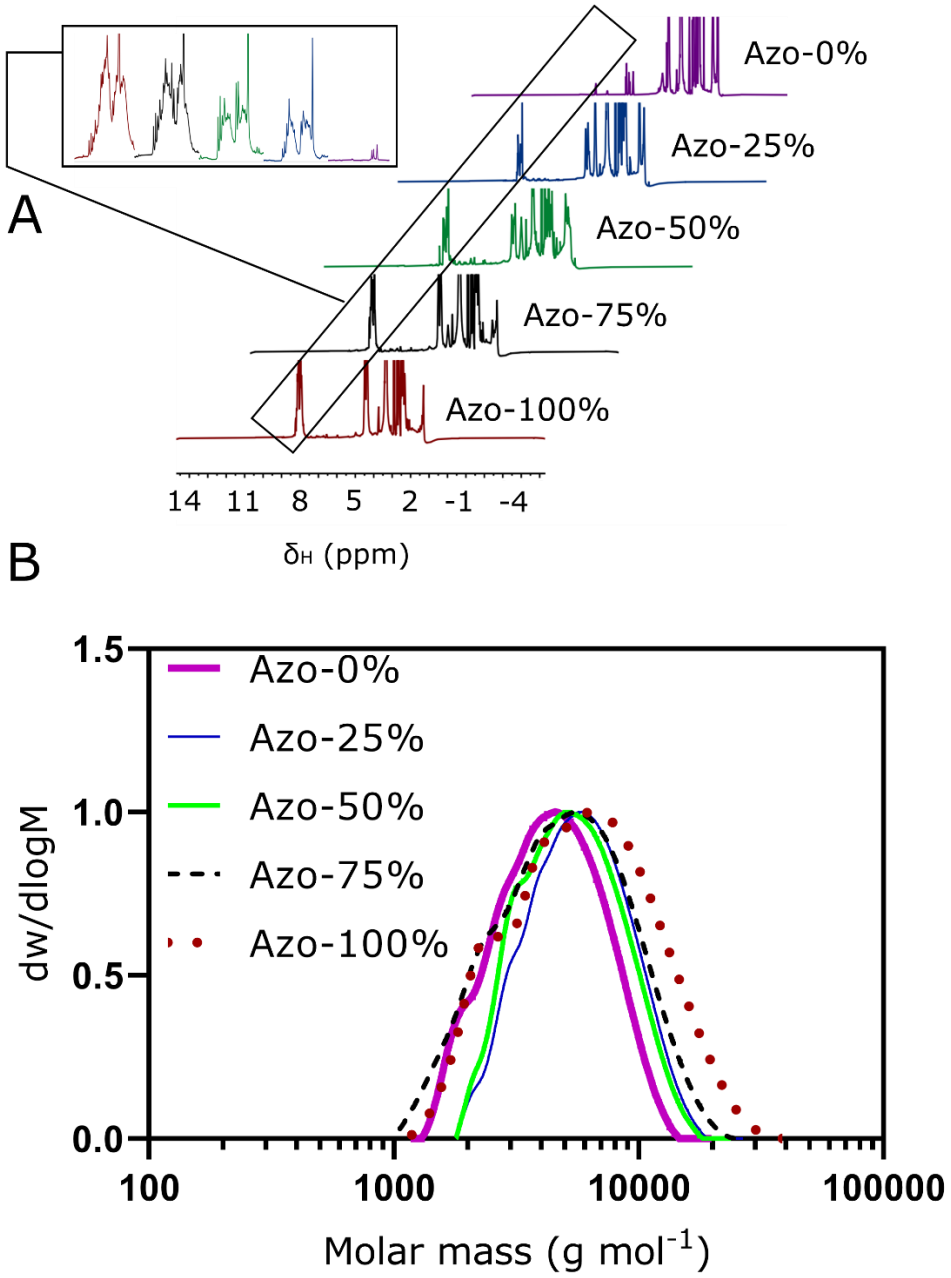


Figure 6.7 Characterisation of PBAE-based polymers. (A) ^{1}H NMR spectra of the PBAE-based polymers highlighting the relevant peaks (4H each) of azobenzene at 8.00 and 8.23 ppm. **(B)** GPC analysis demonstrating the molecular weights and weight distributions of the PBAE-based polymers.

6.3 Polymer formulation

The resulting polymers were then formulated with the anti-EGFR gapmer ASOs to form stable polyplexes via electrostatic interactions. Polymers and ASOs were diluted in 25 mM sodium acetate (NaAc, pH=5) to equal volumes before being thoroughly mixed and incubated for 10 minutes at room temperature (Figure 6.8). To assess the encapsulation stability and the ASO loading of the resulting polyplexes, the azo-100% polymer and the 2nd gapmer ASO were formulated at different weight ratios, loaded into 1% agarose gel and run on an electrophoresis system. As shown in Figure 6.9, the azo-100% polymer appears to fully start encapsulating the ASOs at 30 polymer-to-ASO weight ratio (w/w). The zeta potential analysis also reflects the same findings as the resulting polyplexes started to exhibit a positive zeta potential at 30 w/w, signalling complete ASO complexation.

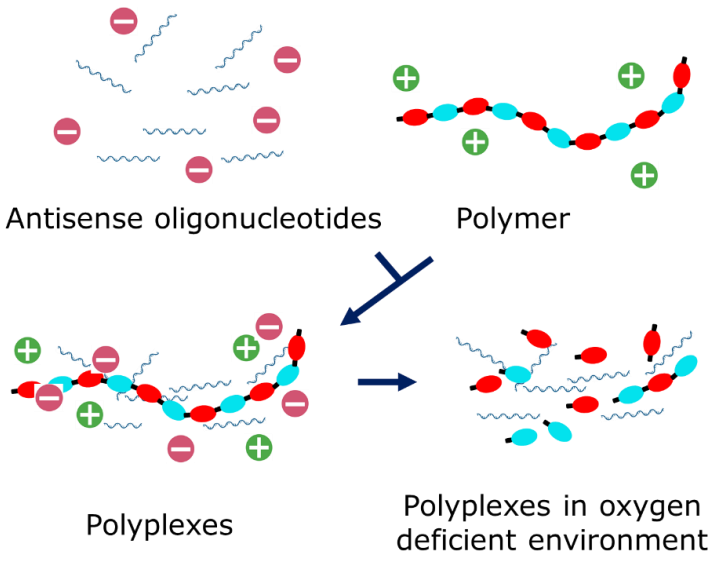


Figure 6.8 Formulation of polyplexes and mechanism for polymer function. Cationic polymers assemble into nanoparticles with the anionic ASOs. Yet these polyplexes get degraded at the azobenzene linkages in an oxygen-deficient environment, allowing for ASO release.

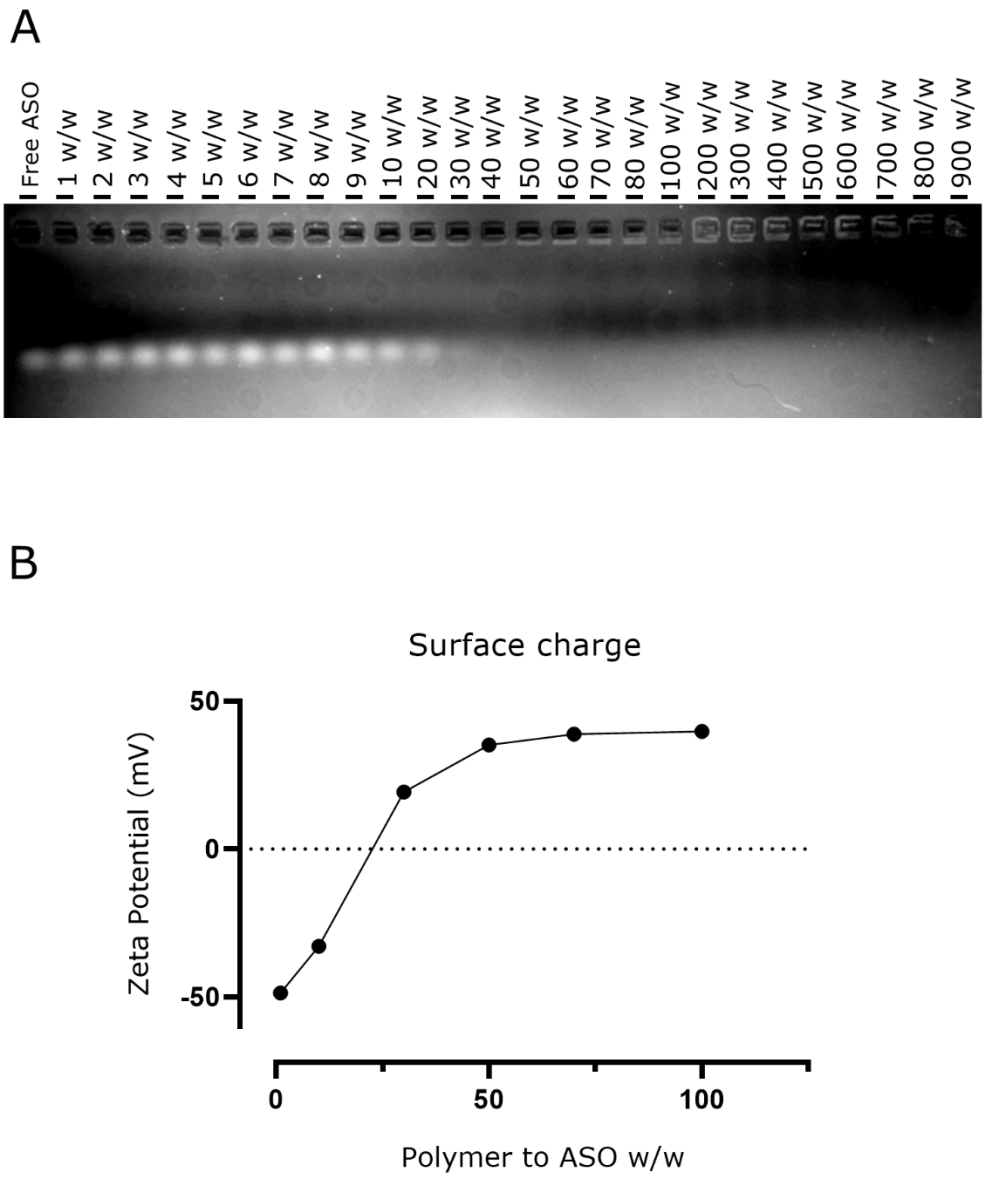


Figure 6.9 ASO loading capacity of nanoparticles. (A) gel retention assay and **(B)** zeta potential measurements of the azo-100% polyplexes demonstrating the complexation potential of these polyplexes formed at varying azo-100% polymer-to-ASO weight ratio (w/w) in 25 mM NaAc (pH=5) which was then supplemented with 10 mM NaCl in an equal volume for zeta potential measurements. Data generated from a single experiment.

After that, the responsiveness of these polyplexes to low oxygen levels in a reducing environment was examined in a gel electrophoresis binding assay (Figure 6.10). Since recombinant azoreductases are not widely available, the azo-100% polyplexes were incubated with the surrogate rat liver microsomes in phosphate-buffered saline (PBS) purged with argon for 120 minutes, mimicking the hypoxic environment in malignant tumours (Perche et al., 2016). Multiple samples were collected throughout the reaction and kept on ice prior to analysis to assess the reaction kinetics.

As can be seen from the densitometric analysis of the ASO bands, reducing the oxygen levels has increased the ASO release by 124.1% in comparison to the normoxic control (Figure 6.10). Under normal oxygen levels, the incubation with rat liver microsomes has also resulted in a significant ASO release, yet it is not comparable to the release observed under low oxygen levels. This normoxic release of complexed ASOs could be attributed to the cleavage of the ester bonds present in the polymer backbone by esterases present in the rat liver microsomes (Hayase and Tappel, 1969). The reaction also appears to proceed almost instantly releasing complexed ASOs within seconds of the start of the reaction (Figure 6.10A).

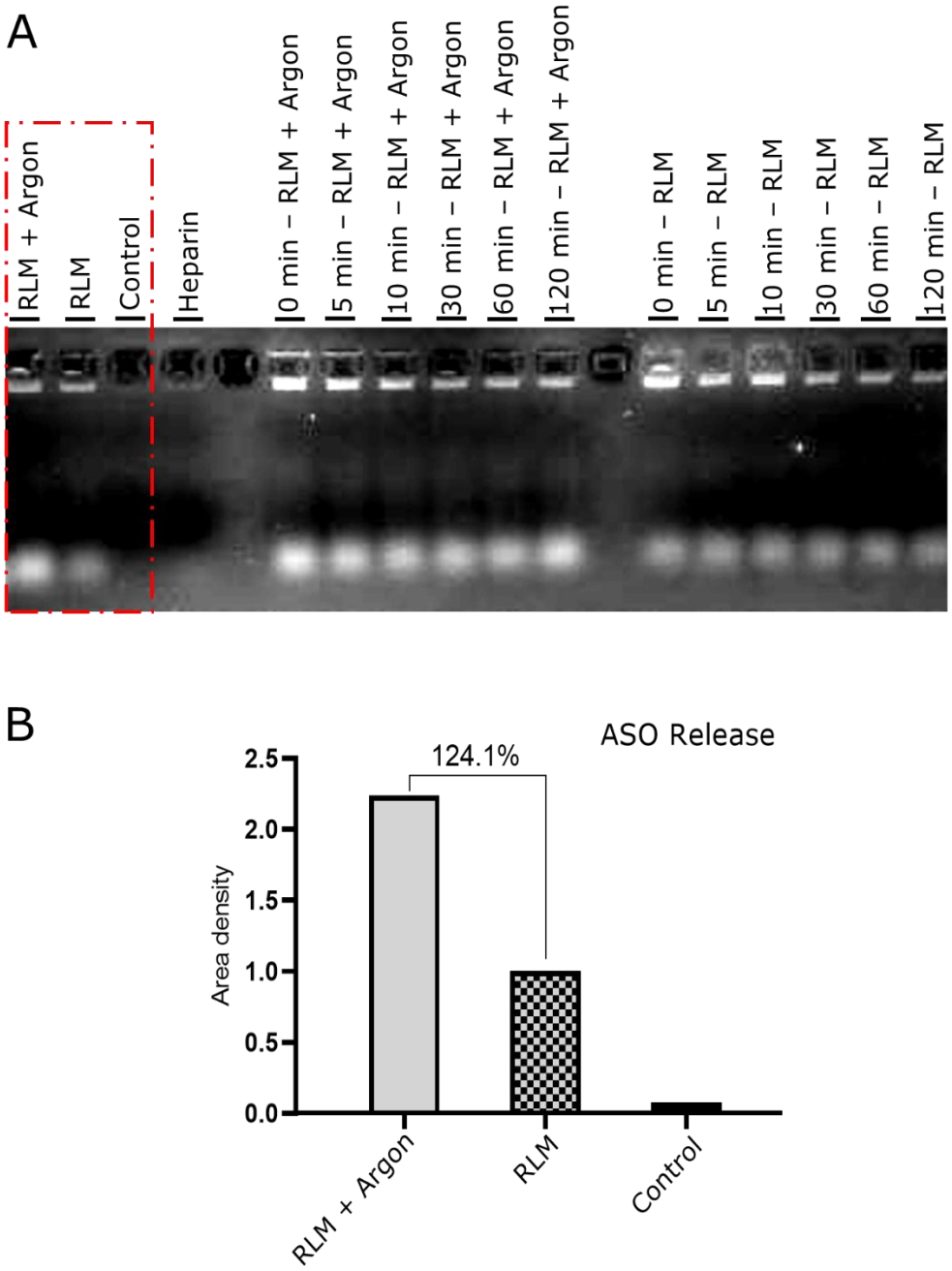


Figure 6.10 Nanoparticles responsiveness to oxygen levels. (A) a representative image of the gel electrophoresis binding assay and **(B)** the quantification of the first three lanes by densitometric analysis showing increased ASO release by 124.1% from the azo-100% polyplexes (formed at 200 w/w) when purged with argon for 120 minutes in comparison to only incubating with rat liver microsomes (RLMs) at 0.5 mg/ml. Control indicates the tube incubated without RLM or argon. Data generated from a single experiment.

This gel retardation assay was then utilised to assess the differential ability of the synthesised PBAE polymers to encapsulate the ASO cargo and release it preferentially under low oxygen levels. As shown in Figure 6.11, all formed polyplexes at 30 w/w were relatively stable when incubated in PBS for two hours. However, all polymers started to release their ASO loads when incubated with the reducing rat liver microsomes. Furthermore, it seems that the release of ASOs has increased under the influence of low oxygen levels especially from polyplexes of polymers with high azobenzene content, as it is the hypoxia-responsive moiety. In comparison to the previous gel retardation assay in which argon was used for 120 minutes, purging with argon for 20 minutes in this assay has decreased the ASO release from the azo-100% polyplexes highlighting the differential responsiveness of the azobenzene bond to different oxygen tensions (Kiyose et al., 2010, Piao et al., 2013).

In addition, particle size and surface charge analyses were conducted for all PBAE-based polyplexes formulated at 30 w/w. As shown in Table 6.2, these polyplexes exhibit varying hydrodynamic diameters ranging from 96.39 nm to 971.2 nm. It seems that there is a positive correlation between the hydrodynamic diameter of polyplexes and their hydrophobicity represented by the azobenzene content. There is a ten-fold difference in hydrodynamic diameter between azo-100% polyplexes and azo-25% polyplexes. It seems that polyplexes with high azobenzene content are less stable in aqueous media, causing them to form nanoparticle aggregates that could potentially affect cellular uptake (Rejman et al., 2004).

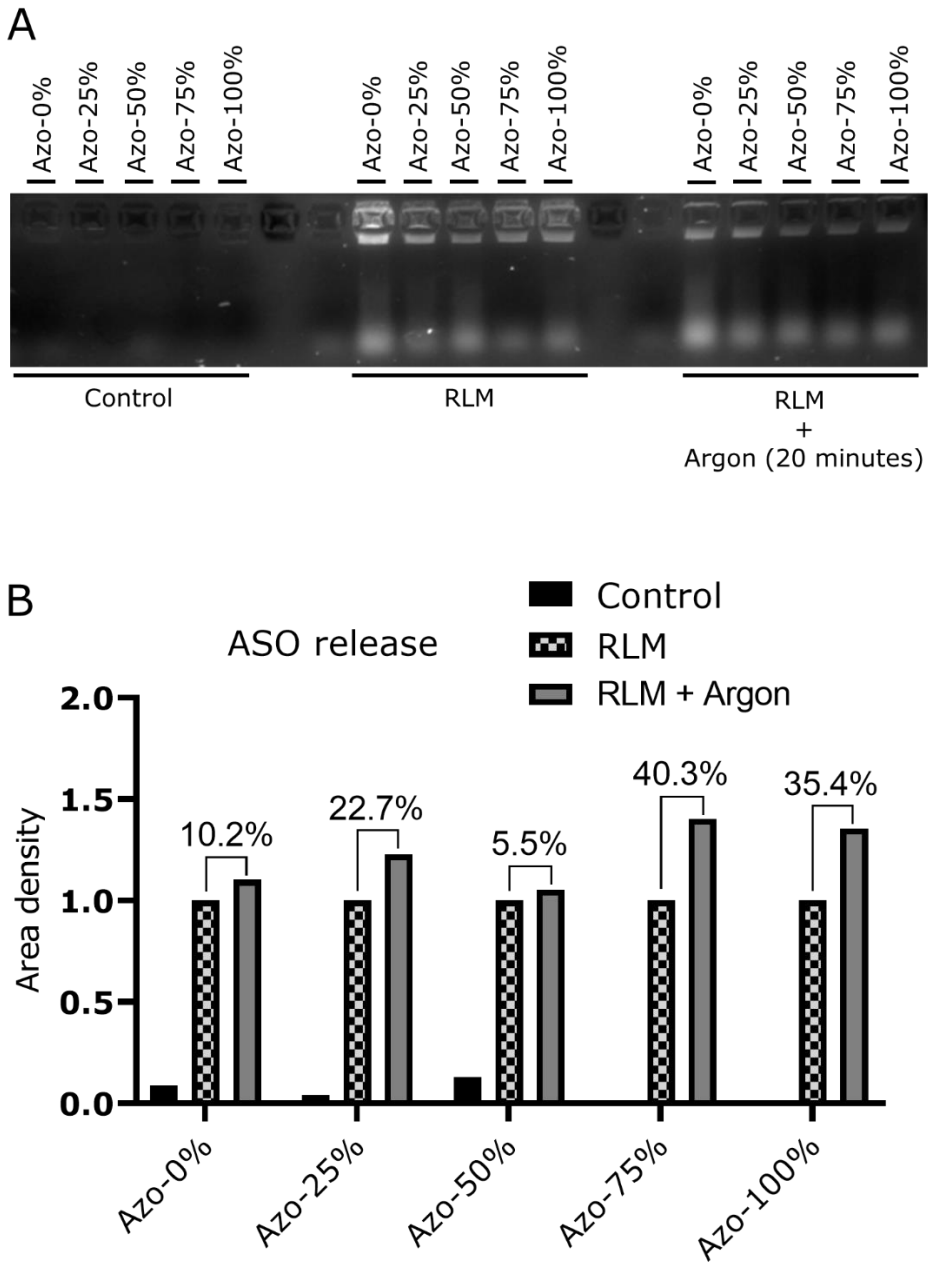


Figure 6.11 Characterisation of ASO release from the PBAE-based polyplexes. This gel retardation assay figure shows **(A)** a representative gel image and **(B)** quantification of the ASOs released from the PBAE-based polyplexes formulated at 30 w/w under the influence of rat liver microsomes (RLMs) at 0.5 mg/ml alone or in combination with purging with argon for 20 minutes. Control indicates tubes incubated without RLM or argon. Data generated from a single experiment.

Table 6.2 Characterisation of PBAE-based polyplexes formulated at 30 w/w. [a]: particle size measurements of the PBAEs-based polyplexes prepared in 25 mM NaAc before mixing with 10 mM NaCl in an equal volume for [b]: zeta potential measurements.

Polyplexes	Hydrodynamic diameter (nm)[a]	Polydispersity index (PDI)[a]	Zeta Potential (mV)[b]
Azo-0%	216.3	0.274	9.11
Azo-25%	96.39	0.251	19.7
Azo-50%	269.8	0.243	25
Azo-75%	539.7	0.328	28.8
Azo-100%	971.2	0.367	31.3

6.4 Polymer Cell-Based Activity

To analyse the ability of polymers to facilitate ASO delivery, PBAE-based polyplexes containing the anti-EGFR ASOs were formulated at 40 w/w and incubated with MCF-7 cells for two hours. The viability, as indicated by the MTT assay, was then assessed 72 hours after transfection. It was assumed that the viability of cells would be affected if the polyplexes were successfully internalised into the diffuse cytoplasm and released their ASO cargo targeting the *EGFR* mRNA. As shown in Figure 6.12, it can be seen that the greatest decrease in viability is associated with polyplexes based on the azo-25% polymer. This is consistent with the particle size analysis (Table 6.2) in which the azo-25% polyplexes exhibited a small-scale hydrodynamic diameter that is more compatible with the clathrin-mediated endocytosis (Rejman et al., 2004). Via this endocytic pathway,

PBAE-based polyplexes have been found to consistently result in successful transfections (Choi et al., 2020). Even though the azo-25% polyplexes were associated with a decrease in viability of cultured cells which could be seen as a successful transfection, this decrease in cellular viability appears to be also mediated by non-specific toxicities derived from the azo-25% polymer itself. It is known that polymers containing bulky hydrophobic cores could induce these toxic interactions in cell-based experiments (Sunshine et al., 2011).

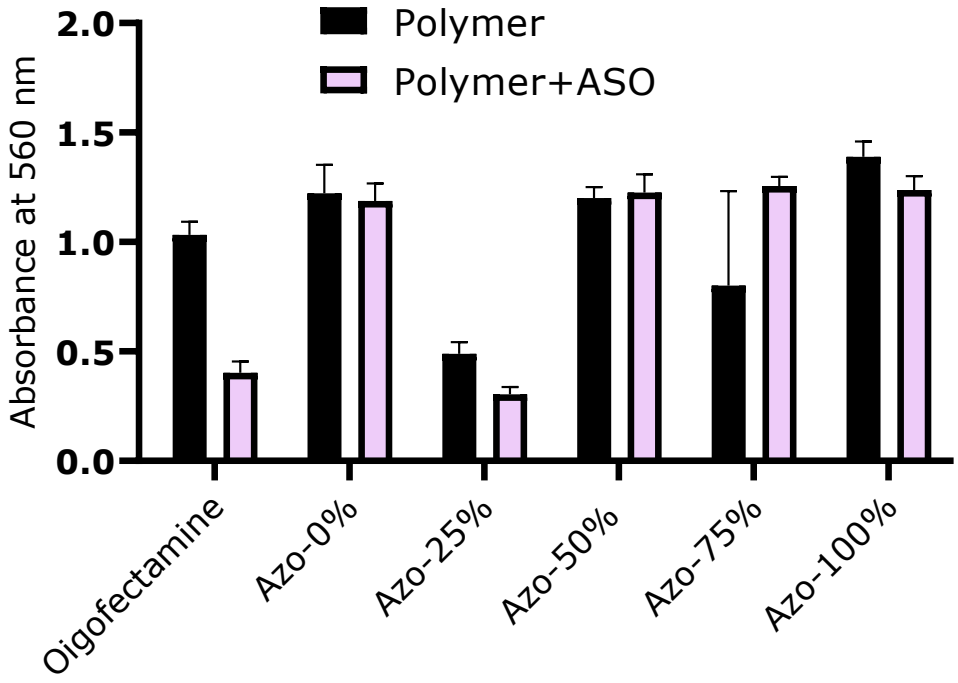


Figure 6.12 Effects of PBAE-based polyplexes targeting *EGFR* on the metabolic activity of MCF-7 cells. MTT assay results after transfecting the anti-EGFR ASOs using the PBAE-based polymers at 0.2 mg/ml for two hours. After that, polyplexes, formed at 40 w/w, were replaced with fresh culture media and cells were incubated for further 72 hours before assessing the cellular metabolic activity. As a positive control, Oligofectamine-mediated transfection of the anti-EGFR ASOs was carried out according to the manufacturer instructions. N = 4. Data derived from a single experiment. Error bars represent standard deviation.

In addition, it was noted that polyplexes at 0.15 mg/ml have precipitated heavily in cell culture media (Figure 6.13A). To address the toxicity and colloidal stability issues of polyplexes in these cell-based experiments, formulating the azo-25% polyplexes was further optimised using lower concentrations and a syringe pump. It was found that to produce monodispersed particles of ~ 124 nm in size, the diluted azo-25% polymer should be added into the ASO solution at a rate of 0.1 min/ml while mixing with a magnetic stirrer at 100 rpm (Figure 6.13B). As shown in Figure 6.13, the sedimentation of the azo-25% polyplexes was greatly minimised following this optimised mixing protocol.

Despite the dose-dependent reduction in toxicity, the azo-25% polyplexes at the reduced concentrations appear also to have reduced ability to deliver the ASOs targeting the *EGFR* mRNA into cultured cells (Figure 6.14). This was confirmed by confocal microscopy images of MCF-7 cells transfected with labelled ASOs using the azo-25% polymer (Figure 6.15). To address this issue, PEG-PEI and the human immunodeficiency virus-1 (HIV-1) Tat protein were separately incorporated into the formulation of the azo-25% polyplexes to improve their colloidal stability and transfectability (Rudolph et al., 2003, Farvadi et al., 2017, Wu et al., 2018, Tang et al., 2015). However, using PEG-PEI was found to increase the overall toxicity, while the HIV-1 Tat protein was found to be ineffective at improving the transfection efficiency of the final formulation (Figure A.7, A.8).

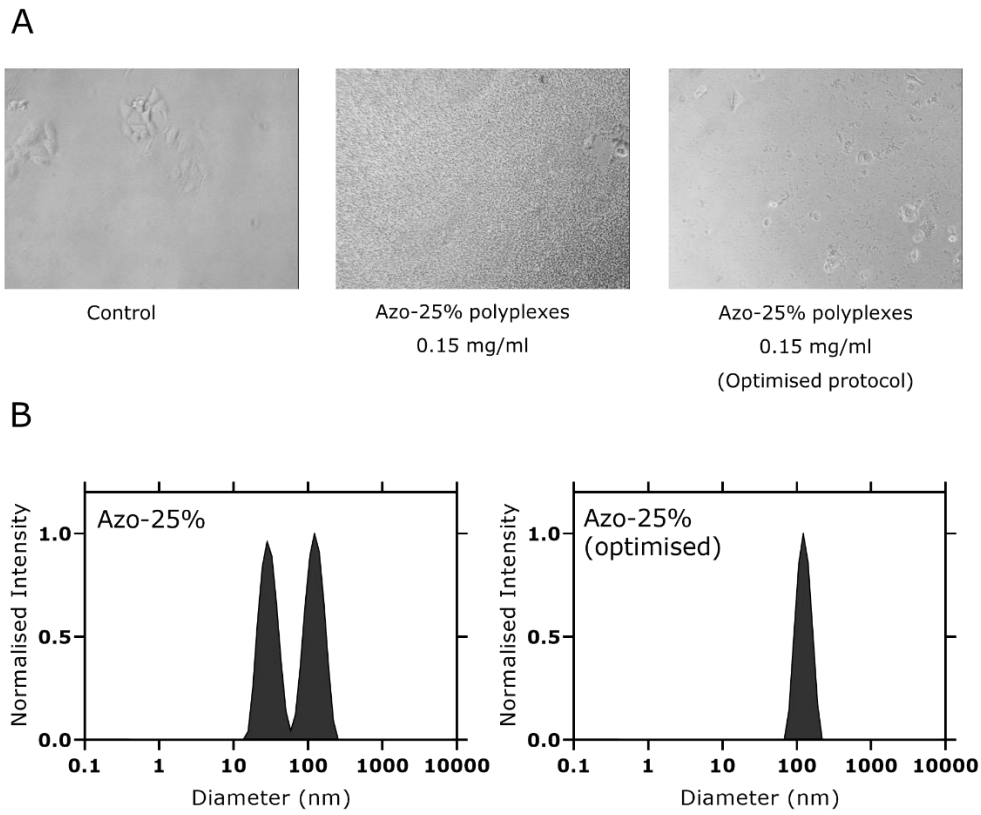


Figure 6.13 Characterising the azo-25% polyplexes in cell culture media. (A) Representative bright-field images at 20x magnification of MCF-7 cells incubated with the azo-25% polyplexes at 0.15 mg/ml in polymer concentration. Control cells received no treatment. **(B)** Dynamic light scattering results showing the difference in the size distribution of azo-25% polyplexes at 30 w/w after optimising the formulation protocol using a syringe pump.

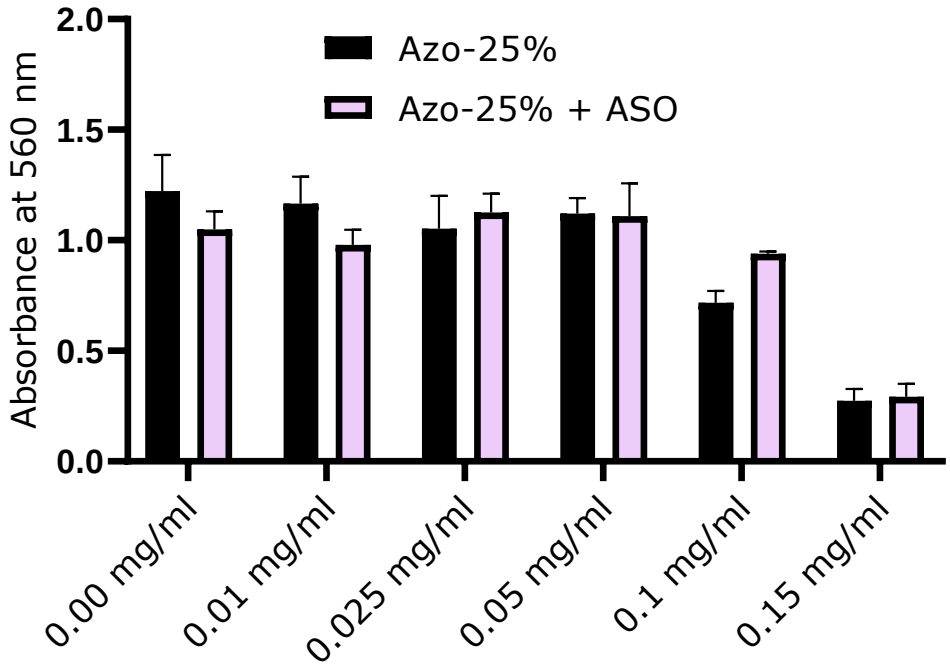


Figure 6.14 Dose-response of the azo-25% polyplexes. MTT assay results after transfection for 2 hours with the azo-25% polyplexes of fixed ASO dose (120 ng) and variable polymer concentration. Cells were then incubated with fresh media for 72 hours before assessing the metabolic activity. N = 4. Data derived from a single experiment. Error bars represent standard deviation.

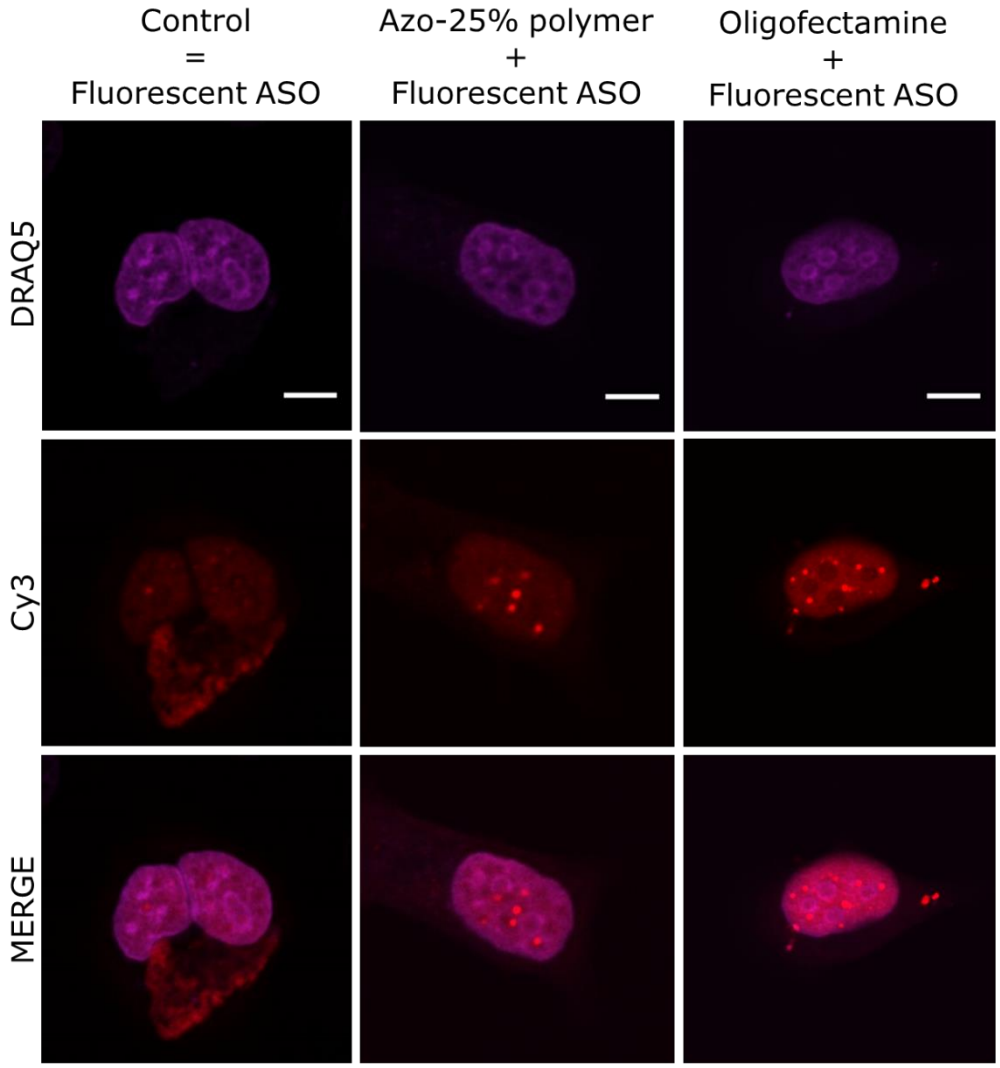


Figure 6.15 Transfection efficiency of the azo-25% polyplexes. Representative fluorescent microscope images of Cy3-labelled ASOs transfected into MCF-7 cells using the azo-25% polymer at 50 w/w and 0.05 mg/ml in polymer concentration. Control group represents cells incubated only with ASOs for 24 hours. Oligofectamine transfection is used as a positive control. Scale bar represents 5 μm. Data generated from a single experiment.

In summary, biodegradable PBAE-based polymers responsive to low oxygen levels were synthesised via the aza-Michael addition reaction. Azobenzene diacrylate was synthesised and incorporated in combination with 1,4-butanediol diacrylate into the polymer backbone at different ratios generating polymers with varied azobenzene content which was reflected by their tuneable hydrophobicity. These PBAE-based polymers were able to fully complex ASOs at 30 w/w and release their ASO load in a reducing environment preferentially under low oxygen levels. However, due to the excessive hydrophobicity of polymers containing azobenzene as the main base monomer, only the azo-25% polymer was found to facilitate the delivery of ASOs to cultured cells, yet with a low transfection efficiency. The reason for this poor transfection efficiency is probably due to the sedimentation of the azo-25% polyplexes in cell-culture media which occurs even at relatively low concentrations. Nevertheless, the results of this research support the concept of incorporating the hypoxia-responsive azobenzene bond into the backbone of hydrophilic PBAE-based polymers.

6.5 Discussion

Prior studies have noted the positive correlation between EGFR, cell survival, tumour hypoxia and overall survival of breast cancer patients (Shen et al., 2013). Thus, this study set out with the aim of preferentially targeting the hypoxic expression of EGFR using the antisense technology. To deliver the anti-EGFR ASOs to hypoxic cancer cells, a small library of PBAE polymers was synthesised and examined for the ability to fully complex the anti-EGFR ASOs and release them preferentially under low oxygen levels. The hypoxic release mechanism is based on the reduction and cleavage of azobenzene moieties

present in the polymer backbone under low oxygen levels. These PBAE polymers were successfully synthesised via bis-Michael addition reaction using two base monomers: the azobenzene diacrylate and 1,4-butanediol diacrylate. This study also characterised the ability of the synthesised PBAE-based polymers to fully complex with ASOs and release them preferentially under low oxygen levels. However, the transfection efficiency of polyplexes imparted by these polymers was found to be compromised by their poor water solubility as indicated by the sedimentation observed in cell-culture media. Overall, this combination of findings provides significant support for the use of PBAE polymers incorporating the azobenzene linkage to preferentially deliver anti-EGFR ASOs to breast cancer cells under hypoxia.

6.5.1 Azobenzene Linkage

The hypoxia-specificity of these azobenzene-containing polymers is an important advantage in cancer treatment as it would greatly minimise off-target toxicities. In a recent study, metal-organic frameworks (MOFs) functionalised with azobenzene were used to deliver siRNA and chemotherapy to hypoxic cancer cells (Huang et al., 2019). It was shown that using these hypoxia-responsive MOFs in mice bearing MCF-7 tumours has resulted in 100% survival after one month of starting treatment, underscoring the potential of azobenzene in cancer therapy. In addition, PBAE-based nanoparticles are known to exhibit high specificity for cancer cell transfection (Kozielski et al., 2019). This cancer specificity is probably due to differences in transfection routes between cancer and healthy cells as cellular uptake and division rate between these different cell types appear to be the same in those studies (Tzeng et al.,

2013, Guerrero-Cázares et al., 2014). Indeed, clathrin-mediated endocytosis was found to result in successful transfections of PBAE-based polyplexes while lipid raft-mediated endocytosis appears to be less likely to produce the same results (Choi et al., 2020). This cancer-targeting property of PBAE polymers and the hypoxia responsiveness of the azobenzene bond were combined for the first time in the polymers generated in this study. Therefore, this study makes a significant contribution to the research on hypoxia-mediated cancer therapy by demonstrating the feasibility of incorporating the azobenzene bond into the backbone of PBAE polymers.

6.5.2 PAA-based Polymers

On the other hand, incorporating the azobenzene bond into the backbone of PAA-based polymers was complicated by the poor solubility of azobenzene in a suitable solvent. Michael-type stepwise polyadditions are best performed in protic solvents as these solvents serve as an important source of mobile hydrogen for the rate-limiting proton transfer step (Manfredi et al., 2007). However, using these solvents such as water and lower alcohols was hindered by the poor solubility of azobenzene diacrylamide. Based on evidence derived from the ester analogues, DMSO was then used as an alternative solvent, however, the reaction has proceeded lethargically as expected. To increase the reaction rate, the reaction was carried out at 90°C in the presence of iodine as a catalyst. Nevertheless, these measures were ineffective in obtaining high polymerization degrees in a reasonable time. This is probably due to the reduced reactivity of the carbonyl group in azobenzene diacrylamide in comparison to its ester counterpart. Since nitrogen is less electronegative than oxygen, the carbonyl group is more resonance stabilized

and less polarised, hence the reduced susceptibility to nucleophilic attacks. Indeed, using the diacrylate derivative of azobenzene has resulted in the formation of high molecular weight species of PBAE-based polymers.

6.5.3 PBAE-based Polymers

These PBAE-polymers were able to bind the anti-EGFR ASOs and release them in a reducing environment preferentially under low oxygen levels. The hypoxia-mediated cleavage of azobenzene has accelerated the degradation of these PBAE polymers resulting in the selective release of ASOs under low oxygen levels. This is consistent with reports in the literature demonstrating the feasibility of incorporating targeting moieties into the backbone of PBAE-based polymers. Due to their glutathione sensitivity and hence cytoplasmic delivery, PBAEs containing disulphide bonds were more effective in gene knockdown and less toxic versus their nonreducible analogues (Kozielski et al., 2013).

The hypoxic release of ASOs from the resulting polyplexes was dependent on the azobenzene content of the polymers in a positive correlation. Under low oxygen levels, polymers with high azobenzene content appear to release more ASOs in comparison to polymers containing lower percentages of azobenzene. Furthermore, increasing the duration of oxygen depletion has also resulted in a notable improvement in the ASO release, highlighting the responsiveness of azobenzene to reduction under hypoxia. In accordance with the present results, previous studies have also demonstrated the differential sensitivity of azobenzene to various oxygen levels in breast cancer cells (Kiyose et al., 2010).

Due to the notable hydrophobicity of azobenzene, the generated polyplexes were characterised by reduced colloidal stability in aqueous suspension leading to aggregation and sedimentation in cell-culture media. It is known that nanoparticles which remain stable in buffered salt solutions can form large aggregates in biological media, a commonly observed phenomenon in such complex environments (Rausch et al., 2010). In cell culture media, the colloidal stability of nanoparticles could be altered not only by the presence of proteins but also due to the high ion content (Zha et al., 2002). Solutions of high ionic strength promote van der Waals interactions and nanoparticle aggregation through compressing the repulsive electrostatic double layer (Edwards and Williams, 2004). To address this issue, a digitally programmable syringe pump was used to optimise the formulation parameters which led to the generation of monodispersed nanoparticles with improved colloidal stability. PEG-PEI and HIV-1 Tat protein were also incorporated into the formulations to provide steric stabilisation and further improvements in transfection efficiency (Farvadi et al., 2017, Rudolph et al., 2003). Yet the PEG-PEI formulations were highly toxic, while the HIV-1 Tat protein formulations were ineffective in preventing sedimentation in cell-culture media.

The generation of large irregular clusters in cell-culture media negatively affects the cellular uptake and transfection efficiency of formulated polyplexes (Moore et al., 2015). The aggregation of nanoparticles was also reported to induce pronounced toxic effects upon cellular uptake which is consistent with the toxicities observed with the azo-25% polyplexes when used at high concentrations (Wick et al., 2007). These toxic effects could be also attributed to the hydrophobic nature of

azobenzene. Even though hydrophobic interactions are important for transfection efficiency and encapsulation stability, excessive hydrophobicity can result in toxicities related to disturbing the integrity of the cell membrane (Sunshine et al., 2011). Therefore, a balanced approach with regards to polymer hydrophobicity is important to generate cationic polymers characterised by high transfectability and reduced toxicity.

An established strategy to address this issue is to randomly combine the hydrophobic monomer with a less hydrophobic one at predetermined ratios in the synthesis reaction. Utilising this approach was shown to improve the overall hydrophobicity-hydrophilicity balance of the resulting polymers (Kozielski et al., 2014). In this regard, 1,4-butanediol diacrylate was incorporated into the synthesis reaction in combination with the hydrophobic azobenzene diacrylate at five different ratios. Even though this strategy has improved the physicochemical properties of polymers containing a high content of 1,4-butanediol diacrylate which was reflected by their nanoparticle size, increased hydrophilicity is still required to further improve the colloidal stability and the toxicity profile in the cell-based experiments.

Gene delivery with non-viral gene vectors is inherently versatile with regards to the size and type of nucleic acid cargo (Vaughan et al., 2019). In concordance with evidence in the literature, the synthesised PBAE polymers in this study exhibited a high loading capacity by fully encapsulating their oligonucleotide load in the sub 30 w/w range. This opens the possibility of complexing different types of ASOs into a single nanoparticle for combinatorial ASO therapy. Silencing complementary targets was shown to be more effective than targeting a single oncogene in inhibiting the proliferation of cancer cells *in vitro*

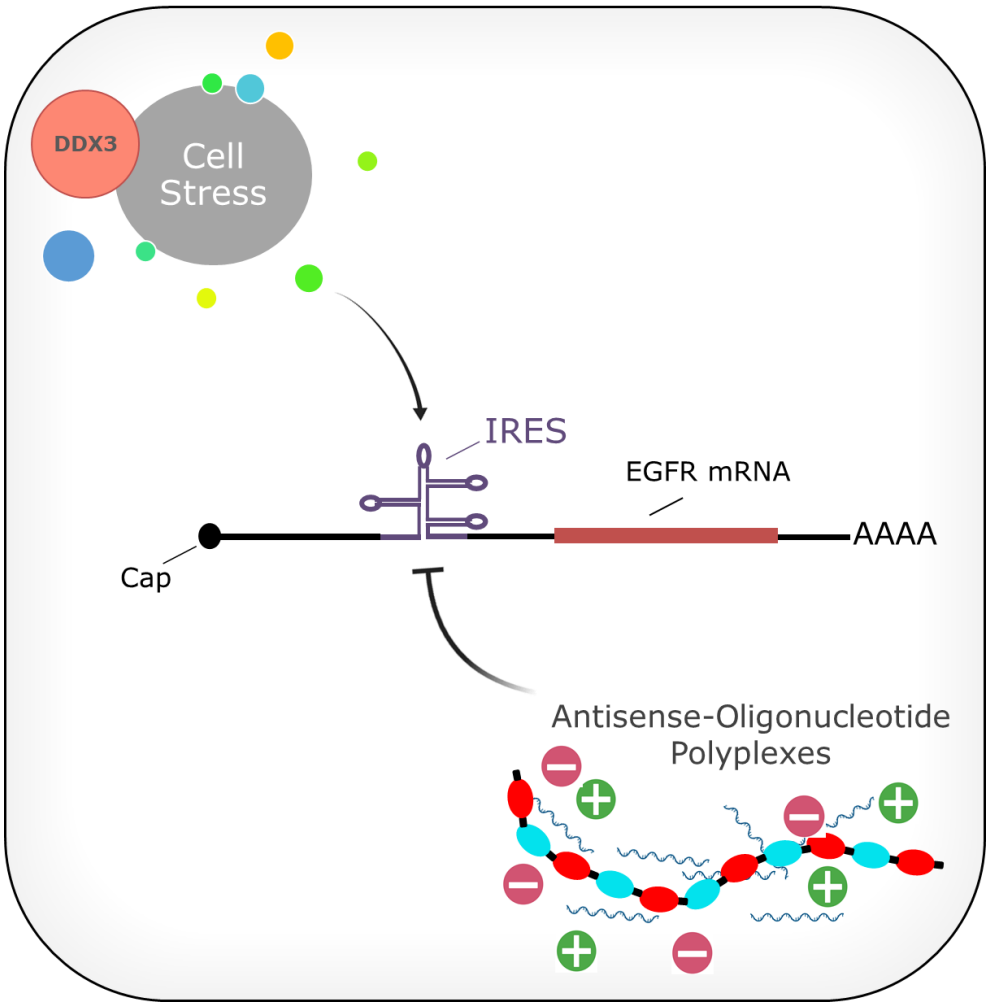
and in *vivo* (Plianwong et al., 2020, Kozielski et al., 2019). Due to the heterogeneous nature of cancer tumours, targeting multiple genes simultaneously can minimise the development of resistance due to the selection of resistant tumour cells. This multimodal agent delivery is particularly an important approach to treat triple-negative breast cancer; a highly heterogeneous disease genetically, histologically, as well as prognostically (Turashvili and Brogi, 2017).

Overall, the present study was designed to determine the effect of targeting the hypoxic expression of EGFR in breast cancer cells using the antisense technology. To deliver the anti-EGFR ASOs to hypoxic cancer cells, novel bioreducible PBAEs with tuneable hydrophobicity were successfully synthesised incorporating the hypoxia-responsive azobenzene bond. These polymers were able to tightly bind ASOs and were capable of releasing them preferentially under low oxygen levels. The hypoxic release from these PBAEs appears to be dependent on the azobenzene content in their polymer backbones. Yet further optimisations are still required to improve the physicochemical properties of the resulting polyplexes for the cell-based assays.

Chapter Seven

7 Discussion and Future Work

Graphical abstract



7.1 Outlook

This project was undertaken to evaluate the expression of EGFR under cell stress and target the *EGFR* mRNA specifically under low oxygen levels. Firstly, the activity of the *EGFR* internal ribosome entry site (IRES) was characterised using bicistronic reporter constructs after treatment with different inducers of cell stress including genotoxic agents. The function of the RNA-helicase DDX3 was also assessed in terms of mediating a gene-specific translational control over the activity of the *EGFR* 5' UTR. In addition, the antisense technology was utilised to target the expression of the *EGFR* mRNA for degradation using poly(β-amino ester) (PBAE) polymers incorporating azobenzene units to preferentially deliver the antisense oligonucleotides (ASOs) into hypoxic cancer cells.

7.1.1 Effect of Cell Stress on the Activity of the *EGFR* IRES

The first aim of this thesis is to investigate the effect of treatment with various cell-stress inducers on the activity of the *EGFR* IRES. The results obtained show that DNA damage induced by certain genotoxic stress measures can increase the use of the *EGFR* IRES activity to mediate the expression of EGFR. These findings complement those of earlier studies recognising the importance of EGFR in promoting resistance in cancer by enhancing the DNA damage response (Liccardi et al., 2011). Considering reports describing high protein levels of EGFR in comparison to its mRNA transcript in breast cancer, the contribution of this study has been to highlight a potential role of IRES-mediated translational regulation in driving the expression of EGFR under the stress of damaged DNA

(Gumuskaya et al., 2010, Meseure et al., 2012). Yet the impact of this intricate translation control to achieve a complex biological output of enhanced DNA damage response during genotoxic stress remains to be established. Furthermore, it is still not clear whether the observed changes in the luciferase reporter assays would be biologically meaningful in terms of maintaining a functional expression of EGFR under genotoxic stress.

To address these issues, the expression of the EGFR protein should be assessed under cell stress against *de novo* total protein synthesis (Esposito and Kinzy, 2014). Furthermore, the induction of DNA damage in cells must be also verified. For example, comet assay could be used to detect single and double DNA strand breaks, while immunological detection could be implemented using anti-CPD or anti-6-4PP antibodies to detect DNA adducts induced by UV-B radiation (Stephanie et al., 2011). This would help in optimising the dose of each genotoxic measure to elicit consistent and comparable cellular responses. In addition, these detection strategies would help in assessing the extent of DNA damage when EGFR is inhibited or depleted and whether transfecting with a cap-independent circular *EGFR* transcript can restore EGFR functions in the context of the DNA damage response (Yang and Wang, 2019).

Further research could be also conducted to examine the molecular pathways involved. For instance, the relevance of eIF4E and eIF2α can be explored in this process (Sanz et al., 2013, White et al., 2011). It would be useful to investigate the effect of knocking down eIF2α on the *EGFR* IRES activity under genotoxic stress induced by cryptolepine and phleomycin. Further research should be also undertaken to investigate whether inhibiting the activity of mTOR using rapamycin could

have any effect on the *EGFR* IRES response following DNA damage (Braunstein et al., 2009, Brenneisen et al., 2000). Additional cell lines including MCF10A, MDA-MB-231 and MDA-MB-468 should be also used for the screening to assess the impact of different genetic backgrounds on the response of the *EGFR* IRES.

7.1.2 Effect of DDX3 on the Activity of the *EGFR* 5' UTR

The second aim of this thesis is to investigate whether DDX3 could modulate the *EGFR* 5' UTR activity with regards to translation initiation in breast cancer. Through bioinformatics analysis, a predicted binding site of DDX3 was identified on the *EGFR* 5' UTR located between the 5' cap end and a highly conserved stem-loop structure. To investigate this potential RNA-protein interaction, the cDNA of *DDX3* was cloned in the mammalian expression vector pcDNA3.1 containing the cytomegalovirus (CMV) promoter. Overexpressing DDX3 in MCF-7 cells was found to increase the reporter activity of monocistronic and bicistronic plasmids containing the 5' UTRs of several genes including *EGFR*. This positive effect on translation initiation is thought to be mediated by the ability of DDX3 to facilitate the assembly of the 80S ribosomes (Geissler et al., 2012).

Interestingly, the results of this investigation show a positive correlation between the expression levels of DDX3 and the expression of the downstream cistron of bicistronic reporter constructs irrespective of the 5' UTR sequence inserted into the intercistronic region. An implication of this cap-independent translation enhancement is the possibility of utilising the co-expression of DDX3 as a strategy to improve the protein titre

from circular transcripts (Costello et al., 2019). Additional studies that involve the transfection with circular RNAs will be needed to validate these findings. Furthermore, experiments that involve the depletion of DDX3 via RNA interference and the transfection with a helicase-disrupted mutant of DDX3 are also required to elucidate the molecular mechanisms behind the observed effects on translation.

Perhaps the absence of a direct correlation between DDX3 and EGFR at the protein level in this study may be due to the low degree of DDX3 overexpression induced in MCF-7 cells. As DDX3 is a dosage-sensitive protein, it seems that the expression levels of DDX3 after transfection were not high enough to elicit a cellular response in which cap-dependent translation is inhibited. Under such conditions, it was shown that the DDX3-mediated expression of selected transcripts is relatively enhanced (Adjibade et al., 2017). Even though the CMV promoter is commonly used for strong induction of protein expression, it is known that this promoter is also prone to transcriptional silencing in some cell types including MCF-7 cells (Winnard Jr et al., 2004). Thus, further research is required using stronger promoters such as the elongation factor-1α *(EF-1α) and SRα* promoters (Shih et al., 2008). Increasing the gene copy number by transfecting more *DDX3* cDNA into cells is an alternative strategy that has been shown to induce a high degree of DDX3 overexpression (Shih et al., 2008).

In addition to DDX3 overexpression, cap-dependent translation can be inhibited by other means including the induction of genotoxic stress. It will be interesting to assess whether overexpressing DDX3 under such conditions would mimic the translational environment in which the selective recruitment of DDX3 to specific mRNAs is relatively significant in terms of

driving their translation (Adjibade et al., 2017, Soto-Rifo et al., 2012). Furthermore, methods for detecting direct interactions between DDX3 and the *EGFR* 5' UTR could be implemented such as RNA pull-down and oligonucleotide-targeted RNase-H protection assays. Fluorescent *in situ* hybridisation co-localization (FISH) can be also utilised to detect the position and abundance of both DDX3 and the *EGFR* mRNA in cells under homeostatic and stressful conditions. While this study did not confirm a direct and specific interaction between DDX3 and the *EGFR* 5' UTR, it adds to the growing body of research that underscores the importance of DDX3 in the translational regulation of mRNA expression (Sharma and Jankowsky, 2014).

7.1.3 Targeting *EGFR* using the Antisense Technology

The third aim of this study is to determine the effectiveness of utilising the antisense technology to target the *EGFR* 5' UTR in hypoxic breast cancer cells. In this regard, two antisense strategies were utilised. First, three occupancy-only ASOs were designed to target the internal landing site of ribosomes within the *EGFR* 5' UTR. However, these ASOs were ineffective in blocking the *EGFR* IRES activity probably due to imprecise ASO targeting of the ribosomal landing site. In the mutagenesis experiments, all introduced AUGs (iAUGs) have negatively affected the translation of the downstream cistron especially the ones introduced downstream on the *EGFR* 5' UTR. Nevertheless, further experiments including additional iAUGs and ASOs targeting the middle region of the *EGFR* 5' UTR are required to investigate the dramatic decrease in luciferase expression associated with iAUG 5 as this decrease could be related to a proximal 40S landing site located upstream to the introduced AUG.

The second approach utilised was based on targeting the *EGFR* 5’ UTR using 2’-O-methyl gapmers containing a phosphorothioate backbone that enables RNase H1–mediated target degradation. The chemical modifications included in the design of these gapmers are widely adopted in the design of therapeutic ASOs to enhance pharmacokinetics, nuclease stability and binding affinity (Bennett and Crooke, 2006). Indeed, ASOs containing the phosphorothioate linkage and the 2’-O-alkyl sugar ring bases represent the most clinically studied class of nucleic acid therapy (Shen et al., 2019, Khvorova and Watts, 2017).

The anti-EGFR gapmers developed in this study have resulted in a significant reduction in EGFR expression and cellular viability of cultured breast cancer cells. Yet further research is still required to assess the gapmer dose-response effects on *EGFR* at the mRNA and protein levels. Furthermore, a functional rescue experiment can be carried out by expressing a resistant mutant of *EGFR* containing silent mutations at the hybridisation sites (Watts and Corey, 2012). Overall, the results of this research support the concept of using the antisense technology to target the expression of EGFR in breast cancer. These findings perhaps highlight the most important advantage of the antisense technology over small-molecule approaches that is once a target sequence is identified, putative ASO therapeutics can be generated rather in a resource-effective manner (Scoles et al., 2019). Progress in the field of the antisense-based drugs continues to grow with four marketed ASOs and several candidates in clinical development (Bennett et al., 2017). Furthermore, opportunities for further progression still exist, considering the potential of the ASO modifications and the novel formulation strategies in improving the therapeutic index and

the bioavailability of these antisense drugs (Bennett et al., 2017). To comprehend the full therapeutic potential of this technology, more efforts are still required to improve our insights about the molecular mechanisms concerning the pharmacokinetics and pharmacodynamics of ASOs in the human body (Shen et al., 2019).

7.1.4 Targeting Hypoxia using Azobenzene-Containing Polymers

The final aim of this investigation is to assess the feasibility of using azobenzene containing polymers to deliver the anti-EGFR gapmers specifically to hypoxic cancer cells. Two approaches were utilised to synthesise these polymers. The first approach was based on synthesising linear polyamidoamine (PAA) polymers containing azobenzene units that could be reduced under an oxygen-deficient environment (Kulkarni et al., 2016, Perche et al., 2016). However, due to the poor solubility of azobenzene in a suitable protic solvent including methanol, the synthesis reaction proceeded rather lethargically resulting in the generation of polymer species with low molecular weights. The second approach utilised was based on synthesising PBAE polymers containing azobenzene. In this regard, five PBAE polymers with different azobenzene content were synthesised via aza-Michael addition reaction. These polymers were able to fully complex ASOs at 30 polymer-to-ASO weight ratio and release them in a reducing environment preferentially under low oxygen levels. In addition, these polymers were able to transfect cells with ASOs, yet the transfection efficiency was greatly compromised by the poor colloidal stability of the resulting polyplexes in cell culture media. This is thought to be stemmed from the hydrophobic nature of azobenzene, as

polymers with a high azobenzene content exhibited larger nanoparticle aggregates in aqueous solution in comparison to polymers with a lower azobenzene content. Nevertheless, the evidence from this study suggests that utilising PBAE polymers containing azobenzene in their backbone to deliver ASOs to hypoxic cancer cells appears to be a promising strategy once the hydrophilic-hydrophobic balance is optimised.

This issue of excessive hydrophobicity can be usefully explored in further research utilising different strategies. A natural progression of this work is to investigate the impact of formulating the resulting polyplexes using the double emulsion solvent evaporation method on their colloidal stability. Utilising this method, it has been shown previously that polymers containing the hydrophobic u-pentadecalactone moiety were successfully formulated into free-standing nanoparticles with an average hydrodynamic diameter of 169 nm (Voevodina et al., 2014). Further experiments that involve the use of polyethene glycol (PEG) chains in either the PBAE synthesis reaction or to produce PEG-PBAE-PEG block copolymers could be effective strategies to optimise the hydrophilic-hydrophobic balance (Kim et al., 2016). It has been also shown that certain disulphide-containing diacrylates such as 2,2- disulfanediylbis(ethane-2,1-diyl) diacrylate can be used as base monomers to improve the hydrophilic content of the resulting polymers while harnessing the functionality of the disulphide bond for cytoplasmic delivery (Rui et al., 2019).

In addition, hydrophilic polymers can be grafted as side chains into the azobenzene-containing polymers via different mechanisms including ring-opening polymerisation using O-carboxyanhydrides and α-amino acid N-carboxyanhydrides (Martin Vaca and Bourissou, 2015, Gradisar et al., 2017). This

graft polymerisation approach has been shown to generate branched copolymers with a hydrophobic core and a hydrophilic shell that is capable of self-assembly into discrete nanoparticles in aqueous solution (Price et al., 2017). Overall, the findings of this research have provided a deep insight into the chemistry of azobenzene-containing PBAEs for nucleic acid delivery.

7.2 Conclusion

This research project was designed to determine the effect of cell stress and DDX3 on the IRES-mediated expression of EGFR and to assess the therapeutic potential of the antisense technology combined with linear cationic polymers to preferentially tackle the hypoxic expression of EGFR in breast cancer. The results of this investigation show that genotoxic stress appears to induce a condition of translational control that increases the dependence on the IRES-mediated expression of EGFR over cap-dependent translation. The RNA helicase DDX3 was found to increase the expression of the downstream cistron in bicistronic constructs irrespective of the inserted 5' UTR sequence indicating a novel function of DDX3 in translation initiation.

In addition, three RNase-H1 dependent ASOs targeting the *EGFR* 5' UTR were developed and characterised with regards to inhibiting the expression of EGFR and hence reducing the viability of breast cancer cells. To deliver these ASOs to hypoxic cancer cells, novel PBAE-based polymers were synthesised incorporating azobenzene as the hypoxia-responsive moiety. Overall, this study underscores the impact of the IRES-mediated translation of EGFR under genotoxic stress, sheds new light into the multifaceted function of DDX3 in translation

initiation and strengthens the concept of using hypoxia-responsive PBAEs to deliver ASOs targeting EGFR in breast cancer cells.

8 Appendix

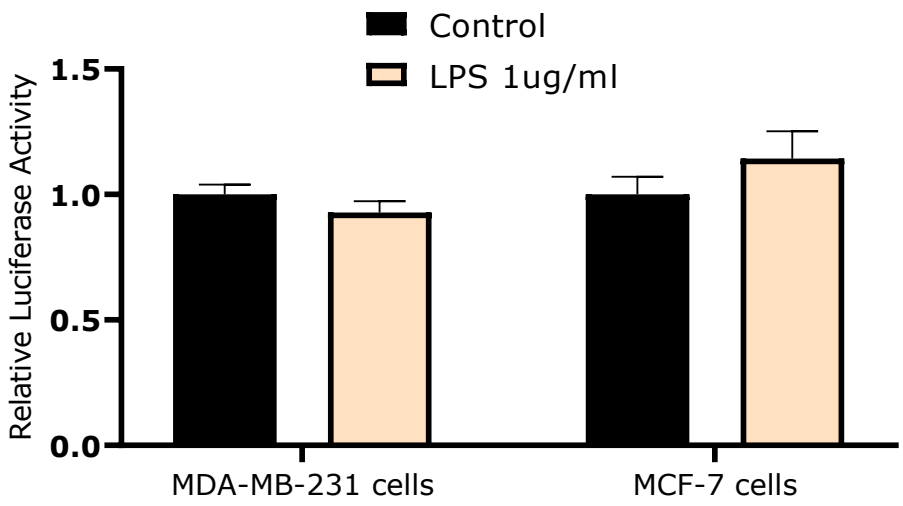


Figure A.1 The relative activity of the *EGFR* IRES following treatment with lipopolysaccharide (LPS). Quantification of the relative activity of firefly luciferase in MDA-MB-231 cells following 24-hour treatment with 1 µg/ml LPS. Control cells received an equivalent solvent amount. Error bars represent standard deviation. N = 3. Data generated from a single experiment.

Table A.1 Accession numbers of sequences included in the *EGFR* 5′ UTR sequence-alignment analysis.

Accession number	Species	Accession number	Species
NC_029519.1	Japanese quail	NW_008354421.1	Blind mole rat
NW_015351236.1	Alpine marmot	NW_020799098.1	Burrowing owl
NW_012267450.1	Kangaroo rat	NW_020269222.1	Dingo
GPS_003819442.1	Aardvark	NC_027874.1	Pygmy chimpanzee
NW_003573425.1	African savanna elephant	NW_017731542.1	Great round-leaf bat
NC_033670.1	Gray mouse lemur	NW_019154135.1	Sea otter
NW_012148552.1	Coquerel's sifaka	NW_006383224.1	Weddell seal
NW_006408562.1	Cape golden mole	NW_018734398.1	Hawaiian monk seal
NW_004454227.1	Southern white rhinoceros	NW_004504433.1	Lesser Egyptian jerboa
NC_009147.3	Horse	NW_017738964.1	Horseshoe bat
NW_006400026.1	Elephant shrew	NW_015495086.1	Egyptian fruit bat
NW_011915941.1	Large flying fox	NW_020092046.1	Vampire bat
NC_018724.3	Domestic cat	NW_003852440.1	Small-ear galago
NW_017619865.1	Leopard	NW_004444050.1	Florida manatee
NW_004451433.1	Pacific walrus	NW_004569145.1	Domestic ferret
NC_013903.1	Common marmoset	NW_016107901.1	White-head capuchin
NW_018514471.1	Ma's night monkey	NW_010824106.1	Golden snub-nosed monkey
NW_020556242.1	Ugandan red colobus	NW_014638556.1	Asinus

NC_027895.1	Southern pig-tailed macaque	NC_018154.2	Olive baboon
NW_016824162.1	Snub-nosed monkey	NC_023662.1	Green monkey
NC_036886.1	Common chimpanzee	NC_022274.1	Crab-eating macaque
NC_000007.14	Human	NC_018154.2	Olive baboon
NC_018431.2	Gorilla	NW_012011522.1	Pig-tailed macaque
NW_004480427.1	Nine-band armadillo	NW_012000909.1	Sooty mangabey
NW_004936678.1	Ground squirrel	NC_037670.1	Gelada baboon
NW_020540423.1	Arctic ground squirrel	NW_020313054	Northern fur seal
NW_004936678.1	Ground squirrel	NC_036910.1	Sumatran orangutan
NW_017871409.1	American beaver	NW_020656122.1	Grizzly bear
NW_004567145.1	Star-nosed mole	NW_003218119.1	Giant panda

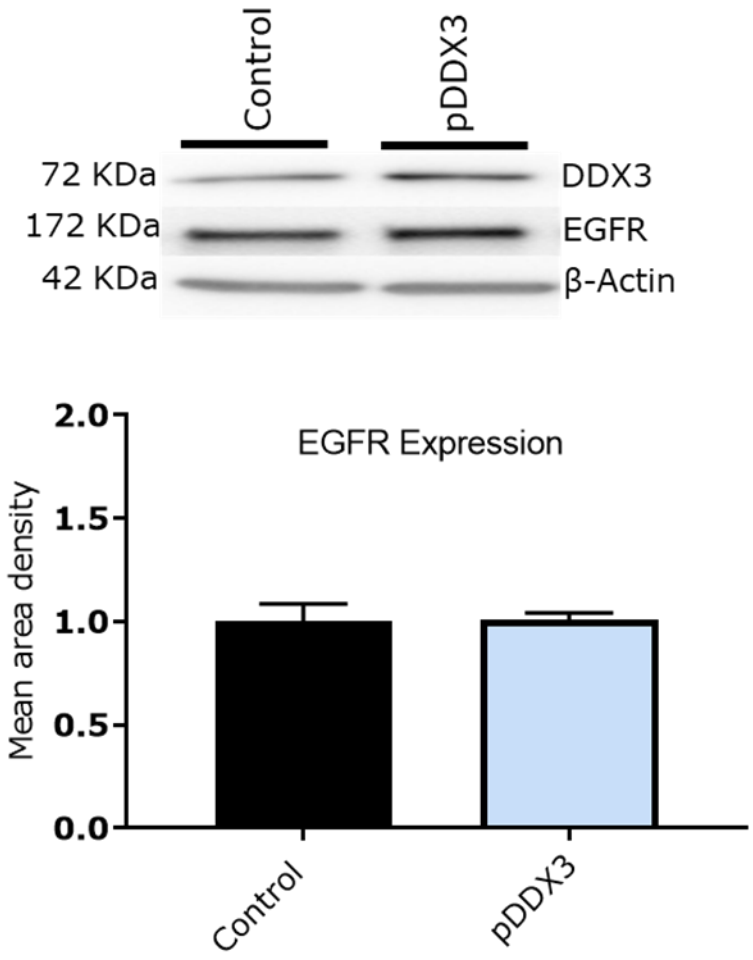


Figure A.2 The effect of overexpressing DDX3 on the protein expression of EGFR. A representative western blot and densitometric analysis of the EGFR protein in MDA-MB-231 cells transfected with pDDX3 for 72 hours. N = 3. Data generated from a single experiment. Control cells were transfected with pcDNA3.1. Error bars represent standard deviation.

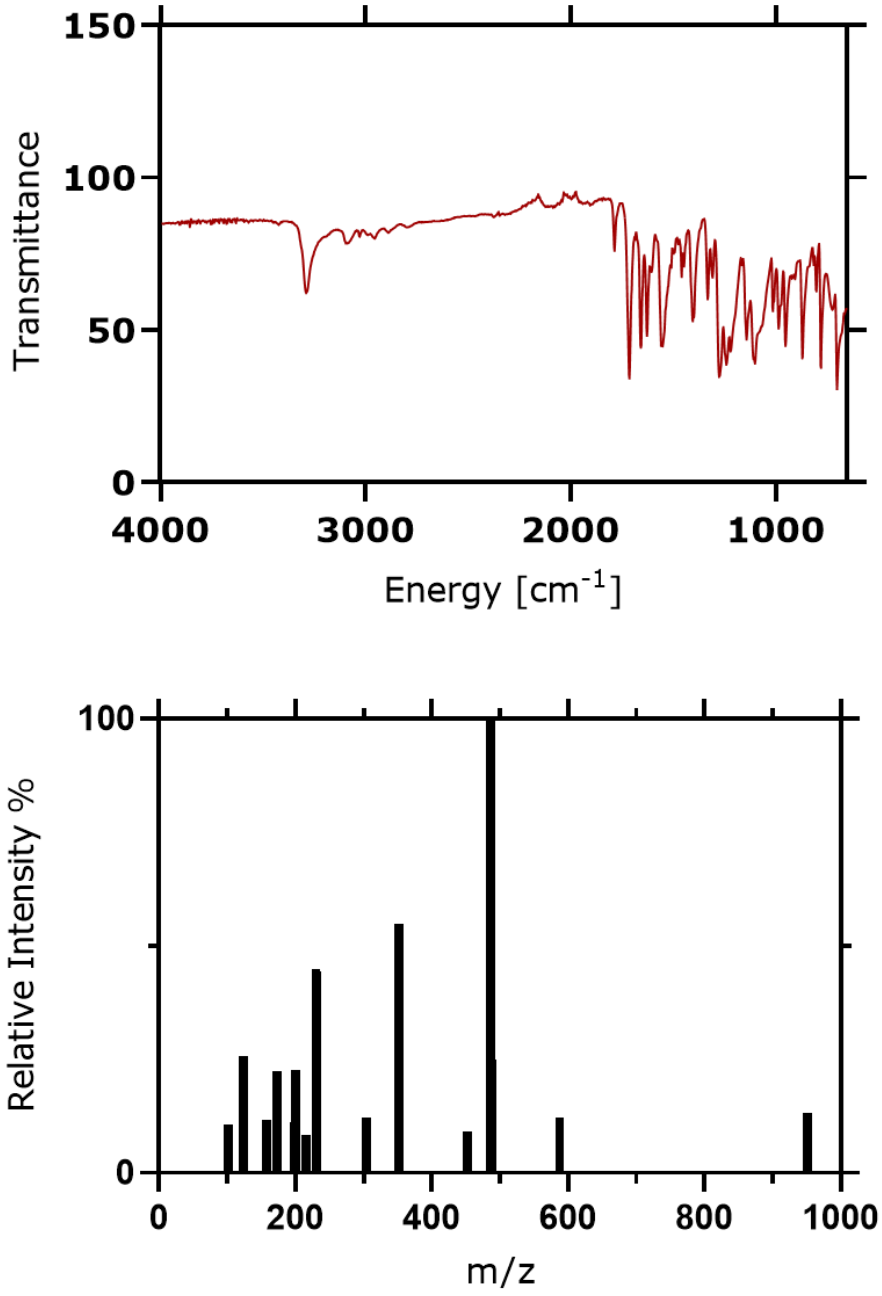


Figure A.3 FT-IR and mass spectra of azobenzene diacrylamide.

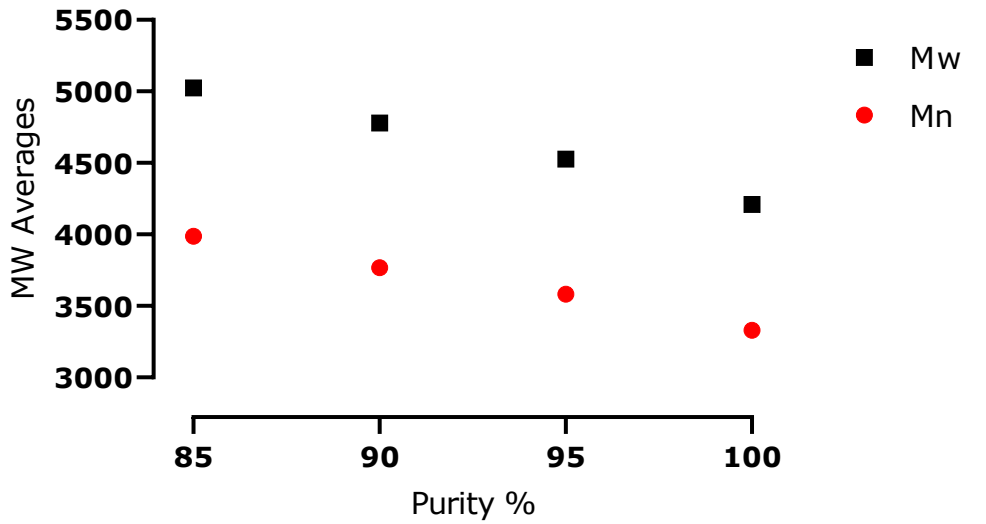


Figure A.4 Molecular weights of azo-0% polymers. 1,4-butanediol diacrylate was used at the purity percentages indicated in the x-axis with 4-aminobutanol to synthesise azo-0% polymers of varied molecular weights.

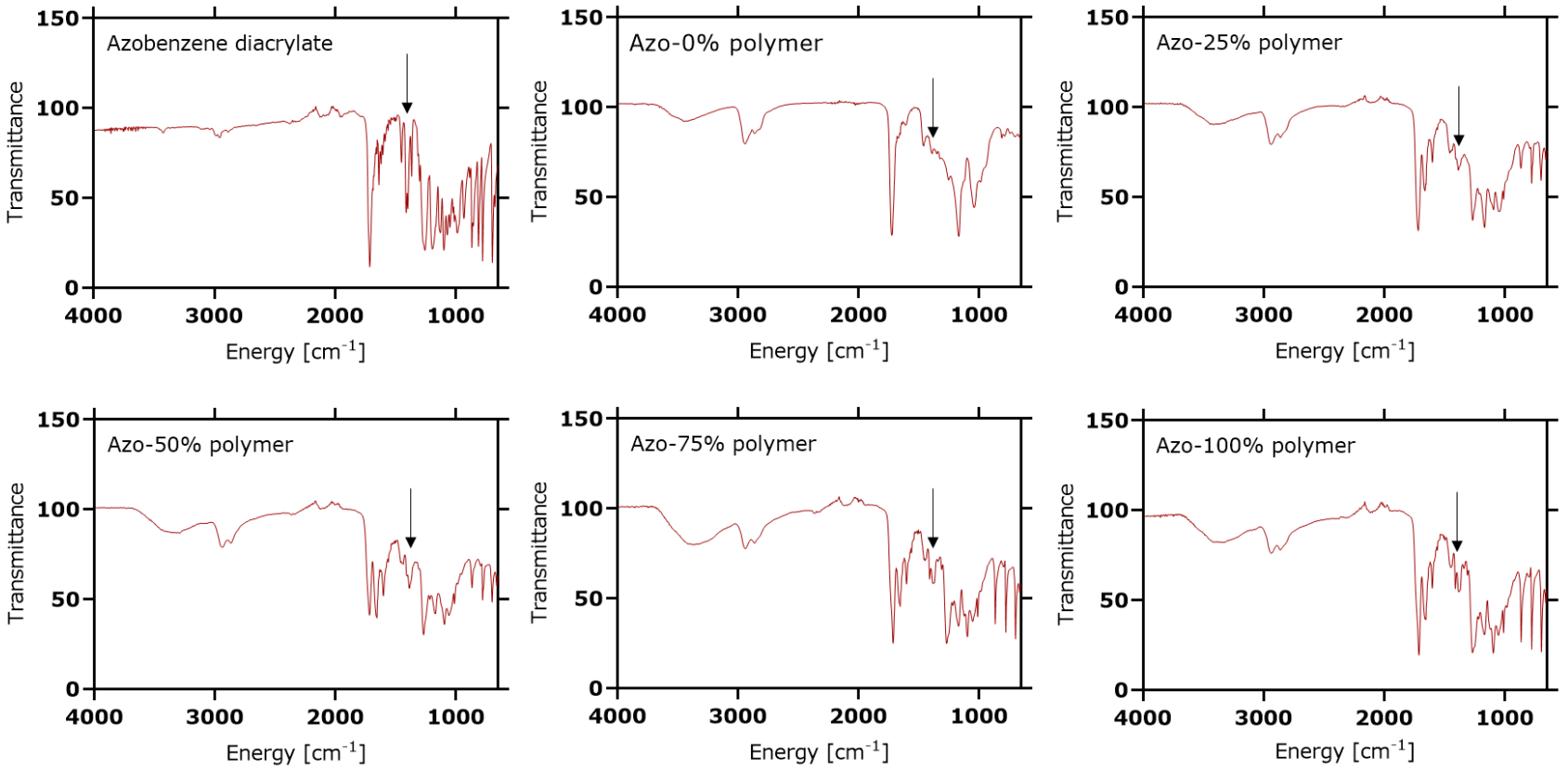


Figure A.5 Fourier Transform Infrared (FT-IR) spectra of the PABE polymers. Vibrational absorption at 1400 cm^{-1} which is indicated by an arrow confirms the presence of the azobenzene bonds.

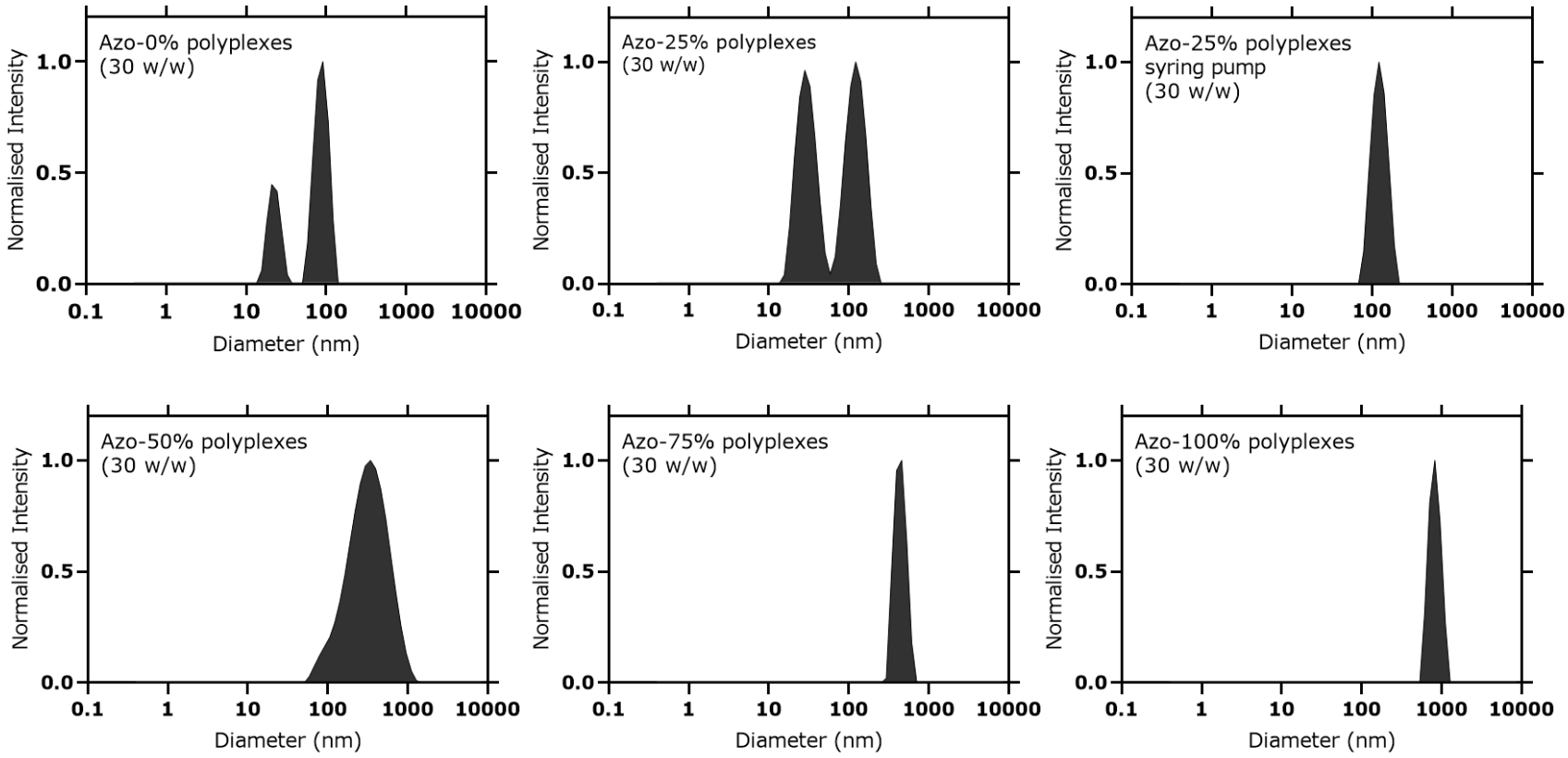


Figure A.6 Size distribution of PBAE polyplexes. Dynamic light scattering results showing the difference in the size distribution of PBAE polyplexes prepared in 25 mM sodium acetate (pH=5) at 30 w/w.

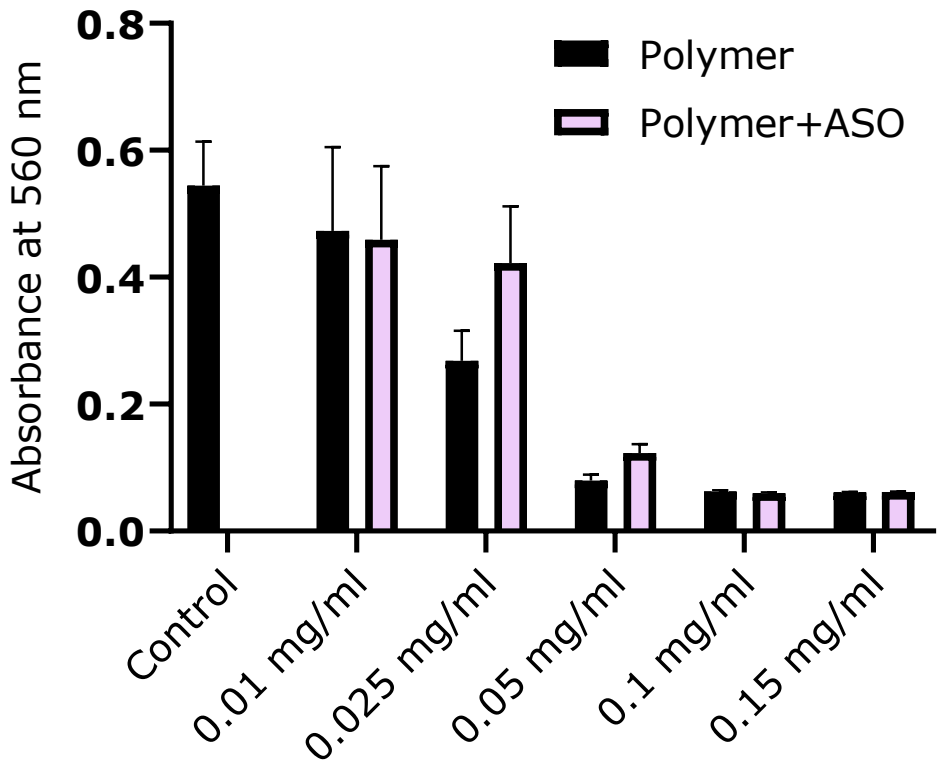


Figure A.7 Effects of PBAE-based polyplexes formulated with PEG-PEI on the metabolic activity of MCF-7 cells. MTT assay results after transfection of anti-EGFR ASOs (120 ng/well) using the azo-25% polymer formulated with PEG-PEI at 0.008 mg/ml for two hours. After that, polyplexes were replaced with fresh cell-culture media and cells were incubated for further 72 hours before assessing the metabolic activity. N = 4. Data generated from a single experiment. Error bars represent standard deviation. Control cells received an equivalent solvent amount.

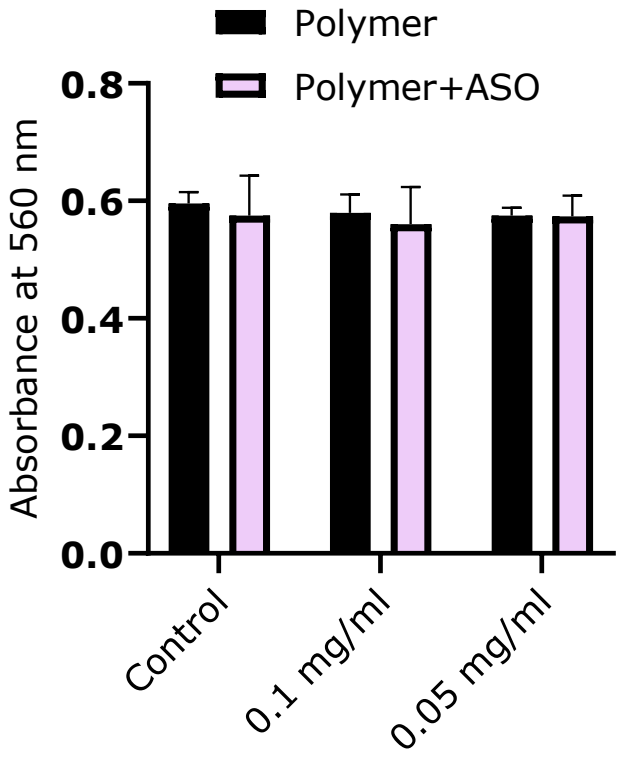


Figure A.8 Effects of PBAE-based polyplexes formulated with the HIV-1 Tat protein on the metabolic activity of MCF-7 cells. MTT assay results after transfection of anti-EGFR ASOs (120 ng/well) using the azo-25% polymer formulated with the HIV-1 Tat protein at 1 µg/ml for two hours. After that, polyplexes were replaced with fresh cell-culture media and cells were incubated for further 72 hours before assessing the metabolic activity. N = 4. Data generated from a single experiment. Error bars represent standard deviation. Control cells received an equivalent solvent amount.

9 References

ABAEVA, I. S., MARINTCHEV, A., PISAREVA, V. P., HELLEN, C. U. & PESTOVA, T. V. 2011. Bypassing of stems versus linear base-by-base inspection of mammalian mRNAs during ribosomal scanning. *Embo j,* 30**,** 115-29.

ABBOTTS, R. & WILSON III, D. M. 2017. Coordination of DNA single strand break repair. *Free Radical Biology and Medicine,* 107**,** 228-244.

ADAMS, J. M. & CORY, S. 2007. The Bcl-2 apoptotic switch in cancer development and therapy. *Oncogene,* 26**,** 1324-1337.

ADJIBADE, P., GRENIER ST-SAUVEUR, V., BERGEMAN, J., HUOT, M. E., KHANDJIAN, E. W. & MAZROUI, R. 2017. DDX3 regulates endoplasmic reticulum stress-induced ATF4 expression. *Sci Rep,* 7**,** 13832.

ADJIBADE, P., ST-SAUVEUR, V. G., HUBERDEAU, M. Q., FOURNIER, M.-J., SAVARD, A., COUDERT, L., KHANDJIAN, E. W. & MAZROUI, R. 2015. Sorafenib, a multikinase inhibitor, induces formation of stress granules in hepatocarcinoma cells. *Oncotarget,* 6**,** 43927.

AGRAWAL, S., TEMSAMANI, J. & TANG, J. Y. 1991. Pharmacokinetics, biodistribution, and stability of oligodeoxynucleotide phosphorothioates in mice. *Proceedings of the National Academy of Sciences,* 88**,** 7595-7599.

AITKEN, C. E. & LORSCH, J. R. 2012. A mechanistic overview of translation initiation in eukaryotes. *Nature structural & molecular biology,* 19**,** 568-576.

AKINC, A., ANDERSON, D. G., LYNN, D. M. & LANGER, R. 2003. Synthesis of poly (β-amino ester) s optimized for highly effective gene delivery. *Bioconjugate chemistry,* 14**,** 979-988.

AKINC, A. & LANGER, R. 2002. Measuring the pH environment of DNA delivered using nonviral vectors: implications for lysosomal trafficking. *Biotechnology and bioengineering,* 78**,** 503-508.

ALEXANDROV, L. B., NIK-ZAINAL, S., WEDGE, D. C., APARICIO, S. A., BEHJATI, S., BIANKIN, A. V., BIGNELL, G. R., BOLLI, N., BORG, A. & BØRRESEN-DALE, A.-L. 2013. Signatures of mutational processes in human cancer. *Nature,* 500**,** 415-421.

ANDERSON, D. G., AKINC, A., HOSSAIN, N. & LANGER, R. 2005. Structure/property studies of polymeric gene delivery

using a library of poly (β-amino esters). *Molecular Therapy,* 11**,** 426-434.

ANDERSON, D. G., LYNN, D. M. & LANGER, R. 2003. Semi-automated synthesis and screening of a large library of degradable cationic polymers for gene delivery. *Angewandte Chemie International Edition,* 42**,** 3153-3158.

ANDERSON, D. G., PENG, W., AKINC, A., HOSSAIN, N., KOHN, A., PADERA, R., LANGER, R. & SAWICKI, J. A. 2004. A polymer library approach to suicide gene therapy for cancer. *Proceedings of the National Academy of Sciences,* 101**,** 16028-16033.

ANDERSON, P. & KEDERSHA, N. 2009. RNA granules: post-transcriptional and epigenetic modulators of gene expression. *Nat Rev Mol Cell Biol,* 10**,** 430-6.

ANDREEV, D. E., O'CONNOR, P. B., FAHEY, C., KENNY, E. M., TERENIN, I. M., DMITRIEV, S. E., CORMICAN, P., MORRIS, D. W., SHATSKY, I. N. & BARANOV, P. V. 2015. Translation of 5′ leaders is pervasive in genes resistant to eIF2 repression. *Elife,* 4.

ARIUMI, Y. 2014. Multiple functions of DDX3 RNA helicase in gene regulation, tumorigenesis, and viral infection. *Front Genet,* 5**,** 423.

ARIUMI, Y., KUROKI, M., ABE, K., DANSAKO, H., IKEDA, M., WAKITA, T. & KATO, N. 2007. DDX3 DEAD-box RNA helicase is required for hepatitis C virus RNA replication. *J Virol,* 81**,** 13922-6.

ARTEAGA, C. L. 2002. Epidermal growth factor receptor dependence in human tumors: more than just expression? *The oncologist,* 7 Suppl 4**,** 31-9.

BABENDURE, J. R., BABENDURE, J. L., DING, J. H. & TSIEN, R. Y. 2006. Control of mammalian translation by mRNA structure near caps. *Rna,* 12**,** 851-61.

BACHE, K. G., SLAGSVOLD, T. & STENMARK, H. 2004. Defective downregulation of receptor tyrosine kinases in cancer. *The EMBO journal,* 23**,** 2707-12.

BADURA, M., BRAUNSTEIN, S., ZAVADIL, J. & SCHNEIDER, R. J. 2012. DNA damage and eIF4G1 in breast cancer cells reprogram translation for survival and DNA repair mRNAs. *Proceedings of the National Academy of Sciences,* 109**,** 18767-18772.

BAILEY, J. K., SHEN, W., LIANG, X.-H. & CROOKE, S. T. 2017. Nucleic acid binding proteins affect the subcellular distribution of phosphorothioate antisense oligonucleotides. *Nucleic acids research,* 45**,** 10649-10671.

BAIRD, S. D., TURCOTTE, M., KORNELUK, R. G. & HOLCIK, M. 2006. Searching for IRES. *Rna,* 12**,** 1755-1785.

BARNER-KOWOLLIK, C. 2009. Acrylate free radical polymerization: From mechanism to polymer design. *Macromolecular rapid communications,* 30**,** 1961-1963.

BARTSCH, H. & NAIR, J. 2006. Chronic inflammation and oxidative stress in the genesis and perpetuation of cancer: role of lipid peroxidation, DNA damage, and repair. *Langenbeck's Archives of Surgery,* 391**,** 499-510.

BASELGA, J. & ARTEAGA, C. L. 2005. Critical update and emerging trends in epidermal growth factor receptor targeting in cancer. *Journal of Clinical Oncology,* 23**,** 2445-2459.

BASTIDE, A., KARAA, Z., BORNES, S., HIEBLOT, C., LACAZETTE, E., PRATS, H. & TOURIOL, C. 2008. An upstream open reading frame within an IRES controls expression of a specific VEGF-A isoform. *Nucleic acids research,* 36**,** 2434-2445.

BEAUDOIN, M. E., POIREL, V.-J. & KRUSHEL, L. A. 2008. Regulating amyloid precursor protein synthesis through an internal ribosomal entry site. *Nucleic acids research,* 36**,** 6835-6847.

BENNETT, C. & CROOKE, S. 2006. Antisense Drug Technology: Principles, Strategies, and Applications. CRC Press Boca Raton.

BENNETT, C. F. 2019. Therapeutic antisense oligonucleotides are coming of age. *Annual review of medicine,* 70**,** 307-321.

BENNETT, C. F., BAKER, B. F., PHAM, N., SWAYZE, E. & GEARY, R. S. 2017. Pharmacology of antisense drugs. *Annual review of pharmacology and toxicology,* 57**,** 81-105.

BENNETT, C. F. & SWAYZE, E. E. 2010. RNA targeting therapeutics: molecular mechanisms of antisense oligonucleotides as a therapeutic platform. *Annual review of pharmacology and toxicology,* 50**,** 259-293.

BENSON, M. D., WADDINGTON-CRUZ, M., BERK, J. L., POLYDEFKIS, M., DYCK, P. J., WANG, A. K., PLANTÉ-BORDENEUVE, V., BARROSO, F. A., MERLINI, G. & OBICI, L. 2018. Inotersen treatment for patients with hereditary transthyretin amyloidosis. *New England Journal of Medicine,* 379**,** 22-31.

BERTOLOTTI, Anne, Yuhong Zhang, Linda M. Hendershot, Heather P. Harding, and David Ron. 2000. "Dynamic Interaction of BiP and ER Stress Transducers in the Unfolded-Protein Response." Nature Cell Biology 2(6):326–32. doi: 10.1038/35014014.

BHATTACHARYYA, D., DIAMOND, P. & BASU, S. 2015. An Independently folding RNA G-quadruplex domain directly recruits the 40S ribosomal subunit. *Biochemistry,* 54**,** 1879-1885.

BLUM, M., DE ROBERTIS, E. M., WALLINGFORD, J. B. & NIEHRS, C. 2015. Morpholinos: antisense and sensibility. *Developmental cell,* 35**,** 145-149.

BOL, G. M., RAMAN, V., VAN DER GROEP, P., VERMEULEN, J. F., PATEL, A. H., VAN DER WALL, E. & VAN DIEST, P. J. 2013. Expression of the RNA helicase DDX3 and the hypoxia response in breast cancer. *PloS one,* 8.

BOL, G. M., VESUNA, F., XIE, M., ZENG, J., AZIZ, K., GANDHI, N., LEVINE, A., IRVING, A., KORZ, D., TANTRAVEDI, S., HEERMA VAN VOSS, M. R., GABRIELSON, K., BORDT, E. A., POLSTER, B. M., COPE, L., VAN DER GROEP, P., KONDASKAR, A., RUDEK, M. A., HOSMANE, R. S., VAN DER WALL, E., VAN DIEST, P. J., TRAN, P. T. & RAMAN, V. 2015. Targeting DDX3 with a small molecule inhibitor for lung cancer therapy. *EMBO Mol Med,* 7**,** 648-69.

BONNEAU, A. & SONENBERG, N. 1987. Involvement of the 24-kDa cap-binding protein in regulation of protein synthesis in mitosis. *Journal of Biological Chemistry,* 262**,** 11134-11139.

BORAH, K. J., PHUKAN, M. & BORAH, R. 2010. Aza-Michael addition of amines to α, β-unsaturated compounds using molecular iodine as catalyst. *Synthetic Communications®,* 40**,** 2830-2836.

BORDELEAU, M.-E., MORI, A., OBERER, M., LINDQVIST, L., CHARD, L. S., HIGA, T., BELSHAM, G. J., WAGNER, G., TANAKA, J. & PELLETIER, J. 2006. Functional characterization of IRESes by an inhibitor of the RNA helicase eIF4A. *Nature chemical biology,* 2**,** 213.

BOS, R., VAN DIEST, P. J., DE JONG, J. S., VAN DER GROEP, P., VAN DER VALK, P. & VAN DER WALL, E. 2005. Hypoxia-inducible factor-1α is associated with angiogenesis, and expression of bFGF, PDGF-BB, and EGFR in invasive breast cancer. *Histopathology,* 46**,** 31-36.

BOSSI, P. & PLATINI, F. 2017. Radiotherapy plus EGFR inhibitors: synergistic modalities. *Cancers of the head & neck,* 2**,** 2.

BOTLAGUNTA, M., KRISHNAMACHARY, B., VESUNA, F., WINNARD JR, P. T., BOL, G. M., PATEL, A. H. & RAMAN, V. 2011. Expression of DDX3 is directly modulated by hypoxia inducible factor-1 alpha in breast epithelial cells. *PloS one,* 6.

BOTLAGUNTA, M., VESUNA, F., MIRONCHIK, Y., RAMAN, A., LISOK, A., WINNARD JR, P., MUKADAM, S., VAN DIEST,

P., CHEN, J. & FARABAUGH, P. 2008. Oncogenic role of DDX3 in breast cancer biogenesis. *Oncogene,* 27**,** 3912.

BOUFFANT Le, Ronan, Patrick Cormier, Odile Mulner-Lorillon, and Robert Bellé. 2006. "Hypoxia and DNA-Damaging Agent Bleomycin Both Increase the Cellular Level of the Protein 4E-BP." Journal of Cellular Biochemistry 99(1):126–32. doi: 10.1002/jcb.20856.

BOUSSIF, O., LEZOUALC'H, F., ZANTA, M. A., MERGNY, M. D., SCHERMAN, D., DEMENEIX, B. & BEHR, J.-P. 1995. A versatile vector for gene and oligonucleotide transfer into cells in culture and in vivo: polyethylenimine. *Proceedings of the National Academy of Sciences,* 92**,** 7297-7301.

BRADFORD, M. M. 1976. A rapid and sensitive method for the quantitation of microgram quantities of protein utilizing the principle of protein-dye binding. *Analytical biochemistry,* 72**,** 248-254.

BRAND, T. M., IIDA, M., LUTHAR, N., STARR, M. M., HUPPERT, E. J. & WHEELER, D. L. 2013. Nuclear EGFR as a molecular target in cancer. *Radiotherapy and Oncology,* 108**,** 370-377.

BRAUNSTEIN, S., BADURA, M. L., XI, Q., FORMENTI, S. C. & SCHNEIDER, R. J. 2009. Regulation of protein synthesis by ionizing radiation. *Molecular and cellular biology,* 29**,** 5645-5656.

BRAUNSTEIN, S., KARPISHEVA, K., POLA, C., GOLDBERG, J., HOCHMAN, T., YEE, H., CANGIARELLA, J., ARJU, R., FORMENTI, S. C. & SCHNEIDER, R. J. 2007. A hypoxia-controlled cap-dependent to cap-independent translation switch in breast cancer. *Molecular cell,* 28**,** 501-512.

BRAY, F., FERLAY, J., SOERJOMATARAM, I., SIEGEL, R. L., TORRE, L. A. & JEMAL, A. 2018. Global cancer statistics 2018: GLOBOCAN estimates of incidence and mortality worldwide for 36 cancers in 185 countries. *CA Cancer J Clin,* 68**,** 394-424.

BRENNEISEN, P., WENK, J., WLASCHEK, M., KRIEG, T. & SCHARFFETTER-KOCHANEK, K. 2000. Activation of p70 ribosomal protein S6 kinase is an essential step in the DNA damage-dependent signaling pathway responsible for the ultraviolet B-mediated increase in interstitial collagenase (MMP-1) and stromelysin-1 (MMP-3) protein levels in human dermal fibroblasts. *Journal of Biological Chemistry,* 275**,** 4336-4344.

BREUGST, M. & VON DER HEIDEN, D. 2018. Mechanisms in iodine catalysis. *Chemistry–A European Journal,* 24**,** 9187-9199.

BROWN, J. M. & WILSON, W. R. 2004. Exploiting tumour hypoxia in cancer treatment. *Nature Reviews Cancer,* 4**,** 437-447.

BUCHAN, J. R. & PARKER, R. 2009. Eukaryotic stress granules: the ins and outs of translation. *Mol Cell,* 36**,** 932-41.

BURDICK, A. D., SCIABOLA, S., MANTENA, S. R., HOLLINGSHEAD, B. D., STANTON, R., WARNEKE, J. A., ZENG, M., MARTSEN, E., MEDVEDEV, A. & MAKAROV, S. S. 2014. Sequence motifs associated with hepatotoxicity of locked nucleic acid—modified antisense oligonucleotides. *Nucleic acids research,* 42**,** 4882-4891.

BUREL, S. A., HART, C. E., CAUNTAY, P., HSIAO, J., MACHEMER, T., KATZ, M., WATT, A., BUI, H.-H., YOUNIS, H. & SABRIPOUR, M. 2015. Hepatotoxicity of high affinity gapmer antisense oligonucleotides is mediated by RNase H1 dependent promiscuous reduction of very long pre-mRNA transcripts. *Nucleic acids research,* 44**,** 2093-2109.

CALFON, M., ZENG, H., URANO, F., TILL, J. H., HUBBARD, S. R., HARDING, H. P., CLARK, S. G. & RON, D. 2002. IRE1 couples endoplasmic reticulum load to secretory capacity by processing the XBP-1 mRNA. *Nature,* 415**,** 92-96.

CALVO, S. E., PAGLIARINI, D. J. & MOOTHA, V. K. 2009. Upstream open reading frames cause widespread reduction of protein expression and are polymorphic among humans. *Proceedings of the National Academy of Sciences,* 106**,** 7507-7512.

CASTAGLIUOLO, I., VALENICK, L., LIU, J. & POTHOULAKIS, C. 2000. Epidermal growth factor receptor transactivation mediates substance P-induced mitogenic responses in U-373 MG cells. *Journal of Biological Chemistry,* 275**,** 26545-26550.

CERRITELLI, S. M. & CROUCH, R. J. 2009. Ribonuclease H: the enzymes in eukaryotes. *The FEBS journal,* 276**,** 1494-1505.

CHAMPION, J. A. & MITRAGOTRI, S. 2006. Role of target geometry in phagocytosis. *Proceedings of the National Academy of Sciences,* 103**,** 4930-4934.

CHAN, C.-P., KOK, K.-H., TANG, H.-M. V., WONG, C.-M. & JIN, D.-Y. 2013. Internal ribosome entry site-mediated translational regulation of ATF4 splice variant in mammalian unfolded protein response. *Biochimica et Biophysica Acta (BBA)-Molecular Cell Research,* 1833**,** 2165-2175.

CHANG, H., ZHANG, J., WANG, H., LV, J. & CHENG, Y. 2017. A combination of guanidyl and phenyl groups on a dendrimer enables efficient siRNA and DNA delivery. *Biomacromolecules,* 18**,** 2371-2378.

CHANG, P. C., CHI, C. W., CHAU, G. Y., LI, F. Y., TSAI, Y. H., WU, J. C. & WU LEE, Y. H. 2006. DDX3, a DEAD box RNA helicase, is deregulated in hepatitis virus-associated hepatocellular carcinoma and is involved in cell growth control. *Oncogene,* 25**,** 1991-2003.

CHANGAVI, A. A., SHASHIKALA, A. & RAMJI, A. S. 2015. Epidermal growth factor receptor expression in triple negative and nontriple negative breast carcinomas. *Journal of laboratory physicians,* 7**,** 79.

CHAO, C. H., CHEN, C. M., CHENG, P. L., SHIH, J. W., TSOU, A. P. & LEE, Y. H. 2006. DDX3, a DEAD box RNA helicase with tumor growth-suppressive property and transcriptional regulation activity of the p21waf1/cip1 promoter, is a candidate tumor suppressor. *Cancer Res,* 66**,** 6579-88.

CHAPPELL, S. A., LEQUESNE, J. P., PAULIN, F. E., STONELEY, M., SOUTAR, R. L., RALSTON, S. H., HELFRICH, M. H. & WILLIS, A. E. 2000. A mutation in the c-myc-IRES leads to enhanced internal ribosome entry in multiple myeloma: a novel mechanism of oncogene de-regulation. *Oncogene,* 19**,** 4437.

CHEN, H. H., YU, H. I., CHO, W. C. & TARN, W. Y. 2015. DDX3 modulates cell adhesion and motility and cancer cell metastasis via Rac1-mediated signaling pathway. *Oncogene,* 34**,** 2790-800.

CHEN, H. H., YU, H. I. & TARN, W. Y. 2016. DDX3 Modulates Neurite Development via Translationally Activating an RNA Regulon Involved in Rac1 Activation. *J Neurosci,* 36**,** 9792-804.

CHEN, S., LIU, X., GONG, W., YANG, H., LUO, D., ZUO, X., LI, W., WU, P., LIU, L. & XU, Q. 2013. Combination therapy with VEGFR2 and EGFR siRNA enhances the antitumor effect of cisplatin in non-small cell lung cancer xenografts. *Oncology reports,* 29**,** 260-268.

CHEN, W.-J., WANG, W.-T., TSAI, T.-Y., LI, H.-K. & LEE, Y.-H. W. 2017. DDX3 localizes to the centrosome and prevents multipolar mitosis by epigenetically and translationally modulating p53 expression. *Scientific reports,* 7**,** 9411-9411.

CHEN, Jane Jane. 2007. "Regulation of Protein Synthesis by the Heme-Regulated EIF2α Kinase: Relevance to Anemias." Blood 109(7):2693–99.

CHENG, Z., AL ZAKI, A., HUI, J. Z., MUZYKANTOV, V. R. & TSOURKAS, A. 2012. Multifunctional nanoparticles: cost versus benefit of adding targeting and imaging capabilities. *Science,* 338**,** 903-910.

CHERY, J. 2016. RNA therapeutics: RNAi and antisense mechanisms and clinical applications. *Postdoc journal: a journal of postdoctoral research and postdoctoral affairs,* 4**,** 35.

CHOI, J., RUI, Y., KIM, J., GORELICK, N., WILSON, D. R., KOZIELSKI, K., MANGRAVITI, A., SANKEY, E., BREM, H. & TYLER, B. 2020. Nonviral polymeric nanoparticles for gene therapy in pediatric CNS malignancies. *Nanomedicine: Nanotechnology, Biology and Medicine,* 23**,** 102115.

CHOU, R.-H., WANG, Y.-N., HSIEH, Y.-H., LI, L.-Y., XIA, W., CHANG, W.-C., CHANG, L.-C., CHENG, C.-C., LAI, C.-C. & HSU, J. L. 2014. EGFR modulates DNA synthesis and repair through Tyr phosphorylation of histone H4. *Developmental cell,* 30**,** 224-237.

CHRISTENSEN, L. V., CHANG, C.-W., KIM, W. J., KIM, S. W., ZHONG, Z., LIN, C., ENGBERSEN, J. F. & FEIJEN, J. 2006. Reducible poly (amido ethylenimine) s designed for triggered intracellular gene delivery. *Bioconjugate chemistry,* 17**,** 1233-1240.

CHRISTMANN, M., TOMICIC, M. T., ROOS, W. P. & KAINA, B. 2003. Mechanisms of human DNA repair: an update. *Toxicology,* 193**,** 3-34.

CHUANG, R.-Y., WEAVER, P. L., LIU, Z. & CHANG, T.-H. 1997. Requirement of the DEAD-Box protein ded1p for messenger RNA translation. *Science,* 275**,** 1468-1471.

CIARDIELLO, F., CAPUTO, R., TROIANI, T., BORRIELLO, G., KANDIMALLA, E. R., AGRAWAL, S., MENDELSOHN, J., BIANCO, A. R. & TORTORA, G. 2001. Antisense oligonucleotides targeting the epidermal growth factor receptor inhibit proliferation, induce apoptosis, and cooperate with cytotoxic drugs in human cancer cell lines. *International journal of cancer,* 93**,** 172-178.

COATES, P. J., LORIMORE, S. A. & WRIGHT, E. G. 2005. Cell and tissue responses to genotoxic stress. *The Journal of Pathology: A Journal of the Pathological Society of Great Britain and Ireland,* 205**,** 221-235.

COBBOLD, L., WILSON, L., SAWICKA, K., KING, H., KONDRASHOV, A., SPRIGGS, K., BUSHELL, M. & WILLIS, A. 2010. Upregulated c-myc expression in multiple myeloma by internal ribosome entry results from increased interactions with and expression of PTB-1 and YB-1. *Oncogene,* 29**,** 2884.

CONNOLLY, E., BRAUNSTEIN, S., FORMENTI, S. & SCHNEIDER, R. J. 2006. Hypoxia inhibits protein synthesis through a 4E-BP1 and elongation factor 2 kinase pathway controlled

by mTOR and uncoupled in breast cancer cells. *Molecular and cellular biology,* 26**,** 3955-3965.

CORCORAN, R. B., EBI, H., TURKE, A. B., COFFEE, E. M., NISHINO, M., COGDILL, A. P., BROWN, R. D., DELLA PELLE, P., DIAS-SANTAGATA, D. & HUNG, K. E. 2012. EGFR-mediated reactivation of MAPK signaling contributes to insensitivity of BRAF-mutant colorectal cancers to RAF inhibition with vemurafenib. *Cancer discovery,* 2**,** 227-235.

CORDEIRO, R. A., SERRA, A., COELHO, J. F. & FANECA, H. 2019. Poly (β-amino ester)-based gene delivery systems: From discovery to therapeutic applications. *Journal of Controlled Release*.

CORDIN, O., BANROQUES, J., TANNER, N. K. & LINDER, P. 2006. The DEAD-box protein family of RNA helicases. *Gene,* 367**,** 17-37.

COSTA, R., SHAH, A. N., SANTA-MARIA, C. A., CRUZ, M. R., MAHALINGAM, D., CARNEIRO, B. A., CHAE, Y. K., CRISTOFANILLI, M., GRADISHAR, W. J. & GILES, F. J. 2017. Targeting epidermal growth factor receptor in triple negative breast cancer: new discoveries and practical insights for drug development. *Cancer treatment reviews,* 53**,** 111-119.

COSTELLO, A., LAO, N. T., BARRON, N. & CLYNES, M. 2019. Continuous translation of circularized mRNA improves recombinant protein titer. *Metabolic engineering,* 52**,** 284-292.

CROOKE, S. T., BAKER, B. F., KWOH, T. J., CHENG, W., SCHULZ, D. J., XIA, S., SALGADO, N., BUI, H.-H., HART, C. E. & BUREL, S. A. 2016. Integrated safety assessment of 2′-O-methoxyethyl chimeric antisense oligonucleotides in nonhuman primates and healthy human volunteers. *Molecular Therapy,* 24**,** 1771-1782.

CROOKE, S. T., BAKER, B. F., WITZTUM, J. L., KWOH, T. J., PHAM, N. C., SALGADO, N., MCEVOY, B. W., CHENG, W., HUGHES, S. G. & BHANOT, S. 2017. The effects of 2′-O-methoxyethyl containing antisense oligonucleotides on platelets in human clinical trials. *nucleic acid therapeutics,* 27**,** 121-129.

CROOKE, S. T., GRAHAM, M. J., ZUCKERMAN, J. E., BROOKS, D., CONKLIN, B. S., CUMMINS, L. L., GREIG, M. J., GUINOSSO, C. J., KORNBRUST, D. & MANOHARAN, M. 1996. Pharmacokinetic properties of several novel oligonucleotide analogs in mice. *Journal of Pharmacology and Experimental Therapeutics,* 277**,** 923-937.

CROOKE, S. T., WITZTUM, J. L., BENNETT, C. F. & BAKER, B. F. 2018. RNA-targeted therapeutics. *Cell metabolism,* 27**,** 714-739.

DAMIANO, F., ROCHIRA, A., TOCCI, R., ALEMANNO, S., GNONI, A. & SICULELLA, L. 2013. hnRNP A1 mediates the activation of the IRES-dependent SREBP-1a mRNA translation in response to endoplasmic reticulum stress. *Biochemical Journal,* 449**,** 543-553.

DASSI, E., RE, A., LEO, S., TEBALDI, T., PASINI, L., PERONI, D. & QUATTRONE, A. 2014. AURA 2: Empowering discovery of post-transcriptional networks. *Translation,* 2**,** e27738.

DAUB, H., WEISS, F. U., WALLASCH, C. & ULLRICH, A. 1996. Role of transactivation of the EGF receptor in signalling by G-protein-coupled receptors. *Nature,* 379**,** 557.

DAVULURI, R. V., SUZUKI, Y., SUGANO, S. & ZHANG, M. Q. 2000. CART classification of human 5′ UTR sequences. *Genome research,* 10**,** 1807-1816.

DE LIMA-BESSA, K. M., ARMELINI, M. G., CHIGANÇAS, V., JACYSYN, J. F., AMARANTE-MENDES, G. P., SARASIN, A. & MENCK, C. F. M. 2008. CPDs and 6-4PPs play different roles in UV-induced cell death in normal and NER-deficient human cells. *DNA repair,* 7**,** 303-312.

DE VILLE DE GOYET, M., MONIOTTE, S., ROBERT, A., DUPONT, S., VERMYLEN, C., VEYCKEMANS, F. & BRICHARD, B. 2013. Iron overload in children undergoing cancer treatments. *Pediatric blood & cancer,* 60**,** 1982-1987.

DEFORGES, J., LOCKER, N. & SARGUEIL, B. 2015. mRNAs that specifically interact with eukaryotic ribosomal subunits. *Biochimie,* 114**,** 48-57.

DENG, J., HARDING, H. P., RAUGHT, B., GINGRAS, A.-C., BERLANGA, J. J., SCHEUNER, D., KAUFMAN, R. J., RON, D. & SONENBERG, N. 2002. Activation of GCN2 in UV-irradiated cells inhibits translation. *Current Biology,* 12**,** 1279-1286.

DENT, P., REARDON, D. B., PARK, J. S., BOWERS, G., LOGSDON, C., VALERIE, K. & SCHMIDT-ULLRICH, R. 1999. Radiation-induced release of transforming growth factor α activates the epidermal growth factor receptor and mitogen-activated protein kinase pathway in carcinoma cells, leading to increased proliferation and protection from radiation-induced cell death. *Molecular biology of the cell,* 10**,** 2493-2506.

DEVER, T. E., YANG, W., ASTRÖM, S., BYSTRÖM, A. S. & HINNEBUSCH, A. G. 1995. Modulation of tRNA (iMet), eIF-2, and eIF-2B expression shows that GCN4 translation is inversely coupled to the level of eIF-2. GTP.

Met-tRNA (iMet) ternary complexes. *Molecular and Cellular Biology,* 15**,** 6351-6363.

DIAS, N. & STEIN, C. 2002. Antisense oligonucleotides: basic concepts and mechanisms. *Molecular cancer therapeutics,* 1**,** 347-355.

DITTMANN, K., MAYER, C., FEHRENBACHER, B., SCHALLER, M., RAJU, U., MILAS, L., CHEN, D. J., KEHLBACH, R. & RODEMANN, H. P. 2005. Radiation-induced epidermal growth factor receptor nuclear import is linked to activation of DNA-dependent protein kinase. *Journal of Biological Chemistry,* 280**,** 31182-31189.

DITTMANN, K., MAYER, C., KEHLBACH, R. & RODEMANN, H. P. 2008. Radiation-induced caveolin-1 associated EGFR internalization is linked with nuclear EGFR transport and activation of DNA-PK. *Molecular cancer,* 7**,** 69.

DITTON, H. J., ZIMMER, J., KAMP, C., RAJPERT-DE MEYTS, E. & VOGT, P. H. 2004. The AZFa gene DBY (DDX3Y) is widely transcribed but the protein is limited to the male germ cells by translation control. *Hum Mol Genet,* 13**,** 2333-41.

DOBBYN, H. C., HILL, K., HAMILTON, T. L., SPRIGGS, K. A., PICKERING, B. M., COLDWELL, M. J., DE MOOR, C. H., BUSHELL, M. & WILLIS, A. E. 2008. Regulation of BAG-1 IRES-mediated translation following chemotoxic stress. *Oncogene,* 27**,** 1167-1174.

DONG, Jinsheng, Hongfang Qiu, Minerva Garcia-Barrio, James Anderson, and Alan G. Hinnebusch. 2000. "Uncharged TRNA Activates GCN2 by Displacing the Protein Kinase Moiety from a Bipartite TRNA-Binding Domain." Molecular Cell 6(2):269–79. doi: 10.1016/S1097-2765(00)00028-9.

DOSTA, P., RAMOS, V. & BORRÓS, S. 2018. Stable and efficient generation of poly (β-amino ester) s for RNAi delivery. *Molecular Systems Design & Engineering,* 3**,** 677-689.

EDER, P. S., DEVINE, R. J., DAGLE, J. M. & WALDER, J. A. 1991. Substrate specificity and kinetics of degradation of antisense oligonucleotides by a 3' exonuclease in plasma. *Antisense research and development,* 1**,** 141-151.

EDWARDS, S. & WILLIAMS, D. 2004. Double layers and interparticle forces in colloid science and biology: analytic results for the effect of ionic dispersion forces. *Physical review letters,* 92**,** 248303.

EL-NAGGAR, A. M., VEINOTTE, C. J., CHENG, H., GRUNEWALD, T. G., NEGRI, G. L., SOMASEKHARAN, S. P., CORKERY, D. P., TIRODE, F., MATHERS, J. & KHAN, D. 2015. Translational activation of HIF1α by YB-1 promotes sarcoma metastasis. *Cancer cell,* 27**,** 682-697.

EL-NAGGAR, A. M. & SORENSEN, P. H. 2018. Translational control of aberrant stress responses as a hallmark of cancer. *The Journal of pathology,* 244**,** 650-666.

ELISEEV, B., YERAMALA, L., LEITNER, A., KARUPPASAMY, M., RAIMONDEAU, E., HUARD, K., ALKALAEVA, E., AEBERSOLD, R. & SCHAFFITZEL, C. 2018. Structure of a human cap-dependent 48S translation pre-initiation complex. *Nucleic acids research,* 46**,** 2678-2689.

ENGELMAN, J. A., ZEJNULLAHU, K., MITSUDOMI, T., SONG, Y., HYLAND, C., PARK, J. O., LINDEMAN, N., GALE, C.-M., ZHAO, X. & CHRISTENSEN, J. 2007. MET amplification leads to gefitinib resistance in lung cancer by activating ERBB3 signaling. *science,* 316**,** 1039-1043.

EPLING, L. B., GRACE, C. R., LOWE, B. R., PARTRIDGE, J. F. & ENEMARK, E. J. 2015. Cancer-associated mutants of RNA helicase DDX3X are defective in RNA-stimulated ATP hydrolysis. *J Mol Biol,* 427**,** 1779-1796.

ESPOSITO, A. M. & KINZY, T. G. 2014. In vivo [35S]-methionine incorporation. *Methods Enzymol,* 536**,** 55-64.

EVDOKIMOVA, V., OVCHINNIKOV, L. P. & SORENSEN, P. H. 2006. Y-box binding protein 1: providing a new angle on translational regulation. *Cell Cycle,* 5**,** 1143-1147.

EVDOKIMOVA, V., TOGNON, C., NG, T., RUZANOV, P., MELNYK, N., FINK, D., SOROKIN, A., OVCHINNIKOV, L. P., DAVICIONI, E. & TRICHE, T. J. 2009. Translational activation of snail1 and other developmentally regulated transcription factors by YB-1 promotes an epithelial-mesenchymal transition. *Cancer cell,* 15**,** 402-415.

FALLETTA, P., SANCHEZ-DEL-CAMPO, L., CHAUHAN, J., EFFERN, M., KENYON, A., KERSHAW, C. J., SIDDAWAY, R., LISLE, R., FRETER, R. & DANIELS, M. J. 2017. Translation reprogramming is an evolutionarily conserved driver of phenotypic plasticity and therapeutic resistance in melanoma. *Genes & development,* 31**,** 18-33.

FARLEY, S. M., PURDY, D. E., RYABININA, O. P., SCHNEIDER, P., MAGUN, B. E. & IORDANOV, M. S. 2008. Fas Ligand-induced Proinflammatory Transcriptional Responses in Reconstructed Human Epidermis RECRUITMENT OF THE EPIDERMAL GROWTH FACTOR RECEPTOR AND ACTIVATION OF MAP KINASES. *Journal of Biological Chemistry,* 283**,** 919-928.

FARMER, H., MCCABE, N., LORD, C. J., TUTT, A. N., JOHNSON, D. A., RICHARDSON, T. B., SANTAROSA, M., DILLON, K. J., HICKSON, I. & KNIGHTS, C. 2005. Targeting the DNA repair defect in BRCA mutant cells as a therapeutic strategy. *Nature,* 434**,** 917-921.

FARVADI, F., TAMADDON, A., SOBHANI, Z. & ABOLMAALI, S. S. 2017. Polyionic complex of single-walled carbon nanotubes and PEG-grafted-hyperbranched polyethyleneimine (PEG-PEI-SWNT) for an improved doxorubicin loading and delivery: development and in vitro characterization. *Artificial cells, nanomedicine, and biotechnology,* 45**,** 855-863.

FAYE, M. D., S. T. Beug, T. E. Graber, N. Earl, X. Xiang, B. Wild, S. Langlois, J. Michaud, K. N. Cowan, R. G. Korneluk, and M. Holcik. 2015. "IGF2BP1 Controls Cell Death and Drug Resistance in Rhabdomyosarcomas by Regulating Translation of CIAP1." Oncogene 34(12):1532–41. doi: 10.1038/onc.2014.90.

FAYE, Mame Daro, and Martin Holcik. 2015. "The Role of IRES Trans-Acting Factors in Carcinogenesis." Biochimica et Biophysica Acta - Gene Regulatory Mechanisms 1849(7):887–97.

FERNANDEZ, J., YAMAN, I., HUANG, C., LIU, H., LOPEZ, A. B., KOMAR, A. A., CAPRARA, M. G., MERRICK, W. C., SNIDER, M. D. & KAUFMAN, R. J. 2005. Ribosome stalling regulates IRES-mediated translation in eukaryotes, a parallel to prokaryotic attenuation. *Molecular cell,* 17**,** 405-416.

FERNANDEZ, J., YAMAN, I., MERRICK, W. C., KOROMILAS, A., WEK, R. C., SOOD, R., HENSOLD, J. & HATZOGLOU, M. 2002. Regulation of internal ribosome entry site-mediated translation by eukaryotic initiation factor-2α phosphorylation and translation of a small upstream open reading frame. *Journal of Biological Chemistry,* 277**,** 2050-2058.

FERRARO, D. A., GABORIT, N., MARON, R., COHEN-DVASHI, H., PORAT, Z., PAREJA, F., LAVI, S., LINDZEN, M., BEN-CHETRIT, N. & SELA, M. 2013. Inhibition of triple-negative breast cancer models by combinations of antibodies to EGFR. *Proceedings of the National Academy of Sciences,* 110**,** 1815-1820.

FERRUTI, P., MARCHISIO, M. A. & DUNCAN, R. 2002. Poly (amido-amine) s: Biomedical Applications. *Macromolecular Rapid Communications,* 23**,** 332-355.

FILOSTO, S., KHAN, E. M., TOGNON, E., BECKER, C., ASHFAQ, M., RAVID, T. & GOLDKORN, T. 2011. EGF receptor exposed to oxidative stress acquires abnormal phosphorylation and aberrant activated conformation that impairs canonical dimerization. *PloS one,* 6**,** e23240.

FRANOVIC, A., GUNARATNAM, L., SMITH, K., ROBERT, I., PATTEN, D. & LEE, S. 2007. Translational up-regulation of the EGFR by tumor hypoxia provides a nonmutational

explanation for its overexpression in human cancer. *Proceedings of the National Academy of Sciences,* 104**,** 13092-13097.

FREED, D. M., BESSMAN, N. J., KIYATKIN, A., SALAZAR-CAVAZOS, E., BYRNE, P. O., MOORE, J. O., VALLEY, C. C., FERGUSON, K. M., LEAHY, D. J. & LIDKE, D. S. 2017. EGFR ligands differentially stabilize receptor dimers to specify signaling kinetics. *Cell,* 171**,** 683-695. e18.

FREIER, S. M. & ALTMANN, K.-H. 1997. The ups and downs of nucleic acid duplex stability: structure-stability studies on chemically-modified DNA: RNA duplexes. *Nucleic acids research,* 25**,** 4429-4443.

FUKUMURA, J., NOGUCHI, E., SEKIGUCHI, T. & NISHIMOTO, T. 2003. A temperature-sensitive mutant of the mammalian RNA helicase, DEAD-BOX X isoform, DBX, defective in the transition from G1 to S phase. *J Biochem,* 134**,** 71-82.

FULDA, S. 2009. Caspase-8 in cancer biology and therapy. *Cancer letters,* 281**,** 128-133.

FULDA, S., GORMAN, A. M., HORI, O. & SAMALI, A. 2010. Cellular stress responses: cell survival and cell death. *International journal of cell biology,* 2010.

FULDA, S., LOS, M., FRIESEN, C. & DEBATIN, K. M. 1998. Chemosensitivity of solid tumor cells in vitro is related to activation of the CD95 system. *International journal of cancer,* 76**,** 105-114.

GARRIDO-CASTRO, A. C., LIN, N. U. & POLYAK, K. 2019. Insights into molecular classifications of triple-negative breast cancer: improving patient selection for treatment. *Cancer discovery,* 9**,** 176-198.

GEARY, R. S., NORRIS, D., YU, R. & BENNETT, C. F. 2015. Pharmacokinetics, biodistribution and cell uptake of antisense oligonucleotides. *Advanced drug delivery reviews,* 87**,** 46-51.

GEARY, R. S., YU, R., SIWKOWSKI, A. & LEVIN, A. A. 2007. Pharmacokinetic/pharmacodynamic properties of phosphorothioate 2′-O-(2-methoxyethyl)-modified antisense oligonucleotides in animals and man. *Antisense drug technology: principles, strategies, and applications***,** 305-326.

GEBAUER, F. & HENTZE, M. W. 2004. Molecular mechanisms of translational control. *Nature reviews Molecular cell biology,* 5**,** 827-835.

GEISSLER, R., GOLBIK, R. P. & BEHRENS, S.-E. 2012. The DEAD-box helicase DDX3 supports the assembly of functional 80S ribosomes. *Nucleic acids research,* 40**,** 4998-5011.

GHAZALPOUR, A., BENNETT, B., PETYUK, V. A., OROZCO, L., HAGOPIAN, R., MUNGRUE, I. N., FARBER, C. R., SINSHEIMER, J., KANG, H. M. & FURLOTTE, N. 2011. Comparative analysis of proteome and transcriptome variation in mouse. *PLoS genetics,* 7**,** e1001393.

GIBSON, D. G., YOUNG, L., CHUANG, R.-Y., VENTER, J. C., HUTCHISON, C. A. & SMITH, H. O. 2009. Enzymatic assembly of DNA molecules up to several hundred kilobases. *Nature methods,* 6**,** 343-345.

GINGRAS, A.-C., KENNEDY, S. G., O'LEARY, M. A., SONENBERG, N. & HAY, N. 1998. 4E-BP1, a repressor of mRNA translation, is phosphorylated and inactivated by the Akt (PKB) signaling pathway. *Genes & development,* 12**,** 502-513.

GINGRAS, A.-C., RAUGHT, B. & SONENBERG, N. 1999. eIF4 initiation factors: effectors of mRNA recruitment to ribosomes and regulators of translation. *Annual review of biochemistry,* 68**,** 913-963.

GOLDING, S. E., MORGAN, R. N., ADAMS, B. R., HAWKINS, A. J., POVIRK, L. F. & VALERIE, K. 2009. Pro-survival AKT and ERK signaling from EGFR and mutant EGFRvIII enhances DNA double-strand break repair in human glioma cells. *Cancer biology & therapy,* 8**,** 730-738.

GONZALEZ, H., HWANG, S. J. & DAVIS, M. 1999. New class of polymers for the delivery of macromolecular therapeutics. *Bioconjugate chemistry,* 10**,** 1068-1074.

GORT, E., GROOT, A., VAN DE VEN, T. D., VAN DER GROEP, P., VERLAAN, I., VAN LAAR, T., VAN DIEST, P., VAN DER WALL, E. & SHVARTS, A. 2006. Hypoxia-inducible factor-1 α expression requires PI 3-kinase activity and correlates with Akt1 phosphorylation in invasive breast carcinomas. *Oncogene,* 25**,** 6123-6127.

GOTO, A., HOSHINO, M., MATSUDA, M. & NAKAMURA, T. 2011. Phosphorylation of STEF/Tiam2 by protein kinase A is critical for Rac1 activation and neurite outgrowth in dibutyryl cAMP-treated PC12D cells. *Molecular biology of the cell,* 22**,** 1780-1790.

GOULD, P. S., DYER, N. P., CROFT, W., OTT, S. & EASTON, A. J. 2014. Cellular mRNAs access second ORFs using a novel amino acid sequence-dependent coupled translation termination–reinitiation mechanism. *RNA,* 20**,** 373-381.

GRADISAR, S., ZAGAR, E. & PAHOVNIK, D. 2017. Ring-opening polymerization of N-carboxyanhydrides initiated by a hydroxyl group. *ACS Macro Letters,* 6**,** 637-640.

GRANT, C. M. & HINNEBUSCH, A. G. 1994. Effect of sequence context at stop codons on efficiency of reinitiation in

GCN4 translational control. *Molecular and cellular biology,* 14**,** 606-618.

GRANT, C. M., MILLER, P. F. & HINNEBUSCH, A. G. 1994. Requirements for intercistronic distance and level of eukaryotic initiation factor 2 activity in reinitiation on GCN4 mRNA vary with the downstream cistron. *Molecular and Cellular Biology,* 14**,** 2616-2628.

GREDELL, J. A., BERGER, A. K. & WALTON, S. P. 2008. Impact of target mRNA structure on siRNA silencing efficiency: a large-scale study. *Biotechnology and bioengineering,* 100**,** 744-755.

GREEN, J. J., LANGER, R. & ANDERSON, D. G. 2008. A combinatorial polymer library approach yields insight into nonviral gene delivery. *Accounts of chemical research,* 41**,** 749-759.

GREEN, J. J., ZUGATES, G. T., TEDFORD, N. C., HUANG, Y. H., GRIFFITH, L. G., LAUFFENBURGER, D. A., SAWICKI, J. A., LANGER, R. & ANDERSON, D. G. 2007. Combinatorial modification of degradable polymers enables transfection of human cells comparable to adenovirus. *Advanced Materials,* 19**,** 2836-2842.

GREIJER, A., DE JONG, M., SCHEFFER, G., SHVARTS, A., VAN DIEST, P. & VAN DER WALL, E. 2005. Hypoxia-induced acidification causes mitoxantrone resistance not mediated by drug transporters in human breast cancer cells. *Analytical Cellular Pathology,* 27**,** 43-49.

GROB, T. J., HEILENKÖTTER, U., GEIST, S., PALUCHOWSKI, P., WILKE, C., JAENICKE, F., QUAAS, A., WILCZAK, W., CHOSCHZICK, M. & SAUTER, G. 2012. Rare oncogenic mutations of predictive markers for targeted therapy in triple-negative breast cancer. *Breast cancer research and treatment,* 134**,** 561-567.

GROUP, E. B. C. T. C. 2006. Effects of radiotherapy and of differences in the extent of surgery for early breast cancer on local recurrence and 15-year survival: an overview of the randomised trials. *The Lancet,* 366**,** 2087-2106.

GUENTHER, U. P., WEINBERG, D. E., ZUBRADT, M. M., TEDESCHI, F. A., STAWICKI, B. N., ZAGORE, L. L., BRAR, G. A., LICATALOSI, D. D., BARTEL, D. P., WEISSMAN, J. S. & JANKOWSKY, E. 2018. The helicase Ded1p controls use of near-cognate translation initiation codons in 5' UTRs. *Nature,* 559**,** 130-134.

GUERRERO-CÁZARES, H., TZENG, S. Y., YOUNG, N. P., ABUTALEB, A. O., QUIÑONES-HINOJOSA, A. & GREEN, J. J. 2014. Biodegradable polymeric nanoparticles show high efficacy and specificity at DNA delivery to human

glioblastoma in vitro and in vivo. *ACS nano,* 8**,** 5141-5153.

GUMUSKAYA, B., ALPER, M., HUCUMENOGLU, S., ALTUNDAG, K., UNER, A. & GULER, G. 2010. EGFR expression and gene copy number in triple-negative breast carcinoma. *Cancer genetics and cytogenetics,* 203**,** 222-229.

GUNGABISSOON, R. A. & BAMBURG, J. R. 2003. Regulation of growth cone actin dynamics by ADF/cofilin. *Journal of Histochemistry & Cytochemistry,* 51**,** 411-420.

GUNIŠOVÁ, S., HRONOVÁ, V., MOHAMMAD, M. P., HINNEBUSCH, A. G. & VALÁŠEK, L. S. 2017. Please do not recycle! Translation reinitiation in microbes and higher eukaryotes. *FEMS microbiology reviews,* 42**,** 165-192.

HABRANT, D., PEUZIAT, P., COLOMBANI, T., DALLET, L., GEHIN, J., GOUDEAU, E., EVRARD, B. R. R., LAMBERT, O., HAUDEBOURG, T. & PITARD, B. 2016. Design of ionizable lipids to overcome the limiting step of endosomal escape: application in the intracellular delivery of mRNA, DNA, and siRNA. *Journal of medicinal chemistry,* 59**,** 3046-3062.

HAC, Aleksandra, Joanna Brokowska, Estera Rintz, Michał Bartkowski, Grzegorz Węgrzyn, and Anna Herman-Antosiewicz. 2020. "Mechanism of Selective Anticancer Activity of Isothiocyanates Relies on Differences in DNA Damage Repair between Cancer and Healthy Cells." European Journal of Nutrition 59(4):1421–32. doi: 10.1007/s00394-019-01995-6.

HAFEZ, I., MAURER, N. & CULLIS, P. 2001. On the mechanism whereby cationic lipids promote intracellular delivery of polynucleic acids. *Gene therapy,* 8**,** 1188-1196.

HAGEDORN, P. H., PONTOPPIDAN, M., BISGAARD, T. S., BERRERA, M., DIECKMANN, A., EBELING, M., MØLLER, M. R., HUDLEBUSCH, H., JENSEN, M. L. & HANSEN, H. F. 2018. Identifying and avoiding off-target effects of RNase H-dependent antisense oligonucleotides in mice. *Nucleic acids research,* 46**,** 5366-5380.

HAIR, P., CAMERON, F. & MCKEAGE, K. 2013. Mipomersen sodium: first global approval. *Drugs,* 73**,** 487-493.

HALATSCH, M.-E., SCHMIDT, U., BEHNKE-MURSCH, J., UNTERBERG, A. & WIRTZ, C. R. 2006. Epidermal growth factor receptor inhibition for the treatment of glioblastoma multiforme and other malignant brain tumours. *Cancer treatment reviews,* 32**,** 74-89.

HAN, W. & LO, H.-W. 2012. Landscape of EGFR signaling network in human cancers: biology and therapeutic

response in relation to receptor subcellular locations. *Cancer letters,* 318**,** 124-134.
HANSEL, T. T., KROPSHOFER, H., SINGER, T., MITCHELL, J. A. & GEORGE, A. J. 2010. The safety and side effects of monoclonal antibodies. *Nature reviews Drug discovery,* 9**,** 325-338.
HARDING, H. P., ZHANG, Y. & RON, D. 1999. Protein translation and folding are coupled by an endoplasmic-reticulum-resident kinase. *Nature,* 397**,** 271-274.
HARRIS, R. C., CHUNG, E. & COFFEY, R. J. 2003. -EGF receptor ligands. *The EGF Receptor Family.* Elsevier.
HARTMAN, T. R., QIAN, S., BOLINGER, C., FERNANDEZ, S., SCHOENBERG, D. R. & BORIS-LAWRIE, K. 2006. RNA helicase A is necessary for translation of selected messenger RNAs. *Nat Struct Mol Biol,* 13**,** 509-16.
HARTMANN, G., WEERATNA, R. D., BALLAS, Z. K., PAYETTE, P., BLACKWELL, S., SUPARTO, I., RASMUSSEN, W. L., WALDSCHMIDT, M., SAJUTHI, D. & PURCELL, R. H. 2000. Delineation of a CpG phosphorothioate oligodeoxynucleotide for activating primate immune responses in vitro and in vivo. *The Journal of Immunology,* 164**,** 1617-1624.
HAYASE, K. & TAPPEL, A. 1969. Microsomal esterase of rat liver. *Journal of Biological Chemistry,* 244**,** 2269-2274.
HAYASHI, S., NISHIMURA, K., FUKUCHI-SHIMOGORI, T., KASHIWAGI, K. & IGARASHI, K. 2000. Increase in cap- and IRES-dependent protein synthesis by overproduction of translation initiation factor eIF4G. *Biochemical and biophysical research communications,* 277**,** 117-123.
HE, Y., GRANDIS, J. R. & HUANG, L. 2010. Inhibition of human squamous cell carcinoma growth in vivo by epidermal growth factor receptor antisense RNA transcribed from a Pol III promoter. Google Patents.
HEERMA VAN VOSS, M. R., VAN KEMPEN, P. M., NOORLAG, R., VAN DIEST, P. J., WILLEMS, S. M. & RAMAN, V. 2015. DDX3 has divergent roles in head and neck squamous cell carcinomas in smoking versus non-smoking patients. *Oral Dis,* 21**,** 270-1.
HEITZ, F., MORRIS, M. C. & DIVITA, G. 2009. Twenty years of cell-penetrating peptides: from molecular mechanisms to therapeutics. *British journal of pharmacology,* 157**,** 195-206.
HELLEN, C. U. & SARNOW, P. 2001. Internal ribosome entry sites in eukaryotic mRNA molecules. *Genes & development,* 15**,** 1593-1612.
HENRY, S., STECKER, K., BROOKS, D., MONTEITH, D., CONKLIN, B. & BENNETT, C. F. 2000. Chemically modified

oligonucleotides exhibit decreased immune stimulation in mice. *Journal of Pharmacology and Experimental Therapeutics,* 292**,** 468-479.

HENRY, S. P., SEGUIN, R., CAVAGNARO, J., BERMAN, C., TEPPER, J. & KORNBRUST, D. 2016. Considerations for the characterization and interpretation of results related to alternative complement activation in monkeys associated with oligonucleotide-based therapeutics. *nucleic acid therapeutics,* 26**,** 210-215.

HERBERT, B.-S., GELLERT, G. C., HOCHREITER, A., PONGRACZ, K., WRIGHT, W. E., ZIELINSKA, D., CHIN, A. C., HARLEY, C. B., SHAY, J. W. & GRYAZNOV, S. M. 2005. Lipid modification of GRN163, an N3'→ P5' thio-phosphoramidate oligonucleotide, enhances the potency of telomerase inhibition. *Oncogene,* 24**,** 5262.

HERDEWIJN, P. 2000. Heterocyclic modifications of oligonucleotides and antisense technology. *Antisense and Nucleic Acid Drug Development,* 10**,** 297-310.

HESSLER, G. & BARINGHAUS, K.-H. 2018. Artificial intelligence in drug design. *Molecules,* 23**,** 2520.

HILLIKER, A., GAO, Z., JANKOWSKY, E. & PARKER, R. 2011. The DEAD-box protein Ded1 modulates translation by the formation and resolution of an eIF4F-mRNA complex. *Molecular cell,* 43**,** 962-972.

HINNEBUSCH, A. G. 2000. Mechanism and regulation of initiator methionyl-tRNA binding to ribosomes. *COLD SPRING HARBOR MONOGRAPH SERIES,* 39**,** 185-244.

HINNEBUSCH, A. G. 2014. The scanning mechanism of eukaryotic translation initiation. *Annual review of biochemistry,* 83**,** 779-812.

HINNEBUSCH, A. G., IVANOV, I. P. & SONENBERG, N. 2016. Translational control by 5'-untranslated regions of eukaryotic mRNAs. *Science,* 352**,** 1413-1416.

HOLCIK, M., LEFEBVRE, C., YEH, C., CHOW, T. & KORNELUK, R. G. 1999. A new internal-ribosome-entry-site motif potentiates XIAP-mediated cytoprotection. *Nature cell biology,* 1**,** 190.

HOLCIK, M. & SONENBERG, N. 2005. Translational control in stress and apoptosis. *Nature reviews Molecular cell biology,* 6**,** 318-327.

HOLCIK, M., SONENBERG, N. & KORNELUK, R. G. 2000. Internal ribosome initiation of translation and the control of cell death. *Trends in Genetics,* 16**,** 469-473.

HOOGSTEEN, I. J., MARRES, H. A., VAN DEN HOOGEN, F. J., RIJKEN, P. F., LOK, J., BUSSINK, J. & KAANDERS, J. H. 2012. Expression of EGFR under tumor hypoxia: identification of a subpopulation of tumor cells responsible

for aggressiveness and treatment resistance. *International Journal of Radiation Oncology* Biology* Physics,* 84**,** 807-814.

HOWARD, K. A. 2009. Delivery of RNA interference therapeutics using polycation-based nanoparticles. *Advanced drug delivery reviews,* 61**,** 710-720.

HSU, S.-C., MILLER, S. A., WANG, Y. & HUNG, M.-C. 2009. Nuclear EGFR is required for cisplatin resistance and DNA repair. *American journal of translational research,* 1**,** 249.

HUANG, C., TAN, W., ZHENG, J., ZHU, C., HUO, J. & YANG, R. 2019. Azoreductase-Responsive Metal–Organic Framework-Based Nanodrug for Enhanced Cancer Therapy via Breaking Hypoxia-induced Chemoresistance. *ACS applied materials & interfaces,* 11**,** 25740-25749.

HUANG, J. S., CHAO, C. C., SU, T. L., YEH, S. H., CHEN, D. S., CHEN, C. T., CHEN, P. J. & JOU, Y. S. 2004. Diverse cellular transformation capability of overexpressed genes in human hepatocellular carcinoma. *Biochem Biophys Res Commun,* 315**,** 950-8.

HUANG, W.-C., CHEN, Y.-J., LI, L.-Y., WEI, Y.-L., HSU, S.-C., TSAI, S.-L., CHIU, P.-C., HUANG, W.-P., WANG, Y.-N. & CHEN, C.-H. 2011. Nuclear translocation of epidermal growth factor receptor by Akt-dependent phosphorylation enhances breast cancer-resistant protein expression in gefitinib-resistant cells. *Journal of Biological Chemistry,* 286**,** 20558-20568.

HUNTER, A. M., LACASSE, E. C. & KORNELUK, R. G. 2007. The inhibitors of apoptosis (IAPs) as cancer targets. *Apoptosis,* 12**,** 1543-1568.

IMATAKA, H. & SONENBERG, N. 1997. Human eukaryotic translation initiation factor 4G (eIF4G) possesses two separate and independent binding sites for eIF4A. *Mol Cell Biol,* 17**,** 6940-7.

INGOLIA, N. T., LAREAU, L. F. & WEISSMAN, J. S. 2011. Ribosome profiling of mouse embryonic stem cells reveals the complexity and dynamics of mammalian proteomes. *Cell,* 147**,** 789-802.

IVANOV, I. P., ATKINS, J. F. & MICHAEL, A. J. 2010. A profusion of upstream open reading frame mechanisms in polyamine-responsive translational regulation. *Nucleic acids research,* 38**,** 353-359.

JACKSON, R. J. 2013. The current status of vertebrate cellular mRNA IRESs. *Cold Spring Harbor perspectives in biology,* 5**,** a011569.

JACKSON, R. J., HELLEN, C. U. T. & PESTOVA, T. V. 2010. The mechanism of eukaryotic translation initiation and

principles of its regulation. *Nature reviews Molecular cell biology,* 11**,** 113-27.

JANSSEN, H. L., REESINK, H. W., LAWITZ, E. J., ZEUZEM, S., RODRIGUEZ-TORRES, M., PATEL, K., VAN DER MEER, A. J., PATICK, A. K., CHEN, A. & ZHOU, Y. 2013. Treatment of HCV infection by targeting microRNA. *New England Journal of Medicine,* 368**,** 1685-1694.

JEONG, J. H., KIM, S. W. & PARK, T. G. 2007. Molecular design of functional polymers for gene therapy. *Progress in Polymer Science,* 32**,** 1239-1274.

JEFFREY, I.W., Bushell, M., Tilleray, V.J., Morley, S. and Clemens, M.J., 2002. Inhibition of protein synthesis in apoptosis: differential requirements by the tumor necrosis factor α family and a DNA-damaging agent for caspases and the double-stranded RNA-dependent protein kinase. Cancer research, 62(8), pp.2272-2280.

JIAN, Z., YI, Z., HUOYU, Z., FENG, L., YUQIONG, Y. & SHIXI, L. 2010. Inhibition of the EGFR with nanoparticles encapsulating antisense oligonucleotides of the EGFR enhances radiosensitivity in SCCVII cells. *Medical Oncology,* 27**,** 715-721.

JOPLING, C. L., SPRIGGS, K. A., MITCHELL, S. A., STONELEY, M. & WILLIS, A. E. 2004. L-Myc protein synthesis is initiated by internal ribosome entry. *Rna,* 10**,** 287-298.

JOPLING, C. L. & WILLIS, A. E. 2001. N-myc translation is initiated via an internal ribosome entry segment that displays enhanced activity in neuronal cells. *Oncogene,* 20**,** 2664.

JUDGE, A. D., BOLA, G., LEE, A. C. & MACLACHLAN, I. 2006. Design of noninflammatory synthetic siRNA mediating potent gene silencing in vivo. *Molecular Therapy,* 13**,** 494-505.

JULIANO, R., ALAHARI, S., YOO, H., KOLE, R. & CHO, M. 1999. Antisense pharmacodynamics: critical issues in the transport and delivery of antisense oligonucleotides. *Pharmaceutical research,* 16**,** 494-502.

JULIANO, R. & CARVER, K. 2015. Cellular uptake and intracellular trafficking of oligonucleotides. *Advanced drug delivery reviews,* 87**,** 35-45.

JUWEID, M., NEUMANN, R., PAIK, C., PEREZ-BACETE, M. J., SATO, J., VAN OSDOL, W. & WEINSTEIN, J. N. 1992. Micropharmacology of monoclonal antibodies in solid tumors: direct experimental evidence for a binding site barrier. *Cancer research,* 52**,** 5144-5153.

KABANOV, A. V. 1999. Taking polycation gene delivery systems from in vitro to in vivo. *Pharmaceutical science & technology today,* 2**,** 365-372.

KAGIYAMA, S., QIAN, K., KAGIYAMA, T. & PHILLIPS, M. I. 2003. Antisense to epidermal growth factor receptor prevents the development of left ventricular hypertrophy. *Hypertension,* 41**,** 824-829.

KANDOTH, C., MCLELLAN, M. D., VANDIN, F., YE, K., NIU, B., LU, C., XIE, M., ZHANG, Q., MCMICHAEL, J. F., WYCZALKOWSKI, M. A., LEISERSON, M. D. M., MILLER, C. A., WELCH, J. S., WALTER, M. J., WENDL, M. C., LEY, T. J., WILSON, R. K., RAPHAEL, B. J. & DING, L. 2013. Mutational landscape and significance across 12 major cancer types. *Nature,* 502**,** 333-339.

KANG, C., ZHANG, Z., JIA, Z., WANG, G., QIU, M., ZHOU, H., YU, S., CHANG, J., JIANG, H. & PU, P. 2006. Suppression of EGFR expression by antisense or small interference RNA inhibits U251 glioma cell growth in vitro and in vivo. *Cancer gene therapy,* 13**,** 530-538.

KASSAM, F., ENRIGHT, K., DENT, R., DRANITSARIS, G., MYERS, J., FLYNN, C., FRALICK, M., KUMAR, R. & CLEMONS, M. 2009. Survival outcomes for patients with metastatic triple-negative breast cancer: implications for clinical practice and trial design. *Clinical breast cancer,* 9**,** 29-33.

KAUFMAN, R. J. 1999. Stress signaling from the lumen of the endoplasmic reticulum: coordination of gene transcriptional and translational controls. *Genes & development,* 13**,** 1211-1233.

KERSTING, C., TIDOW, N., SCHMIDT, H., LIEDTKE, C., NEUMANN, J., BOECKER, W., VAN DIEST, P. J., BRANDT, B. & BUERGER, H. 2004. Gene dosage PCR and fluorescence in situ hybridization reveal low frequency of egfr amplifications despite protein overexpression in invasive breast carcinoma. *Laboratory investigation,* 84**,** 582.

KHVOROVA, A. & WATTS, J. K. 2017. The chemical evolution of oligonucleotide therapies of clinical utility. *Nature biotechnology,* 35**,** 238.

KIEFT, J. S., ZHOU, K., JUBIN, R., MURRAY, M. G., LAU, J. Y. & DOUDNA, J. A. 1999. The hepatitis C virus internal ribosome entry site adopts an ion-dependent tertiary fold. *Journal of molecular biology,* 292**,** 513-529.

KIM, J., KANG, Y., TZENG, S. Y. & GREEN, J. J. 2016. Synthesis and application of poly (ethylene glycol)-co-poly (β-amino ester) copolymers for small cell lung cancer gene therapy. *Acta biomaterialia,* 41**,** 293-301.

KIM, J. H., PARK, S. M., PARK, J. H., KEUM, S. J. & JANG, S. K. 2011. eIF2A mediates translation of hepatitis C viral

mRNA under stress conditions. *The EMBO journal,* 30**,** 2454-2464.

KIMBALL, S. R. 1999. Eukaryotic initiation factor eIF2. *The international journal of biochemistry & cell biology,* 31**,** 25-29.

KINALI, M., ARECHAVALA-GOMEZA, V., FENG, L., CIRAK, S., HUNT, D., ADKIN, C., GUGLIERI, M., ASHTON, E., ABBS, S. & NIHOYANNOPOULOS, P. 2009. Local restoration of dystrophin expression with the morpholino oligomer AVI-4658 in Duchenne muscular dystrophy: a single-blind, placebo-controlled, dose-escalation, proof-of-concept study. *The Lancet Neurology,* 8**,** 918-928.

KIYOSE, K., HANAOKA, K., OUSHIKI, D., NAKAMURA, T., KAJIMURA, M., SUEMATSU, M., NISHIMATSU, H., YAMANE, T., TERAI, T. & HIRATA, Y. 2010. Hypoxia-sensitive fluorescent probes for in vivo real-time fluorescence imaging of acute ischemia. *Journal of the American Chemical Society,* 132**,** 15846-15848.

KOFF, J. L., SHAO, M. X., UEKI, I. F. & NADEL, J. A. 2008. Multiple TLRs activate EGFR via a signaling cascade to produce innate immune responses in airway epithelium. *American Journal of Physiology-Lung Cellular and Molecular Physiology,* 294**,** L1068-L1075.

KOLLER, E., VINCENT, T. M., CHAPPELL, A., DE, S., MANOHARAN, M. & BENNETT, C. F. 2011. Mechanisms of single-stranded phosphorothioate modified antisense oligonucleotide accumulation in hepatocytes. *Nucleic acids research,* 39**,** 4795-4807.

KOMAR, A. A. & HATZOGLOU, M. 2011. Cellular IRES-mediated translation: the war of ITAFs in pathophysiological states. *Cell cycle,* 10**,** 229-240.

KONDASKAR, A., KONDASKAR, S., FISHBEIN, J. C., CARTER-COOPER, B. A., LAPIDUS, R. G., SADOWSKA, M., EDELMAN, M. J. & HOSMANE, R. S. 2013. Structure-based drug design and potent anti-cancer activity of tricyclic 5: 7: 5-fused diimidazo [4, 5-d: 4′, 5′-f][1, 3] diazepines. *Bioorganic & medicinal chemistry,* 21**,** 618-631.

KOYNOVA, R. & TENCHOV, B. 2009. Cationic phospholipids: structure–transfection activity relationships. *Soft Matter,* 5**,** 3187-3200.

KOZAK, M. 1987. Effects of intercistronic length on the efficiency of reinitiation by eucaryotic ribosomes. *Molecular and cellular biology,* 7**,** 3438-3445.

KOZAK, M. 1989. Circumstances and mechanisms of inhibition of translation by secondary structure in eucaryotic mRNAs. *Mol Cell Biol,* 9**,** 5134-42.

KOZAK, M. 1991. Structural features in eukaryotic mRNAs that modulate the initiation of translation. *J Biol Chem,* 266**,** 19867-70.

KOZAK, M. 2001. Constraints on reinitiation of translation in mammals. *Nucleic acids research,* 29**,** 5226-5232.

KOZAK, M. 2002. Pushing the limits of the scanning mechanism for initiation of translation. *Gene,* 299**,** 1-34.

KOZAK, M. 2005. A second look at cellular mRNA sequences said to function as internal ribosome entry sites. *Nucleic acids research,* 33**,** 6593-6602.

KOZIELSKI, K. L., RUIZ-VALLS, A., TZENG, S. Y., GUERRERO-CÁZARES, H., RUI, Y., LI, Y., VAUGHAN, H. J., GIONET-GONZALES, M., VANTUCCI, C. & KIM, J. 2019. Cancer-selective nanoparticles for combinatorial siRNA delivery to primary human GBM in vitro and in vivo. *Biomaterials,* 209**,** 79-87.

KOZIELSKI, K. L., TZENG, S. Y. & GREEN, J. J. 2013. A bioreducible linear poly (β-amino ester) for siRNA delivery. *Chemical Communications,* 49**,** 5319-5321.

KOZIELSKI, K. L., TZENG, S. Y., HURTADO DE MENDOZA, B. A. & GREEN, J. J. 2014. Bioreducible cationic polymer-based nanoparticles for efficient and environmentally triggered cytoplasmic siRNA delivery to primary human brain cancer cells. *ACS nano,* 8**,** 3232-3241.

KRIEG, A. M., WU, T., WEERATNA, R., EFLER, S. M., LOVE-HOMAN, L., YANG, L., YI, A.-K., SHORT, D. & DAVIS, H. L. 1998. Sequence motifs in adenoviral DNA block immune activation by stimulatory CpG motifs. *Proceedings of the National Academy of Sciences,* 95**,** 12631-12636.

KRIEG, A. M., YI, A.-K., MATSON, S., WALDSCHMIDT, T. J., BISHOP, G. A., TEASDALE, R., KORETZKY, G. A. & KLINMAN, D. M. 1995. CpG motifs in bacterial DNA trigger direct B-cell activation. *Nature,* 374**,** 546.

KRIEGS, M., KASTEN-PISULA, U., RIECKMANN, T., HOLST, K., SAKER, J., DAHM-DAPHI, J. & DIKOMEY, E. 2010. The epidermal growth factor receptor modulates DNA double-strand break repair by regulating non-homologous end-joining. *DNA repair,* 9**,** 889-897.

KU, Y. C., LAI, M. H., LO, C. C., CHENG, Y. C., QIU, J. T., TARN, W. Y. & LAI, M. C. 2019. DDX3 Participates in Translational Control of Inflammation Induced by Infections and Injuries. *Mol Cell Biol,* 39.

KULKARNI, J. A., CULLIS, P. R. & VAN DER MEEL, R. 2018. Lipid nanoparticles enabling gene therapies: from concepts to clinical utility. *Nucleic acid therapeutics,* 28**,** 146-157.

KULKARNI, P., HALDAR, M. K., YOU, S., CHOI, Y. & MALLIK, S. 2016. Hypoxia-responsive polymersomes for drug delivery to hypoxic pancreatic cancer cells. *Biomacromolecules,* 17**,** 2507-2513.

KUO, L. J. & YANG, L.-X. 2008. γ-H2AX-a novel biomarker for DNA double-strand breaks. *In vivo,* 22**,** 305-309.

LAI, F. P., SZCZODRAK, M., BLOCK, J., FAIX, J., BREITSPRECHER, D., MANNHERZ, H. G., STRADAL, T. E., DUNN, G. A., SMALL, J. V. & ROTTNER, K. 2008. Arp2/3 complex interactions and actin network turnover in lamellipodia. *The EMBO journal,* 27**,** 982-992.

LAI, M. C., CHANG, W. C., SHIEH, S. Y. & TARN, W. Y. 2010. DDX3 regulates cell growth through translational control of cyclin E1. *Mol Cell Biol,* 30**,** 5444-53.

LAI, M. C., SUN, H. S., WANG, S. W. & TARN, W. Y. 2016. DDX3 functions in antiviral innate immunity through translational control of PACT. *Febs j,* 283**,** 88-101.

LARAIA, L., ROBKE, L. & WALDMANN, H. 2018. Bioactive compound collections: from design to target identification. *Chem,* 4**,** 705-730.

LE QUESNE, J. P., STONELEY, M., FRASER, G. A. & WILLIS, A. E. 2001. Derivation of a structural model for the c-myc IRES1. *Journal of molecular biology,* 310**,** 111-126.

LE, S.-Y. & MAIZEL JR, J. V. 1997. A common RNA structural motif involved in the internal initiation of translation of cellular mRNAs. *Nucleic acids research,* 25**,** 362-369.

LECLERC, G. M., F. R. Boockfor, W. J. Faught, and L. S. Frawley. 2000. "Development of a Destabilized Firefly Luciferase Enzyme for Measurement of Gene Expression." BioTechniques 29(3):590–601. doi: 10.2144/00293rr02.

LEE, A. S., KRANZUSCH, P. J. & CATE, J. H. 2015. eIF3 targets cell-proliferation messenger RNAs for translational activation or repression. *Nature,* 522**,** 111.

LEE, C. S., DIAS, A. P., JEDRYCHOWSKI, M., PATEL, A. H., HSU, J. L. & REED, R. 2008. Human DDX3 functions in translation and interacts with the translation initiation factor eIF3. *Nucleic Acids Res,* 36**,** 4708-18.

LEE, S.-H., KOO, K. H., PARK, J.-W., KIM, H.-J., YE, S.-K., PARK, J. B., PARK, B.-K. & KIM, Y.-N. 2009. HIF-1 is induced via EGFR activation and mediates resistance to anoikis-like cell death under lipid rafts/caveolae-disrupting stress. *Carcinogenesis,* 30**,** 1997-2004.

LEMP, Nathan A., Kei Hiraoka, Noriyuki Kasahara, and Christopher R. Logg. 2012. "Cryptic Transcripts from a Ubiquitous Plasmid Origin of Replication Confound Tests for Cis-Regulatory Function." Nucleic Acids Research 40(15):7280–90. doi: 10.1093/nar/gks451.

LEMMON, M. A., SCHLESSINGER, J. & FERGUSON, K. M. 2014. The EGFR family: not so prototypical receptor tyrosine kinases. *Cold Spring Harbor perspectives in biology,* 6**,** a020768.

LEPPEK, K., DAS, R. & BARNA, M. 2017. Functional 5′ UTR mRNA structures in eukaryotic translation regulation and how to find them. *Nature Reviews Molecular Cell Biology*.

LEVIN, A. A. 2019. Treating disease at the RNA level with oligonucleotides. *New England Journal of Medicine,* 380**,** 57-70.

LI, Q., ZHANG, P., ZHANG, C., WANG, Y., WAN, R., YANG, Y., GUO, X., HUO, R., LIN, M., ZHOU, Z. & SHA, J. 2014. DDX3X regulates cell survival and cell cycle during mouse early embryonic development. *J Biomed Res,* 28**,** 282-91.

LI, S., LIU, C., GUO, J., MARCONDES, A., DEEG, J., LI, X. & GUAN, F. 2016. Iron overload induced by ferric ammonium citrate triggers reactive oxygen species-mediated apoptosis via both extrinsic and intrinsic pathways in human hepatic cells. *Human & experimental toxicology,* 35**,** 598-607.

LI, T., ZENG, Z., WANG, L., QIU, S., ZHOU, J., ZHI, X., YU, H. & TANG, Z. 2011. Radiation enhances long-term metastasis potential of residual hepatocellular carcinoma in nude mice through TMPRSS4-induced epithelial–mesenchymal transition. *Cancer gene therapy,* 18**,** 617-626.

LIANG, Xue Hai, Hong Sun, Joshua G. Nichols, and Stanley T. Crooke. 2017. "RNase H1-Dependent Antisense Oligonucleotides Are Robustly Active in Directing RNA Cleavage in Both the Cytoplasm and the Nucleus." Molecular Therapy 25(9):2075–92. doi: 10.1016/j.ymthe.2017.06.002.

LIANG, X.-H., SHEN, W., SUN, H., MIGAWA, M. T., VICKERS, T. A. & CROOKE, S. T. 2016. Translation efficiency of mRNAs is increased by antisense oligonucleotides targeting upstream open reading frames. *Nature biotechnology,* 34**,** 875.

LIANG, X.-H., SHEN, W., SUN, H., PRAKASH, T. P. & CROOKE, S. T. 2014. TCP1 complex proteins interact with phosphorothioate oligonucleotides and can co-localize in oligonucleotide-induced nuclear bodies in mammalian cells. *Nucleic acids research,* 42**,** 7819-7832.

LIBERMAN, N., GANDIN, V., SVITKIN, Y. V., DAVID, M., VIRGILI, G., JARAMILLO, M., HOLCIK, M., NAGAR, B., KIMCHI, A. & SONENBERG, N. 2015. DAP5 associates with eIF2β and eIF4AI to promote Internal Ribosome

Entry Site driven translation. *Nucleic acids research,* 43**,** 3764-3775.
LICCARDI, G., HARTLEY, J. A. & HOCHHAUSER, D. 2011. EGFR nuclear translocation modulates DNA repair following cisplatin and ionizing radiation treatment. *Cancer research,* 71**,** 1103-1114.
LIM, S. M., SYN, N. L., CHO, B. C. & SOO, R. A. 2018. Acquired resistance to EGFR targeted therapy in non-small cell lung cancer: mechanisms and therapeutic strategies. *Cancer treatment reviews,* 65**,** 1-10.
LIMA, W., WU, H. & CROOKE, S. T. 2007. The RNase H mechanism. *Antisense Drug Technology Principles, Strategies, and Applications,* 2**,** 47-74.
LIMA, W. F., MURRAY, H. M., DAMLE, S. S., HART, C. E., HUNG, G., DE HOYOS, C. L., LIANG, X.-H. & CROOKE, S. T. 2016. Viable RNaseH1 knockout mice show RNaseH1 is essential for R loop processing, mitochondrial and liver function. *Nucleic acids research,* 44**,** 5299-5312.
LINDER, P. & JANKOWSKY, E. 2011. From unwinding to clamping—the DEAD box RNA helicase family. *Nature reviews Molecular cell biology,* 12**,** 505.
LING, Y.-H., LI, T., PEREZ-SOLER, R. & HAIGENTZ, M. 2009. Activation of ER stress and inhibition of EGFR N-glycosylation by tunicamycin enhances susceptibility of human non-small cell lung cancer cells to erlotinib. *Cancer chemotherapy and pharmacology,* 64**,** 539-548.
LIU, M., XIE, S. & ZHOU, J. 2017. Use of animal models for the imaging and quantification of angiogenesis. *Experimental animals***,** 17-0054.
LIU, N., ZOU, Z., LIU, J., ZHU, C., ZHENG, J. & YANG, R. 2019. A fluorescent nanoprobe based on azoreductase-responsive metal–organic frameworks for imaging VEGF mRNA under hypoxic conditions. *Analyst,* 144**,** 6254-6261.
LIU, Z., ZHANG, Z., ZHOU, C. & JIAO, Y. 2010. Hydrophobic modifications of cationic polymers for gene delivery. *Progress in Polymer Science,* 35**,** 1144-1162.
LO, H.-W., HSU, S.-C., ALI-SEYED, M., GUNDUZ, M., XIA, W., WEI, Y., BARTHOLOMEUSZ, G., SHIH, J.-Y. & HUNG, M.-C. 2005. Nuclear interaction of EGFR and STAT3 in the activation of the iNOS/NO pathway. *Cancer cell,* 7**,** 575-589.
LOPEZ-BERTONI, H., KOZIELSKI, K. L., RUI, Y., LAL, B., VAUGHAN, H., WILSON, D. R., MIHELSON, N., EBERHART, C. G., LATERRA, J. & GREEN, J. J. 2018. Bioreducible polymeric nanoparticles containing multiplexed cancer stem cell regulating miRNAs inhibit

glioblastoma growth and prolong survival. *Nano letters,* 18**,** 4086-4094.
LORD, C. J. & ASHWORTH, A. 2012. The DNA damage response and cancer therapy. *Nature,* 481**,** 287.
LORENZ, P., BAKER, B. F., BENNETT, C. F. & SPECTOR, D. L. 1998. Phosphorothioate antisense oligonucleotides induce the formation of nuclear bodies. *Molecular biology of the cell,* 9**,** 1007-1023.
LOVE, D., KIM, K., DOMAILLE, D. W., WILLIAMS, O., STANSBURY, J., MUSGRAVE, C. & BOWMAN, C. 2019. Catalyst-free, aza-Michael polymerization of hydrazides: polymerizability, kinetics, and mechanistic origin of an α-effect. *Polymer chemistry,* 10**,** 5790-5804.
LOWE, S. W., CEPERO, E. & EVAN, G. 2004. Intrinsic tumour suppression. *Nature,* 432**,** 307-315.
LUO, D. & SALTZMAN, W. M. 2000. Synthetic DNA delivery systems. *Nature biotechnology,* 18**,** 33-37.
LUUKKONEN, B., TAN, W. & SCHWARTZ, S. 1995. Efficiency of reinitiation of translation on human immunodeficiency virus type 1 mRNAs is determined by the length of the upstream open reading frame and by intercistronic distance. *Journal of virology,* 69**,** 4086-4094.
LYNCH, T. J., BELL, D. W., SORDELLA, R., GURUBHAGAVATULA, S., OKIMOTO, R. A., BRANNIGAN, B. W., HARRIS, P. L., HASERLAT, S. M., SUPKO, J. G. & HALUSKA, F. G. 2004. Activating mutations in the epidermal growth factor receptor underlying responsiveness of non–small-cell lung cancer to gefitinib. *New England Journal of Medicine,* 350**,** 2129-2139.
LYNN, D. M., ANDERSON, D. G., PUTNAM, D. & LANGER, R. 2001. Accelerated discovery of synthetic transfection vectors: parallel synthesis and screening of a degradable polymer library. *Journal of the American Chemical Society,* 123**,** 8155-8156.
LYNN, D. M. & LANGER, R. 2000. Degradable poly (β-amino esters): synthesis, characterization, and self-assembly with plasmid DNA. *Journal of the American Chemical Society,* 122**,** 10761-10768.
LYTTON, J., WESTLIN, M. & HANLEY, M. R. 1991. Thapsigargin inhibits the sarcoplasmic or endoplasmic reticulum Ca-ATPase family of calcium pumps. *Journal of Biological Chemistry,* 266**,** 17067-17071.
MAEDA, H. 2015. Toward a full understanding of the EPR effect in primary and metastatic tumors as well as issues related to its heterogeneity. *Advanced drug delivery reviews,* 91**,** 3-6.

MANFREDI, A., RANUCCI, E., SUARDI, M. & FERRUTI, P. 2007. Polymerization kinetics of poly (amidoamine) s in different solvents. *Journal of bioactive and compatible polymers,* 22**,** 219-231.

MARTIN VACA, B. & BOURISSOU, D. 2015. O-carboxyanhydrides: useful tools for the preparation of well-defined functionalized polyesters. ACS Publications.

MARTINAND-MARI, C., LEBLEU, B. & ROBBINS, I. 2003. Oligonucleotide-based strategies to inhibit human hepatitis C virus. *Oligonucleotides,* 13**,** 539-548.

MASSARWEH, S., OSBORNE, C. K., JIANG, S., WAKELING, A. E., RIMAWI, M., MOHSIN, S. K., HILSENBECK, S. & SCHIFF, R. 2006. Mechanisms of tumor regression and resistance to estrogen deprivation and fulvestrant in a model of estrogen receptor–positive, HER-2/neu-positive breast cancer. *Cancer research,* 66**,** 8266-8273.

MATSUMURA, Y. & MAEDA, H. 1986. A new concept for macromolecular therapeutics in cancer chemotherapy: mechanism of tumoritropic accumulation of proteins and the antitumor agent smancs. *Cancer research,* 46**,** 6387-6392.

MATTOON, D. R., LAMOTHE, B., LAX, I. & SCHLESSINGER, J. 2004. The docking protein Gab1 is the primary mediator of EGF-stimulated activation of the PI-3K/Akt cell survival pathway. *BMC biology,* 2**,** 24.

MAURO, V. P. & EDELMAN, G. M. 1997. rRNA-like sequences occur in diverse primary transcripts: implications for the control of gene expression. *Proceedings of the National Academy of Sciences,* 94**,** 422-427.

MCKEOWN, S. R. 2014. "Defining Normoxia, Physoxia and Hypoxia in Tumours - Implications for Treatment Response." British Journal of Radiology 87(1035).

MCMAHON, B. M., MAYS, D., LIPSKY, J., STEWART, J. A., FAUQ, A. & RICHELSON, E. 2002. Pharmacokinetics and tissue distribution of a peptide nucleic acid after intravenous administration. *Antisense and Nucleic Acid Drug Development,* 12**,** 65-70.

MEISTER, A. 1988. Glutathione metabolism and its selective modification. *Journal of biological chemistry,* 263**,** 17205-17208.

MENDELSOHN, J. & BASELGA, J. 2003. Status of epidermal growth factor receptor antagonists in the biology and treatment of cancer. *Journal of clinical oncology,* 21**,** 2787-2799.

MESEURE, D., VACHER, S., DRAK ALSIBAI, K., TRASSARD, M., SUSINI, A., LE RAY, C., LEREBOURS, F., LE SCODAN, R., SPYRATOS, F. & MARC GUINEBRETIERE, J. 2012. Profiling

of EGFR mRNA and protein expression in 471 breast cancers compared with 10 normal tissues: a candidate biomarker to predict EGFR inhibitor effectiveness. *International journal of cancer,* 131**,** 1009-1010.

MEYER, K. D., PATIL, D. P., ZHOU, J., ZINOVIEV, A., SKABKIN, M. A., ELEMENTO, O., PESTOVA, T. V., QIAN, S.-B. & JAFFREY, S. R. 2015. 5′ UTR m6A promotes cap-independent translation. *Cell,* 163**,** 999-1010.

MIAO, X., YANG, Z. L., XIONG, L., ZOU, Q., YUAN, Y., LI, J., LIANG, L., CHEN, M. & CHEN, S. 2013. Nectin-2 and DDX3 are biomarkers for metastasis and poor prognosis of squamous cell/adenosquamous carcinomas and adenocarcinoma of gallbladder. *Int J Clin Exp Pathol,* 6**,** 179-90.

MISALE, S., DI NICOLANTONIO, F., SARTORE-BIANCHI, A., SIENA, S. & BARDELLI, A. 2014. Resistance to anti-EGFR therapy in colorectal cancer: from heterogeneity to convergent evolution. *Cancer discovery,* 4**,** 1269-1280.

MITCHELL, S. A., SPRIGGS, K. A., BUSHELL, M., EVANS, J. R., STONELEY, M., LE QUESNE, J. P. C., SPRIGGS, R. V. & WILLIS, A. E. 2005. Identification of a motif that mediates polypyrimidine tract-binding protein-dependent internal ribosome entry. *Genes & development,* 19**,** 1556-1571.

MITCHELL, S. A., SPRIGGS, K. A., COLDWELL, M. J., JACKSON, R. J. & WILLIS, A. E. 2003. The Apaf-1 internal ribosome entry segment attains the correct structural conformation for function via interactions with PTB and unr. *Molecular cell,* 11**,** 757-771.

MOK, T. S., WU, Y.-L., THONGPRASERT, S., YANG, C.-H., CHU, D.-T., SAIJO, N., SUNPAWERAVONG, P., HAN, B., MARGONO, B. & ICHINOSE, Y. 2009. Gefitinib or carboplatin–paclitaxel in pulmonary adenocarcinoma. *New England Journal of Medicine,* 361**,** 947-957.

MONIA, B. P., LESNIK, E., GONZALEZ, C., LIMA, W., MCGEE, D., GUINOSSO, C., KAWASAKI, A., COOK, P. D. & FREIER, S. 1993. Evaluation of 2'-modified oligonucleotides containing 2'-deoxy gaps as antisense inhibitors of gene expression. *Journal of Biological Chemistry,* 268**,** 14514-14522.

MOORE, T. L., RODRIGUEZ-LORENZO, L., HIRSCH, V., BALOG, S., URBAN, D., JUD, C., ROTHEN-RUTISHAUSER, B., LATTUADA, M. & PETRI-FINK, A. 2015. Nanoparticle colloidal stability in cell culture media and impact on cellular interactions. *Chemical Society Reviews,* 44**,** 6287-6305.

MORIMOTO, R. I., KROEGER, P. & COTTO, J. 1996. The transcriptional regulation of heat shock genes: a plethora

of heat shock factors and regulatory conditions. *Stress-inducible cellular responses.* Springer.

MORSE, L. & CALARESE, P. EGFR-targeted therapy and related skin toxicity. Seminars in oncology nursing, 2006. Elsevier, 152-162.

MOTEKI, S. & PRICE, D. 2002. Functional coupling of capping and transcription of mRNA. *Molecular cell,* 10**,** 599-609.

MURANEN, T., SELFORS, L. M., WORSTER, D. T., IWANICKI, M. P., SONG, L., MORALES, F. C., GAO, S., MILLS, G. B. & BRUGGE, J. S. 2012. Inhibition of PI3K/mTOR leads to adaptive resistance in matrix-attached cancer cells. *Cancer cell,* 21**,** 227-239.

NAJAR, A. G., PASHAEI-ASL, R., OMIDI, Y., FARAJNIA, S. & NOURAZARIAN, A. R. 2013. EGFR antisense oligonucleotides encapsulated with nanoparticles decrease EGFR, MAPK1 and STAT5 expression in a human colon cancer cell line. *Asian Pacific Journal of Cancer Prevention,* 14**,** 495-498.

NANDURI, Sambasivarao, Fahima Rahman, Bryan R. G. Williams, and Jun Qin. 2000. "A Dynamically Tuned Double-Stranded RNA Binding Mechanism for the Activation of Antiviral Kinase PKR." EMBO Journal 19(20):5567–74. doi: 10.1093/emboj/19.20.5567.

NEAMNARK, A., SUWANTONG, O., KC, R. B., HSU, C. Y., SUPAPHOL, P. & ULUDAG, H. 2009. Aliphatic lipid substitution on 2 kDa polyethylenimine improves plasmid delivery and transgene expression. *Molecular Pharmaceutics,* 6**,** 1798-1815.

NEL, A. E., MÄDLER, L., VELEGOL, D., XIA, T., HOEK, E. M., SOMASUNDARAN, P., KLAESSIG, F., CASTRANOVA, V. & THOMPSON, M. 2009. Understanding biophysicochemical interactions at the nano–bio interface. *Nature materials,* 8**,** 543-557.

NICKEL, G. C., BARNHOLTZ-SLOAN, J., GOULD, M. P., MCMAHON, S., COHEN, A., ADAMS, M. D., GUDA, K., COHEN, M., SLOAN, A. E. & LAFRAMBOISE, T. 2012. Characterizing mutational heterogeneity in a glioblastoma patient with double recurrence. *PloS one,* 7**,** e35262.

NIJKAMP, M. M., SPAN, P. N., BUSSINK, J. & KAANDERS, J. H. 2013. Interaction of EGFR with the tumour microenvironment: implications for radiation treatment. *Radiotherapy and Oncology,* 108**,** 17-23.

NISHINA, K., PIAO, W., YOSHIDA-TANAKA, K., SUJINO, Y., NISHINA, T., YAMAMOTO, T., NITTA, K., YOSHIOKA, K., KUWAHARA, H. & YASUHARA, H. 2015. DNA/RNA heteroduplex oligonucleotide for highly efficient gene silencing. *Nature communications,* 6**,** 7969.

NORMANNO, N., DE LUCA, A., BIANCO, C., STRIZZI, L., MANCINO, M., MAIELLO, M. R., CAROTENUTO, A., DE FEO, G., CAPONIGRO, F. & SALOMON, D. S. 2006. Epidermal growth factor receptor (EGFR) signaling in cancer. *Gene,* 366**,** 2-16.

NOURAZARIAN, A. R., NAJAR, A. G., FARAJNIA, S., KHOSROUSHAHI, A. Y., PASHAEI-ASL, R. & OMIDI, Y. 2012. Combined EGFR and c-Src antisense oligodeoxynucleotides encapsulated with PAMAM Denderimers inhibit HT-29 colon cancer cell proliferation. *Asian Pacific Journal of Cancer Prevention,* 13**,** 4751-4756.

O'BRIEN, M. E., WIGLER, N., INBAR, M., ROSSO, R., GRISCHKE, E., SANTORO, A., CATANE, R., KIEBACK, D., TOMCZAK, P. & ACKLAND, S. 2004. Reduced cardiotoxicity and comparable efficacy in a phase III trial of pegylated liposomal doxorubicin HCl (CAELYX™/Doxil®) versus conventional doxorubicin for first-line treatment of metastatic breast cancer. *Annals of oncology,* 15**,** 440-449.

ODA, K., MATSUOKA, Y., FUNAHASHI, A. & KITANO, H. 2005. A comprehensive pathway map of epidermal growth factor receptor signaling. *Molecular systems biology,* 1.

OGRIS, M., BRUNNER, S., SCHÜLLER, S., KIRCHEIS, R. & WAGNER, E. 1999. PEGylated DNA/transferrin–PEI complexes: reduced interaction with blood components, extended circulation in blood and potential for systemic gene delivery. *Gene therapy,* 6**,** 595-605.

OH, S., FLYNN, R. A., FLOOR, S. N., PURZNER, J., MARTIN, L., DO, B. T., SCHUBERT, S., VAKA, D., MORRISSY, S. & LI, Y. 2016. Medulloblastoma-associated DDX3 variant selectively alters the translational response to stress. *Oncotarget,* 7**,** 28169.

OLIVEIRA, S., FRETZ, M. M., HØGSET, A., STORM, G. & SCHIFFELERS, R. M. 2007. Photochemical internalization enhances silencing of epidermal growth factor receptor through improved endosomal escape of siRNA. *Biochimica et Biophysica Acta (BBA)-Biomembranes,* 1768**,** 1211-1217.

OSHIUMI, H., IKEDA, M., MATSUMOTO, M., WATANABE, A., TAKEUCHI, O., AKIRA, S., KATO, N., SHIMOTOHNO, K. & SEYA, T. 2010. Hepatitis C virus core protein abrogates the DDX3 function that enhances IPS-1-mediated IFN-beta induction. *PLoS One,* 5**,** e14258.

ÖZEŞ, A. R., FEOKTISTOVA, K., AVANZINO, B. C. & FRASER, C. S. 2011. Duplex unwinding and ATPase activities of the

DEAD-box helicase eIF4A are coupled by eIF4G and eIF4B. *Journal of molecular biology,* 412**,** 674-687.

PAL, H. C. & KATIYAR, S. K. 2016. Cryptolepine, a plant alkaloid, inhibits the growth of non-melanoma skin cancer cells through inhibition of topoisomerase and induction of DNA damage. *Molecules,* 21**,** 1758.

PANEK, J., KOLÁŘ, M., VOHRADSKÝ, J. & SHIVAYA VALÁŠEK, L. 2013. An evolutionary conserved pattern of 18S rRNA sequence complementarity to mRNA 5′ UTRs and its implications for eukaryotic gene translation regulation. *Nucleic acids research,* 41**,** 7625-7634.

PARKIN, N. T., COHEN, E. A., DARVEAU, A., ROSEN, C., HASELTINE, W. & SONENBERG, N. 1988. Mutational analysis of the 5' non-coding region of human immunodeficiency virus type 1: effects of secondary structure on translation. *Embo j,* 7**,** 2831-7.

PARSEGHIAN, C. M., NAPOLITANO, S., LOREE, J. M. & KOPETZ, S. 2019. Mechanisms of innate and acquired resistance to anti-EGFR therapy: a review of current knowledge with a focus on rechallenge therapies. *Clinical Cancer Research,* 25**,** 6899-6908.

PARSYAN, A., SHAHBAZIAN, D., MARTINEAU, Y., PETROULAKIS, E., ALAIN, T., LARSSON, O., MATHONNET, G., TETTWEILER, G., HELLEN, C. U., PESTOVA, T. V., SVITKIN, Y. V. & SONENBERG, N. 2009. The helicase protein DHX29 promotes translation initiation, cell proliferation, and tumorigenesis. *Proc Natl Acad Sci U S A,* 106**,** 22217-22.

PARSYAN, A., SVITKIN, Y., SHAHBAZIAN, D., GKOGKAS, C., LASKO, P., MERRICK, W. C. & SONENBERG, N. 2011. mRNA helicases: the tacticians of translational control. *Nat Rev Mol Cell Biol,* 12**,** 235-45.

PASSINI, M. A., BU, J., RICHARDS, A. M., KINNECOM, C., SARDI, S. P., STANEK, L. M., HUA, Y., RIGO, F., MATSON, J. & HUNG, G. 2011. Antisense oligonucleotides delivered to the mouse CNS ameliorate symptoms of severe spinal muscular atrophy. *Science translational medicine,* 3**,** 72ra18-72ra18.

PATEL, C. V., HANDY, I., GOLDSMITH, T. & PATEL, R. C. 2000. PACT, a stress-modulated cellular activator of interferon-induced double-stranded RNA-activated protein kinase, PKR. *J Biol Chem,* 275**,** 37993-8.

PAULIN, F., WEST, M. J., SULLIVAN, N. F., WHITNEY, R. L., LYNE, L. & WILLIS, A. E. 1996. Aberrant translational control of the c-myc gene in multiple myeloma. *Oncogene,* 13**,** 505-513.

PAULIN, F. E., CHAPPELL, S. A. & WILLIS, A. E. 1998. A single nucleotide change in the c-myc internal ribosome entry segment leads to enhanced binding of a group of protein factors. *Nucleic acids research,* 26**,** 3097-3103.

PERCHE, F., BISWAS, S., PATEL, N. R. & TORCHILIN, V. P. 2016. Hypoxia-responsive copolymer for siRNA delivery. *RNA Imaging.* Springer.

PERCHE, F., BISWAS, S., WANG, T., ZHU, L. & TORCHILIN, V. 2014. Hypoxia-Targeted siRNA Delivery. *Angewandte Chemie International Edition,* 53**,** 3362-3366.

PERKINS, N. & GILMORE, T. 2006. Good cop, bad cop: the different faces of NF-κB. *Cell Death & Differentiation,* 13**,** 759-772.

PERRAULT, S. D., WALKEY, C., JENNINGS, T., FISCHER, H. C. & CHAN, W. C. 2009. Mediating tumor targeting efficiency of nanoparticles through design. *Nano letters,* 9**,** 1909-1915.

PESOLE, G., MIGNONE, F., GISSI, C., GRILLO, G., LICCIULLI, F. & LIUNI, S. 2001. Structural and functional features of eukaryotic mRNA untranslated regions. *Gene,* 276**,** 73-81.

PESTOVA, T. V., DE BREYNE, S., PISAREV, A. V., ABAEVA, I. S. & HELLEN, C. U. 2008. eIF2-dependent and eIF2-independent modes of initiation on the CSFV IRES: a common role of domain II. *The EMBO journal,* 27**,** 1060-1072.

PESTOVA, T. V. & KOLUPAEVA, V. G. 2002. The roles of individual eukaryotic translation initiation factors in ribosomal scanning and initiation codon selection. *Genes Dev,* 16**,** 2906-22.

PIAO, W., TSUDA, S., TANAKA, Y., MAEDA, S., LIU, F., TAKAHASHI, S., KUSHIDA, Y., KOMATSU, T., UENO, T. & TERAI, T. 2013. Development of azo-based fluorescent probes to detect different levels of hypoxia. *Angewandte Chemie International Edition,* 52**,** 13028-13032.

PICCIRILLO, C. A., BJUR, E., TOPISIROVIC, I., SONENBERG, N. & LARSSON, O. 2014. Translational control of immune responses: from transcripts to translatomes. *Nature immunology,* 15**,** 503-511.

PICKERING, B. M., MITCHELL, S. A., EVANS, J. R. & WILLIS, A. E. 2003. Polypyrimidine tract binding protein and poly r (C) binding protein 1 interact with the BAG-1 IRES and stimulate its activity in vitro and in vivo. *Nucleic acids research,* 31**,** 639-646.

PICKERING, B. M., MITCHELL, S. A., SPRIGGS, K. A., STONELEY, M. & WILLIS, A. E. 2004. Bag-1 internal ribosome entry segment activity is promoted by structural

changes mediated by poly (rC) binding protein 1 and recruitment of polypyrimidine tract binding protein 1. *Molecular and cellular biology,* 24**,** 5595-5605.

PICKERING, B. M. & WILLIS, A. E. The implications of structured 5′ untranslated regions on translation and disease. Seminars in cell & developmental biology, 2005. Elsevier, 39-47.

PINNIX, Z. K., MILLER, L. D., WANG, W., D'AGOSTINO, R., KUTE, T., WILLINGHAM, M. C., HATCHER, H., TESFAY, L., SUI, G. & DI, X. 2010. Ferroportin and iron regulation in breast cancer progression and prognosis. *Science translational medicine,* 2**,** 43ra56-43ra56.

PINTENS, S., NEVEN, P., DRIJKONINGEN, M., VAN BELLE, V., MOERMAN, P., CHRISTIAENS, M.-R., SMEETS, A., WILDIERS, H. & BEMPT, I. V. 2009. Triple negative breast cancer: a study from the point of view of basal CK5/6 and HER-1. *Journal of clinical pathology,* 62**,** 624-628.

PISAREVA, V. P., PISAREV, A. V., KOMAR, A. A., HELLEN, C. U. & PESTOVA, T. V. 2008. Translation initiation on mammalian mRNAs with structured 5′ UTRs requires DExH-box protein DHX29. *Cell,* 135**,** 1237-1250.

PISKOUNOVA, E., AGATHOCLEOUS, M., MURPHY, M. M., HU, Z., HUDDLESTUN, S. E., ZHAO, Z., LEITCH, A. M., JOHNSON, T. M., DEBERARDINIS, R. J. & MORRISON, S. J. 2015. Oxidative stress inhibits distant metastasis by human melanoma cells. *Nature,* 527**,** 186-191.

PLAISANCE, V., BRAJKOVIC, S., TENENBAUM, M., FAVRE, D., EZANNO, H., BONNEFOND, A., BONNER, C., GMYR, V., KERR-CONTE, J. & GAUTHIER, B. R. 2016. Endoplasmic reticulum stress links oxidative stress to impaired pancreatic Beta-cell function caused by human oxidized LDL. *PloS one,* 11**,** e0163046.

PLANK, C., OBERHAUSER, B., MECHTLER, K., KOCH, C. & WAGNER, E. 1994. The influence of endosome-disruptive peptides on gene transfer using synthetic virus-like gene transfer systems. *Journal of Biological Chemistry,* 269**,** 12918-12924.

PLANK, C., ZELPHATI, O. & MYKHAYLYK, O. 2011. Magnetically enhanced nucleic acid delivery. Ten years of magnetofection—Progress and prospects. *Advanced drug delivery reviews,* 63**,** 1300-1331.

PLIANWONG, S., THAPA, B., KC, R. B., KUCHARSKI, C., ROJANARATA, T. & ULUDAĞ, H. 2020. Enabling Combinatorial siRNA Delivery against Apoptosis-Related Proteins with Linoleic Acid and α-Linoleic Acid Substituted Low Molecular Weight Polyethylenimines. *Pharmaceutical Research,* 37**,** 46.

POSTOW, M. A., CALLAHAN, M. K. & WOLCHOK, J. D. 2015. Immune checkpoint blockade in cancer therapy. *Journal of clinical oncology,* 33**,** 1974.

Powley, Ian R., Alexander Kondrashov, Lucy A. Young, Helen C. Dobbyn, Kirsti Hill, Ian G. Cannell, Mark Stoneley, Yi Wen Kong, Julia A. Cotes, Graeme C. M. Smith, Ron Wek, Christopher Hayes, Timothy W. Gant, Keith A. Spriggs, Martin Bushell, and Anne E. Willis. 2009. "Translational Reprogramming Following UVB Irradiation Is Mediated by DNA-PKcs and Allows Selective Recruitment to the Polysomes of MRNAs Encoding DNA Repair Enzymes." Genes and Development 23(10):1207–20. doi: 10.1101/gad.516509.

PÖYRY, T. A., KAMINSKI, A., CONNELL, E. J., FRASER, C. S. & JACKSON, R. J. 2007. The mechanism of an exceptional case of reinitiation after translation of a long ORF reveals why such events do not generally occur in mammalian mRNA translation. *Genes & development,* 21**,** 3149-3162.

PRAHALLAD, A., SUN, C., HUANG, S., DI NICOLANTONIO, F., SALAZAR, R., ZECCHIN, D., BEIJERSBERGEN, R. L., BARDELLI, A. & BERNARDS, R. 2012. Unresponsiveness of colon cancer to BRAF (V600E) inhibition through feedback activation of EGFR. *Nature,* 483**,** 100-103.

PRAKASH, T. P., GRAHAM, M. J., YU, J., CARTY, R., LOW, A., CHAPPELL, A., SCHMIDT, K., ZHAO, C., AGHAJAN, M. & MURRAY, H. F. 2014. Targeted delivery of antisense oligonucleotides to hepatocytes using triantennary N-acetyl galactosamine improves potency 10-fold in mice. *Nucleic acids research,* 42**,** 8796-8807.

PRAKASH, T. P., SIWKOWSKI, A., ALLERSON, C. R., MIGAWA, M. T., LEE, S., GAUS, H. J., BLACK, C., SETH, P. P., SWAYZE, E. E. & BHAT, B. 2010. Antisense oligonucleotides containing conformationally constrained 2′, 4′-(N-methoxy) aminomethylene and 2′, 4′-aminooxymethylene and 2′-O, 4′-C-aminomethylene bridged nucleoside analogues show improved potency in animal models. *Journal of medicinal chemistry,* 53**,** 1636-1650.

PRICE, D. J., KHUPHE, M., DAVIES, R. P., MCLAUGHLAN, J. R., INGRAM, N. & THORNTON, P. D. 2017. Poly (amino acid)-polyester graft copolymer nanoparticles for the acid-mediated release of doxorubicin. *Chemical Communications,* 53**,** 8687-8690.

PUTZ, M. V., DUDA-SEIMAN, C., DUDA-SEIMAN, D., PUTZ, A.-M., ALEXANDRESCU, I., MERNEA, M. & AVRAM, S. 2016. Chemical structure-biological activity models for

pharmacophores' 3D-interactions. *International journal of molecular sciences,* 17**,** 1087.

QIU, Q. 2003. Inhibitory Effect of Antisense Oligonucleotides on EGFR Expression, Proliferation and Migration of Retinal Pigment Epithelium Cells In Vivo. *Investigative Ophthalmology & Visual Science,* 44**,** 2342-2342.

QUARANTA, V., REJNIAK, K. A., GERLEE, P. & ANDERSON, A. R. Invasion emerges from cancer cell adaptation to competitive microenvironments: quantitative predictions from multiscale mathematical models. Seminars in Cancer Biology, 2008. Elsevier, 338-348.

RADEN, Martin, Syed M. Ali, Omer S. Alkhnbashi, Anke Busch, Fabrizio Costa, Jason A. Davis, Florian Eggenhofer, Rick Gelhausen, Jens Georg, Steffen Heyne, Michael Hiller, Kousik Kundu, Robert Kleinkauf, Steffen C. Lott, Mostafa M. Mohamed, Alexander Mattheis, Milad Miladi, Andreas S. Richter, Sebastian Will, Joachim Wolff, Patrick R. Wright, and Rolf Backofen. 2018. "Freiburg RNA Tools: A Central Online Resource for RNA-Focused Research and Teaching." Nucleic Acids Research 46(W1):W25–29. doi: 10.1093/nar/gky329.

RADER, D. J. & KASTELEIN, J. J. 2014. Lomitapide and mipomersen: two first-in-class drugs for reducing low-density lipoprotein cholesterol in patients with homozygous familial hypercholesterolemia. *Circulation,* 129**,** 1022-1032.

RAMAN, S. N. T., LIU, G., PYO, H. M., CUI, Y. C., XU, F., AYALEW, L. E., TIKOO, S. K. & ZHOU, Y. 2016. DDX3 interacts with influenza A virus NS1 and NP proteins and exerts antiviral function through regulation of stress granule formation. *Journal of virology,* 90**,** 3661-3675.

RANUCCI, E. & MANFREDI, A. 2019. Polyamidoamines: Versatile bioactive polymers with potential for biotechnological applications. *Chemistry Africa,* 2**,** 167-193.

RAUSCH, K., REUTER, A., FISCHER, K. & SCHMIDT, M. 2010. Evaluation of nanoparticle aggregation in human blood serum. *Biomacromolecules,* 11**,** 2836-2839.

RAVID, T., SWEENEY, C., GEE, P., CARRAWAY, K. L. & GOLDKORN, T. 2002. Epidermal growth factor receptor activation under oxidative stress fails to promote c-Cbl mediated down-regulation. *Journal of Biological Chemistry,* 277**,** 31214-31219.

REARDON, D. B., CONTESSA, J. N., MIKKELSEN, R. B., VALERIE, K., AMIR, C., DENT, P. & SCHMIDT-ULLRICH, R. K. 1999. Dominant negative EGFR-CD533 and inhibition of MAPK modify JNK1 activation and enhance radiation

toxicity of human mammary carcinoma cells. *Oncogene,* 18.

REJMAN, J., OBERLE, V., ZUHORN, I. S. & HOEKSTRA, D. 2004. Size-dependent internalization of particles via the pathways of clathrin-and caveolae-mediated endocytosis. *Biochemical journal,* 377**,** 159-169.

RICHARDSON, E., YANG, Y. & HALL, J. 2009. *A novel meta database for relationships between Bioinformatics databases*.

RICHARDSON, S. C., PATTRICK, N. G., LAVIGNAC, N., FERRUTI, P. & DUNCAN, R. 2010. Intracellular fate of bioresponsive poly (amidoamine) s in vitro and in vivo. *Journal of controlled release,* 142**,** 78-88.

RIGO, F., CHUN, S. J., NORRIS, D. A., HUNG, G., LEE, S., MATSON, J., FEY, R. A., GAUS, H., HUA, Y. & GRUNDY, J. S. 2014. Pharmacology of a central nervous system delivered 2′-O-methoxyethyl–modified survival of motor neuron splicing oligonucleotide in mice and nonhuman primates. *Journal of Pharmacology and Experimental Therapeutics,* 350**,** 46-55.

RIMAWI, M. F., SHETTY, P. B., WEISS, H. L., SCHIFF, R., OSBORNE, C. K., CHAMNESS, G. C. & ELLEDGE, R. M. 2010. Epidermal growth factor receptor expression in breast cancer association with biologic phenotype and clinical outcomes. *Cancer,* 116**,** 1234-1242.

ROCAK, S. & LINDER, P. 2004. DEAD-box proteins: the driving forces behind RNA metabolism. *Nature reviews Molecular cell biology,* 5**,** 232-241.

RODRIGUES, T. & BERNARDES, G. J. 2020. Machine learning for target discovery in drug development. *Current opinion in chemical biology,* 56**,** 16-22.

RON, D. & WALTER, P. 2007. Signal integration in the endoplasmic reticulum unfolded protein response. *Nature reviews Molecular cell biology,* 8**,** 519-529.

ROSIE, Z. Y., LEMONIDIS, K. M., GRAHAM, M. J., MATSON, J. E., CROOKE, R. M., TRIBBLE, D. L., WEDEL, M. K., LEVIN, A. A. & GEARY, R. S. 2009. Cross-species comparison of in vivo PK/PD relationships for second-generation antisense oligonucleotides targeting apolipoprotein B-100. *Biochemical pharmacology,* 77**,** 910-919.

RUBIO, Claudia A., Benjamin Weisburd, Matthew Holderfield, Carolina Arias, Eric Fang, Joseph L. DeRisi, and Abdallah Fanidi. 2014. "Transcriptome-Wide Characterization of the EIF4A Signature Highlights Plasticity in Translation Regulation." Genome Biology 15(10):476. doi: 10.1186/s13059-014-0476-1.

RUDOLPH, C., PLANK, C., LAUSIER, J., SCHILLINGER, U., MÜLLER, R. H. & ROSENECKER, J. 2003. Oligomers of the arginine-rich motif of the HIV-1 TAT protein are capable of transferring plasmid DNA into cells. *Journal of Biological Chemistry,* 278**,** 11411-11418.

RUGGERO, D. 2013. Translational control in cancer etiology. *Cold Spring Harb Perspect Biol,* 5.

RUHANEN, H., USHAKOV, K. & YASUKAWA, T. 2011. Involvement of DNA ligase III and ribonuclease H1 in mitochondrial DNA replication in cultured human cells. *Biochimica et Biophysica Acta (BBA)-Molecular Cell Research,* 1813**,** 2000-2007.

RUI, Y., WILSON, D. R., SANDERS, K. & GREEN, J. J. 2019. Reducible branched ester-amine quadpolymers (rBEAQs) codelivering plasmid DNA and RNA oligonucleotides enable CRISPR/Cas9 genome editing. *ACS applied materials & interfaces,* 11**,** 10472-10480.

SADLER, J. L. & BARD, A. J. 1968. Electrochemical reduction of aromatic azo compounds. *Journal of the American Chemical Society,* 90**,** 1979-1989.

SAGLIOCCO, F. A., VEGA LASO, M. R., ZHU, D., TUITE, M. F., MCCARTHY, J. E. & BROWN, A. J. 1993. The influence of 5'-secondary structures upon ribosome binding to mRNA during translation in yeast. *J Biol Chem,* 268**,** 26522-30.

SAITO, A., OCHIAI, K., KONDO, S., TSUMAGARI, K., MURAKAMI, T., CAVENER, D. R. & IMAIZUMI, K. 2011. Endoplasmic reticulum stress response mediated by the PERK-eIF2α-ATF4 pathway is involved in osteoblast differentiation induced by BMP2. *Journal of biological chemistry,* 286**,** 4809-4818.

SAMAL, S. K., ROUTRAY, S., VEERAMACHANENI, G. K., DASH, R. & BOTLAGUNTA, M. 2015. Ketorolac salt is a newly discovered DDX3 inhibitor to treat oral cancer. *Scientific reports,* 5**,** 9982.

SAMALI, A., HOLMBERG, C. I., SISTONEN, L. & ORRENIUS, S. 1999. Thermotolerance and cell death are distinct cellular responses to stress: dependence on heat shock proteins. *FEBS letters,* 461**,** 306-310.

SANDS, H., GOREY-FERET, L. J., COCUZZA, A. J., HOBBS, F. W., CHIDESTER, D. & TRAINOR, G. L. 1994. Biodistribution and metabolism of internally 3H-labeled oligonucleotides. I. Comparison of a phosphodiester and a phosphorothioate. *Molecular pharmacology,* 45**,** 932-943.

SANZ, M. A., REDONDO, N., GARCÍA-MORENO, M. & CARRASCO, L. 2013. Phosphorylation of eIF2α is responsible for the failure of the picornavirus internal

ribosome entry site to direct translation from Sindbis virus replicons. *Journal of General Virology,* 94**,** 796-806.
SCHAFFER, D. V., FIDELMAN, N. A., DAN, N. & LAUFFENBURGER, D. A. 2000. Vector unpacking as a potential barrier for receptor-mediated polyplex gene delivery. *Biotechnology and bioengineering,* 67**,** 598-606.
SCHLESSINGER, J. 2002. Ligand-induced, receptor-mediated dimerization and activation of EGF receptor. *Cell,* 110**,** 669-672.
SCHMID, S. R. & LINDER, P. 1991. Translation initiation factor 4A from Saccharomyces cerevisiae: analysis of residues conserved in the DEAD family of RNA helicases. *Molecular and cellular biology,* 11**,** 3463-3471.
SCHOFIELD, James P. R., Joanne L. Cowan, and Mark J. Coldwell. 2015. "G-Quadruplexes Mediate Local Translation in Neurons." Biochemical Society Transactions 43(3):338–42. doi: 10.1042/BST20150053.
SCHRODER, M., BARAN, M. & BOWIE, A. G. 2008. Viral targeting of DEAD box protein 3 reveals its role in TBK1/IKKepsilon-mediated IRF activation. *Embo j,* 27**,** 2147-57.
SCHWANHÄUSSER, B., BUSSE, D., LI, N., DITTMAR, G., SCHUCHHARDT, J., WOLF, J., CHEN, W. & SELBACH, M. 2011. Global quantification of mammalian gene expression control. *Nature,* 473**,** 337.
SCOLES, D. R., MINIKEL, E. V. & PULST, S. M. 2019. Antisense oligonucleotides: A primer. *Neurology. Genetics,* 5**,** e323-e323.
SETH, P. P., JAZAYERI, A., YU, J., ALLERSON, C. R., BHAT, B. & SWAYZE, E. E. 2012. Structure activity relationships of α-L-LNA modified phosphorothioate gapmer antisense oligonucleotides in animals. *Molecular Therapy-Nucleic Acids,* 1**,** e47.
SHAKIN, S. & LIEBHABER, S. 1986. Destabilization of messenger RNA/complementary DNA duplexes by the elongating 80 S ribosome. *Journal of Biological Chemistry,* 261**,** 16018-16025.
SHAMOVSKY, I. & NUDLER, E. 2008. New insights into the mechanism of heat shock response activation. *Cellular and Molecular Life Sciences,* 65**,** 855-861.
SHARMA, D. & JANKOWSKY, E. 2014. The Ded1/DDX3 subfamily of DEAD-box RNA helicases. *Critical reviews in biochemistry and molecular biology,* 49**,** 343-360.
SHARMA, S. V., BELL, D. W., SETTLEMAN, J. & HABER, D. A. 2007. Epidermal growth factor receptor mutations in lung cancer. *Nature reviews Cancer,* 7**,** 169-81.

SHEEHAN, J. P. & PHAN, T. M. 2001. Phosphorothioate oligonucleotides inhibit the intrinsic tenase complex by an allosteric mechanism. *Biochemistry,* 40**,** 4980-4989.
SHEN, J., XIA, W., KHOTSKAYA, Y. B., HUO, L., NAKANISHI, K., LIM, S.-O., DU, Y., WANG, Y., CHANG, W.-C. & CHEN, C.-H. 2013. EGFR modulates microRNA maturation in response to hypoxia through phosphorylation of AGO2. *Nature,* 497**,** 383-387.
SHEN, L., SIWKOWSKI, A., WANCEWICZ, E. V., LESNIK, E., BUTLER, M., WITCHELL, D., VASQUEZ, G., ROSS, B., ACEVEDO, O. & INAMATI, G. 2003. Evaluation of C-5 propynyl pyrimidine-containing oligonucleotides in vitro and in vivo. *Antisense and Nucleic Acid Drug Development,* 13**,** 129-142.
SHEN, W., DE HOYOS, C. L., MIGAWA, M. T., VICKERS, T. A., SUN, H., LOW, A., BELL, T. A., RAHDAR, M., MUKHOPADHYAY, S. & HART, C. E. 2019. Chemical modification of PS-ASO therapeutics reduces cellular protein-binding and improves the therapeutic index. *Nature biotechnology,* 37**,** 640-650.
SHEN, W., LIANG, X.-H. & CROOKE, S. T. 2014. Phosphorothioate oligonucleotides can displace NEAT1 RNA and form nuclear paraspeckle-like structures. *Nucleic acids research,* 42**,** 8648-8662.
SHIH, J.-W., WANG, W.-T., TSAI, T.-Y., KUO, C.-Y., LI, H.-K. & LEE, Y.-H. W. 2012. Critical roles of RNA helicase DDX3 and its interactions with eIF4E/PABP1 in stress granule assembly and stress response. *Biochemical Journal,* 441**,** 119-129.
SHIH, J., TSAI, T., CHAO, C. & LEE, Y. W. 2008. Candidate tumor suppressor DDX3 RNA helicase specifically represses cap-dependent translation by acting as an eIF4E inhibitory protein. *Oncogene,* 27**,** 700.
SHIH, J. W. & LEE, Y. H. 2014. Human DExD/H RNA helicases: emerging roles in stress survival regulation. *Clin Chim Acta,* 436**,** 45-58.
SHIN, M. S., KIM, H. S., LEE, S. H., PARK, W. S., KIM, S. Y., PARK, J. Y., LEE, J. H., LEE, S. K., LEE, S. N. & JUNG, S. S. 2001. Mutations of tumor necrosis factor-related apoptosis-inducing ligand receptor 1 (TRAIL-R1) and receptor 2 (TRAIL-R2) genes in metastatic breast cancers. *Cancer research,* 61**,** 4942-4946.
SI, X., MA, S., XU, Y., ZHANG, D., SHEN, N., YU, H., ZHANG, Y., SONG, W., TANG, Z. & CHEN, X. 2020. Hypoxia-sensitive supramolecular nanogels for the cytosolic delivery of ribonuclease A as a breast cancer therapeutic. *Journal of Controlled Release*.

SIEVERS, F. & HIGGINS, D. G. 2018. Clustal Omega for making accurate alignments of many protein sequences. *Protein Science,* 27**,** 135-145.

SILVERA, D., ARJU, R., DARVISHIAN, F., LEVINE, P. H., ZOLFAGHARI, L., GOLDBERG, J., HOCHMAN, T., FORMENTI, S. C. & SCHNEIDER, R. J. 2009. Essential role for eIF4GI overexpression in the pathogenesis of inflammatory breast cancer. *Nature cell biology,* 11**,** 903-908.

SIRSI, S. R., HERNANDEZ, S. L., ZIELINSKI, L., BLOMBACK, H., KOUBAA, A., SYNDER, M., HOMMA, S., KANDEL, J. J., YAMASHIRO, D. J. & BORDEN, M. A. 2012. Polyplex-microbubble hybrids for ultrasound-guided plasmid DNA delivery to solid tumors. *Journal of controlled release,* 157**,** 224-234.

SKABKIN, M. A., SKABKINA, O. V., HELLEN, C. U. & PESTOVA, T. V. 2013. Reinitiation and other unconventional posttermination events during eukaryotic translation. *Molecular cell,* 51**,** 249-264.

SLEIGH, M. 1976. The mechanism of DNA breakage by phleomycin in vitro. *Nucleic acids research,* 3**,** 891-902.

SMITH, A. E. 1995. Viral vectors in gene therapy. *Annual review of microbiology,* 49**,** 807-838.

SMITH, C. E. & ZAIN, R. 2019. Therapeutic oligonucleotides: state of the art. *Annual review of pharmacology and toxicology,* 59**,** 605-630.

SOMERS, J., PÖYRY, T. & WILLIS, A. E. 2013. A perspective on mammalian upstream open reading frame function. *The international journal of biochemistry & cell biology,* 45**,** 1690-1700.

SON, S., NAMGUNG, R., KIM, J., SINGHA, K. & KIM, W. J. 2012. Bioreducible polymers for gene silencing and delivery. *Accounts of chemical research,* 45**,** 1100-1112.

SONENBERG, N. & HINNEBUSCH, A. G. 2009. Regulation of translation initiation in eukaryotes: mechanisms and biological targets. *Cell,* 136**,** 731-745.

SONENBERG, N., MORGAN, M. A., MERRICK, W. C. & SHATKIN, A. J. 1978. A polypeptide in eukaryotic initiation factors that crosslinks specifically to the 5'-terminal cap in mRNA. *Proceedings of the National Academy of Sciences,* 75**,** 4843-4847.

SONNENBLICK, A., DE AZAMBUJA, E., AZIM JR, H. A. & PICCART, M. 2015. An update on PARP inhibitors—moving to the adjuvant setting. *Nature reviews Clinical oncology,* 12**,** 27.

SOTO-RIFO, R. & OHLMANN, T. 2013. The role of the DEAD-box RNA helicase DDX3 in mRNA metabolism. *Wiley Interdisciplinary Reviews: RNA,* 4**,** 369-385.

SOTO-RIFO, R., RUBILAR, P. S., LIMOUSIN, T., DE BREYNE, S., DECIMO, D. & OHLMANN, T. 2012. DEAD-box protein DDX3 associates with eIF4F to promote translation of selected mRNAs. *The EMBO journal,* 31**,** 3745-3756.

SPRIGGS, K., BUSHELL, M., MITCHELL, S. & WILLIS, A. 2005. Internal ribosome entry segment-mediated translation during apoptosis: the role of IRES-trans-acting factors. *Cell death and differentiation,* 12**,** 585.

SPRIGGS, K. A., COBBOLD, L. C., JOPLING, C. L., COOPER, R. E., WILSON, L. A., STONELEY, M., COLDWELL, M. J., PONCET, D., SHEN, Y. C., MORLEY, S. J., BUSHELL, M. & WILLIS, A. E. 2009. Canonical initiation factor requirements of the Myc family of internal ribosome entry segments. *Mol Cell Biol,* 29**,** 1565-74.

SPRIGGS, K. A., STONELEY, M., BUSHELL, M. & WILLIS, A. E. 2008. Re-programming of translation following cell stress allows IRES-mediated translation to predominate. *Biology of the Cell,* 100**,** 27-38.

SRIRAM, A., BOHLEN, J. & TELEMAN, A. A. 2018. Translation acrobatics: how cancer cells exploit alternate modes of translational initiation. *EMBO reports,* 19.

STARESINCIC, L., FAGBEMI, A. F., ENZLIN, J. H., GOURDIN, A. M., WIJGERS, N., DUNAND-SAUTHIER, I., GIGLIA-MARI, G., CLARKSON, S. G., VERMEULEN, W. & SCHÄRER, O. D. 2009. Coordination of dual incision and repair synthesis in human nucleotide excision repair. *The EMBO journal,* 28**,** 1111-1120.

STECHOW von, Louise, Dimitris Typas, Jordi Carreras Puigvert, Laurens Oort, Ramakrishnaiah Siddappa, Alex Pines, Harry Vrieling, Bob van de Water, Leon H. F. Mullenders, and Erik H. J. Danen. 2015. "The E3 Ubiquitin Ligase ARIH1 Protects against Genotoxic Stress by Initiating a 4EHP-Mediated MRNA Translation Arrest." Molecular and Cellular Biology 35(7):1254–68. doi: 10.1128/mcb.01152-14.

STEIN, C., HANSEN, J. B., LAI, J., WU, S., VOSKRESENSKIY, A., H⊘ G, A., WORM, J., HEDTJÄRN, M., SOULEIMANIAN, N. & MILLER, P. 2009. Efficient gene silencing by delivery of locked nucleic acid antisense oligonucleotides, unassisted by transfection reagents. *Nucleic acids research,* 38**,** e3-e3.

STEIN, C., SUBASINGHE, C., SHINOZUKA, K. & COHEN, J. S. 1988. Physicochemical properties of phospborothioate

oligodeoxynucleotides. *Nucleic acids research,* 16**,** 3209-3221.

STEIN, D., FOSTER, E., HUANG, S.-B., WELLER, D. & SUMMERTON, J. 1997. A specificity comparison of four antisense types: morpholino, 2′-O-methyl RNA, DNA, and phosphorothioate DNA. *Antisense and Nucleic Acid Drug Development,* 7**,** 151-157.

STEPHANIE, K., URSULA, O. & THOMAS, S. 2011. Immunological detection of UV induced cyclobutane pyrimidine dimers and (6–4) photoproducts in DNA from reference bacteria and natural aquatic populations. *Journal of microbiological methods,* 84**,** 435-441.

STEPHENSON, M. L. & ZAMECNIK, P. C. 1978. Inhibition of Rous sarcoma viral RNA translation by a specific oligodeoxyribonucleotide. *Proceedings of the National Academy of Sciences,* 75**,** 285-288.

STONELEY, M., PAULIN, F. E., QUESNE, J. P. L., CHAPPELL, S. A. & WILLIS, A. E. 1998. C-Myc 5'untranslated region contains an internal ribosome entry segment. *Oncogene,* 16**,** 423-428.

STUCHINSKAYA, T., MORENO, M., COOK, M. J., EDWARDS, D. R. & RUSSELL, D. A. 2011. Targeted photodynamic therapy of breast cancer cells using antibody–phthalocyanine–gold nanoparticle conjugates. *Photochemical & Photobiological Sciences,* 10**,** 822-831.

SUMMERTON, J. 1999. Morpholino antisense oligomers: the case for an RNase H-independent structural type. *Biochimica et Biophysica Acta (BBA)-Gene Structure and Expression,* 1489**,** 141-158.

SUN, C. & BERNARDS, R. 2014. Feedback and redundancy in receptor tyrosine kinase signaling: relevance to cancer therapies. *Trends in biochemical sciences,* 39**,** 465-474.

SUN, M., SONG, L., LI, Y., ZHOU, T. & JOPE, R. S. 2008. Identification of an antiapoptotic protein complex at death receptors. *Cell Death Differ,* 15**,** 1887-900.

SUN, M., SONG, L., ZHOU, T., GILLESPIE, G. Y. & JOPE, R. S. 2011. The role of DDX3 in regulating Snail. *Biochimica et biophysica acta,* 1813**,** 438-447.

SUN, M., ZHOU, T., JONASCH, E. & JOPE, R. S. 2013. DDX3 regulates DNA damage-induced apoptosis and p53 stabilization. *Biochim Biophys Acta,* 1833**,** 1489-97.

SUNSHINE, J. C., AKANDA, M. I., LI, D., KOZIELSKI, K. L. & GREEN, J. J. 2011. Effects of base polymer hydrophobicity and end-group modification on polymeric gene delivery. *Biomacromolecules,* 12**,** 3592-3600.

SUNSHINE, J. C., PENG, D. Y. & GREEN, J. J. 2012. Uptake and transfection with polymeric nanoparticles are dependent

on polymer end-group structure, but largely independent of nanoparticle physical and chemical properties. *Molecular pharmaceutics,* 9**,** 3375-3383.

SVITKIN, Y. V., PAUSE, A., HAGHIGHAT, A., PYRONNET, S., WITHERELL, G., BELSHAM, G. J. & SONENBERG, N. 2001. The requirement for eukaryotic initiation factor 4A (eIF4A) in translation is in direct proportion to the degree of mRNA 5' secondary structure. *Rna,* 7**,** 382-94.

SWAYZE, E. E., SIWKOWSKI, A. M., WANCEWICZ, E. V., MIGAWA, M. T., WYRZYKIEWICZ, T. K., HUNG, G., MONIA, B. P., BENNETT & FRANK, C. 2006. Antisense oligonucleotides containing locked nucleic acid improve potency but cause significant hepatotoxicity in animals. *Nucleic acids research,* 35**,** 687-700.

SWINSON, D. E. B. & O'BYRNE, K. J. 2006. Interactions between hypoxia and epidermal growth factor receptor in non–small-cell lung cancer. *Clinical lung cancer,* 7**,** 250-256.

TAKAYANAGI, T., KAWAI, T., FORRESTER, S. J., OBAMA, T., TSUJI, T., FUKUDA, Y., ELLIOTT, K. J., TILLEY, D. G., DAVISSON, R. L. & PARK, J.-Y. 2015. Role of epidermal growth factor receptor and endoplasmic reticulum stress in vascular remodeling induced by angiotensin II. *Hypertension***,** HYPERTENSIONAHA. 115.05344.

TALLET-LOPEZ, B., ALDAZ-CARROLL, L., CHABAS, S., DAUSSE, E., STAEDEL, C. & TOULMÉ, J. J. 2003. Antisense oligonucleotides targeted to the domain IIId of the hepatitis C virus IRES compete with 40S ribosomal subunit binding and prevent in vitro translation. *Nucleic acids research,* 31**,** 734-742.

TALLÓCZY, Z., JIANG, W., VIRGIN, H. W., LEIB, D. A., SCHEUNER, D., KAUFMAN, R. J., ESKELINEN, E.-L. & LEVINE, B. 2002. Regulation of starvation-and virus-induced autophagy by the eIF2α kinase signaling pathway. *Proceedings of the National Academy of Sciences,* 99**,** 190-195.

TANG, S., YIN, Q., SU, J., SUN, H., MENG, Q., CHEN, Y., CHEN, L., HUANG, Y., GU, W. & XU, M. 2015. Inhibition of metastasis and growth of breast cancer by pH-sensitive poly (β-amino ester) nanoparticles co-delivering two siRNA and paclitaxel. *Biomaterials,* 48**,** 1-15.

TERENIN, Ilya M., Victoria V. Smirnova, Dmitri E. Andreev, Sergey E. Dmitriev, and Ivan N. Shatsky. 2017. "A Researcher's Guide to the Galaxy of IRESs." Cellular and Molecular Life Sciences 74(8):1431–55.

THAKOR, N. & HOLCIK, M. 2011. IRES-mediated translation of cellular messenger RNA operates in eIF2α-independent

manner during stress. *Nucleic acids research,* 40**,** 541-552.
THOMPSON, S. R. 2012. So you want to know if your message has an IRES? *Wiley Interdisciplinary Reviews: RNA,* 3**,** 697-705.
THORNE, Natasha, James Inglese, and Douglas S. Auld. 2010. "Illuminating Insights into Firefly Luciferase and Other Bioluminescent Reporters Used in Chemical Biology." Chemistry and Biology 17(6):646–57.
TOMAS, A., FUTTER, C. E. & EDEN, E. R. 2014. EGF receptor trafficking: consequences for signaling and cancer. *Trends in cell biology,* 24**,** 26-34.
TRUITT, M. L. & RUGGERO, D. 2017. New frontiers in translational control of the cancer genome. *Nature reviews Cancer,* 17**,** 332.
TURASHVILI, G. & BROGI, E. 2017. Tumor heterogeneity in breast cancer. *Frontiers in medicine,* 4**,** 227.
TZENG, S. Y., HIGGINS, L. J., POMPER, M. G. & GREEN, J. J. 2013. Biomaterial-mediated cancer-specific DNA delivery to liver cell cultures using synthetic poly (beta-amino esters). *Journal of biomedical materials research. Part A,* 101**,** 1837.
TZENG, S. Y., HUNG, B. P., GRAYSON, W. L. & GREEN, J. J. 2012. Cystamine-terminated poly (beta-amino ester) s for siRNA delivery to human mesenchymal stem cells and enhancement of osteogenic differentiation. *Biomaterials,* 33**,** 8142-8151.
ULE, J., JENSEN, K. B., RUGGIU, M., MELE, A., ULE, A. & DARNELL, R. B. 2003. CLIP identifies Nova-regulated RNA networks in the brain. *Science,* 302**,** 1212-1215.
UNIACKE, J., HOLTERMAN, C. E., LACHANCE, G., FRANOVIC, A., JACOB, M. D., FABIAN, M. R., PAYETTE, J., HOLCIK, M., PAUSE, A. & LEE, S. 2012. An oxygen-regulated switch in the protein synthesis machinery. *Nature,* 486**,** 126.
URADE, R., HAYASHI, Y. & KITO, M. 1988. Endosomes differ from plasma membranes in the phospholipid molecular species composition. *Biochimica et Biophysica Acta (BBA)-Biomembranes,* 946**,** 151-163.
VADER, P., VAN DER AA, L. J., ENGBERSEN, J. F., STORM, G. & SCHIFFELERS, R. M. 2012. Physicochemical and biological evaluation of siRNA polyplexes based on PEGylated poly (amido amine) s. *Pharmaceutical research,* 29**,** 352-361.
VALENTIN-VEGA, Y. A., WANG, Y.-D., PARKER, M., PATMORE, D. M., KANAGARAJ, A., MOORE, J., RUSCH, M., FINKELSTEIN, D., ELLISON, D. W., GILBERTSON, R. J., ZHANG, J., KIM, H. J. & TAYLOR, J. P. 2016. Cancer-

associated DDX3X mutations drive stress granule assembly and impair global translation. *Scientific reports,* 6**,** 25996-25996.

VALERIE, K. & POVIRK, L. F. 2003. Regulation and mechanisms of mammalian double-strand break repair. *Oncogene,* 22**,** 5792-5812.

VAN MEER, L., MOERLAND, M., GALLAGHER, J., VAN DOORN, M. B., PRENS, E. P., COHEN, A. F., RISSMANN, R. & BURGGRAAF, J. 2016. Injection site reactions after subcutaneous oligonucleotide therapy. *British journal of clinical pharmacology,* 82**,** 340-351.

VAN VOSS, M. H., VESUNA, F., BOL, G. M., AFZAL, J., TANTRAVEDI, S., BERGMAN, Y., KAMMERS, K., LEHAR, M., MALEK, R. & BALLEW, M. 2018. Targeting mitochondrial translation by inhibiting DDX3: a novel radiosensitization strategy for cancer treatment. *Oncogene,* 37**,** 63-74.

VAUGHAN, H. J., GREEN, J. J. & TZENG, S. Y. 2019. Cancer-Targeting Nanoparticles for Combinatorial Nucleic Acid Delivery. *Advanced Materials***,** 1901081.

VEO, B. L. & KRUSHEL, L. A. 2012. Secondary RNA structure and nucleotide specificity contribute to internal initiation mediated by the human tau 5′ leader. *RNA biology,* 9**,** 1344-1360.

VERMA, A. & STELLACCI, F. 2010. Effect of surface properties on nanoparticle–cell interactions. *small,* 6**,** 12-21.

VIALE, G. 2012. The current state of breast cancer classification. *Annals of Oncology,* 23**,** x207-x210.

VICKERS, T. A., WYATT, J. R. & FREIER, S. M. 2000. Effects of RNA secondary structure on cellular antisense activity. *Nucleic Acids Research,* 28**,** 1340-1347.

VISVANATHAN, A., PATIL, V., ARORA, A., HEGDE, A., ARIVAZHAGAN, A., SANTOSH, V. & SOMASUNDARAM, K. 2018. Essential role of METTL3-mediated m 6 A modification in glioma stem-like cells maintenance and radioresistance. *Oncogene,* 37**,** 522-533.

VOEVODINA, I., SCANDOLA, M., ZHANG, J. & JIANG, Z. 2014. Exploring the solid state properties of enzymatic poly (amine-co-ester) terpolymers to expand their applications in gene transfection. *RSC advances,* 4**,** 8953-8961.

WALTERS, B. & THOMPSON, S. R. 2016. Cap-independent translational control of carcinogenesis. *Frontiers in oncology,* 6.

WANG, B., ZHANG, J., SONG, F., TIAN, M., SHI, B., JIANG, H., XU, W., WANG, H., ZHOU, M. & PAN, X. 2016. EGFR regulates iron homeostasis to promote cancer growth

through redistribution of transferrin receptor 1. *Cancer letters,* 381**,** 331-340.

WANG, H. & RYU, W. S. 2010. Hepatitis B virus polymerase blocks pattern recognition receptor signaling via interaction with DDX3: implications for immune evasion. *PLoS Pathog,* 6**,** e1000986.

WANG, S., ALLEN, N., VICKERS, T. A., REVENKO, A. S., SUN, H., LIANG, X.-H. & CROOKE, S. T. 2018. Cellular uptake mediated by epidermal growth factor receptor facilitates the intracellular activity of phosphorothioate-modified antisense oligonucleotides. *Nucleic acids research,* 46**,** 3579-3594.

WANG, X., REYES, M. E., ZHANG, D., FUNAKOSHI, Y., TRAPE, A. P., GONG, Y., KOGAWA, T., ECKHARDT, B. L., MASUDA, H. & PIRMAN JR, D. A. 2017. EGFR signaling promotes inflammation and cancer stem-like activity in inflammatory breast cancer. *Oncotarget,* 8**,** 67904.

WATERMAN, H., KATZ, M., RUBIN, C., SHTIEGMAN, K., LAVI, S., ELSON, A., JOVIN, T. & YARDEN, Y. 2002. A mutant EGF-receptor defective in ubiquitylation and endocytosis unveils a role for Grb2 in negative signaling. *The EMBO journal,* 21**,** 303-313.

WATTS, J. K. & COREY, D. R. 2012. Gene silencing by siRNAs and antisense oligonucleotides in the laboratory and the clinic. *The Journal of pathology,* 226**,** 365.

WEBB, T. E., HUGHES, A., SMALLEY, D. S. & SPRIGGS, K. A. 2015. An internal ribosome entry site in the 5' untranslated region of epidermal growth factor receptor allows hypoxic expression. *Oncogenesis,* 4**,** e134.

WELLS, S. E., HILLNER, P. E., VALE, R. D. & SACHS, A. B. 1998. Circularization of mRNA by eukaryotic translation initiation factors. *Molecular cell,* 2**,** 135-140.

WENGEL, J. 1999. Synthesis of 3 ‘-C-and 4 ‘-C-branched oligodeoxynucleotides and the development of locked nucleic acid (LNA). *Accounts of Chemical Research,* 32**,** 301-310.

WESTON, C. R. & DAVIS, R. J. 2007. The JNK signal transduction pathway. *Current opinion in cell biology,* 19**,** 142-149.

WHITE, J. P., REINEKE, L. C. & LLOYD, R. E. 2011. Poliovirus switches to an eIF2-independent mode of translation during infection. *Journal of virology,* 85**,** 8884-8893.

WHITESIDE, T. 2008. The tumor microenvironment and its role in promoting tumor growth. *Oncogene,* 27**,** 5904-5912.

WICK, P., MANSER, P., LIMBACH, L. K., DETTLAFF-WEGLIKOWSKA, U., KRUMEICH, F., ROTH, S., STARK, W. J. & BRUININK, A. 2007. The degree and kind of

agglomeration affect carbon nanotube cytotoxicity. *Toxicology letters,* 168**,** 121-131.

WICKSTROM, E. 1986. Oligodeoxynucleotide stability in subcellular extracts and culture media. *Journal of biochemical and biophysical methods,* 13**,** 97-102.

WIGHTMAN, L., KIRCHEIS, R., RÖSSLER, V., CAROTTA, S., RUZICKA, R., KURSA, M. & WAGNER, E. 2001. Different behavior of branched and linear polyethylenimine for gene delivery in vitro and in vivo. *The Journal of Gene Medicine: A cross‐disciplinary journal for research on the science of gene transfer and its clinical applications,* 3**,** 362-372.

WILLIFORD, J.-M., ARCHANG, M. M., MINN, I., REN, Y., WO, M., VANDERMARK, J., FISHER, P. B., POMPER, M. G. & MAO, H.-Q. 2016. Critical length of PEG grafts on lPEI/DNA nanoparticles for efficient in vivo delivery. *ACS biomaterials science & engineering,* 2**,** 567-578.

WILSON, D. R., RUI, Y., SIDDIQ, K., ROUTKEVITCH, D. & GREEN, J. J. 2019. Differentially branched ester amine quadpolymers with amphiphilic and pH-sensitive properties for efficient plasmid DNA delivery. *Molecular pharmaceutics,* 16**,** 655-668.

WILSON, K. J., MILL, C., LAMBERT, S., BUCHMAN, J., WILSON, T. R., HERNANDEZ-GORDILLO, V., GALLO, R. M., ADES, L. M., SETTLEMAN, J. & RIESE, D. J. 2012. EGFR ligands exhibit functional differences in models of paracrine and autocrine signaling. *Growth factors,* 30**,** 107-116.

WINNARD JR, P., MIRONCHIK, Y. & RAMAN, V. 2004. Robust expression of transgenes in MCF-7 breast cancer cells is expression vector-dependent. *BioTechniques,* 37**,** 370-374.

WITTERS, L., KUMAR, R., MANDAL, M., BENNETT, C. F., MIRAGLIA, L. & LIPTON, A. 1999. Antisense oligonucleotides to the epidermal growth factor receptor. *Breast cancer research and treatment,* 53**,** 41-50.

WÓJCIK, M., CIEŚLAK, M., STEC, W. J., GODING, J. W. & KOZIOŁKIEWICZ, M. 2007. Nucleotide pyrophosphatase/phosphodiesterase 1 is responsible for degradation of antisense phosphorothioate oligonucleotides. *Oligonucleotides,* 17**,** 134-145.

WOLFE, Andrew L., Kamini Singh, Y. Zhong, Philipp Drewe, Vinagolu K. Rajasekhar, Viraj R. Sanghvi, Konstantinos J. Mavrakis, Man Jiang, Justine E. Roderick, Joni Van der Meulen, Jonathan H. Schatz, Christina M. Rodrigo, Chunying Zhao, Pieter Rondou, Elisa de Stanchina, Julie Teruya-Feldstein, Michelle A. Kelliher, Frank Speleman, John A. Porco, Jerry Pelletier, Gunnar Rätsch, and Hans

Guido Wendel. 2014. "RNA G-Quadruplexes Cause EIF4A-Dependent Oncogene Translation in Cancer." Nature 513(7516):65–70. doi: 10.1038/nature13485.

WONG, E. & GOLDBERG, T. 2014. Mipomersen (kynamro): a novel antisense oligonucleotide inhibitor for the management of homozygous familial hypercholesterolemia. *Pharmacy and Therapeutics,* 39**,** 119.

WU, C., LI, J., WANG, W. & HAMMOND, P. T. 2018. Rationally designed polycationic carriers for potent polymeric siRNA-mediated gene silencing. *ACS nano,* 12**,** 6504-6514.

WU, D. W., LIN, P. L., CHENG, Y. W., HUANG, C. C., WANG, L. & LEE, H. 2016. DDX3 enhances oncogenic KRASinduced tumor invasion in colorectal cancer via the betacatenin/ZEB1 axis. *Oncotarget,* 7**,** 22687-99.

WU, D. W., LIU, W. S., WANG, J., CHEN, C. Y., CHENG, Y. W. & LEE, H. 2011. Reduced p21(WAF1/CIP1) via alteration of p53-DDX3 pathway is associated with poor relapse-free survival in early-stage human papillomavirus-associated lung cancer. *Clin Cancer Res,* 17**,** 1895-905.

WU, H., LIMA, W. F. & CROOKE, S. T. 1999. Properties of cloned and expressed human RNase H1. *Journal of Biological Chemistry,* 274**,** 28270-28278.

XIE, M., VESUNA, F., BOTLAGUNTA, M., BOL, G. M., IRVING, A., BERGMAN, Y., HOSMANE, R. S., KATO, Y., WINNARD JR, P. T. & RAMAN, V. 2015. NZ51, a ring-expanded nucleoside analog, inhibits motility and viability of breast cancer cells by targeting the RNA helicase DDX3. *Oncotarget,* 6**,** 29901.

XIE, S. & ZHOU, J. 2017. Harnessing plant biodiversity for the discovery of novel anticancer drugs targeting microtubules. *Frontiers in plant science,* 8**,** 720.

XIE, W. & ZHOU, J. 2018. Aberrant regulation of autophagy in mammalian diseases. *Biology letters,* 14**,** 20170540.

XUE, S., TIAN, S., FUJII, K., KLADWANG, W., DAS, R. & BARNA, M. 2015. RNA regulons in Hox 5′ UTRs confer ribosome specificity to gene regulation. *Nature,* 517**,** 33.

YANG, L., MAO, H., WANG, Y. A., CAO, Z., PENG, X., WANG, X., DUAN, H., NI, C., YUAN, Q. & ADAMS, G. 2009. Single chain epidermal growth factor receptor antibody conjugated nanoparticles for in vivo tumor targeting and imaging. *Small,* 5**,** 235-243.

YANG, Q. & SARNOW, P. 1997. Location of the internal ribosome entry site in the 5′ non-coding region of the immunoglobulin heavy-chain binding protein (BiP) mRNA: evidence for specific RNA-protein interactions. *Nucleic acids research,* 25**,** 2800-2807.

YANG, X., CHEN, Z., CAI, Y., HUANG, Y.-Y. & SHIBATA, N. 2014. An aza-Michael addition protocol to fluoroalkylated β-amino acid derivatives and enantiopure trifluoromethylated N-heterocycles. *Green Chemistry,* 16**,** 4530-4534.

YANG, Y. & WANG, Z. 2019. IRES-mediated cap-independent translation, a path leading to hidden proteome. *Journal of molecular cell biology,* 11**,** 911-919.

YANG, Z. & TAM, K. Y. 2018. Combination strategies using EGFR-TKi in NSCLC therapy: learning from the gap between pre-clinical results and clinical outcomes. *International journal of biological sciences,* 14**,** 204.

YAO, Y. & DAI, W. 2014. Genomic instability and cancer. *Journal of carcinogenesis & mutagenesis,* 5.

YEDAVALLI, V. S., NEUVEUT, C., CHI, Y. H., KLEIMAN, L. & JEANG, K. T. 2004. Requirement of DDX3 DEAD box RNA helicase for HIV-1 Rev-RRE export function. *Cell,* 119**,** 381-92.

YOSHIDA, T., NAITO, Y., SASAKI, K., UCHIDA, E., SATO, Y., NAITO, M., KAWANISHI, T., OBIKA, S. & INOUE, T. 2018. Estimated number of off-target candidate sites for antisense oligonucleotides in human mRNA sequences. *Genes to Cells,* 23**,** 448-455.

YU, R. Z., GRUNDY, J. S. & GEARY, R. S. 2013. Clinical pharmacokinetics of second generation antisense oligonucleotides. *Expert opinion on drug metabolism & toxicology,* 9**,** 169-182.

YU, Y.-L., CHOU, R.-H., WU, C.-H., WANG, Y.-N., CHANG, W.-J., TSENG, Y.-J., CHANG, W.-C., LAI, C.-C., LEE, H.-J. & HUO, L. 2012. Nuclear EGFR suppresses ribonuclease activity of polynucleotide phosphorylase through DNAPK-mediated phosphorylation at serine 776. *Journal of Biological Chemistry,* 287**,** 31015-31026.

YUAN, Y. Y., MAO, C. Q., DU, X. J., DU, J. Z., WANG, F. & WANG, J. 2012. Surface charge switchable nanoparticles based on zwitterionic polymer for enhanced drug delivery to tumor. *Advanced materials,* 24**,** 5476-5480.

ZAMECNIK, P. C. & STEPHENSON, M. L. 1978. Inhibition of Rous sarcoma virus replication and cell transformation by a specific oligodeoxynucleotide. *Proceedings of the National Academy of Sciences,* 75**,** 280-284.

ZBAIDA, S. & LEVINE, W. G. 1991. A novel application of cyclic voltammetry for direct investigation of metabolic intermediates in microsomal azo reduction. *Chemical research in toxicology,* 4**,** 82-88.

ZELENKA, J., KONCOŠOVÁ, M. & RUML, T. 2018. Targeting of stress response pathways in the prevention and

treatment of cancer. *Biotechnology advances,* 36**,** 583-602.

ZHA, L., HU, J., WANG, C., FU, S. & LUO, M. 2002. The effect of electrolyte on the colloidal properties of poly (N-isopropylacrylamide-co-dimethylaminoethylmethacrylate) microgel latexes. *Colloid and Polymer Science,* 280**,** 1116-1121.

ZHANG, R., LI, Y., ZHANG, M., TANG, Q. & ZHANG, X. 2016. Hypoxia-responsive drug–drug conjugated nanoparticles for breast cancer synergistic therapy. *RSC advances,* 6**,** 30268-30276.

ZHANG, Y.-L., ZHANG, X., FEI, X.-C., WANG, S.-L. & GAO, H.-W. 2010. Binding of bisphenol A and acrylamide to BSA and DNA: insights into the comparative interactions of harmful chemicals with functional biomacromolecules. *Journal of hazardous materials,* 182**,** 877-885.

ZHAO, J., ULLAH, I., GAO, B., GUO, J., REN, X.-K., XIA, S., ZHANG, W. & FENG, Y. 2020. Agmatine-grafted bioreducible poly (L-lysine) for gene delivery with low cytotoxicity and high efficiency. *Journal of Materials Chemistry B*.

ZHU, G., FAN, Z., DING, M., ZHANG, H., MU, L., DING, Y., ZHANG, Y., JIA, B., CHEN, L. & CHANG, Z. 2015. An EGFR/PI3K/AKT axis promotes accumulation of the Rac1-GEF Tiam1 that is critical in EGFR-driven tumorigenesis. *Oncogene,* 34**,** 5971.

ZINTCHENKO, A., OGRIS, M. & WAGNER, E. 2006. Temperature dependent gene expression induced by PNIPAM-based copolymers: potential of hyperthermia in gene transfer. *Bioconjugate chemistry,* 17**,** 766-772.

ZUKER, M. 2003. Mfold web server for nucleic acid folding and hybridization prediction. *Nucleic acids research,* 31**,** 3406-3415.